



## Durham E-Theses

---

### *Epidermal Notch1 recruits innate lymphoid cells to orchestrate normal skin repair*

LI, ZHI

#### How to cite:

---

LI, ZHI (2014) *Epidermal Notch1 recruits innate lymphoid cells to orchestrate normal skin repair*, Durham theses, Durham University. Available at Durham E-Theses Online: <http://etheses.dur.ac.uk/10524/>

#### Use policy

---

The full-text may be used and/or reproduced, and given to third parties in any format or medium, without prior permission or charge, for personal research or study, educational, or not-for-profit purposes provided that:

- a full bibliographic reference is made to the original source
- a [link](#) is made to the metadata record in Durham E-Theses
- the full-text is not changed in any way

The full-text must not be sold in any format or medium without the formal permission of the copyright holders.

Please consult the [full Durham E-Theses policy](#) for further details.

**Zhi Li**

**Epidermal Notch1 recruits innate lymphoid cells to orchestrate normal skin repair**

**Abstract**

Skin constitutes a barrier between our body and outside environment providing the first line defence against microbial infection. Epithelial repair and skin wound healing starts with inflammation to clear up invading pathogens and debris followed by cell proliferation and tissue remodelling. The immune response is vital for protecting the body from infection and diseases, however, it remains controversial whether the immune cells contribute to wound closure and tissue repair, or cause scarring and pathology. In this thesis, I investigate the role of Notch signalling in epithelial tissue repair. I demonstrate Notch1 signalling activation in epidermal keratinocytes following acute skin injury recruits innate lymphoid cells (i.e. ILC3s) to the site of injury in a TNF- $\alpha$ /CCL20-dependent mechanism and controls macrophage/monocyte recruitment via ILC3-dependent CCL3. Notch1 also induces epidermal production of IL23 which facilitates ILC3s to produce IL22 for re-epithelialization and skin repair.

**Epidermal Notch1 recruits innate lymphoid cells to orchestrate normal skin repair**

**Zhi Li**

**PhD**

**School of Biological and Biomedical Sciences**

**Durham University**

**March 2014**

## Table of Contents

List of Figures .....	8
List of Tables .....	12
List of Abbreviations .....	13
Statement of Copyright .....	16
Acknowledgments .....	16
Chapter 1 Introduction .....	17
1.1 Notch signalling .....	17
1.1.1 Background .....	17
1.1.2 Notch signalling facilitates cell-to-cell communication .....	17
1.1.3 Ligand endocytosis is required for Notch receptor activation .....	22
1.1.4 Anti-NRR1/NRR2 blocking antibodies target individual Notch receptor .....	27
1.2 Skin .....	28
1.2.1 Background .....	28
1.2.2 Epidermis is a self-renewing stratified epithelium with multiple lineages .....	29
1.2.3 Epidermal barrier protects from penetrance of microbes .....	34
1.2.4 Notch signalling in skin .....	36
1.3 Immune system in skin .....	47
1.3.1 Background .....	47
1.3.2 Origin, location and classification of immune cells .....	48
1.3.3 Major circulating immune cells accessible to skin .....	53
1.3.4 Entry of circulating immune cells into dermis .....	56
1.3.5 Skin resident immune sentinels .....	57

1.3.6 Notch signalling in skin immune system .....	58
1.4 Skin wound healing .....	58
1.4.1 Background .....	59
1.4.2 Mechanism of wound healing .....	59
1.4.3 The role of immune cells in wound closure .....	63
1.4.4 The role of innate lymphoid cells in epithelial repair .....	66
1.4.5 Notch signalling in wound healing .....	67
1.5 Hypothesis .....	71
Chapter 2 Methods .....	73
2.1 Research animals .....	73
2.2 Wound healing .....	75
2.3. HE staining and antibody labelling .....	78
2.4 Isolation of cells for flow cytometry .....	79
2.5 Antibody staining for flow cytometry .....	80
2.6 Protein extraction/ Western blotting .....	81
2.7 RNA extraction .....	81
2.8 Quantitative polymerase chain reaction (QPCR) .....	82
2.9 Primary dermal cells .....	83
2.10 Systems Biology Analysis of Gene Expression Data Sets .....	84
2.11 Statistical Analysis .....	84
Chapter 3 Involvement of immune cells in normal skin wound healing .....	86
3.1 Introduction .....	86
3.2 Results .....	87

3.2.1 Timing of the healing process of skin wound .....	87
3.2.2 Myeloid cells .....	91
3.2.3 T cells .....	107
3.2.4 B cells .....	114
3.2.5 NK cells .....	114
3.2.6 Innate lymphoid cells (ILCs) .....	122
3.3 Summary .....	133
Chapter 4 The function of Group 3 ILCs (ILC3s) in skin wound healing .....	138
4.1 Introduction .....	138
4.2 Results .....	139
4.2.1 ROR $\gamma$ <sup>-/-</sup> mice have poorly healed wounds partly due to delayed epidermal proliferation .....	139
4.2.2 CCL3 dependent monocyte/macrophage recruitment is delayed in wounded ROR $\gamma$ <sup>-/-</sup> back skin .....	142
4.2.3 Loss of ILC3s directly causes wound healing defect in ROR $\gamma$ <sup>-/-</sup> mice .....	145
4.2.4 ILC3s supply early IL-22 in skin wound healing .....	147
4.2.5 IL-23 from dendritic/Langerhans cells is required for IL-22 production in skin wounds .....	151
4.2.6 IL-23 is required for IL22-dependent epidermal proliferation but not for monocyte/macrophage recruitment .....	154
4.3 Summary .....	157

Chapter 5 Epidermal Notch1 signalling promotes skin wound healing through recruiting ILC3s .....	159
5.1 Introduction .....	159
5.2 Results .....	160
5.2.1 Skin injury activates epidermal Notch1 and Notch2 .....	161
5.2.2 Treating with anti-NRR1 and anti-NRR2 blocking antibodies specifically reduce Notch1 or Notch2 activity in wounded skin .....	164
5.2.3 Inhibiting Notch1 activity causes wound healing delay partly due to lack of early IL22.....	171
5.2.4 IL22-producing ILC3s are recruited to dermis in a Notch1-dependent manner .....	174
5.2.5 Recruitment of monocytes/macrophages, but not of neutrophils or dendritic/Langerhans cells, is dependent on epidermal Notch1 signalling .....	181
5.2.6 Notch1 signalling has no significant effect on NK cell recruitment .....	186
5.2.7 Epidermal Notch1 signalling may play a role in regulating maintenance of dendritic epidermal T cells.....	186
5.3 Summary .....	191
Chapter 6 Mechanism of how epidermal Notch1 regulate ILC3s .....	193
6.1 Introduction .....	193
6.2 Results .....	194

6.2.1 Epidermal Notch1 up-regulates cytokine and chemokine production, including TNF $\alpha$ , CCL20, CXCL13 and IL-23 .....	194
6.2.2 CXCL13 is not required for ILC3 recruitment .....	196
6.2.3 Notch regulated factor TNF $\alpha$ mediates ILC3 recruitment .....	196
6.2.4 TNF $\alpha$ regulates ILC3 recruitment by inducing CCL20 expression in dermal fibroblasts.....	198
6.2.5 Epidermal Notch1 signalling might activate Langerhans cells to secrete IL-23 that is required for ILC3s as well as dermal fibroblasts to produce IL-22.....	205
6.3 Summary .....	207
Chapter 7 Discussion .....	209
Bibliography .....	218



## List of Figures

Figure 1.1 The structures of Notch receptors and ligands .....	18
Figure 1.2 Cleavage sites in Notch receptor and its precursor .....	19
Figure 1.3 Recycling model for ligand endocytosis to activate Notch signalling.....	24
Figure 1.4 Pulling force model for ligand endocytosis and the downstream signalling after Notch activation .....	26
Figure 1.5 Epidermis is composed of hair follicles and interfollicular epidermis ....	30
Figure 1.6 Schematic diagram of human skin barrier .....	35
Figure 1.7 Sites of Notch activity in interfollicular epidermis and hair follicles in neonatal mice .....	38
Figure 1.8 The role of Notch signalling in regulating epidermal homeostasis .....	44
Figure 1.9 The vast majority of immune cells are derived from bone marrow hematopoietic stem cell in the presence of different soluble cytokines and growth factors .....	49
Figure 1.10 Schematics of normal skin wound healing .....	61
Figure 2.1 Ectopically activated Notch signalling in 4OHT treated K14NICDER mice .....	74
Figure 2.2 Surgical wounding model .....	76
Figure 2.3 Collection and frozen sectioning of skin wounds .....	77
Figure 3.1 Skin wound healing is initiated by immune response .....	89
Figure 3.2 Quantification of myeloid cells and dendritic/Langerhans cells in skin wounds .....	93

Figure 3.3 Dendritic cells are recruited into dermis in wound edges .....	95
Figure 3.4 Langerhans cells reside in epidermis and are replenished early following wound healing .....	99
Figure 3.5 Neutrophils are recruited into dermis in wound edges .....	101
Figure 3.6 Monocytes/Macrophages are recruited into dermis in wound edges.....	105
Figure 3.7 Quantification of T cell subsets in skin wounds .....	108
Figure 3.8 T cells reside in epidermis and rare dermis, and are replenished late following wounding .....	112
Figure 3.9 B cells are not involved in skin wound healing .....	115
Figure 3.10 NK cells are recruited early into wound site determined by flow cytometry .....	118
Figure 3.11 NKp46 <sup>+</sup> cells are hardly detectable in skin wound sections .....	120
Figure 3.12 The phenotypes of the vast majority of ROR $\gamma$ -expressing cells recruited in skin wounds are CD3 <sup>-</sup> CD4 <sup>dim to +</sup> CD127 <sup>dim to +</sup> CD117 <sup>-</sup> NKp46 <sup>-</sup> .....	124
Figure 3.13 Phenotypes of ROR $\gamma$ -expressing cells are confirmed by immunofluorescence chemistry on skin wound sections .....	128
Figure 3.14 ILC3s are recruited into dermis following wounding and are most abundant on day 5 post-wounding .....	131
Figure 3.15 Summary of inflammation response in skin wound healing .....	134
Figure 4.1 Skin wound healing in ROR $\gamma$ KO mice are delayed partly due to reduced epidermal proliferation .....	140
Figure 4.2 Macrophage recruitment is delayed in wounded ROR $\gamma$ <sup>-/-</sup> back skin .....	143
Figure 4.3 Loss of ILC3s directly causes wound healing defects .....	146
Figure 4.4 ILC3s are an important early source of IL22 .....	149

Figure 4.5 IL22 production is dependent on IL23 supplied mainly by dendritic/ Langerhans cells .....	152
Figure 4.6 IL23 is required for epidermal proliferation but not for macrophage/monocyte recruitment .....	155
Table 5.1 Epidermal Notch1 and Notch2 are activated upon skin injury .....	162
Figure 5.2 Systemic effects of anti-NRR1 and anti-NRR2 treatment .....	165
Figure 5.3 Epidermal Notch1 and Notch2 activities are reduced by anti-NRR1 or anti-NRR2 treatment .....	169
Figure 5.4 Inhibiting Notch1 activity delays wound closure .....	172
Figure 5.5 Inhibiting Notch1 blocks ILC3 recruitment following wounding .....	175
Figure 5.6 Ectopic activation of Notch1 receptor signaling promotes ILC3 recruitment into uninjured skin dermis .....	178
Figure 5.7 Inhibiting Notch1 activity dramatically reduces monocyte/ macrophage recruitment .....	182
Figure 5.8 Ectopic activation of epidermal Notch1 activity results in monocyte/macrophage recruitment in uninjured skin dermis, but has no evident effects on neutrophils or dendritic/Langerhans cells .....	184
Figure 5.9 Inhibiting Notch1 activity has no significant effects on NK cell recruitment .....	187
Figure 5.10 Ectopic activation of Notch1 activity causes the expansion of epidermal dendritic T cell .....	189
Figure 6.1 Ingenuity Pathway Analysis of secreted factors that can interact with receptors expressed on ILC3s .....	195

Figure 6.2 CXCL13 is not required for ILC recruitment into skin wound.....	197
Figure 6.3 Notch-regulated factor TNF $\alpha$ regulates ILC3 recruitment and activation.....	199
Figure 6.4 TNF $\alpha$ antagonist (Adalimumab) blocks Notch1-induced ILC3 recruitment.....	201
Figure 6.5 CCL20 are immediately produced in skin wounds and can be expressed by dermal fibroblasts after stimulation by TNF $\alpha$ .....	203
Figure 6.6 IL-22 can be produced by dermal fibroblasts after stimulation by TNF $\alpha$ .....	206
Figure 7.1 Notch1 orchestrates wound healing through control of Innate Lymphoid Cells (i.e. ILC3s) .....	217

## **List of Tables**

Table 1.1 Consequences of modulation of Notch signalling in epidermis .....	41
Table 1.2 Phenotypes and functions of immune cells residing in mouse skin in steady state .....	51
Table 1.3 Family of innate lymphoid cells (ILCs) in mouse .....	69
Table 7.1 Major cellular events of normal skin wound healing process .....	210

## List of Abbreviations

4OHT	4-hydroxytamoxifen
AKN	<u>A</u> n <u>k</u> yrin repeat
APC	<u>A</u> llo <u>ph</u> ycoc <u>ya</u> nin
APC-Cy7	<u>A</u> llo <u>ph</u> ycoc <u>ya</u> nin- <u>C</u> ya <u>n</u> ine <u>7</u>
BCR	<u>B</u> <u>c</u> ell <u>r</u> eceptor
BME	$\beta$ - <u>m</u> er <u>c</u> ap <u>t</u> o <u>e</u> thanol
cDC	Conventional dendritic cell
CR	<u>C</u> ysteine rich <u>d</u> omain
DAMP	<u>D</u> anger <u>a</u> ssociated <u>m</u> olecular <u>p</u> attern
DC	<u>D</u> endritic <u>c</u> ell
DETC	<u>D</u> endritic <u>e</u> pidermal <u>T</u> <u>c</u> ells
DMEM	Dulbecco's modified Eagle medium
DSL	<u>D</u> elta- <u>S</u> errate- <u>L</u> ag2 region
ECL	<u>E</u> nhanced <u>C</u> hemil <u>u</u> minescence
ECM	<u>E</u> xtrac <u>e</u> llular <u>m</u> atrix
EGF	<u>E</u> pidermal <u>g</u> rowth <u>f</u> actor
ELISA	<u>E</u> nzyme- <u>l</u> inked <u>i</u> mmuno <u>s</u> orbent <u>a</u> ssay
FAM	<u>F</u> luorescein <u>A</u> midite
FCS	<u>F</u> etal <u>c</u> alf <u>s</u> erum
GSI	$\gamma$ - <u>s</u> ecretase <u>i</u> nhibitor
HD	<u>H</u> eterodimerization <u>d</u> omains
HE	<u>H</u> ematoxylin and <u>e</u> osin
Hes	<u>H</u> airy and <u>e</u> nhancer of <u>s</u> plit
HF	<u>H</u> air <u>f</u> ollicles

HRP	<u>H</u> or <u>s</u> er <u>a</u> dish <u>p</u> eroxidase
IFE	<u>I</u> nter <u>f</u> ollicular <u>e</u> pidermis
IFN	Interferon
IL	<u>I</u> nter <u>l</u> eukin
ILCs	<u>I</u> nnate <u>l</u> ymphoid <u>c</u> ells
ILC3	Group <u>3</u> innate lymphoid <u>c</u> ells, also known as ROR $\gamma^+$ ILCs
<i>i.p.</i>	<u>I</u> ntra <u>p</u> eritoneal
IRS	<u>I</u> nn <u>e</u> r <u>r</u> ooter <u>s</u> heath
K	<u>K</u> eratin
KGF	<u>K</u> eratinocyte growth <u>f</u> actor
LC	<u>L</u> angerhans <u>c</u> ell
LNRs	<u>L</u> in12- <u>N</u> otch <u>r</u> epeats
MAML	<u>M</u> aster <u>m</u> ind- <u>l</u> ike
MIP	<u>M</u> acrophage <u>i</u> nflammatory <u>p</u> rotein
NCR	<u>N</u> atural <u>c</u> ytotoxicity triggering <u>r</u> eceptor
NECD	<u>N</u> otch <u>e</u> xtracellular <u>d</u> omain
NICD	<u>N</u> otch <u>i</u> ntracellular <u>d</u> omain
NK	<u>N</u> atural <u>k</u> iller cells
NKT	<u>N</u> atural <u>k</u> iller-like <u>T</u> cells
NRR	<u>N</u> otch negative <u>r</u> egulatory <u>r</u> egion
OCT	Optimal cutting temperature compound
ORS	<u>O</u> uter <u>r</u> ooter <u>s</u> heath
PAMP	<u>P</u> athogen <u>a</u> ssociated <u>m</u> olecular <u>p</u> attern
PE	<u>P</u> hyco <u>e</u> rythrin
PEST	Domain rich in proline, <u>a</u> spartic acid, <u>s</u> erine and <u>t</u> hreonine residues

PRRs	<u>P</u> attern <u>r</u> ecognition <u>r</u> eceptor
PVDF	<u>P</u> oly <u>v</u> inylidene <u>d</u> ifluoride
RAM	<u>R</u> BP- <u>J</u> $\kappa$ <u>a</u> ssociated <u>m</u> olecule
RBP-J $\kappa$	<u>R</u> ecombination signal sequence <u>b</u> inding <u>p</u> rotein <u>J</u> $\kappa$
RIPA	<u>R</u> adio- <u>i</u> mmunoprecipitation <u>a</u> ssay
RPMI	<u>R</u> oswell <u>P</u> ark <u>M</u> emorial <u>I</u> nstitute
SEM	<u>S</u> tandard <u>e</u> rror of the <u>m</u> ean
SG	<u>S</u> ebaceous gland
Tc	<u>C</u> ytotoxic <u>T</u> cells
TCR	<u>T</u> cell <u>r</u> eceptor
TGF- $\beta$	<u>T</u> ransforming growth factor <u><math>\beta</math></u>
Th	<u>T</u> helper cells
TNF- $\alpha$	<u>T</u> umor <u>n</u> ecrosis <u>f</u> actor- <u><math>\alpha</math></u>



### **Statement of Copyright**

The copyright of this thesis rests with the author. No quotation from it should be published without the author's prior written consent and information derived from it should be acknowledged.

### **Acknowledgements**

I am grateful to my supervisor, Dr. Carrie Ambler for expert advice on experiment design, data analysis and time management. I wish to thank Dr. Mark Coles at York University for great support on immunological aspects. I also would like to thank Dr. Ian Cummins, Miss Rebecca Lamb and Mrs Soulmaz Boroumand for their efforts and cooperation to produce some data. Work was funded by the British Skin Foundation.

## **Chapter 1 Introduction**

### **1.1 Notch Signalling**

#### **1.1.1 Background**

The Notch gene was first discovered 100 years ago in fruit fly, *Drosophila Melanogaster* (Dexter, 1914). Mutant Notch gene has a distinct phenotype of ‘notched’ wing tips during embryonic development (Dexter, 1914). Since that first discovery, it has become clear that Notch, as an evolutionary conserved gene, plays a key role in a range of developmental processes (Bray 2006; Penton et al., 2012; Watt et al., 2008). However, the implication of Notch in human development and disease was not revealed until early 1990s when a gain-of-function mutation in human Notch1 gene was reported to cause T-cell acute lymphoblastic leukaemia (Ellisen et al., 1991). Since that first link to human diseases, mutations of Notch family genes have now been related to a wide spectrum of diseases and cancers (Louvi and Artavanis-Tsakonas, 2012; Penton et al., 2012). The aim of this thesis is to define the role of Notch in skin wound healing particularly in respect to the regulation of immune cell recruitment and function.

#### **1.1.2 Notch signalling facilitates cell-to-cell communication**

Notch signalling is named after Notch and is essential for communication and interaction between different cells expressing a Notch gene encoded receptor and its ligand respectively at cell surface (Chiba 2006, Fortini 2009; Musse et al., 2012). In mammals there are four Notch (receptors), Notch1-4, with similar protein structures (Figure 1.1) (Chiba 2006; Musse et al., 2012). In Golgi apparatus Notch protein precursor undergoes post translational modification involving two events: the S1 cleavage (Figure 1.2) mediated by furin like convertase to form a heterodimer in

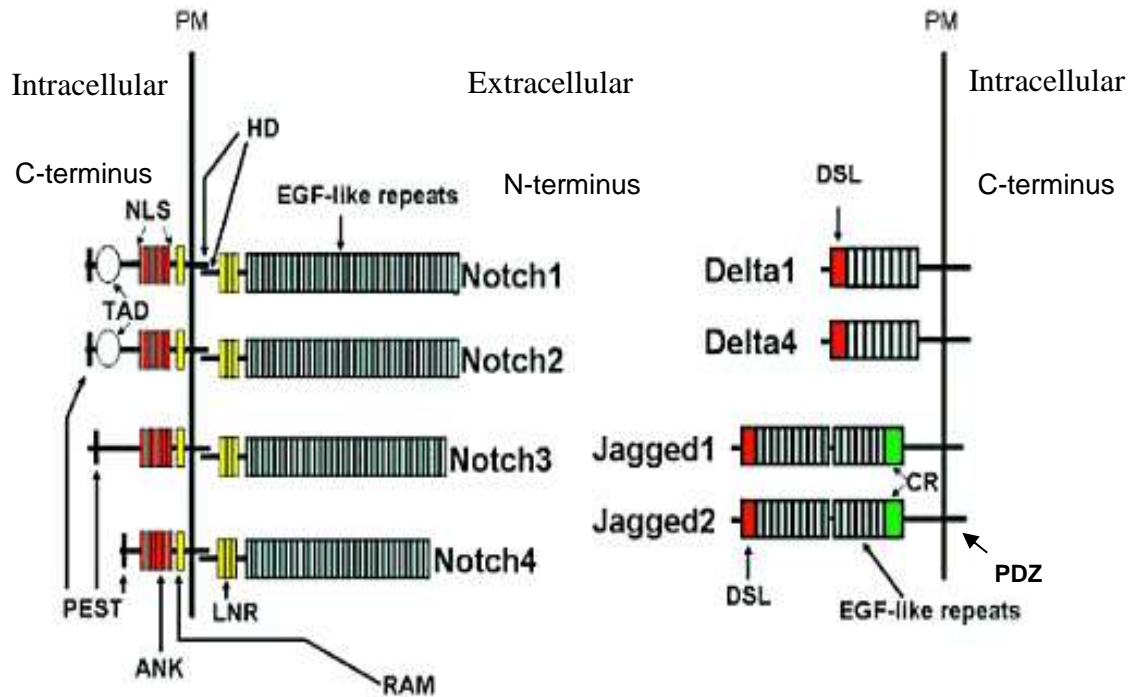


**Figure 1.1 The structures of Notch receptors and ligands** (Modified from Shigeru Chiba, 2006). There are 36 EGF-like repeats in Notch1 and Notch2, 34 repeats in Notch3, 29 repeats in Notch4, 16 repeats in Jagged1 and Jagged2, and 5-9 repeats in Delta1 and Delta4. LNR and HD form negative regulatory region (NRR). Ligand binding site is located in EGF-like repeats 11 and 12. ANK, ankyrin repeat; CR, cysteine-rich repeat; DSL, Delta-Serrate-Lag2 domain; EGF, epidermal growth factor; HD, heterodimerization domain; LNR, Lin12-Notch repeat; NLS, nuclear localization signal; PEST, rich in proline, aspartic acid, serine and threonine residues; PM, plasma membrane; RAM, RBP-Jk associated molecule; TAD, transactivation domain.

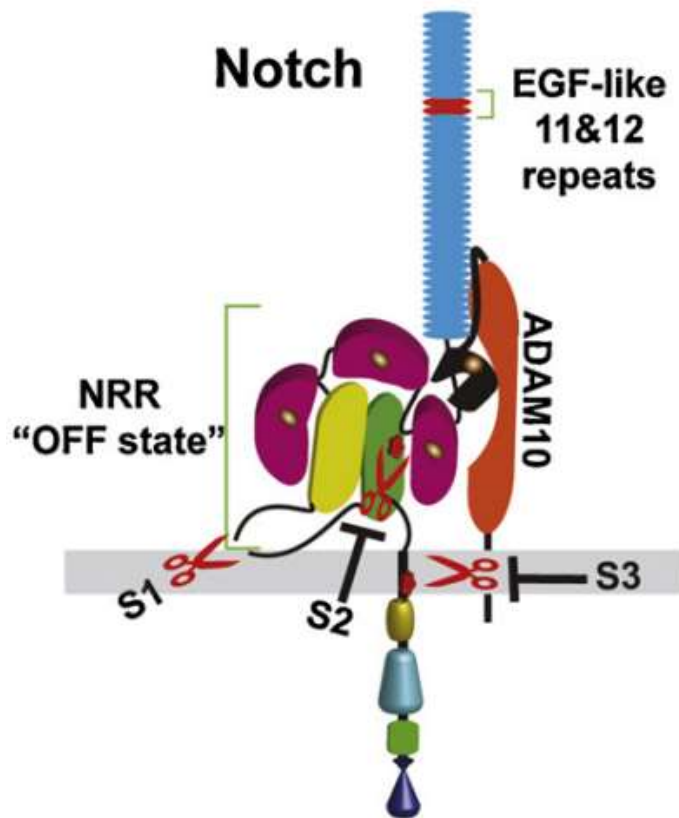


**Figure 1.2 Cleavage sites in Notch receptor and its precursor** (Adapted from Musse et al., 2012). Mature transmembrane Notch protein is a heterodimer formed by furin cleavage at S1 site between N-terminal HD (yellow) and C-terminal HD (green) in Notch extracellular domain during post translational modification. Metalloproteinase ADAM10 mediated cleavage S2 site is located within C-terminal HD and is buried deep by Notch NRR (negative regulatory region) domain in which three Notch12-Lin repeats (NLR) (purple) are conformationally compacted and wrap over HD to keep Notch inactivated ‘OFF state’ in the absence of ligand. The S3 cleavage occurs in Notch intra-membrane domain and requires the substrate produced by S2 cleavage. The ligand binding site containing EGF (epidermal growth factor) like repeats 11 and 12 is indicated in red.

which cleaved N-terminal and C-terminal fragments remain stably associated through multiple non-covalent interactions between their heterodimerization domains (HD) HD-N and HD-C, and Fringe N-acetylglucosamine transferase mediated glycosylation that regulates the intensity of Notch signalling through altering the Notch binding affinity for ligand (Chillakuri et al., 2012; Fortini 2009; Musse et al., 2012). Then mature Notch receptor is transported and tethered to cell membrane (Chillakui et al., 2012; Fortini 2009; Musse et al., 2012). Upon binding to one of its ligands through epidermal growth factor (EGF) like repeats 11 and 12 in Notch extracellular domain, Notch undergoes sequential S2 and S3 proteolysis cleavages mediated by metalloproteinase ADAM10 and  $\gamma$ -secretase respectively (Figure 1.2) (Musse et al., 2012). In unbound receptors, the S2 cleavage is blocked by highly compacted and folded Lin12-Notch repeats (LNRs) in Notch negative regulatory region (NRR) (Figure 1.2) (Musse et al., 2012). The ligand binding stimulates a conformational change in NRR to expose the S2 site to ADAM10-mediated cleavage which then permits S3 cleavage within Notch intra-membrane domain by providing a substrate for the  $\gamma$ -secretase enzyme catalysis (Musse et al., 2012; Watt et al., 2008). Following S3 cleavage, Notch intracellular domain (NICD) is subsequently released from cell membrane and translocated into nucleus where NICD interacts with a DNA binding protein, recombination signal sequence binding protein J $\kappa$  (RBP-J $\kappa$ , also known as CSL), and a co-activator, Mastermind-like (MAML), through its RBP-J $\kappa$  associated molecule (RAM) and ankyrin repeat (AKN) domain respectively (Figure1.1) to directly activate transcription of Notch target genes (Ambler and Watt, 2010; Chilarkuri et al., 2012; Iso et al., 2003; Watt et al., 2008). Notch target genes typically include basic helix-loop-helix family, such as Hes and Hey genes which encode transcriptional factors that in turn influence cell

fate and differentiation (Guruharsha et al., 2012; Kageyama et al., 2007, Watt et al., 2008). Similar to other short-life intracellular proteins, the turnover of the NICD is controlled by C-terminal PEST domain, rich in proline, aspartic acid, serine and threonine residues, which induces NICD degradation via ubiquitin/proteasome mechanism to stop Notch signalling when not in need (Chillakuri et al., 2012; Spencer et al., 2004).

Similar to Notch receptors, canonical Notch ligands are also membrane-bound proteins containing EGF like repeats in the extracellular domain (Figure 1.1). Adjacent to the EGF like repeats is Notch-binding site Delta-Serrate-Lag2 (DSL) region. The intracellular PDZ domain has a role in promoting cell adhesion and inhibiting cell motility (Chillakuri et al., 2012). Notch ligands are divided into two families namely Jagged (Jag, also known as Serrate) and Delta (also known as Delta like, DLL), which are distinguished from each other by the presence or absence of a cysteine rich (CR) domain (Figure 1.1). At least 5 Notch ligands, Jagged1, Jagged2, Delta1, Delta3 and Delta4 have been detected in mammals (Musse et al., 2012).

Notch and its ligands are both bound to cell membrane, thus Notch is involved in cell-to-cell communication and interaction. The most pronounced function of this interaction is to regulate cell fate decision (Blanpain et al., 2006; Moriyama et al., 2008; Watt et al., 2008). However, new evidence suggests that Notch controls expression and activities of growth factors and cytokines, such as tumor necrosis factor- $\alpha$  (TNF- $\alpha$ ), which facilitates communication between different cell types beyond immediate contact, for instance between epithelial cells and immune cells (Ambler and Watt, 2010). Furthermore, recent studies have shown that Notch

activation up-regulates Jagged1 expression in signal-receiving cell via nuclear factor  $\text{N}\kappa\text{B}$  or P63 pathway, which in turn relay and amplify Notch signaling from cell to cell (Ambler and Watt, 2010; Foldi et al., 2010; Ross and Kadesch, 2004).

In conclusion, Notch, as a family of evolutionary conserved gene, has been linked to a range of developmental processes and human diseases (Louvi and Artavanis-Tsakonas, 2012). Notch signaling activation in Notch-expressing cells is dependent on ligand-induced NRR conformational change that permits a series of proteolysis cleavages in Notch extracellular domain and intra-membrane domain followed by release of NICD to activate transcription of target genes and a signaling cascade in nucleus (Chillakui et al., 2012; Musse et al., 2012). Notch and its ligands are both bound to cell membrane, thus Notch is involved in cell-to-cell communication and interaction. Notch also controls expression and activity of several growth factors and cytokines, such as  $\text{TNF-}\alpha$  (Ambler and Watt, 2010).

### **1.1.3 Ligand endocytosis is required for Notch receptor activation**

Similar to other membrane-bound proteins, the surface level of Notch receptors and ligands are maintained appropriately through ubiquitylation-dependent endocytotic degradation in order to prevent over-activation of Notch signaling (Weinmaster and Fischer, 2011). In mammals, ubiquitin ligases Itch/AIP4 and Neur have been found to promote constant endocytosis of Notch receptor and ligand respectively (Chastagner et al., 2008; Lai et al., 2001). By contrast, recent studies have suggested particular ligand endocytosis is critically required for activating ligand-induced NRR conformational change rather than limiting Notch signaling (Chen et al., 2009; Nichols et al., 2007; Wang and Struhl, 2005). They found either genetic ablation of

endosomal pathway components that are known to participate in ligand internalization, such as dynamin, epsin and clathrin, or deletion of ligand intracellular domain that contains ubiquitin ligase binding sites and nuclear localization signal, resulted in accumulation of ligands on cell surface as expected, but failure in sending a signal to Notch-expressing cells (Chen et al., 2009; Nichols et al., 2007; Wang and Struhl, 2005). This signaling-specific endocytosis of ligand is thought to be unique to Notch signaling (Weinmaster and Fischer, 2011) and requires a specific ubiquitin ligase Mib distinct from Neur which down-regulates surface ligand level through constitutive ligand endocytosis (Wang and Struhl, 2005). The underlying mechanism is not completely understood, however, two models involving ligand recycling and pulling force have been proposed in order to explain how ligand endocytosis in signal sending cells promotes Notch activation.

The recycling model is based on the finding that recycling proteins such as Rab11 and Sec15 which are known to promote membrane-bound protein to traffic back to cell surface through endocytosis and exocytosis have been detected in some ligand-expressing cells and deletion of these recycling proteins in ligand cells led to failure in Notch activation (Emery et al., 2005; Jafar-Nejad et al., 2005). This model (Figure 1.3) hypothesizes that the Notch ligand initially transported to cell membrane may not be able to physically bind to Notch receptor in an adjacent cell due to the poor position of ligand against receptor, therefore dislocation of ligand into a specific microdomain may be required through Rab11 and Sec15 dependent ligand recycling to juxtapose ligand to Notch receptor before they can bind to each other (Benhra et al., 2010; Musse et al., 2012; Rajan et al., 2009; Weinmaster and Fischer, 2011). However, this proposed recycling model may only apply to polarized cells such as



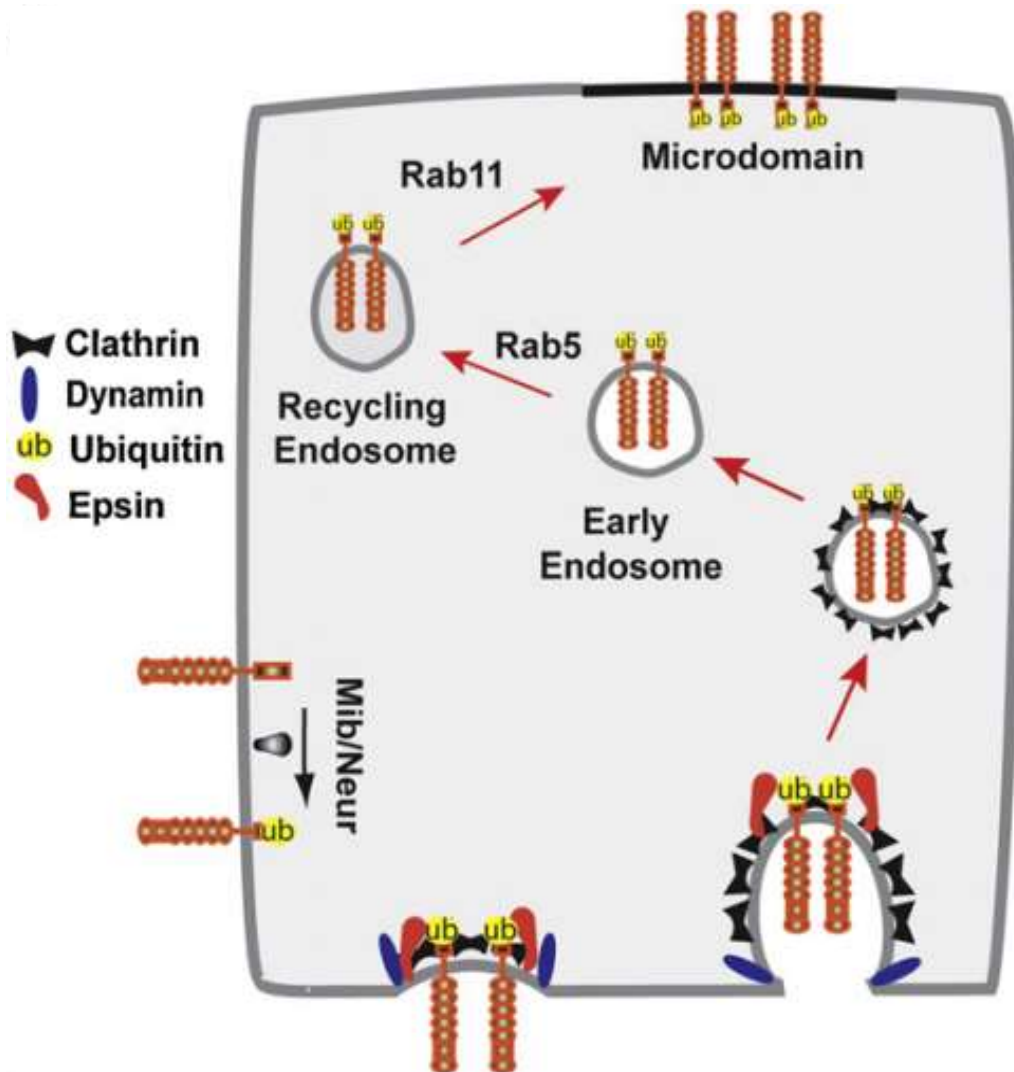


**Figure 1.3 Recycling model for ligand endocytosis to activate Notch signaling** (Reproduced from Musse et al, 2012). The recycling model proposes ligand initially delivered to the cell surface is ubiquitylated (Ub) by E3 ubiquitin ligase Mindbomb (Mib) alone in mammals or Mib together with Neurlized (Neur) in drosophila which facilitates interactions with the endocytic adapter epsin, GTPase dynamin and vesicle coating protein clathrin to promote ligand endocytosis. Following internalization, ligand enters recycling endosome and traffics back a cell surface microdomain which supplies a better position for ligand to bind Notch receptor in adjacent cell.

epithelial cells since Rab11 is not required to activate Notch signaling in some other types of cells (Windler and Bilder, 2010). It is also believed by some researchers that Notch ligand might require further processing through recycling to become a more competent ligand with higher binding affinity for Notch, however, such an active form of ligand has yet to be identified (Weinmaster and Fischer, 2011).

In contrast, the pulling force model (Figure 1.4) proposes ligand-Notch binding alone may not be sufficient to induce NRR conformational change that relieves the repression of S2 cleavage, and additional force may be required to pull LNR away from HD. This mechanical force could be generated by ligand endocytosis, and could invaginate cell membrane and pull ligand back into signal-sending cell during endosome formation. Since the fringe-enhanced binding between Notch receptor and ligand is strong enough, this force may unfold, stretch and pull the whole ligand-receptor complex towards signal-sending cell and thus expose S2 site for ADAM10-mediated cleavage. (Liu et al., 2010; Musse et al., 2012; Nichols et al., 2007; Parks et al., 2000; Weinmaster et al., 2011). This model was first raised by Parks et al. (2000) who detected co-localization of Delta and NECD in endosomes of Delta-expressing drosophila imaginal disc cells. It was supported by a more recent study in which ligand with endocytic defects was still able to physically bind to Notch, but failed to induce Notch signaling (Gordon et al., 2008, Nichols et al., 2007).

In summary, the surface level of Notch receptor and ligand and subsequent Notch activity are regulated by ubiquitylation-dependent constitutive endocytosis that induces protein degradation (Weinmaster and Fischer, 2011). Notch activation requires specific ligand endocytosis which may either dislocate ligand to a better

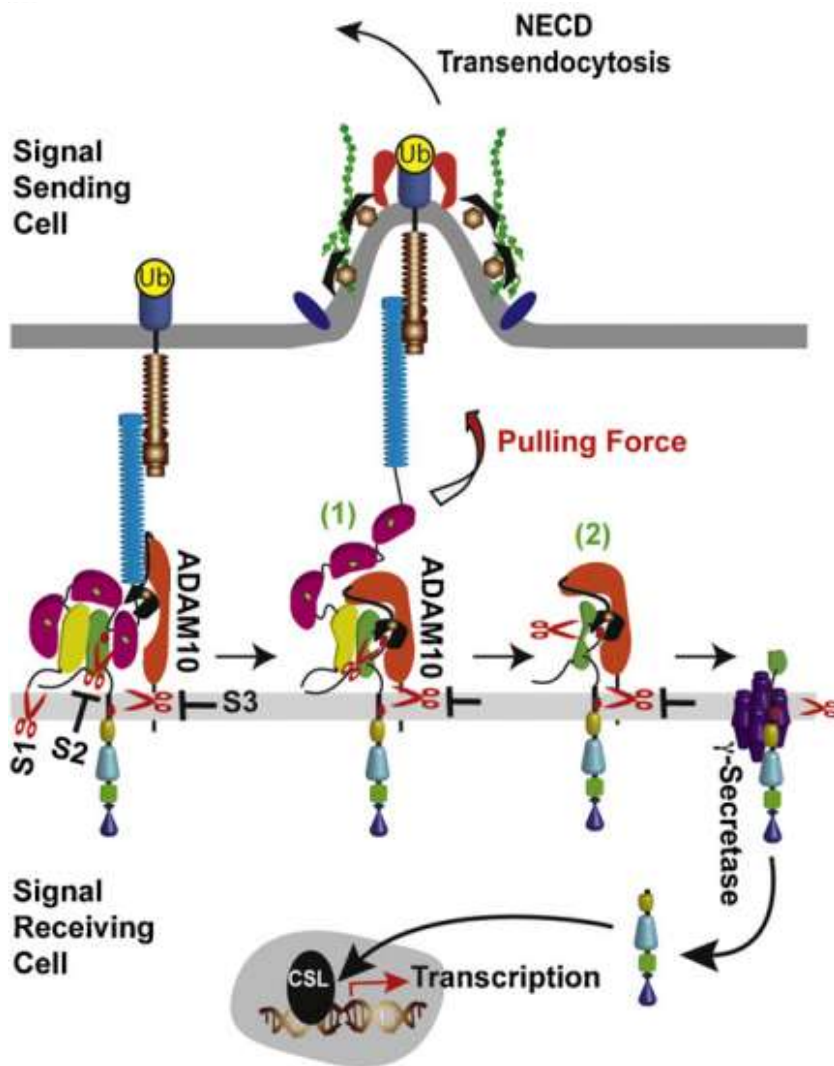


**Figure 1.4 Pulling force model for ligand endocytosis and the downstream signaling after Notch activation** (Adapted from Musse et al., 2012). Pulling force generated by endocytosis of Notch-bound ligand pulls the LNR modules (purple) away from HDs (yellow and green) to directly expose S2 site in N-terminal HD (green) (1). Alternatively, this force unfolds HD structure and induces HD physical dissociation thereby removing N-terminal fragment from intact Notch dimer prior to S2 cleavage (2). In both cases NRR domain is targeted to expose S2 site in the remaining membrane bound Notch receptor for ADAM10 cleavage which directly generates a substrate for  $\gamma$ -secretase S3 cleavage. After proteolysis NICD is released and translocated into nucleus to bind CSL (also known as RBP-Jk) and co-regulator MAML to activate transcription of target genes.

position for binding Notch or provide pulling force for inducing NRR conformational change (Musse et al, 2012).

#### **1.1.4 Anti-NRR1/ NRR2 blocking antibodies target individual Notch receptor**

Since gain-of-function mutations in Notch receptor are implicated in a number of diseases and cancers, most notably T-cell acute lymphoblastic leukaemia, the current exploration of therapeutic drugs for altering Notch signaling is focusing on how to block Notch signaling, ideally to block activation of individual Notch receptor (Groth and Fortini, 2012). Researchers were formerly interested in  $\gamma$ -secretase inhibitor (GSI) which represses  $\gamma$ -secretase mediated events including the S3 cleavage of Notch, since a small number of GSIs, such as LY450139 invented by Eli Lilly, had entered phase III clinical trial for treating Alzheimer's Disease by preventing the proteolysis of amyloid precursor protein into pathogenic amyloid plaques (Lanz et al., 2006; Tolia and De Strooper, 2009). However, all of these GSIs resulted in serious gastrointestinal toxicity and immune system defects owing to pan-inhibition of all Notch receptors and possibly other  $\gamma$ -secretase-involved pathways (Groth and Fortini, 2012). More recently, the development by Genotech of individual Notch1 and Notch2 blocking antibodies, anti-NRR1 and anti-NRR2, are favoured and promising due to increased specificity and reduced side effects (Wu et al., 2010). These individual blocking antibodies stabilize the compacted conformation of NRR1 or NRR2 and maintain the 'off' status of Notch1 or Notch2 even when they are bound to a ligand (Wu et al., 2010).

In summary, Notch is involved in a range of developmental processes and human diseases through cell-to-cell interaction (Bray 2006; Louvi and Artavanis-Tsakonas,

2010; Penton et al., 2012). Notch activation requires ligand endocytosis-dependent NRR conformational change which permits proteolysis cleavages and subsequently releases NICD (Musse et al., 2012). This activated form of Notch then translocates into nucleus to activate target gene transcription and a signaling cascade that usually functions to regulate cell fate decision (Bray 2006). Notch also controls expression and activity of growth factors and cytokines, such as TNF- $\alpha$  (Ambler and Watt, 2010). Recently, new therapy for blocking Notch signaling has been developed by using anti-NRR1 or anti-NRR2 antibody to target individual Notch1 or Notch2 receptors with high specificity and reduced side effects (Wu et al., 2010).

## **1.2 Skin**

### **1. 2.1 Background**

The outer surface of our body is covered by skin which is composed of epidermal epithelium tissue and underlying dermal connective tissue. Skin as a physical barrier provides first-line defence against chemical insults and microbial penetrance from outside environment, and prevents excess loss of water and water-soluble salts from inner body (Baroni et al., 2012; Fuchs, 2007). The skin color is rendered by melanocytes located in epidermis via releasing pigment granules to keratinocytes to help protect cell nucleus from ultraviolet radiation such as sunshine (Baroni et al., 2012). The sense of touch and other sensations are provided by epidermal Merkel cells which are connected with enriched nervous endings in dermis (Baroni et al., 2012). The tensile strength of skin is supplied by dermal myofibroblasts which are differentiated from dermal fibroblasts to produce components of extracellular matrix (ECM) such as collagen and elastic fibres (Baroni et al., 2012). The nutrients are supplied by blood capillaries distributed in dermis. In this section, I will focus on the

development and maintenance of epidermal lineages, and the properties of epidermal barrier.

### **1.2.2 Epidermis is a self-renewing stratified epithelium with multiple lineages**

Epidermis is a self-renewing stratified epithelium with multiple lineages including interfollicular epidermis (IFE) and its specialized appendages, such as hair follicles (HF) and associated sebaceous gland (SG) and sweat gland (Fuchs, 2007) (Figure 1.5a). During embryogenesis these lineages are all differentiated from a single epithelium (Fuchs, 2007). Invagination and down-growth of regularly spaced epithelium form hair follicles which are in charge of producing hairs (Alonso and Fuchs, 2006; Fuchs, 2007). Inside hair follicles, sebaceous and sweat glands are developed for producing oil-filled sebocytes and sweat (Ambler and Määttä, 2009). The remaining epidermis, namely interfollicular epidermis, undergoes cornification and stratification into several layers populated by cells with differential status of differentiation to form a permeability barrier at body surface for tackling the potential risks of excess water loss and penetrance of microbes and chemicals from outside environment throughout postnatal life (Ambler and Määttä, 2009; Fuchs, 2007; Segre, 2006).

Once established epidermal lineages are physiologically maintained by their own epidermal stem cells or progenitor cells located in distinct compartments to supply the needed cells through proliferation followed by terminal differentiation (Ambler and Määttä, 2009; Fuchs, 2007; Fuchs, 2008; Lechler and Fuchs, 2005; Plikus et al., 2012; Watt et al., 2006). The final products of terminal differentiation, such as hairs and corneocytes, undergo apoptosis after a limited lifespan and shed from our body

a

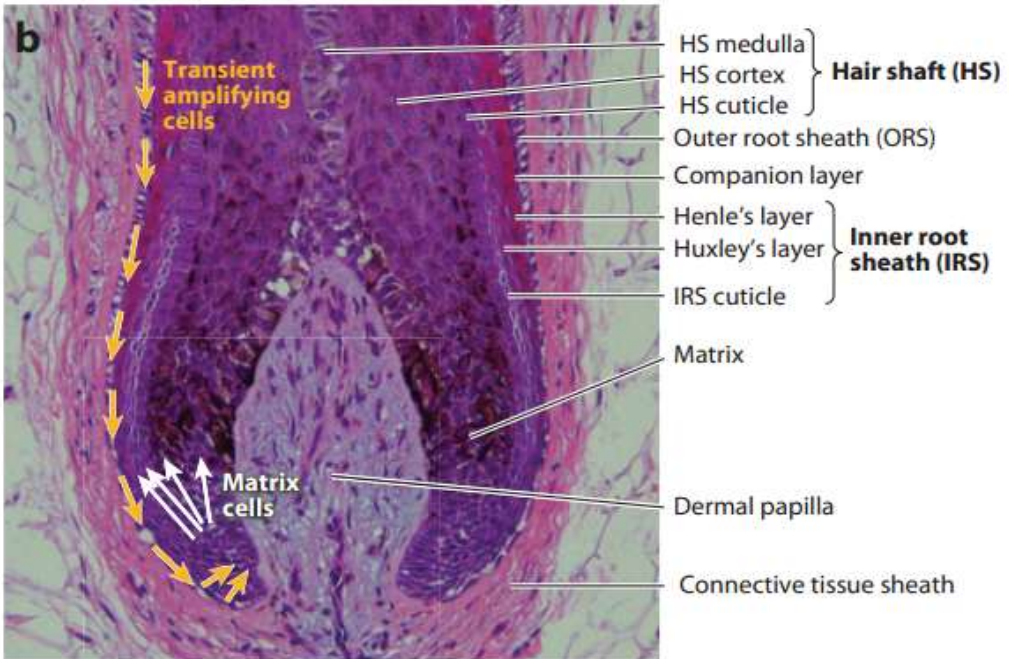
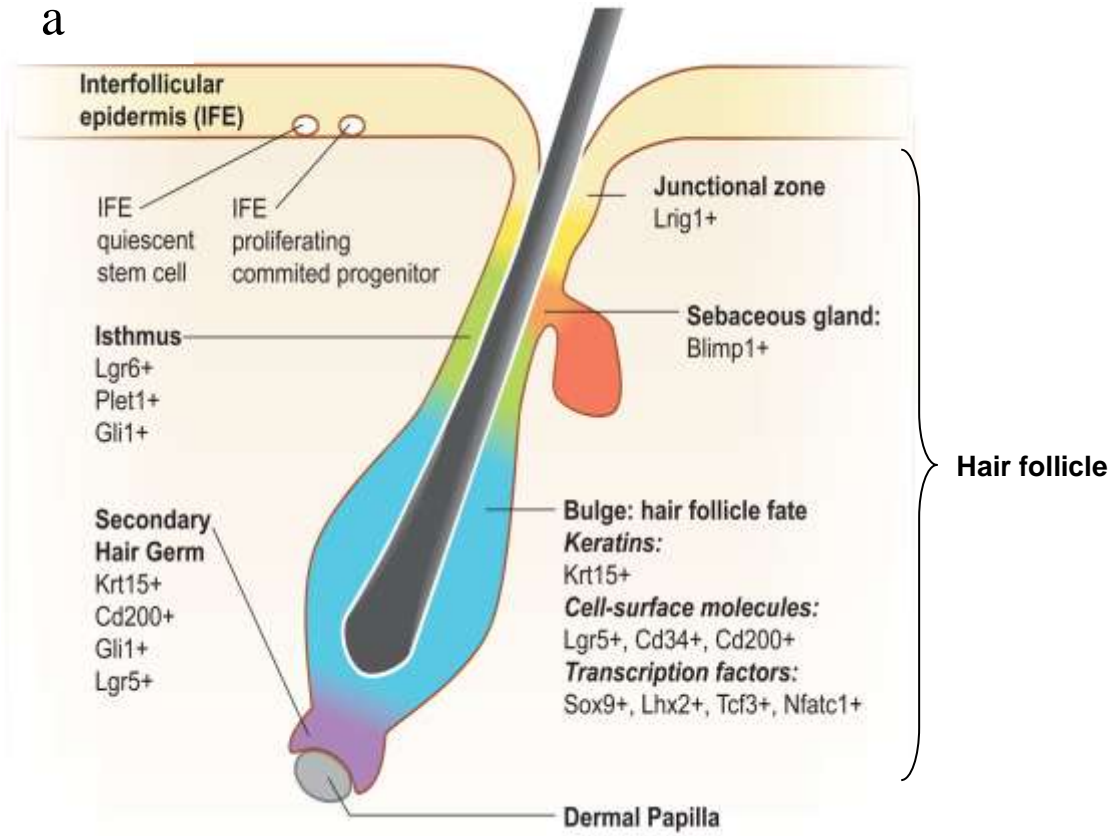


**Figure 1.5 Epidermis is composed of hair follicles and interfollicular epidermis**

(Adapted from Plikus et al., 2012; Shimomura and Christinano, 2010) (a) Schematic diagram illustrating anagen hair follicle (HF), interfollicular epidermis (IFE) and distinct epidermal stem cell populations. (b) Hematoxylin and eosin staining of bulb portion of human anagen HF. Transient amplifying cells derived from the bulge stem cells migrate to the matrix region (orange arrows) through outer root sheath (ORS). The matrix cells then differentiate into hair shaft (HS) and inner root sheath (IRS) layers of the HF (white arrows). The bulge stem cell also has the potential to form IFE.



to maintain homeostasis of epidermis.

The predominant cell type in interfollicular epidermis is keratinocytes which are continuously replenished by IFE stem cells or progenitor cells in basal layer in adult homeostatic epidermis (Figure 1.5a) (Ambler and Määttä, 2009; Fuchs, 2007; Ito et al., 2005; Levi et al., 2005; Plikus et al., 2012). The currently favoured model proposes a proliferation-active basal cell divides into two daughter cells, one of which remains as progenitor cell in basal layer while the other one proceed with further rounds of divisions as a transient amplifying progenitor before committing terminal differentiation (Ambler and Määttä, 2009; Fuchs et al., 2008; Plikus et al., 2012; Watt et al., 2006). This terminal differentiation involves withdrawal from cell division cycle, detachment from basement membrane, move outwards through spinous layer, granular layer and cornified layer while switching gene expression and finally production of a keratin-filled dead keratinocyte (corneocyte) in cornified layer (Ambler and Määttä, 2009; Fuchs et al., 2008; Watt et al., 2006). In healthy adults, a homeostasis is achieved to maintain normal thickness and function of IFE, in which only a small proportion (around 15%) of basal cells (Blanpain et al., 2006) are active at a time to regularly replace the older keratinocytes in interfollicular epidermis, which takes 4 weeks in human throughout life, while the remaining basal cells are resting or quiescent (Ambler and Määttä, 2009; Segre, 2006; Watt et al., 2008). However, a larger number and more variety of epidermal stem cells localized in interfollicular epidermis as well as in hair follicles (e.g. bulge, isthmus and junctional zone) (Figure 1.5a) will be activated for re-epithelialization under certain circumstances, e.g. post injury (Ambler and Määttä, 2009; Blanpain et al., 2006a; Plikus et al., 2012).

Adult hair follicle composes of three concentric layers, outer rooter sheath (ORS), inner rooter sheath (IRS) and the final product hair shaft (HS) (Figure 1.5b) (Pan et al., 2004; Shimomura and Christinano, 2010). Hair follicle stem or progenitor cells were first found in bulge area (Cotsarelis et al., 1990), a protruding structure in the upper portion of ORS that is contiguous with IFE basal layer (Ambler and Määttä, 2009). Bulge progenitor cells produce transient amplifying cells that migrate to the matrix of HF through ORS and differentiate into IRS and HF (Ambler and Määttä, 2009; Shimomura and Christinano, 2010). Recently, distinct hair follicle stem cell populations have also been found in other areas of hair follicles, e.g. isthmus and junctional zone (Plikus et al., 2012). Unlike IFE terminal differentiation which is continuous, existing hair follicles undergo cycles of growing (anagen), repressing (catagen) and resting (telogen) phases, in which the upper portion of ORS including bulge is permanent while the rest of ORS and entire IRS and HS are degraded and replaced by new hair follicles (Alonso and Fuchs, 2006). Catagen is the transition from anagen to telogen, which is accompanied by skin color changes from the dark gray to black of anagen to pale pink by telogen in pigmented mice (Alonso and Fuchs, 2006). Catagen is very short, lasts only 3 or 4 days in mice, while anagen and telogen usually last 2 or 3 weeks (Alonso and Fuchs, 2006; Oh and Smart, 1996). A collection of studies have suggested that the progenies of hair follicle stem cells also contribute to re-epithelialization of interfollicular epidermis by migrating towards the centre of the wounds (Ansell et al., 2011; Langton et al., 2008; Plikus et al., 2012). Bulge stem cells from peri-wound hair follicles contribute to wound repair transiently in early stage particularly during anagen (Ansell et al., 2011; Ito et al., 2005), while a long-term role of isthmus and junctional zone stem cells in providing

additional interfollicular epidermal cells during wound repair has been observed (Langton et al., 2008; Ito and Cotsarelis, 2008; Plikus et al., 2012).

### **1.2.3 Epidermal barrier protects from penetrance of microbes**

The cornified layer of IFE constitutes the primary barrier of skin that prevents penetrance of microbes and water-soluble molecules (Figure 1.6) (Segre, 2006). In cornified layer, keratinocytes undergo profound changes in their cell structures including losing nucleus and organelles (Baroni et al., 2012). Subsequently, the entire intracellular space is filled by structure proteins, predominantly keratins, which are continuously synthesized by keratinocytes and accumulated in cytoplasm during terminal differentiation (Baroni et al., 2012). The abundant keratin filaments are encased and supported by cornified envelopes formed by the other structure proteins, which provide a durable stress-resistant framework for corneocytes (Baroni et al., 2012). The individual corneocytes are held together by lipids which are produced by keratinocytes, stored in lamellar bodies in spinous and granular layer and finally extruded into intercellular space in cornified layer (Baroni et al., 2012). As a consequence, the primary skin barrier is now built like a wall, with protein-enriched corneocytes resembling the bricks and lipid-enriched intercellular media mimicking the cements (Baroni et al., 2012; Fuchs, 2007, Segre, 2006)

In addition to preventing microbial penetrance by acting as a physical barrier, epidermis constitutively expresses low level of antimicrobial peptides, such as  $\beta$ -defensins-1, which directly inhibit colonization of a wide spectrum of microbes by disrupting their phospholipid bilayer membrane in a way similar to antibiotics (Afshar and Gallo, 2013; Niyangsaba et al., 2007). In normal skin in steady state,

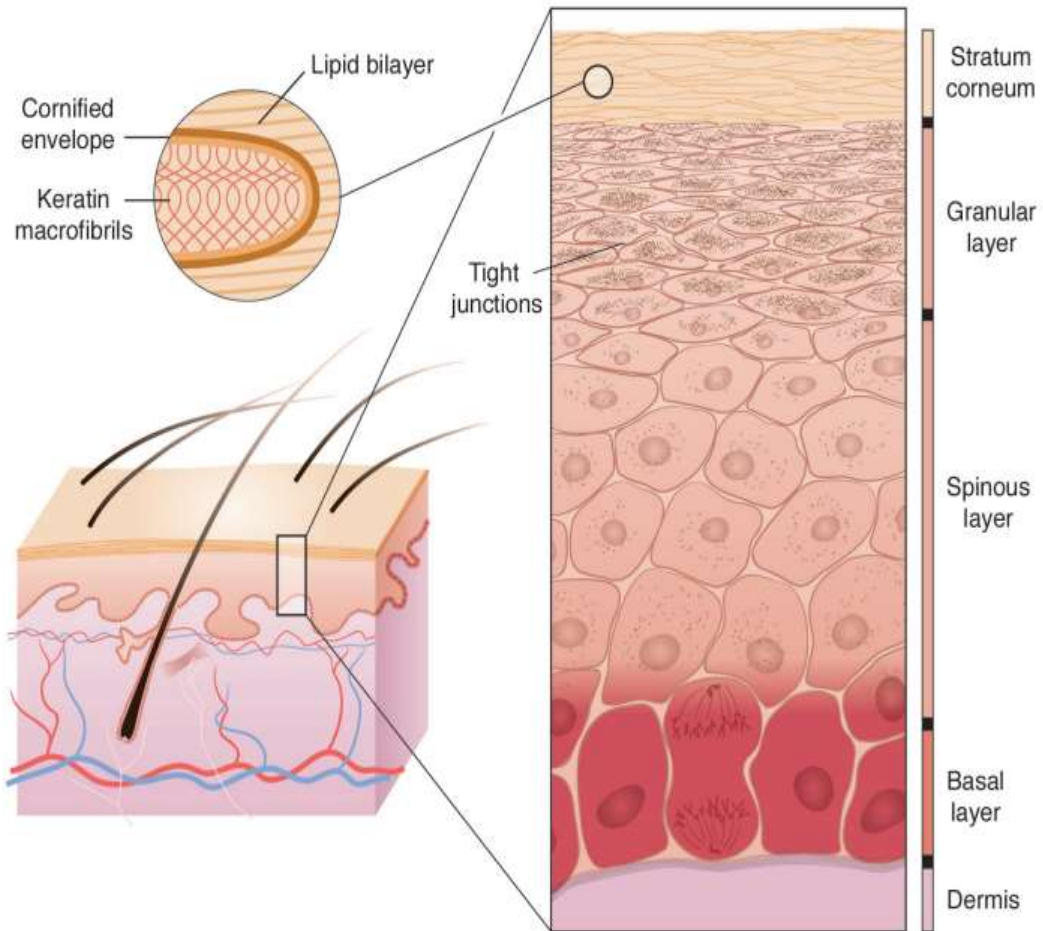


**Figure 1.6 Schematic diagram of human skin barrier** (Adapted from Segre, 2006).

Stratum corneum also known as cornified layer which is composed of keratin macrofibrils and cross-linked cornified envelopes encased in lipid bilayers at the outmost surface of interfollicular epidermis (IFE) provides the primary barrier, like a wall built by bricks and mortar. The granular cells held together by tight junctions also play an essential role in defence against physical trauma, invading pathogens and fluid loss.

keratinocytes are the main source of antimicrobial peptides which are packaged in lamellar bodies in spinous and granular layer, and extruded into intercellular media in cornified layer (Afshar and Gallo, 2013). Upon breakage of epidermal barrier, keratinocytes also produce an array of inflammatory cytokines and growth factors, such as TNF- $\alpha$ , interferon- $\gamma$  (IFN- $\gamma$ ) and interleukin-1(IL-1), which play a role in activating immune system (Afshar and Gallo, 2013). In this state, the task of antimicrobial peptide production is primarily fulfilled by immune cells such as neutrophils (Afshar and Gallo, 2013).

#### **1.2.4 Notch signaling in skin**

Notch signaling, as a key regulator for cell fate decision, is typically involved in epithelial stratification, epidermal homeostasis and lineage decision (Ambler and Watt, 2010; Nicolas et al., 2003; Okuyama et al., 2008; Watt et al., 2008). The presence of Notch receptor and ligand including Notch1-4, Jagged1, Jagged2 and Delta1 has been well documented in developing as well as adult epidermis throughout human and mouse, with the exception of Notch4 which has only been reported in human in rare suprabasal cells and Delta1 which is rarely detectable in adult mouse (Favier et al., 2000; Nickoloff et al., 2002). Nevertheless, the sub-locations of these Notch receptors and ligands are less clear and even contradicted among different studies (Ambler and Watt, 2010; Blanpain et al., 2006; Estrach et al., 2006; Estrach et al., 2007; Moriyama et al., 2008; Nickoloff et al., 2002; Pan et al., 2004; Thelu et al., 2002). By validating the most consistent findings from these studies, Fiona Watt and her colleagues (2008) have drawn a diagram illustrating the expression pattern of Notch1-3 and Jagged1-2 in neonatal mouse IFE and HF (Figure 1.7). While the expressions of Notch1-3 are somewhat overlapping with

abundance in neonatal suprabasal cells, complementary location of Jagged1 and Jagged2 are detected with Jagged1 preferentially expressed in suprabasal cells and Jagged2 confined to basal cells (Ambler and Watt, 2010; Blanpain et al., 2006; Estrach et al., 2006; Estrach et al., 2007; Moriyama et al., 2008; Nickoloff et al., 2002; Pan et al., 2004; Thelu et al., 2002). Deletion of Notch1, Jagged1 or Delta1 alone causes epidermal phenotypes in mouse while loss of Notch2, Notch3, Notch4 or Jagged2 alone has no overt impact on epidermis, suggesting Notch1 and Jagged1 are the primary Notch receptor and ligand that may play indispensable roles in adult epidermis while Delta1 is essential for epidermis development (Ambler and Watt, 2010; Estrach et al., 2007; Kerabs et al., 2000; Kerabs et al., 2003; Pan et al., 2004; Watt et al., 2008).

However, the presence of Notch receptor and ligand does not necessarily trigger an active Notch signaling which normally requires ligand endocytosis-dependent NRR conformational change (Musse et al., 2012). Notch signaling activity in mouse embryonic and neonate epidermis is then confirmed by the presence of NICD and expression of Notch target gene Hes1 which are both abundant in suprabasal layer but also detectable in basal layer corresponding to the location of Notch1 and Jagged1 (Estrach et al., 2006; Moriyama et al., 2008). However, Notch activity seems to be rapidly decreased after birth (during the first few weeks in mouse) and maintained at a low level throughout adult life, since the expression of Hes1 only detected in rare epidermal cells in older mice at age of 7 week old (Ambler and Watt, 2010). The decrease in mouse epidermal Notch activity after birth might be related to the diminished expression of Delta1 (Powell et al., 1998).

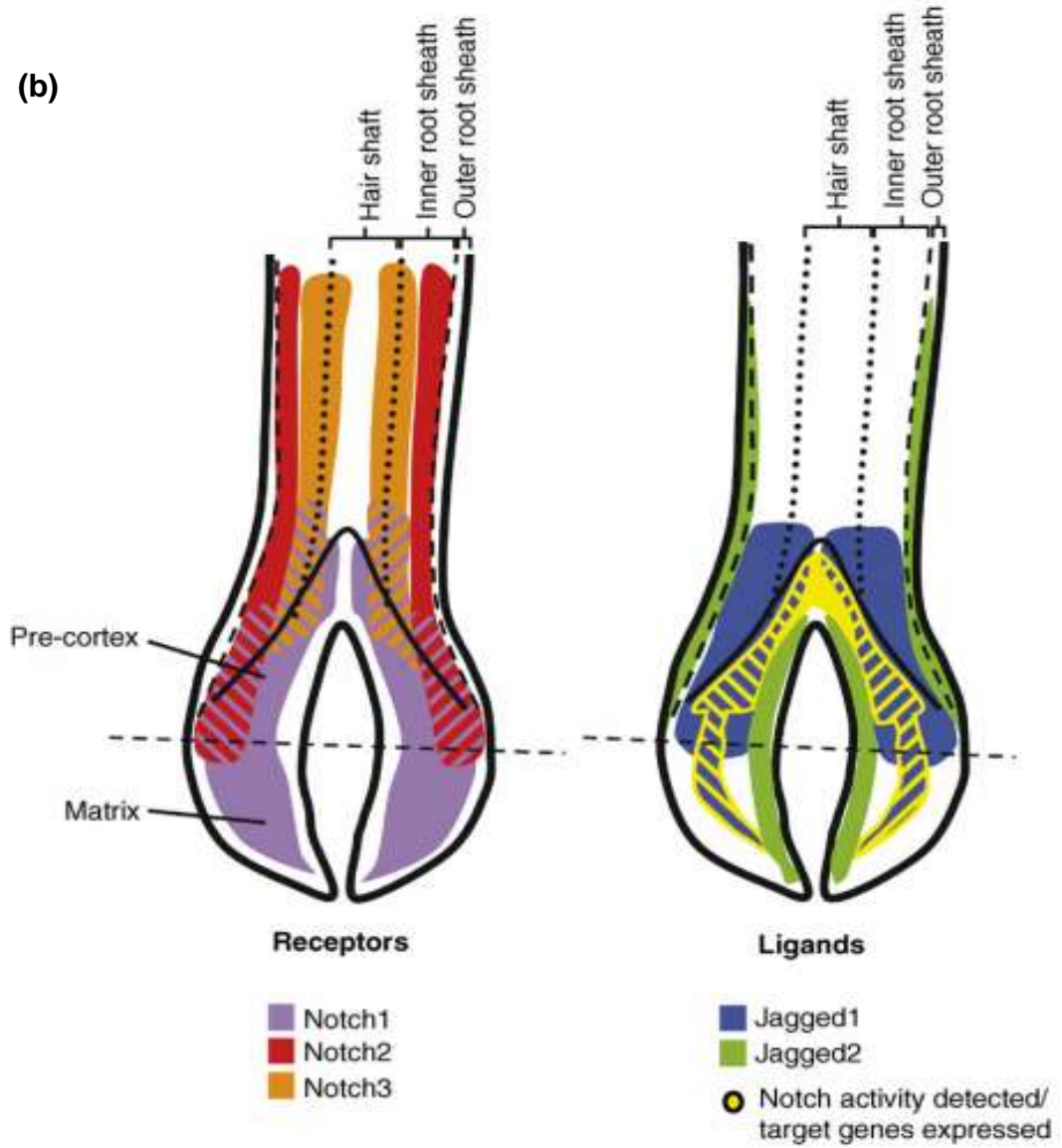
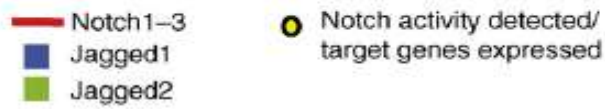
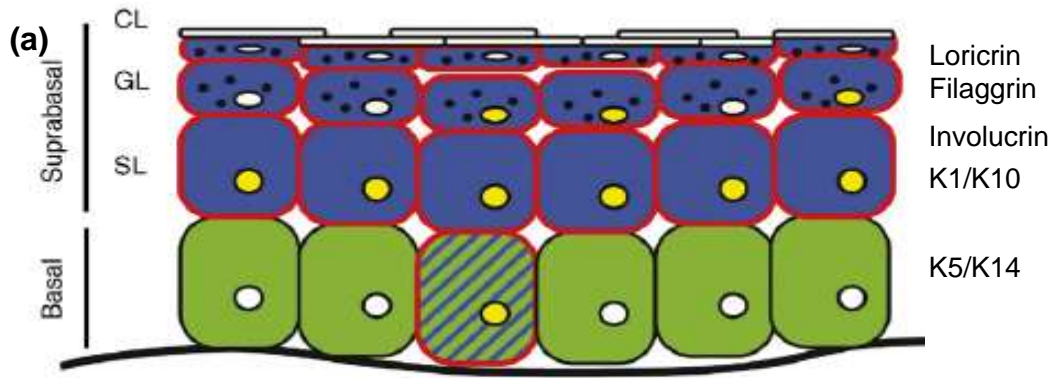


**Figure 1.7 Sites of Notch activity in interfollicular epidermis and hair follicles in neonatal mice** (Adapted from Watt et al., 2008). (a) Schematic diagram illustrating the presence and location of Notch pathway components in neonatal interfollicular epidermis (IFE). CL: cornified layer; GL: granular layer; SL: spinous layer. (b) Schematic diagram illustrating the presence and location of Notch pathway components in hair follicles at anagen (growing stage). Hatched shading indicates co-expression.



To investigate the function of epidermal Notch signaling, a variety of genetically modified mouse models have been used to mimic either loss or gain of function of Notch signaling by ‘knocking out’ or ‘knocking in’ a sequence that encodes a key component of Notch pathway, such as NICD1, Hes1 or BRP-Jκ (Table 1.1) (Ambler and Watt, 2010; Blanpain et al., 2006; Estrach et al., 2006; Moriyama et al., 2008; Nicolas et al., 2003; Rangarajan et al., 2001; Uyttendaele et al., 2004). In these models, Notch signaling is altered either completely throughout body or conditionally within epidermis under the control of epidermis-specific promoter such as the promoter of keratin14 (K14) etc. Most of these studies demonstrated loss of Notch function in IFE resulted in decrease in basal cell fate and increase in suprabasal fate while gain of Notch function led to increase in basal fate and increase in suprabasal fate, suggesting Notch signaling promotes constitutive differentiation of epidermal keratinocytes from basal cell into granular cell via spinous cell. However, differences were noted among different studies especially among individual gain-of-function models and between embryo and adult models, which could be explained by Notch non-cell autonomous effects on adjacent layer of epidermis due to altered Notch activity in a single layer (Rangarajan et al. 2001) or skin barrier defects in adult models as a secondary effect of Notch alteration (Blanpain et al., 2006b). In basal layer, Notch signaling promotes transition of basal cell into spinous cell by repressing basal cell-specific gene expression such as hemidesmosome component  $\alpha 6\beta 4$  integrin (Figure 1.8) (Blanpain et al., 2006b; Estrach et al., 2006; Moriyama et al., 2008) which associates basal cell with the underlying basement membrane while favouring spinous cell-specific gene expression such as K1 and K10 through a mechanism independent of Hes1 (Moriyama et al., 2008). In spinous layer, Notch signaling plays an essential role in

Modulation of Notch signaling	Molecule targeted	Mouse model	Tissue targeted	Epidermis thickness	Proliferation potential	Basal fate	Spinous fate	Granular fate	Reference
Loss of function	Notch1 & 2	Embryo	Epidermis	↓↓	UD	↑	↓↓	↓↓	Moriyama et al., 2008
	RBP-Jk	Embryo	Epidermis	↓↓	↓	—	↓↓	↓↓	Blanpain et al., 2006
	RBP-Jk	Embryo graft in adult	Epidermis	UD	↑	—	UD	UD	Blanpain et al., 2006
	Notch1	Adult (inducible)	Epidermis	↑↑	↑↑	↑↑	—	↑↑	Nicolas et al., 2003; Rangarajan et al., 2001
	Hes1	Embryo	Global	↓↓	↓↓	↓	↓↓	↓	Moriyama et al., 2008
	Hes1	Embryo graft in adult	Global	—	UD	—	—	—	Moriyama et al., 2008
Gain of function	Hes1	Embryo	Basal	—	UD	—	—	UD	Moriyama et al., 2008
	NICD1	Embryo	Basal	↑	UD	↓↓	↑↑	UD	Moriyama et al., 2008
	NICD1	Embryo	Basal	↑↑	↑	↓	↑↑↑	↓↓	Blanpain et al., 2006
	NICD1	Adult (inducible)	Basal	↑↑	↑↑	↑↑ patchy	↓↓ patchy	—	Estrach et al., 2006; Ambler and Watt, 2010
	Hes1	Embryo	Spinous	↑↑	UD	—	↑↑	—	Moriyama et al., 2008
	NICD1	Embryo	Spinous	—	UD	UD	↑	↑↑	Moriyama et al., 2008
	NICD1	Adult	Granular	↑↑	UD	—	↑	↑↑	Uyttendaele et al., 2004

**Table 1.1 Consequences of modulation of Notch signaling in epidermis.** Arrow upward indicates increase; arrow downward indicates decrease. The number of arrows indicates the extent of the change. Horizontal line indicates no obvious change. UD represents undetermined.

homeostasis of spinous cells by maintaining spinous fate in a manner dependent on Hes1 while promoting transition of spinous cell into granular cell through upregulation of another Notch/RBP-Jk target gene *Ascl2* (Moriyama et al., 2008). However, expression of *Ascl2* gene is repressed in the presence of Hes1, thus the induction of granular fate in spinous cell only occurs when Hes1 is down-regulated probably by an auto-regulatory feedback loop (Moriyama et al., 2008). Since either ectopic activating or blocking Notch signaling causes abnormal differentiation of epidermis, epidermal barrier disruption may eventually occur as a side effect of Notch modulation (Ambler and Watt, 2010; Blanpain et al., 2006) making the analysis of Notch signaling function much more complicated.

In addition to promoting terminal differentiation, Notch signaling also plays a role in regulating IFE proliferation through a mechanism which is less clear. Two separate studies reported that deletion of Notch1 promoted epidermal proliferation in adult mice through down-regulation of p21 expression which is known to induce cell growth arrest, suggesting Notch signaling might repress proliferation by directly activating transcription of p21 as a target gene (Nicolas et al., 2003; Rangarajan et al., 2001). By contrast, a couple of studies found loss of Notch activity by deleting Hes-1 or RBP-Jk resulted in reduced rather than increased epidermal proliferation in mouse embryos. Furthermore, they found such thinned hypo-proliferated epidermis experienced thickening and hyper-proliferation after several weeks of grafting into conditional RBP-Jk or NICD1 knockout adult mice (Blanpain et al., 2006; Moriyama et al., 2008). Blanpain et al. (2006) and Rangarajan et al. (2001) suggested the distinct proliferation phenotypes observed between embryos or neonates and adults might be related to epidermal barrier disruption which usually causes a secondary

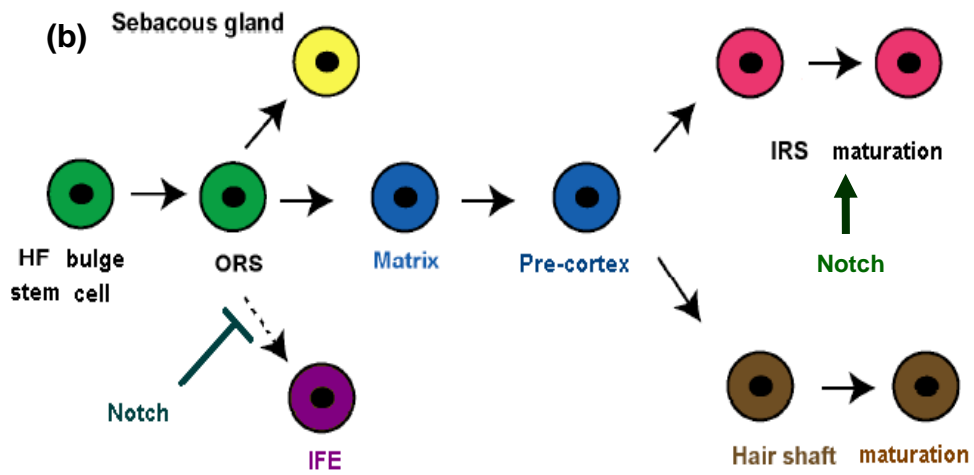
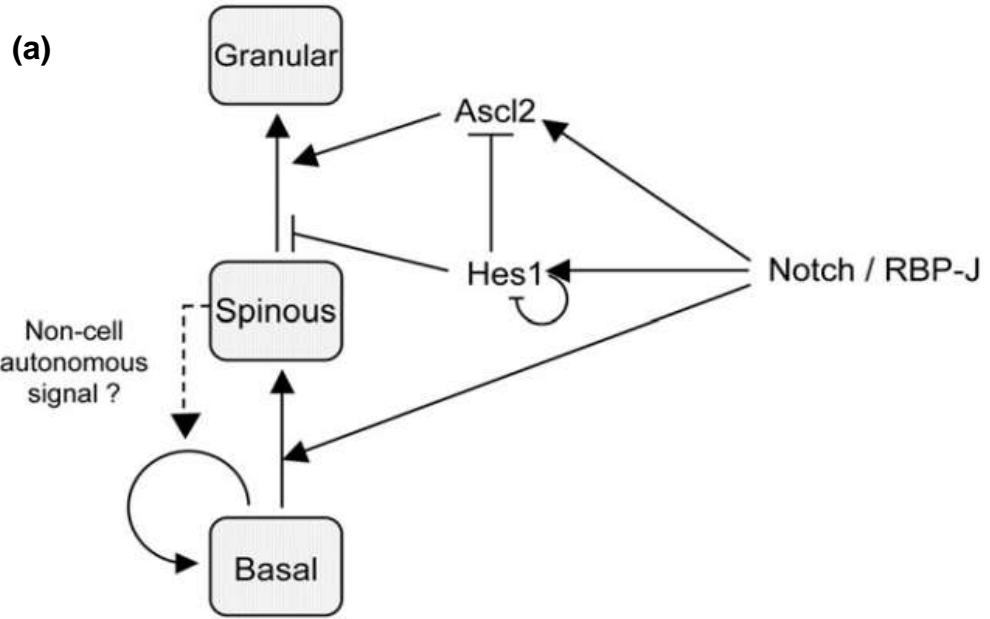


**Figure 1.8 The role of Notch signaling in regulating epidermal homeostasis**

(Adapted from Blanpain et al., 2006; Moriyama et al., 2008). (a) Schematic diagram illustrating the role of Notch signaling in regulation of normal IFE differentiation and proliferation. Canonical Notch signaling (Notch/RBP-Jk) promotes basal cell detachment from underlying basement membrane and differentiation into spinous cell by repressing basal cell genes such as  $\alpha 6$ ,  $\beta 4$  integrin and Keratin (K) 14 while inducing spinous cell genes such as K1 and K10 via a mechanism independent of Hes1. Then Notch signaling plays an essential role in maintenance of spinous fate and repressing transition in a manner dependent on Hes1. On the other hand, Notch signaling also promotes spinous cells transition into granular cells by directly activating Ascl2 gene expression. However, Ascl2 promoter is repressed in the presence of Hes1, thus the induction of granular differentiation will not occur until Hes1 is down-regulated in spinous layer probably by an auto-regulatory feedback loop. In addition, non-cell-autonomous Notch signaling from spinous cells may promote proliferation of basal cells probably via upregulation of p63 (Moriyama et al., 2008). (b) Schematic diagram illustrating Notch signaling regulates hair follicle maintenance by repressing the fate decision of bi-potential bulge stem cells into IFE (interfollicular epidermis) and promoting IRS (inner rooter sheath) differentiation and maturation. ORS, outer root sheath (Blanpain et al., 2006).

hyper-proliferation response. Moreover, Moriyama et al. (2008) suggested that a non-cell-autonomous Notch signaling sent by spinous cells might be constitutively activated in basal cells, the major population possessing proliferation potential in epidermis, as a result of differential levels of Notch activity between these two cell populations to contribute to basal cell proliferation possibly via upregulation of p63 (Moriyama et al., 2008). Whereas, ectopic induction of NICD1 specifically in basal cells was sufficient to drive basal cell proliferation, suggesting epidermal proliferation might be independent of non-cell-autonomous Notch signaling sent by spinous cells (Ambler and Watt, 2010; Blanpain et al., 2006; Estrach et al., 2006). Although epidermal barrier defects could contribute to hyper-proliferation in postnatal epidermis, this increased proliferation phenotype was also detected in neonates with ectopic NICD1 induction suggesting a direct role of Notch signaling for promoting proliferation (Blanpain et al., 2006). Furthermore, it has been suggested that Notch signaling plays this role through a mechanism dependent of Jagged1, since deletion of Jagged1 eliminates the hyper-proliferation phenotype in K14NICDER mice with ectopic induction of NICD1 (Ambler and Watt, 2010). However, it is still unknown how Notch, via Jagged 1, directs keratinocytes to proliferate.

Notch signaling also plays a direct role in regulating the terminal differentiation of IRS and/or HF and maintaining the existing hair follicle lineages by repressing the transition of bi-potential bulge progenitor cells into IFE fate (Ambler and Watt, 2010; Blanpain et al., 2006b; Estrach et al., 2006; Lin et al., 2000; Pan et al., 2004). However, Notch signaling is not capable to induce new hair follicle generation (Estrach et al., 2006).

In summary, skin is composed of epidermis and dermis, which are connected to each other via basement membrane. Adult epidermis is a self-renewing stratified epithelium with multiple lineages including IFE and its associated specialized appendages such as HF (Fuchs, 2007). IFE and HF are maintained by their own progenitor cells located in basal layer and outer root sheet through homeostasis and hair cycles respectively (Ambler and Määttä, 2009). The terminally differentiated cornified layer constitutes the primary skin barrier that prevents the penetrance of microbes and other insults (Baroni et al., 2012; Segre, 2006). The predominant epidermal cell type keratinocyte also secretes antimicrobial peptides to prevent microbe colonization in steady state and produce a range of inflammatory cytokines upon barrier disruption and microbial infection (Baroni et al., 2012). Notch signaling plays an essential role in maintaining homeostasis of epidermis by controlling the fate decision of HF bulge progenitor cells towards HF lineage, promoting terminal differentiation of both IFE and HF through cell-autonomous and non-cell-autonomous effects (Blanpain et al., 2006b; Moriyama et al., 2008). Notch also plays a role in epidermal proliferation through a mechanism that is less clear (Ambler and Watt, 2010; Estrach et al., 2006).

### **1.3 Immune system in skin**

#### **1.3.1 Background**

Although skin keratinocytes constitute a physical barrier that provides first-line defence against pathogen invasion and secretes antimicrobial peptides that have a direct role in killing microbes (Baroni et al., 2012), these mechanisms may not be sufficient to prevent microbial infection especially when epidermal barrier is broken by injury. In that case, a variety of immune cells, also known as white blood cells or



leukocytes, are recruited into skin through dermal blood capillaries and activated by inflammatory cytokines leading to inflammatory response against different sorts of infections, damages or host cell pathogenesis (e.g. tumorigenesis) (Delves et al., 2011). A number of immune cells are also present in skin as sentinels in steady state to provide immune surveillance (Nestle and Nickoloff, 2007). In this section, origin, location and classification of major types of immune cells circulating in blood vessels as well as residing in skin will be reviewed. Then the role of Notch signaling in immune system will be discussed.

### **1.3.2 Origin, location and classification of immune cells**

In adults, immune cells are derived from self-renewing hematopoietic stem cell (HSC) in bone marrow (Figure 1.9) and released into blood circulation to patrol the whole body (Delves et al., 2011). However, macrophages and myeloid dendritic cells are localized and matured in peripheral tissues only and share a common blood circulating progenitor called monocytes in inflamed state (Merad et al., 2013). Thymus-derived lymphocytes (T cells) require further processing and development in thymus before joining circulation (Blum et al., 2013). While bone marrow and thymus constitutes the primary lymphoid tissue which produce immune cells, the battlefronts of immunological defences are usually localized in spleen and lymph nodes spreading throughout the body, called secondary lymphoid tissues which are loaded and formed by massive immune cells (Delves et al., 2011). In addition, a number of immune cells are also accumulated in steady state in certain non-lymphoid tissues such as epithelial tissues at the body surface (e.g. skin, intestine and lung) (Table 1.2) where the risk of pathogen insults is higher than the other tissues (Dupasquier et al., 2004; Luci et al., 2009; Macleod and Havran., 2011;

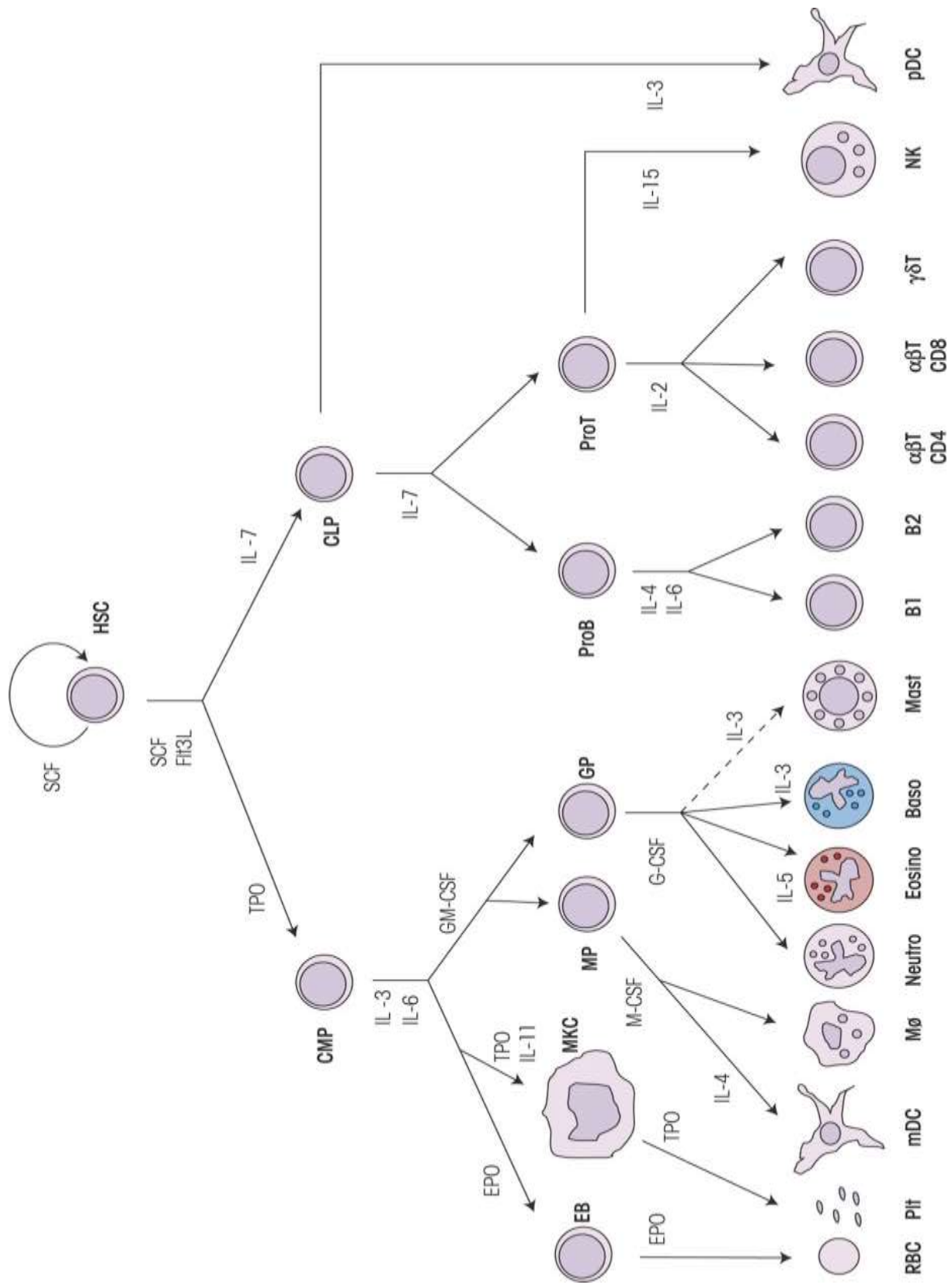


**Figure 1.9 The vast majority of immune cells are derived from bone marrow hematopoietic stem cell in the presence of different soluble cytokines and growth factors** (Adapted from Delves et al., 2011). SCF, stem cell factor; HSC, hematopoietic stem cell; Flt3L, FMS-like tyrosine kinase-3 ligand; TPO, thrombopoietin; IL, interleukin; CMP, common myeloid precursor; CLP, common lymphoid precursor; EPO, erythropoietin; GM-CSF, granulocyte–macrophage colony-stimulating factor; EB, erythroblast; MKC, megakaryocyte; MP, monocyte progenitor; GP, granulocyte progenitor; M-CSF, monocyte colony-stimulating factor; G-CSF, granulocyte colony-stimulating factor; RBC, red blood cell; Plt, platelet; mDC, myeloid dendritic cell; M $\phi$ , macrophage; Neutro, neutrophil; Eosino, eosinophil; Baso, basophil; NK, natural killer; pDC, plasmacytoid dendritic cell.

Skin resident immune cells	Location	Signature marker	Key features	Reference
Langerhans cell	Epidermis	CD207 (Langerin)	Proliferative and self-renewing in situ, classified as a unique subtype of dendritic cells	Romani et al., 2010
Dendritic epidermal T cell (DETC)	Epidermis	TCR $\gamma\delta$	Promote skin repair by producing keratinocyte growth factor, Promote macrophage migration into wounds	Macleod and Havran., 2011
Macrophage	Dermis	F4/80	Professional phagocyte that engulf microbes and cell debris followed by intracellular digestion	Dupasquier et al., 2004
Dendritic cell	Dermis	CD11c	Professional antigen presentation cell that activates adaptive response by matured T cell	Dupasquier et al., 2004
Mast cell	Dermis	UD	Increase vascular permeability by releasing mediators such as histamine	Stone et al., 2010
$\gamma\delta$ T cell	Dermis	TCR $\gamma\delta$	Proliferative and self-renewing in situ, produce IL-17 that controls neutrophil recruitment	Sumaria et al., 2011
Natural killer cell	Dermis	NKp46 NK1.1	Innate immunity against virus and tumor by producing interferon $-\gamma$ (IFN- $\gamma$ ) and mildly releasing cytotoxic granules	Luci et al., 2009

**Table 1.2 Phenotypes and functions of immune cells residing in mouse skin in steady state.** UD, undetermined.

Romani et al., 2010; Stone et al., 2009; Sumaria et al., 2011).

Depending on their differentiation pathways, immune cells are broadly classified into two families, lymphoid cells which includes T cells, B cells and NK cells, and myeloid cells which are subdivided into monocytes (including macrophages and most dendritic cells), granulocytes (including neutrophils, eosinophils and basophils) and mast cells (Delves et al., 2011). The majority of myeloid cells, NK cells and a small number (less than 5% of total circulating T cells) of T cells ( $\gamma\delta$  T cell) bearing  $\gamma$  and  $\delta$  chains in their T cell receptor (TCR $\gamma\delta$ ) participate in rapid innate immune response by directly recognizing pathogens, infected cells or damaged cells (Dupasquier et al., 2004; Luci et al., 2009; Macleod and Havran., 2011; Romani et al., 2010; Stone et al., 2010; Sumaria et al., 2011). Conventional T cells ( $\alpha\beta$  T cells) and B cells participate in adaptive immune response by producing specific cytotoxic T cells and antibody respectively for adapting to a particular antigen processed and presented by professional antigen presenting cells (i.e. dendritic cells) or stressed host cells (non-professional antigen presenting cells) (Blum et al., 2013; Delves et al., 2011). Compared to rapid innate immune response, adaptive immune response allows time for antigen presentation (Blum et al., 2013; Delves et al., 2011). However, adaptive system has long-lasting memory which allows it to be prepared for the next threat event by the microbe bearing the same antigen (Mueller et al., 2013).

### **1.3.3 Major circulating immune cells accessible to skin**

To confront the risk of microbial infection, a variety of circulating immune cells are recruited into the site of pathogen invasion or damage in dermis through blood

capillaries and activated to perform innate or adaptive immune reactions against different sorts of threats. The roles of immune cells are conserved throughout human and mammals, however, the phenotypes (i.e. the cell surface markers) can be slightly different (Delves et al., 2011; Mestas and Hughes, 2004). Here, I use mouse model to review the immune system.

Neutrophils ( $CD11b^+F4/80^-Gr1^+$ ) and inflammatory monocyte ( $CD11b^+F4/80^+Gr1^+$ )-derived macrophages ( $CD11b^+F4/80^+Gr1^-$ ), which are known as professional phagocytes, are the key players of innate immune system defending against bacteria, fungi as well as cell damage (Amulic et al., 2012; Wynn and Barron, 2010). They, via a range of cell surface pattern recognition receptor (PRRs) such as Toll-like receptor, recognize a highly conserved component either present in common infectious agents called pathogen associated molecular pattern (PAMP) or released by necrotic host cells undergoing uncontrolled death upon severe damage (danger associated molecular pattern, DAMP) (Amulic et al., 2012; Delves et al., 2011; Dupasquier et al., 2004). Upon recognition of a PAMP or DAMP, the pathogens or necrotic cells displaying the same PAMP or DAMP are engulfed by these professional phagocytes followed by intracellular digestion via destructive enzyme, chemicals or radicals (Delves et al., 2011; Dupasquier et al., 2004). Compared to neutrophils, macrophages are more powerful in phagocytosis, they can engulf apoptotic cells undergoing natural or programmed death, such as short-life neutrophils (Wynn and Barron, 2010).

The minority of granulocytes, such as basophils and eosinophils, are often involved in innate immune defence against parasites which are too large to be engulfed by

professional phagocytes and thus require membrane lysis mediated by basophils and eosinophils before phagocytosis can take place (Stone et al., 2010).

NK cells ( $CD3^-NKp46^+NK1.1^+$ ) play a key role in innate killing of virally infected host cells as well as host cells committed to undergo tumorigenesis (Cameron et al., 2002; Delves et al., 2011; Luci et al., 2009). Although macrophages are the powerful phagocytes to engulf bacteria, fungi and damaged cells, they are not capable to target viruses, since viruses live inside host cells and use host ribosomes to replicate themselves, the recognition of PAMP or DAMP from these viruses is hindered by the intact host cell membrane (Delves et al., 2011; Luci et al., 2009). In that case, the recognition of abnormal host cells is performed by NK cells which detect missing or reduced expression of MHC-I that is normally expressed by all nucleated host cells, or MHC-related molecules (non-classical MHC) which is expressed by certain stressed cell types such as epithelial cells to convey a danger signal and thus allow themselves to be recognized (Delves et al., 2011; Luci et al., 2009). Following recognition, NK cells then induce apoptosis (assisted suicide) of these abnormal cells via releasing cytotoxic granules or activating death receptor in host cells, and produce interferon- $\gamma$  (IFN- $\gamma$ ) that directly inhibit viral replication (Delves et al., 2011; Luci et al., 2009). Dead cells are finally engulfed and cleared by macrophages (Delves et al., 2011; Luci et al., 2009; Wynn and Barron, 2010). A small number of T cells called NK-like T cells (NKT cells,  $CD3^+NK1.1^+NKp46^+$ ) have the similar properties of NK cells, and plays a role in innate immune system (Cameron et al., 2002; Delves et al., 2011).

Dendritic cells (most of them are CD11c<sup>high</sup>) are the major type of so called professional antigen presenting cells which also include macrophages and B cells, which activate adaptive immune response (Blum et al., 2012; Kushwah and Hu, 2011; Merad et al., 2013). They can capture specific protein structures called antigens from outside pathogens followed by internalizing and processing these antigens and expressing the antigen peptides on their cell surface MHC-II, which allows the pathogen fragments to be recognized by CD4<sup>+</sup> T cells (Blum et al., 2012; Dupasquier et al., 2004; Kushwah and Hu, 2011; Merad et al., 2013). Compared to macrophages, dendritic cells have limited capacity to directly kill the pathogen they have phagocytosed (Kushwah and Hu, 2011; Merad et al., 2013). However, pathogen-encountered dendritic cells are competent to activate adaptive immune system by migrating to the nearest lymph node and present an antigen derived from the pathogen to CD4<sup>+</sup> T cells (Kushwah and Hu, 2011; Merad et al., 2013).

Conventional T and B lymphocytes mediate antigen-specific adaptive immune response (Delves et al., 2011). Under inflamed state, B cells undergo clonal expansion and differentiation into effector plasma cell to produce an antibody that specifically target pathogens displaying a particular antigen. Naive CD8<sup>+</sup> T cells induce apoptosis of infected cells expressing a foreign antigen via differentiation into effector cytotoxic T cell (Tc), while naive CD4<sup>+</sup> T cell differentiates into various subsets of helper T cell (Th) to facilitate co-activation of B cell and enhance intracellular killing by macrophages and Tc (Delves et al., 2011; Zhu et al., 2011). This antigen-specific defence usually takes place 4-5 days later (Delves et al., 2011) than innate immune response because activation of conventional T and B cells is dependent on antigen presentation. Naive CD4<sup>+</sup> or CD8<sup>+</sup> T cells cannot recognize



antigen through T cell receptor (TCR) until antigen-derived peptide is expressed by professional APC, predominantly dendritic cells, via MHC-II or by viral infected cells via MHC-I (Zhu et al., 2011). B cells directly recognize extracellular antigen through B cell receptor (BCR), but antibody cannot be produced until B cell presents this antigen, via MHC-II, to a particular Th cell which has been encountered by the same antigen (Delves et al., 2011; Zhu et al., 2011). As a consequence, the extracellular pathogens which have not been phagocytosed by macrophage-predominant innate immune system are targeted by B cell-mediated humoral immunity. The intracellular pathogens which have been phagocytosed but not been killed by macrophages and those pathogens living and replicating within the host cells which have not been targeted by NK cells are challenged by Tc cell mediated cytotoxicity (Delves et al., 2011; Zhu et al., 2010).

#### **1.3.4 Entry of circulating immune cells into dermis**

The motility and recruitment of circulating immune cells are regulated by a family of specialized message protein called chemokines, such as CCL and CXCL families, that attract immune cells bearing a corresponding chemokine receptor from adjacent tissue or blood circulation into the inflamed site (Dupasquier et al., 2004; Henri et al., 2009). The penetrance of immune cells through blood vascular wall is mainly facilitated by mast cells which release mediators such as histamine to increase vascular permeability (Stone et al., 2010). After entering dermis, the clonal expansion and activity of these migratory immune cells are activated by another family of message proteins called cytokines such as interleukins (IL) and TNF that function over a shorter range. Then the activated immune cells can in turn, via NFκB pathway, produce their own cytokines and growth factors that influence the activity

of the other immune cells as well as non-immune cells nearby with an appropriate receptor (Delves et al., 2011; Dupasquier et al., 2004; Henri et al., 2009). As a consequence, the extra cells and fluids gathered at the site of infection or cell damage result in a so called inflammation reaction which is featured by swelling, redness and heating of local tissue (Delves et al., 2011).

### **1.3.5 Skin resident immune sentinels**

In steady state, skin is constantly populated by a number of immune cells which provide immune surveillance by watching the signs for pathogen insults and cell damages, and produce cytokines that amplify inflammatory response by activating and attracting blood-circulating immune cells. These skin resident immune sentinels mainly include most common innate immune cells such as macrophages, dendritic cells, NK cells, mast cells (Dupasquier et al., 2004; Luci et al., 2009) as well as those which are seeded in skin particularly in epidermis very early during fetal development with a long lifespan and thus are thought to be absent or rare in blood circulation, such as Langerhans cells (LCs, CD207<sup>+</sup>CD11c<sup>low</sup>) and dendritic epidermal T cells (DETCs, CD3<sup>+</sup>TCR $\gamma\delta$ <sup>+</sup>V $\gamma$ 3<sup>+</sup>) (Macleod and Havran., 2011; Merad et al., 2013). Langerhans cells are classified as a particular subset of dendritic cells participating in antigen presentation. In contrast to conventional DCs which are characterized by high expression of CD11c integrin and replenished by blood circulating monocytes, LCs express low level of CD11c and are primarily produced in sac yolk and fetal liver and maintained by local proliferation (Merad et al., 2013). DETCs belong to a rare subset of T cells ( $\gamma\delta$  T cells) bearing TCR  $\gamma\delta$  chains, distinct from the majority (95%) of circulating T cells) of T cells which express TCR  $\alpha\beta$  chains (Delves et al., 2011). DETCs are only present in rodent epidermis where they

produce keratinocyte growth factor (KGF), insulin-like growth factor-1 (IGF-1) and hyaluronan in response to damaged keratinocytes, which protects epidermal barrier integrity by promoting keratinocyte proliferation and recruits macrophages to the site of damage respectively (Bolleville, 2012; Macleod and Havran., 2011). Recently  $\gamma\delta$  T cells have also been detected in steady state dermis where they produce IL-17 that plays a role in neutrophils (Sumaria et al., 2011). In contrast to  $\alpha\beta$  T cells,  $\gamma\delta$  T cells directly recognize antigen or non-classical MHC molecules expressed by stressed and damaged host cells without a requirement of antigen presentation (Zhu et al., 2010). Therefore,  $\gamma\delta$  T cells usually do not express CD4 or CD8 which acts as co-receptor for antigen within the context of MHC-II or MHC-I (Delves et al., 2011).

### **1.3.6 Notch signaling in skin immune system**

Notch signaling, as key regulator of cell fate decision in a range of developmental process, also plays a role in the development of immune system. Notch1 signaling controls thymic T-cell maturation (Izon et al., 2001) and Notch2 signaling maintains splenic marginal zone B cells (Saito et al., 2003). However, new evidence suggests Notch signaling may play a role for epidermal keratinocytes to contact immune cells (Ambler and Watt., 2010; Estrach et al., 2006). In their studies, Notch activation by inducing ectopic NICD1 in epidermal keratinocytes resulted in epidermal production of inflammatory cytokines such as  $\text{TNF}\alpha$  and dermal accumulation of  $\text{CD4}^+$  immune cells via a mechanism dependent on epidermal Jagged1 expression (Ambler and Watt., 2010; Estrach et al., 2006). Although the role of Jagged1 in downstream Notch signaling is less clear, other studies have suggested Jagged1 as a target gene of  $\text{BRP-J}\kappa$  (Foldi et al., 2011), may relays and amplifies Notch signaling from cell to cell, which seems to be consistent to these studies.

In summary, immune system provides professional defence against various insults such as bacteria, fungi, viruses as well as abnormal host cells (Delves et al., 2011). The majority of immune cells are circulating throughout body via blood vessels, lymph vessels and lymphoid organs, such as spleen and lymph nodes, to provide immune surveillance (Delves et al., 2011). Some immune cells such as LC and DETCs (specific to rodents) are exclusively residing in epithelial epidermis to play a role in local immunity (Macleod and Havran, 2011; Merad et al., 2013; Nestle and Nickoloff, 2007). Under the inflamed state, a variety of circulating immune cells are recruited into skin especially dermis by chemokines and activated by cytokines to perform innate and adaptive immune response via direct killing and producing cytokines to amplify the inflammation (Delves et al., 2011). Notch signaling plays a role in regulating the development of immune system as well as the recruitment of immune cells into dermis via TNF- $\alpha$  (Ambler and Watt, 2010; Estrach et al., 2006; Izon et al., 2001; Saito et al., 2003).

## **1.4 Skin wound healing**

### **1.4.1 Background**

Wound healing in epithelial tissue is a sequential process which is initiated by immune cell mediated inflammation to clear wound of any damaged cells, debris and microbes (inflammation phase), followed by epidermal proliferation and dermal extracellular matrix deposition to close the wound (proliferation phase), and finished with remodelling of dermal tissue and resolution of excessive extracellular matrix to restore the normal structure and function of skin (remodelling phase) (Figure 1.10). These events are co-ordinated in terms of timing, duration and intensity in order to keep the repair progressing and maintain an equilibrium between tissue synthesis and

degradation (Guo and DiPietro, 2010; Martin and Leibovich, 2005; Rodero and Khosrotehrani, 2010). In this section, wound healing mechanism and the role of immune system and Notch signaling in wound closure will be reviewed.

#### **1.4.2 Mechanism of wound healing**

In wounded area, the normal skin structures are completely lost leaving dermal blood capillaries with open ends (Martin et al., 2005). However, blood loss is rapidly ceased by a platelet-composed blood plug which is then stabilized by fibrin fibers converted from fibrinogen (Figure 1.10) (Rodero and Khosrotehrani, 2010). Skin injury also directly induces damage and stress to the local cells at the wound edge by exposing the skin and inner body to potential pathogens in the environment. Stressed keratinocytes produce antimicrobial peptides and inflammatory cytokines such as TNF- $\alpha$  (Grone, 2002). In the meanwhile, the skin resident immune sentinels which are already present at the time of injury are activated to clear the dead cells, cellular debris and any invading pathogens and produce pro-inflammatory cytokines, chemokines and antimicrobial peptides. The cytokines and chemokines produced by stressed keratinocytes as well as skin resident immune cells amplify the inflammatory reaction by attracting and activating more immune cells into wound site through dilated blood vessels with the help of skin resident mast cells. Neutrophils are the first cells recruited into wound site with a very short lifespan, while monocyte-derived macrophages become the predominant cell type from approximately day 2 post injury to intensively phagocytose wound debris, microbes and apoptotic neutrophils (Rodero and Khosrotehrani, 2010). The adaptive immune cells such as conventional T cells and B cells are thought not to be significantly involved in inflammation phase in acute wound healing (Stout, 2010), probably

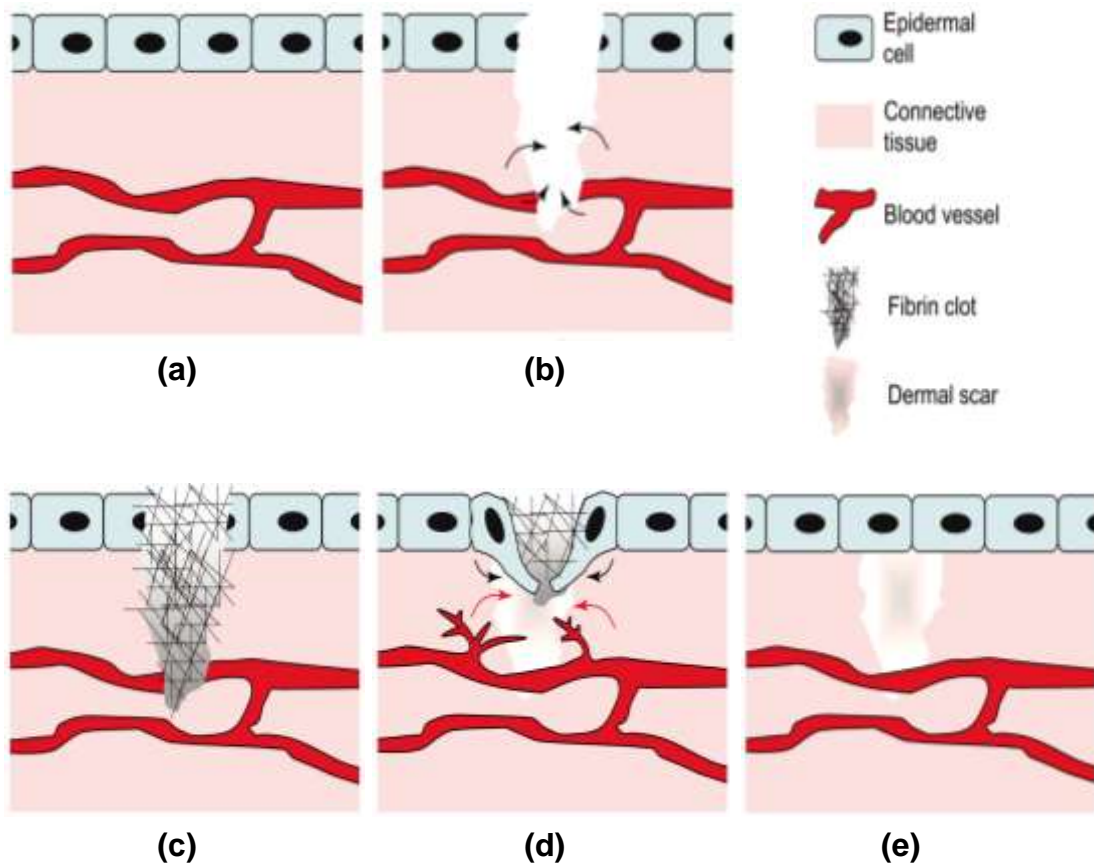


**Figure 1.10 Schematics of normal skin wound healing** (Modified from Martin and Leibovich, 2005). (a) Normal skin consists of epidermal barrier and underlying dermis enriched with capillary blood vessels. (b) Physical injury causes disruption of epidermal barrier and damage of dermis. Platelets are immediately activated and aggregated to prevent blood loss. Massive immune cells from adjacent dermis and from circulating blood vessels are recruited into wound site to promote a protective inflammatory response to clear damaged cells and invading microbes. (c) Fibrin clot is formed to cover the wound edge and (d) serve as a matrix that allows keratinocytes proliferation and migration along its undersurface to close the wound. Dermis undergoes massive angiogenesis and deposition of extracellular matrix (dermal scar) that gradually replaces the fibrin clot. (e) When the epidermis has healed over the exposed wound, dermis undergoes remodelling involving resolution of vascular sprouting and dermal scar to restore tissue strength.

because the defence against common environmental pathogens do not require antigen-specific response.

The later stage of inflammation phase is overlapped with proliferation phase where fibrin clot acts as a scaffold for keratinocytes at the wound edge to proliferate and migrate along the undersurface of fibrin clot to bridge the gap between wound edges (Martin and Leibovich, 2005). In wound dermis, a large number of fibroblasts from adjacent dermis and derived from circulating fibrocytes are accumulated to form so called granulation tissues with macrophages to promote dermal extracellular matrix deposition and wound contraction as well as inflammation. In these specialized granulation tissues, massive blood vessels are generated to supply cytokines, growth factors as well as nutrients to tissue repair, some fibroblasts are converted to myofibroblasts which synthesize extracellular matrix components such as collagens, contract wound edges and drawing up wound bed thereby promoting wound closure (Rodero and Khosrotehrani, 2010).

Subsequently, wound is closed when keratinocytes migrated from wound edges confront and adhere to one another. Whereas, wound dermis, which is largely composed of granulation tissues and collagen scar, requires remodeling to replace collagen-producing granulation tissue and restore the normal structure and tensile. This remodeling could last for years involving apoptosis of myofibroblasts, vascular endothelial cells and macrophages, degradation of excessive extracellular matrix via metalloproteinases which are expressed by epidermal cells, fibroblasts and remaining macrophages (Guo and DiPietro, 2010). However, it is not always possible to restore adult skin to its pre-injury state and scar formation usually occurs as a common

result of adult wound healing, although incisional fetal wound may heal perfectly without scar (Guo and DiPietro, 2010).

### **1.4.3 The role of immune cells in wound closure**

The three phases of wound healing are coordinated and occur in an order. Inflammation phase is typically mediated by immune cells that protect host body from infection and clear wound of damaged cells and debris, proliferation phase contributes to wound closure, while remodeling phase replace dermal scar with normal skin structure. However, inflammation must be self-sustained once pathogen infection and wound clearance is under control to allow proliferation phase to proceed. Therefore, the entry and exit of inflammatory immune cells in appropriate timing are equally important for wound closure (Guo and DiPietro, 2010; Martin and Leibovich, 2005; Rodero and Khosrotehrani, 2010). Macrophages have long been considered the key regulator for wound healing, since they not only act as a predominant type of inflammatory cells (M1 macrophage) in inflammation phase, but also are involved in proliferation phase (M2 macrophage) as well as remodeling phase, following being activated by different pathways (Rodero and Khosrotehrani, 2010).

As a main type of professional phagocyte, macrophages are recruited into wound site following neutrophils and become the predominant immune cells present in the wound approximately from day 2 post injuries (Rodero and Khosrotehrani, 2010). In the initial inflammation phase, the majority of macrophages are classically activated by interferon- $\gamma$  (IFN- $\gamma$ ) (M1 macrophages) to perform extensive phagocytosis to clear wound of any debris including the short-life neutrophils and secrete pro-inflammatory cytokines such as TNF- $\alpha$ , IL-1 $\beta$ , IL-6 (Rodero and Khosrotehrani,



2010). During later inflammation phase and proliferation phase, the functional phenotypes of macrophages are converted (M2) to promote granulation tissue formation angiogenesis, collagen synthesis, ECM deposition and wound contraction through producing transforming growth factor  $\beta$  (TGF $\beta$ ) (Rodero and Khosrotehrani, 2010). These macrophages displaying M2 phenotypes are thought to be alternatively activated by IL-4 or IL-13 (Martin and Leibovich, 2005; Rodero and Khosrotehrani, 2010). As the main source of TGF- $\beta$  that activates dermal myofibroblast differentiation, which in turn switches on collagen production to generate extracellular matrix, macrophages have also been considered as a key contributor to fibrosis and scarring formation especially when inflammation is persistent or repeated (Wynn and Barron, 2010). However, the issue of fibrotic and scarring wound healing is beyond the focus of this thesis. In remodeling phase, macrophages undergo apoptosis and remaining macrophages play a minor role in promoting degradation of excessive extracellular matrix via directly producing metalloproteinase (Wynn and Barron, 2010; Leibovich and Ross, 1975). The critical importance of macrophages over the other common immune cells to normal wound healing is supported by a collection of studies, where depletion of macrophages during inflammation phase or proliferation phase of wound healing by using anti-macrophage serum or macrophage- knockout animals hinders wound closure (Goren et al., 2009; Leibovich and Ross, 1975; Lucas et al., 2009; Mirza et al., 2009; Rodero and Khosrotehrani, 2010), while depletion of neutrophils, mast cells or conventional T cells (Grawnska-Kozak et al., 2006) by using antiserum or genetic knock-out animals leads to normal or speedier healing (Simpson and Ross al., 1972; Dovi et al., 2003; Egozi et al., 2003; Martin and Leibovich, 2005). These studies suggest that

macrophages may play a non-redundant role in inflammation and proliferation phases in normal wound healing.

However, the non-redundant role of macrophages and even the requirement for immune cells in adult wound closure are disfavored by an older study. In the year of 2003, Martin et al. reported that PU.1 null mice which lacked macrophages along with neutrophils and were pre-treated with antibiotics to prevent infection, had decreased levels of granulation tissues, less efficient phagocytosis and reduced TGF- $\beta$  production in their skin wounds. However, these PU.1 null mice had similar reconstitution rate of both wound epidermis and dermis and no overt wound closure defects compared to wild type mice (Martin et al., 2003). Furthermore, the normal presence of myofibroblasts which is associated with wound contraction was detected in PU.1 null wound and dermal fibroblasts were found to act as candidate phagocytes to clear cell and matrix debris to compensate for the absence of macrophages (Martin et al., 2003). Therefore, it was suggested that immune cells are not absolutely needed for tissue repair (Martin et al., 2003). Whereas, the author admitted that the administration of antibiotics and deficiency in neutrophils might have led to reduced requirement for macrophage-associated phagocytosis and following intracellular killing, thus the candidate phagocyte dermal fibroblasts was proved to be capable to play macrophages role in that case (Martin and Leibovich, 2005).

In addition, skin-resident DETCs have shown a role in promoting skin wound healing by activating keratinocytes proliferation via KGF and IGF-1 and by recruiting macrophages into wound site via hyaluronan (Jameson et al., 2002; Macleod and Havran, 2011). In their studies, TCR- $\delta$  deficient mice had a 2- or 3-

day delay in wound closure and reduced epidermal thickness compared to wild type mice (Jameson et al., 2002; Macleod and Havran, 2011).

New evidence suggested IL-22 as a key signaling for epithelial tissue repair promotes fibroblast-mediated skin repair (Dudakov et al., 2012; McGee et al., 2013). Their study demonstrated IL-22 receptor which was thought to be exclusively expressed by epithelial cells is also expressed by dermal fibroblasts *in vivo* and IL-22 knockout mice had wound closure defects resulting from the failure in myofibroblast differentiation (McGee et al., 2013). However, the source of IL-22 needs to be determined yet, although IL-22 has been reported to be produced by novel innate lymphoid cells in intestine to promote epithelial proliferation (Spits and Cupedo, 2012; Spits and Santo, 2011).

#### **1.4.4 The role of Innate lymphoid cells in epithelial repair**

A novel group of innate lymphoid cells (ILCs) (ILC3s, characterized by CD3<sup>-</sup>CD127<sup>+</sup>ROR $\gamma$ <sup>+</sup>) distinct from NK cells which belong to Group 1 innate lymphoid cells, has drawn our attention due to its role in promoting epithelial tissue repair in intestine via producing IL-22 that induce epithelial tissue proliferation (Spits and Cupedo, 2012; Spits et al., 2013; Spits and Santo, 2011). Activation of IL-22 production in these ILCs requires IL-23 released from dendritic cells (Spits and Cupedo, 2012). The term innate lymphoid cells (ILCs) have been recently given to a heterogeneous immune cell family that have morphological characteristics of lymphoid cells and share cytokine production profile with various T helper cells (Th) subsets, but lack a specific antigen receptor which is usually required for adaptive immune cells (Spits and Cupedo, 2012). Therefore, ILCs are likely to be derived

from common lymphoid precursor but do not express CD3 which is considered as a T cell marker (Spits and Cupedo, 2012). They participate in innate immune response and function in lymphoid organogenesis, tissue remodeling, antimicrobial immunity, and inflammation, particularly at barrier surfaces (Spits and Cupedo, 2012). ILCs can be grouped into three major categories (Table 1.3): (1) Group 1 ILCs (ILC1s) including NK cells, which mainly produce IFN- $\gamma$ ; (2) Group 2 ILCs (ILC2), which are ROR $\gamma$  t-independent and function in helminth immunity; (3) Group 3 ILCs (ILC3s, also known as ROR $\gamma^+$  ILC), which are dependent on IL-7 and retinoid-related orphan receptor gamma (ROR $\gamma$ , a key nuclear transcriptional factor) during development and maturation, express IL-7 receptor (CD127) and ROR $\gamma$ t, and produce IL-17, IL-22 or both in a mechanism dependent on IL-23 (Spits and Cupedo, 2012; Spits and Santo, 2011). ILC3s may contain several distinct subsets such as lymphoid tissue inducer cells (LTi), IL17-expressing cells (ILC17), IL22 expressing cells (ILC22), depending on the main cytokines they produce (Spits and Cupedo, 2012). However, the current classification and nomenclature within this category are not clear or uniform, and require further knowledge of lineage development and relationship (Spits and Cupedo, 2012; Spits et al., 2013). Although the presence of ILC3s has not been reported in skin, the finding that IL-22 has a significant role in skin repair suggests the repair mechanism might be conserved among tissues containing epithelium.

#### **1.4.5 Notch signaling in wound healing**

It has been suggested that Notch signaling might be involved in wound healing by a study using topically-applied pan-Notch activator and inhibitor (Chigurupai et al., 2007). However, the action site and mechanism remain less clear. Recently our lab

has demonstrated forced activation of epidermal Notch signaling promotes dermal accumulation of immune cells via epidermal production of TNF and epidermal proliferation, resembling the remarks of early and middle stages of wound healing (Ambler and Watt 2010; Estrach et al., 2006). These results suggest a potential link between epidermal Notch signaling and skin wound healing.

In summary, skin wound healing is a coordinated and sequential process including inflammation phase which clears wound of any damaged or dead cells, debris and microbes, proliferation phase which involves epidermal proliferation, dermal extracellular matrix deposition and remodeling phase which restore the normal architecture of skin (Martin and Leibovich, 2005). Macrophages have long been the key immune cells that participate in normal wound healing by serving as major professional phagocytes that stimulating inflammation and by acting as the main source of TGF- $\beta$  that promotes wound contraction and dermal extracellular matrix deposition (Rodero and Khosrotehrani, 2010). However, the redundant role of immune cells in skin repair is in dispute. Recent studies suggest IL-22 which could be produced by a novel population ILC3s plays a key role in promoting intestine epithelial repair and dermal repair by mediating the interaction between immune cells and non-immune cells (Luci et al., 2009; McGee et al., 2013; Sonnenberg et al., 2012). Notch signaling might be involved in skin wound healing (Ambler and Watt, 2010; Chigurupai et al., 2007; Estrach et al., 2006).

Group of innate lymphoid cells	Subset	Key cytokine required	Signature cytokine produced	Main function
ILC1 (NK cell)	—	IL-18, IL-12, and IL-15	Interferon- $\gamma$	Innate immunity against virus and tumor
ILC2	—	IL-25 and IL-33	IL-5 and IL-13	Innate immunity against parasites
ILC3 (ROR $\gamma$ + ILCs)	Lymphoid tissue inducer (LTi) cells	IL-1 $\beta$ and IL-23	IL17 and/or IL22	Secondary lymphoid tissue formation during fetal development
	IL-22 producing ILCs (ILC22 or NCR <sup>+</sup> ILC3)		IL-22	Promote innate immunity and tissue repair in intestine
	IL-17 producing ILCs (ILC17)		IL17 and/or IL22	Innate immunity against bacteria

**Table 1.3 Family of innate lymphoid cells (ILCs) in mouse.** (Information based on Luci et al., 2011; Sonnenberg et al., 2011; Spits and Cupedo, 2012; Spits et al., 2013; Spits and Santo, 2011)

## **1.5 Hypothesis**

Slow or non-healing wounds have affected many people especially for diabetics and elderly people (Guo and DiPietro, 2010). Wound healing requires immune cells especially innate immune cells, such as macrophages and DETCs, to stimulate an acute inflammatory response to remove pathogen threats and damaged cells, and to communicate with epidermal keratinocytes, dermal fibroblast and vascular endothelial cells to start epidermal proliferation, dermal extracellular matrix deposition and wound contraction via releasing cytokines and growth factors. The timing of inflammation is tightly controlled to allow healing proceed with proliferation phase. Persistent inflammation infiltrate could impact this coordinated process and lead to massive scar formation (Guo and DiPietro, 2010; Martin and Leibovich, 2005).

I hypothesize that some currently poorly defined immune cells, such as ILC3s, a novel group of innate lymphoid cells recently found to promote epithelial repair in intestine via IL-22 (Luci et al., 2009; McGee et al., 2012; Sonnenberg et al., 2012), other than macrophages (Stout, 2010) or DETCs (Jameson et al., 2002; Macleod and Havran., 2011) may play a uncovered role in skin repair. Recently a skin study suggests dermal fibroblasts require IL-22 signal to start differentiation and skin repair (MacGee et al., 2013). However, the role of IL-22 in epidermal compartment and the source of IL-22 in skin wound healing have not been determined. It is possible that this possible key signal in skin repair could be provided by ILC3s as demonstrated by recent studies in intestinal repair (Luci et al., 2009; Sonnenberg et al., 2012). It is possible that ILC3s also be recruited in wound inflammatory phase and produce IL-22 in skin, which orchestrates skin repair by mediating the



interaction between immune cells, epidermal keratinocytes and dermal fibroblasts. I will examine the presence of ILC3s in post injury skin, determine the role of ILC3s (ROR $\gamma$ <sup>+</sup>ILCs) in wound healing by comparing the wound closure rate between ROR $\gamma$ <sup>-/-</sup> mice and wild type mice, and study the mechanism of how ILC3s mediates skin repair.

I also hypothesize epidermal Notch signaling might be involved in skin wound healing by promoting a prompt inflammation reaction and mediating the interaction between keratinocytes and immune cells. Previous studies suggests a role of Notch signaling in promoting skin wound healing by using pan-Notch inhibitor (Chigurupai et al., 2007). However, the underlying mechanism is less clear, and the individual roles of Notch1 and Notch2 are unknown due to lack of appropriate agents. Recent studies showed forced activation of epidermal Notch signaling promotes dermal accumulation of immune cells via epidermal production of TNF- $\alpha$  and stimulates epidermal proliferation via a mechanism that is less clear (Ambler and Watt 2010; Estrach et al., 2006). These two striking phenotypes highly resemble the remarks of inflammation and proliferation stages of wound healing. It is possible that Notch signaling might play a role in recruitment of ILC3s that produce IL-22, which might in turn activate epidermal epithelial cells to proliferate as it does in intestinal epithelial cells (Luci et al., 2009; McGee et al., 2012; Sonnenberg et al., 2012). Therefore, I will examine the correlation between ILC3s and Notch activity using Notch activation and blocking models. With the recent progress in development of Notch individual antibodies, I will be able to study the individual roles of Notch1 and Notch2 signaling in ILC3 recruitment (Wu et al., 2010). I will also determine the mechanism of how Notch signaling, via TNF- $\alpha$ , regulates ILC3 recruitment.

## Chapter 2 Methods

### 2.1 Research animals

K14NICDER,  $ROR\gamma^{GFP/GFP}$  ( $ROR\gamma^{-/-}$ ),  $Rag2^{-/-}$ ,  $CD11c^{Cre}Rosa26^{iDTR}$  and  $CXCL13^{-/-}$  mice have been described previously (Ambler and Watt, 2010; Ansel et al., 2000; Buch et al., 2005; Estrach et al., 2006; Johnston et al., 2013; Jung et al., 2002; Luther et al., 2000; Sun et al., 2000). All experimental procedures were performed with ethical permission by Durham Universities under appropriate UK government Home Office licenses. Experiments followed the national and institutional guidelines for the care and use of animals based on the Animal [Scientific Procedures] Act 1986. In every experiment mice were age and sex matched with wild type littermate controls used when possible and within each experiment 3 or more mice per genotype/experimental group were included. Experiments were repeated 2 to 4 times to confirm results. The majority of mice reported were females between 6 and 9 weeks of age. Occasionally, male mice or mice between 9 and 18 weeks were included in an experiment, however RNA and protein analysis was performed on age and sex-matched tissues and analysis was performed amongst experimental replicates where appropriate. Mice were housed in pathogen-free facilities and had access to food and water. In K14NICDER mice, estrogen-inducible ectopic Notch activity (i.e. fragment of Notch1 intracellular domain (NICD1) was induced and activated specifically in epidermal basal cells under the control of Keratin 14 (K14) promoter by topical application of 2mg of 4-hydroxytamoxifen (4OHT, H6278 from Sigma) dissolved in acetone (Figure 2.1). In  $ROR\gamma^{GFP/GFP}$  ( $ROR\gamma^{-/-}$ ) mice, a 200-bp fragment containing the exon encoding the DNA-binding domain of  $ROR\gamma$  gene was replaced with the 1.2-kb neomycin resistance gene and flanking a coding sequence of enhanced green fluorescence protein (eGFP) (Sun et al., 2000).  $ROR\gamma^{-/-}$  were born

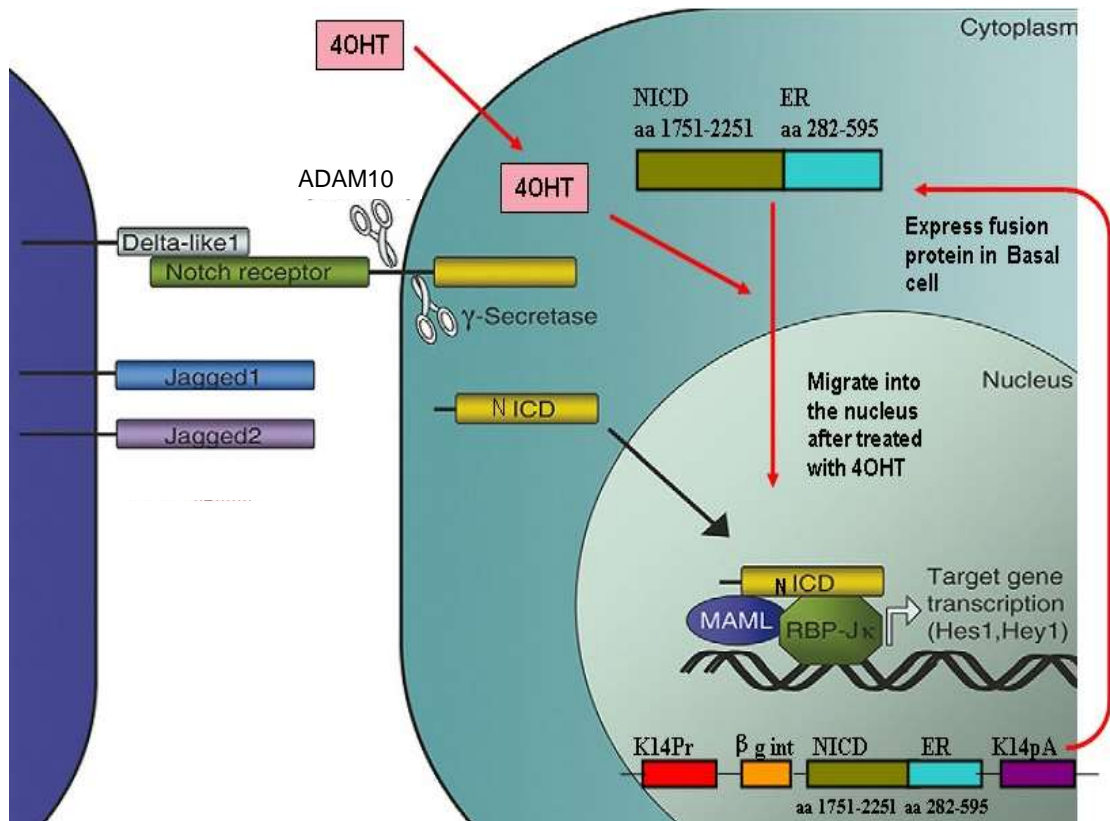


**Figure 2.1 Ectopically activated Notch signaling in 4OHT treated K14NICDER mice** (Adapted from Estrach et al., 2006; Watt et al., 2008). Black arrow represents normal Notch signaling. Red arrow represents ectopically activated Notch signaling. In K14NICDER mice, ectopic Notch1 intracellular domain is specifically induced in basal cells of epidermis under the control of keratin 14 promoter (K14Pr) and enters nucleus to activate Notch signaling when a chemical drug 4-hydroxytamoxifen (4OHT) is topically applied. To make this transgenic model, a vector containing the sequence encoding amino acid 1751-2290 of NICD1 and a modified 4OHT responsive human oestrogen receptor (ER) was generated. For stabilizing its transcript, a rabbit  $\beta$ -globin untranslated region (UTR) encompassing a human  $\beta$ -globin gene intronic sequence to a BamHI site ( $\beta$ g int), K14 UTR and polyadenylation signal from human K14 mRNA (K14pA) was added into this vector. Then this stable NICDER construct was sub-cloned into the BamHI restriction site of the K14 promoter cassette and injected into the pronucleus of F1 embryos.

healthy, had no discernible physical defect, and were fertile. However, these mice completely lack lymph nodes and Peyer's patches (Sun et al., 2000). Mice heterozygous for this targeted mutation  $ROR\gamma^{+/-}$  ( $ROR\gamma^{+eGFP}$ ) were used as controls by breeding  $ROR\gamma^{-/-}$  mice to wildtype C57Bl/6 mice. In  $Rag2^{-/-}$  mice, mature T and B cells are depleted (Hao and Rajewsky, 2001).  $CD11c^{Cre}Rosa26^{iDTR}$  mice were produced by cross-breeding  $B6.Rosa26^{iDTR}$  mice to  $B6.CD11c^{cre}$  mice. In  $CD11c^{Cre}Rosa26^{iDTR}$  mice, Cre recombinase is expressed under the control of CD11c promoter permitting the expression of induced simian Diphtheria Toxin Receptor (iDTR) in  $CD11c^{+}$  cells (Buch et al., 2005; Jung et al., 2002). When being treated with 100 nanograms of Diphtheria Toxin (DT) (D0564, Sigma) per mouse via intraperitoneal (*i.p.*) injection for 4 consecutive days before wounding, mouse  $CD11c^{+}$  cells are killed by DT via uptake through Cre-induced iDTR.  $CXCL13^{-/-}$  mice do not display any gross physical or behavioral abnormalities but have defects in lymphoid tissue (e.g. lymph node) development (Luther et al., 2000).

## 2.2 Wound healing

Mice were anesthetized using 2% inhaled isoflurane and then injected subcutaneously with the analgesic, Vetergesic (0.05mg/kg, Alstoe Animal Health). The back skin was shaved and sterilized with Videne surgical scrub (from Ecolab) then rinsed with sterile water. Two full-thicknesses, 4mm diameter back skin wounds were made using a punch biopsy (from Stiefel) (Figure 2.2). Some wounds were then topically treated daily with recombinant  $TNF\alpha$  (8  $\mu$ g/kg, product code: PNRMTNFAI, Thermo Scientific Pierce),  $TNF\alpha$  antagonist (10 mg/kg, Adalimumab, Humira, Abbott Laboratories) or PBS until humanely sacrificed 2 days or 5 days post-wounding. Some mice were *i.p.* injected with anti-NRR1 (5mg/kg, from

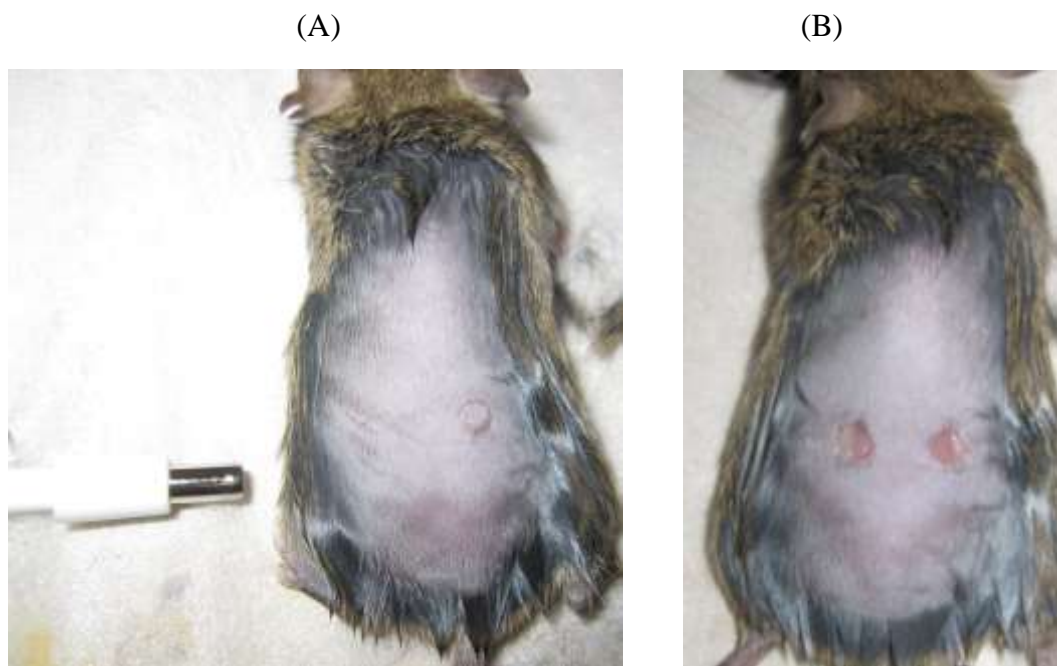


**Figure 2.2 Surgical wounding model.** (a) Full thickness-skin wounds were created by using a 4mm punch biopsy on mouse back skin with hairs shaved. (b) Mice with two wounds on back skin were kept up to 8 days post injury for examining the wound closure rate, cytokine production profile and immune cell recruitment.

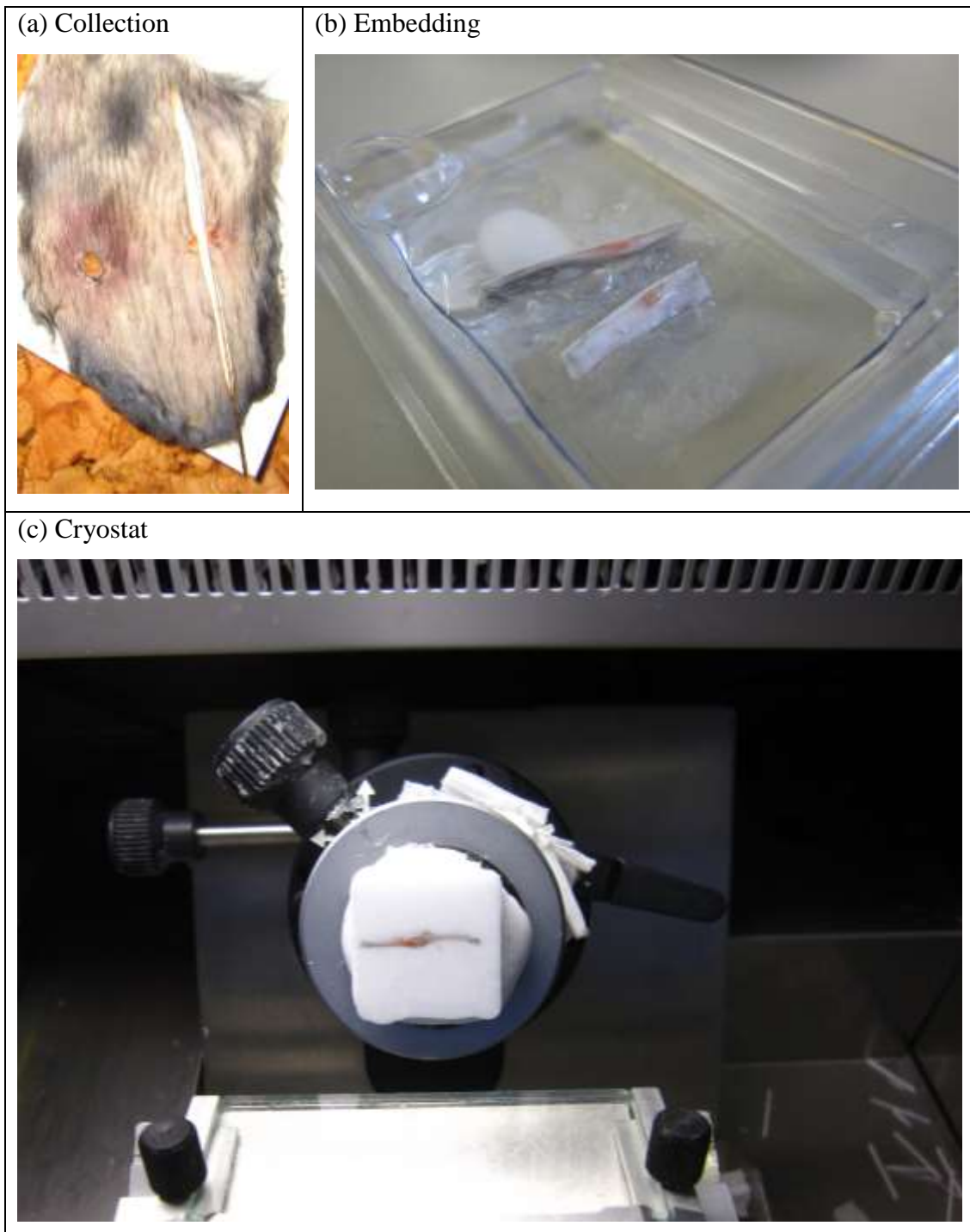


**Figure 2.3 Collection and frozen sectioning of skin wounds.** (a) Back skin from wounded mice was collected. (b) 1.5cm x 0.5cm piece of skin sample including half a wound and surrounding area was immersed into optimal cutting temperature compound (OCT) in a 24cm x 24cm mold before being frozen in liquid nitrogen or in cold isopentane. (c) Frozen sample was cut into 8 micron sections using a cryostat.

Genotech), anti-NRR2 (5mg/kg, from Genotech), or both anti-NRR1 and anti- NRR2 (2.5mg/kg for each), or control (anti-ragweed, 5mg/kg, from Genotech) for 7 days prior to wounding and then every 2 to 3 days post-wounding for the duration of the experiment (Wu et al., 2010). CD11c<sup>Cre</sup>Rosa26<sup>iDTR</sup> mice were treated with 100ng/mouse DT via *i.p.* for 4 consecutive days prior to wounding. Some ROR $\gamma$ <sup>-/-</sup> mice received splenocyte transplantation 1 day prior to wounding. In these ROR $\gamma$ <sup>-/-</sup> mice 1x10<sup>6</sup> cells harvested from Rag2<sup>-/-</sup> spleen were injected via tail vein. Wounds were photographed daily using a Canon digital camera.

### **2.3. HE staining and antibody labeling**

Back skin tissue was collected and processed as previously described (Figure 2.3) (Braun et al., 2003; Estrach et al., 2006). For Haematoxylin and Eosin (HE) staining, 8 $\mu$ m-thick paraffin sections were dewaxed by immersing into xylene, ethanol and distilled water sequentially and stained with Harris' haematoxylin for 10 minutes. Then sections were washed and stained with Eosin for 30 seconds. Finally, the slides were mounted with DPX media (06552, Sigma). For antibody labeling, 8 $\mu$ m-thick frozen or paraffin sections were fixed in 4% or 0.4% paraformaldehyde (PFA) for 15 minutes, blocked in 10% goat or donkey serum, 0.25% fish skin gelatin and 0.2% bovine serum albumin for 30 minutes, and then stained with the following antibodies diluted in blocking solution (dilutions in brackets) for 1 hour or overnight: activated Notch1 (1:200, Abcam, ab8925), Activated Notch2 (1:200, Abcam, ab8926), CD3 (1:100, BD Biosciences, clone 17A2), CD4 (1:100, BD Biosciences, clone RM4-5), CD8a (1:100, BD Biosciences, 53-6.7), CD11b (1:100, BD Biosciences, clone M1/70), CD11c (1:100, Biolegend, clone N418), CD19 (1:100, BD Biosciences, clone 1D3), CD117 (also known as C-kit, 1:100, BD Biosciences, clone 2B8),

CD127 (also known as IL7R, 1:100, eBiosciences, clone SB/199), CD207 (also known as Langerin, 1:100, eBioscience); F4/80 (1:100, eBiosciences, clone BM8), Gr-1 (Ly-6G, 1:100, eBiosciences, clone BR6-8C5), NKp46 (also known as CD335, NCR1, 1:100, eBiosciences, clone 29A1.4), Ki67 (1:400, NeoMarkers), CXCL13 (also known as BLC, BCA-1, 1:300, eBiosciences, polyclone). Tissue sections were stained with appropriate fluorescent secondary antibodies (1:1000, Invitrogen), counterstained with DAPI and mounted with Mowiol (2.4g Mowiol, 6g glycerol, 12.5ml Tris pH8.5, topping up to 50ml with water) before imaging tissues using a Leica Tandem SP5 confocal microscope. To detect ROR $\gamma$ , 8 $\mu$ m frozen sections were fixed in 4% PFA for 10 minutes then incubated with antibody as described above. Sections were incubated with PE-conjugated ROR $\gamma$  antibody (eBiosciences, clone AFKJS-9, Cat. 12-6988-82) diluted to 1:100 in permeabilization buffer (eBiosciences, Kit 00-5521) for 1 hour. Brightness of images was adjusted using Adobe Photoshop CS3 software.

#### **2.4 Isolation of cells for flow cytometry**

A 4-5 cm<sup>2</sup> piece mouse back skin was removed then dermal surface was gently scraped to remove subcutaneous fat and muscle. Tissue was floated in freshly-prepared 2mg/ml dispase (17105-041, Invitrogen) 0.01% DNase I (Roche) in Roswell Park Memorial Institute (RPMI) 1640 medium (R8758, Sigma) with dermal side down overnight at 4°C. The following day, epidermis was separated from dermis using forceps, then dermis was chopped into tiny pieces and dermis and/or epidermis were incubated with 1mg/ml collagenase type I (17100-017, Invitrogen) and collagenase type II (LS004176, Worthington) in RPMI 1640 media in an orbital mixer for 2 hours at 37°C. After incubation the suspension of digested tissue was put



through a 70µm strainer to isolate single cells. Thymocytes were collected by gentle disruption of the thymus in RPMI media. Cutaneous lymph nodes from axillary and inguinal regions and splenocytes were collected by using a syringe to gently smash the tissue through cell strainer. Then splenocytes were subjected by incubation with red blood cell lysis buffer (0.15M NH<sub>4</sub>Cl, 1mM NaHCO<sub>3</sub>, 0.1mM EDTA) for 1 minute. Cell suspensions from all types of tissue were pelleted and re-suspended in 0.5% BSA in PBS prior to antibody staining for flow cytometry.

## **2.5 Antibody staining for flow cytometry**

Antibody staining was performed in 96-well V-bottom plates with the following antibodies: CD3 Alexa-647 (BD Bioscience, clone 17A2) or Allophycocyanin-Cyanine 7 (APC-Cy7) (Biolegend, clone 17A2), CD4 Alex-488 or Phycoerythrin (PE) or Allophycocyanin (APC) (BD Bioscience, clone RM4-5), CD5 (BD Biosciences, clone 53-7.3), CD8a PE (BD Biosciences, clone 53-6.7) or APC, CD11b Alexa-647 (BD Bioscience, clone M1/70), CD19 Alexa-647 or PE-Cy7 (BD Biosciences, clone 1D3), CD21 Alexa 647 (BD Bioscience, clone 7G6), CD23 Alexa 488 (BD Bioscience, clone B3B4), CD45 Peridinin Chlorophyll (PerCP) (BD Biosciences, clone 30-F11) or pacific blue (Biolegend, clone 30-F11), CD45R PerCP (also known as B220, BD Bioscience, clone RA3-6B2), TCR-β PE-Cy7 (Biolegend, clone H57-597), Vγ3 APC (Biolegend, clone 536), Gr-1 FITC (Biolegend, clone BR6-8C5), CD11c PE (Biolegend, clone N418), F4/80 PE-Cy7 (Biolegend, BM8), CD127 PE or APC (Biolegend, clone SB/199), NK1.1 PE-Cy5 (Biolegend, clone PK136), NKp46 Alexa-647 (eBiosciences, clone 29A1.4), CD117 PE-Cy7 (BD Bioscience, clone 2B8) incubated with cells for 1 hour on ice. Following surface labeling, cells were prepared for intracellular staining and fixed overnight in Fixation

buffer (kit 00-5521, eBiosciences). After incubation, PE-conjugated ROR $\gamma$ t antibody was added to the cells for 1 hour with permeabilization buffer (00-5521, eBiosciences) before analyzing cells. Cells were analysed using a FACSCaliber Flow Cytometer (BD Bioscience) or CYAN (Beckman-Coulter).

## **2.6 Protein extraction/ Western blotting**

Pieces of back skin (0.5-1 cm<sup>2</sup>) were snap-frozen in liquid nitrogen and stored in -80°C freezer. Frozen tissue was homogenized in Radio-immunoprecipitation Assay (RIPA) buffer [150 mM NaCl, 50 mM Tris-HCl (pH 7.5), 1% Nonidet P-40, 0.25% sodium deoxycholate with cComplete, Mini, EDTA-free proteinase inhibitor cocktail tablet (1 tablet in 10ml RIPA buffer, product No. 04693159001, Roche)]. Lysates were run on a 10% gradient polyacrylamide gel (Invitrogen), transferred to polyvinylidene difluoride (PVDF) membrane, blocked with 3% cold water fish skin gelatin (Sigma)/0.2% Tween-20/PBS or 5% powdered skimmed milk/0.2% Tween-20/PBS and hybridised with antibodies to activated Notch1 (ab8925, 1:400, Abcam), activated Notch2 (1:400, Abcam, ab8926) or beta-actin (A5441, 1:3000, Sigma). Blots were rinsed in 0.2% Tween-20/PBS, incubated with horseradish peroxidase (HRP)-conjugated anti-rabbit or anti-mouse secondary antibody (Sigma) and visualized with enhanced chemiluminescence (ECL) Western Blotting Substrate (Pierce). Following film detection of blots, band intensity was quantified using ImageJ and the mean band intensity value was calculated against the loading control.

## **2.7 RNA extraction**

RNA extraction methods have been described previously (Ambler and Watt, 2010). In summary, freshly-isolated tissues were immediately snap-frozen in liquid nitrogen

or immersed in RNAlater (Invitrogen) for 24 hours prior to freezing. Tissues were homogenized using polytron tissue homogenizer then RNA was isolated using a Qiagen, RNeasy Mini Kit following manufacturer's instructions including the optional, on-column DNase I digestion step. An additional proteinase K digestion step was performed in the protocol. Briefly, after homogenising lysates in Qiagen RLT buffer (from RNeasy Mini kit) + 1%  $\beta$ -mercaptoethanol (BME), 40 microliters of proteinase K (20mg.ml, P6556, Sigma) and RNase-free water were added to a final volume of 1.8 ml and incubated at 55°C for 10 minutes. RNA concentrations were quantified using a Nanodrop microspectrophotometer and cDNA prepared using a High Capacity cDNA Reverse Transcription Kit (Cat. 4368814, Life Technology).

## **2.8 Quantitative polymerase chain reaction (QPCR)**

To quantify the mRNA levels of IL-22, IL-23a (p19), CCL20 and TNF $\alpha$ , QPCR was performed using a Rotor-Gene Q instrument (Qiagen), with a two-step rapid-cycling procedure as described by the manufacturer (Rotor-Gene Probe Handbook, Qiagen). Triplicate reactions (20 microlitre) of each experimental sample were analysed using fluorescein amidite (FAM) probes for the gene of interest (TNF $\alpha$ , Mm00443258.m1; CCL20, Mm01268754.m1; IL23a (P19), Mm01160011.g1, Life Technologies) at a final concentration of 900 nM for each primer and 250nM for the probe and TaqMan Fast Universal PR master mix (ABI) at 1x. Reactions were subjected to an initial 3-minute denaturation step at 95°C, followed by 45 cycles of 95°C for 3 seconds and 60°C for 10 seconds. Data was analysed using the Comparative Quantitation algorithm in the Rotor-Gene software, with calibrator samples for each run being compared in a common experiment. MIP1 $\alpha$  and IL-22 mRNA levels were examined

using unlabelled primers (MIP1 $\alpha$ : Forward 5'-GTTCTTCTCTGTACCATGAC-3'; Reverse 5'-CTCTTAGTCAGGAAAATGAC-3', final concentration 400 nM; IL-22: PPM05481A-200, Qiagen) in a reaction using SYBR-green master mix (Sigma). Reactions were subjected to an initial 3-minute denaturation step at 95°C, followed by 45 cycles of 95°C for 10 seconds, 60°C for 10 seconds and 72°C for 10 seconds. Reference genes Glyceraldehyde 3-phosphate dehydrogenase (GAPDH) and  $\beta$ -2 microglobulin (B2M) were used to quantify genes of interest.

## **2.9 Primary dermal cells**

Primary mouse fibroblasts were isolated using a method based on Jahoda and Oliver (1984). In brief, after sacrificing the mouse, the back skin hair was clipped and then the skin tissue was washed in Dulbecco's modified Eagle's medium (DMEM) (Invitrogen) with double strength antibiotics (2x Pen/Strep - Penicillin 100 Unit/ml Streptomycin 100  $\mu$ g/ml, Fisher). The fat and non-dermal tissue was gently scrapped from the tissue before cutting into pieces of approximately 10mm<sup>2</sup>. Each piece of tissue was cut repeatedly using curved blade scissors until it became slurry and the tissue was spread onto the bottom of a 6-well plate. The tissue was then covered with DMEM + 10% fetal calf serum (FCS, PAA Laboratories) and 1x Pen/Strep and placed in a 37°C incubator at 5% CO<sub>2</sub>. After 12 days cells were passaged.

Then passaged (P1) mouse fibroblasts when 90% confluent were treated with either TNF $\alpha$  (20 ng/ml, product code: PNRMTNFAI, Thermo Scientific Pierce), TNF $\alpha$  antagonist (50  $\mu$ g/ml, Adalimumab, Humira, Abbott Laboratories) or both diluted in DMEM + 10% FCS and 1x strength Penicillin/Streptomycin. Some passaged (P1) cells were left untreated. Cells were incubated for an additional 24 hours then lysed

by using Qiagen RLT buffer (Qiagen RNeasy Mini Kit) + 1% BME and RNA collected using an RNeasy Mini Kit (Qiagen) following the manufacturer's protocol.

## **2.10 Systems Biology Analysis of Gene Expression Data Sets**

To determine the key signaling pathways involved in Notch-mediated wound healing, unbiased analysis of gene arrays from ROR $\gamma^+$  innate lymphoid cells (NIH GEO: GSE29777, in Reynders et al., 2011 and unpublished results) and from uninjured, K14NICDER transgenic mouse back skin epidermis and dermis (NIH GEO: GSE23782, in Ambler and Watt, 2010) was used. The MAS5-processed datasets of differentially expressed genes were imported into Ingenuity Pathway Analysis software (Ingenuity® Systems, [www.ingenuity.com](http://www.ingenuity.com)) for analysis. All secreted, skin-derived factors that could interact with a cytokine or chemokine receptor on ILCs were determined. The highly upregulated genes in the epidermis and the dermis were filtered by the "extracellular matrix" gene ontology term. Ingenuity Pathway Analysis was used to build direct connections from the upregulated genes to their possible target receptors. The genes displayed in Figure 6.1 were further selected to show the most probable/relevant/interesting interactions between secreted factors and their target receptors.

## **2.11 Statistical Analysis**

For western blotting and mRNA quantification samples were normalized where the average of uninjured skin control unless otherwise stated was designated as 1 or 100%. Independent samples from at least 3 individual animals or wounds were used

to calculate group averages. Standard error of the mean (SEM) was calculated and significance determined using a Student's t-test to compare the means of two unpaired samples. Results are shown as mean  $\pm$  SEM. In figure legends, \* denotes p value  $< 0.05$ ; \*\* denotes p value  $< 0.005$ ; \*\*\* denotes p value  $< 0.0005$  unless otherwise stated.

## **Chapter 3 Involvement of immune cell in normal skin wound healing**

### **3.1 Introduction**

Skin wound healing is a coordinated and sequential process which is initiated by inflammation phase where a large number of immune cells either migrate from adjacent skin or are recruited by chemokines from blood circulation into the wound site and are activated by cytokines to clear damaged cells, debris and pathogens (Martin and Leibovich, 2005). This inflammatory reaction is thought to be largely mediated by innate immune system, especially professional phagocytes such as neutrophils and macrophages (Rodero and Khosrotehrani 2010; Stout, 2010). By contrast, antigen-specific adaptive system including conventional  $\alpha\beta$  T cells and B cells, is considered not to be significantly involved in wound healing (Stout, 2010). Neutrophils are the earliest immune cell type that are recruited into wound site within hours, while blood-derived macrophages arrives at wound site approximately day 2 post-wounding to perform intensive phagocytosis of wound debris and microbes and apoptotic short-life neutrophils (Stout, 2010). However, the evidence for the infiltration of skin wound by the other cells of innate immune system, such as NK cells, dendritic cells, etc., is less clear (Liu et al., 2012).

In addition to promote inflammation after injury, some immune cells have shown roles in tissue regeneration by communicating with other cell types. Wound associated M2 macrophages, via TGF $\beta$ , contact dermal fibroblasts to activate their differentiation into myofibroblasts that are in charge of producing matrix collagens and wound contraction (Rodero and Khosrotehrani, 2010). DETCs contact keratinocytes to promote their proliferation after damage via IGF-1 and KGF, and promote macrophage recruitment via hyaluronan (Jameson et al., 2002; Macleod and

Havran, 2011). Given the new evidence that subsets of emerging ROR $\gamma$ t<sup>+</sup> innate lymphoid cells (ILC3s) play key roles in epithelial tissue homeostasis and repair in thymus and intestine after damage or infection via producing IL-22 (Dudakov et al., 2012) and IL-22 contributes to epidermal proliferation during skin wound healing (McGee et al., 2012), I hypothesize ILC3s might be present in skin and involved in skin wound healing through IL-22 production.

To examine the presence and involvement of individual immune cell subsets in skin wound healing, flow cytometry and immunofluorescence chemistry were performed using a variety of antibodies to analyze the quantification and location of well-defined immune cell types, such as neutrophils (CD11b<sup>+</sup>CD11c<sup>-</sup>Gr-1<sup>+</sup>F4/80<sup>-</sup>), mature macrophages (CD11b<sup>+</sup>CD11c<sup>-</sup>Gr-1<sup>-</sup>F4/80<sup>+</sup>), conventional dendritic cells (cDC, CD11b<sup>+/+</sup>CD11c<sup>high</sup>), Langerhans cells (LC, CD11b<sup>+</sup>CD11c<sup>low</sup>), inflamed monocytes (CD11b<sup>+</sup>CD11c<sup>-</sup>Gr-1<sup>+</sup>F4/80<sup>+</sup>, which give rise to macrophages, cDC and possibly LC), NK cells (NK1.1<sup>+</sup>NKp46<sup>+</sup>CD3<sup>-</sup>), NK-like T cells (NKT cells, NK1.1<sup>+</sup>NKp46<sup>+</sup>CD3<sup>+</sup>), dendritic epidermal T cells (DETCs, CD3<sup>+</sup>TCR $\beta$ <sup>-</sup>V $\gamma$ 3<sup>+</sup>),  $\alpha\beta$  T cells (CD3<sup>+</sup>TCR $\beta$ <sup>+</sup>V $\gamma$ 3<sup>-</sup>), dermal  $\gamma\delta$  T cells (CD3<sup>+</sup>TCR $\beta$ <sup>-</sup>V $\gamma$ 3<sup>-</sup>) and B cells (CD19<sup>+</sup>) as well as ILC3s (ROR $\gamma$ <sup>+</sup>CD127<sup>+</sup>CD3<sup>-</sup>) at different time-points following wounding in wildtype mouse back skin. To determine the phenotypical markers and subsets of ROR $\gamma$ t<sup>+</sup> ILCs in skin, punch-wounded wildtype as well as GFP-expressing ROR $\gamma$ <sup>+/+</sup> mice were analyzed.

## **3.2 Results**

### **3.2.1 Timing of the healing process of skin wound**



To examine skin wound healing process, wounded mouse model was used. Two 4-mm diameter full-thickness wounds were made by using punch biopsy on wildtype mouse back skin. Wounded skin including central wound as well as surrounding area was collected on day 2, 5 and 8 post-wounding representing the early, middle and late stages of wound healing. To examine the histology of normal healing of skin wound, skin sections were analyzed by using hematoxylin and eosin (HE) stainings. On day 2, the wound was covered by a clot (Figure 3.1A) composed of platelets and fibrin (Martin and Leibovich, 2005). The cellular density in dermis at the wound edges is increased resulting from infiltration of immune cells (Figure 3.1E) and other cell types (Martin and Leibovich, 2005). Epidermis at the wound edges was slightly thickened (Figure 3.1A) suggesting epidermal proliferation had just started, which is consistent with the fact that the wound healing is a coordinated process, sequential inflammation and proliferation phases in wound healing are somewhat overlapped (Martin and Leibovich, 2005). On day 5, hyper-thickening of epidermis was detected underneath the clot and migrated towards the wound (Data not shown). Dermal cellular density was continuously increased resulting from persistent inflammation infiltration (Figure 3.1F), granular tissue generation and dermal matrix deposition (Martin and Leibovich, 2005). These results suggested the healing programme was in intensive proliferation phase on day 5 post-wounding. On day 8, the wound was almost closed and drawn up to the normal level parallel to the surrounding area (Figure 3.1B). This was accompanied by dramatically reduced immune cell infiltration (Figure 3.1G). These results suggested the healing programme had started remodeling phase.

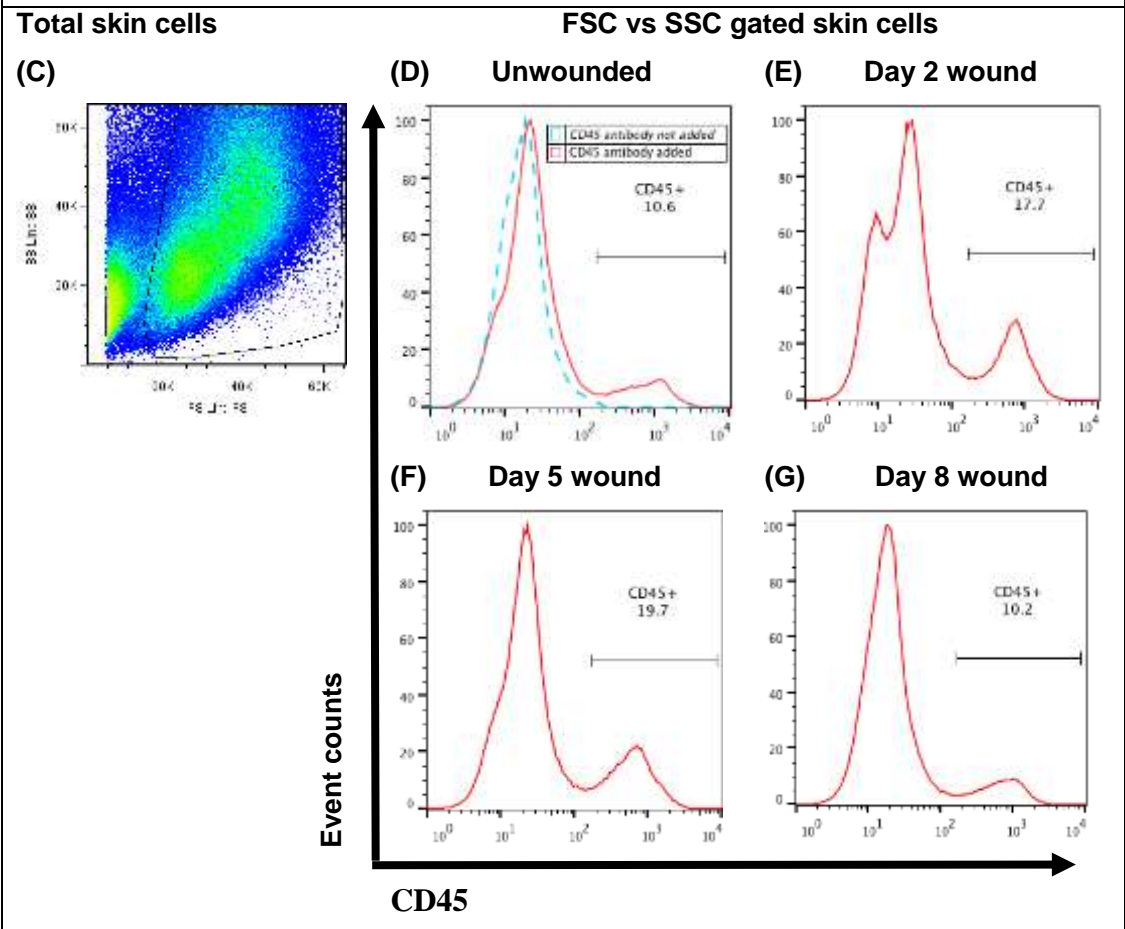
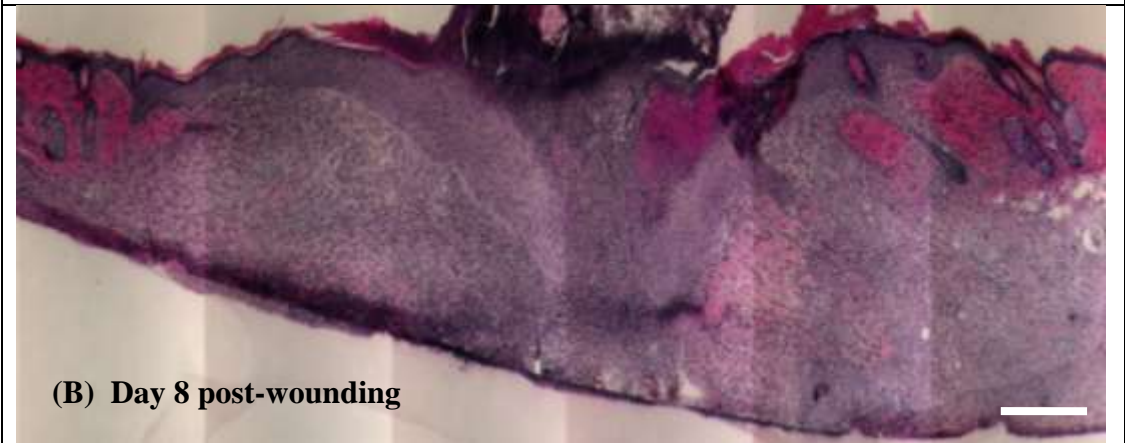
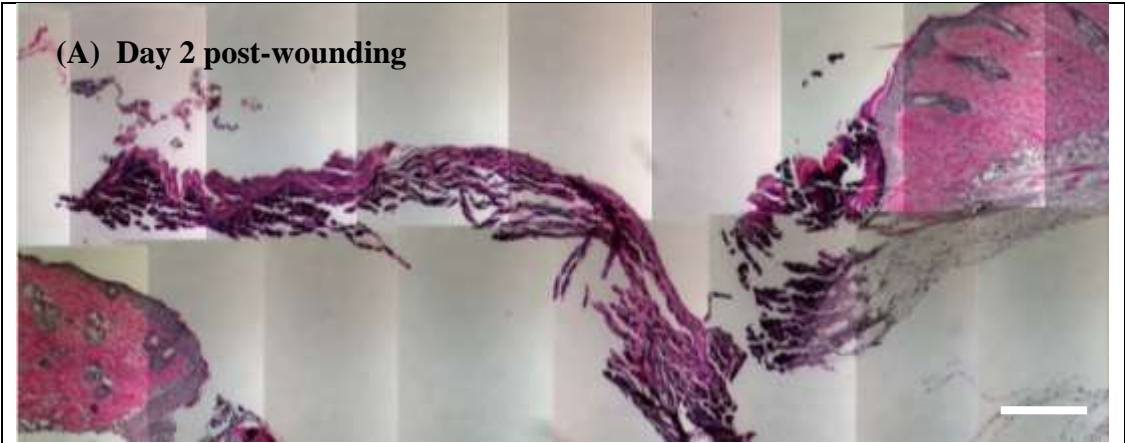


**Figure 3.1 Skin wound healing is initiated by immune response.** (A-B) Histology of wounded mouse back skin is shown by HE staining on paraffin sections at early stage (day 2 post-wounding) (A) and late stage (day 8 post-wounding) (B) of wound healing. (C-G) Cells isolated from wounded skin were analyzed by flow cytometry for CD45, a pan marker for immune cells. Total skin cells are first gated on forward scatter and side scatter to remove dead cells and debris (C). (D-G) show flow cytometry histograms of CD45 staining (red line) of total skin cells gated on FSC vs SSC from unwounded back skin (D), wounded back skin on day 2 (E), 5 (F) and 8 (G) post-wounding. Negative control without adding CD45 antibody is indicated in blue line. Gate frequencies are indicated in percentages. Shown one biological sample; 3 individual biological replicates were tested (not shown). Scale bars equal 300 micron.

To define the timing of inflammatory cell infiltration, wounded skin was analyzed for CD45, a pan cell surface marker for immune cells, by flow cytometry. A same size of skin with the same location in unwound mice was used as control. Total skin cells were gated by forward scatter (FSC) and side scatter (SSC) (Figure 3.1C). In unwounded skin, immune cells accounted for around 8-12% of total skin cells (Figure 3.1D), which represents the skin resident immune cells in steady state. This percentage was dramatically increased by nearly 2 fold by day 5 post-wounding (Figure 3.1F) with the sharpest rise within the first 2 days post-wounding (Figure 3.1E), confirming the inflammation phase is initiated early upon injury. On day 8 post-wounding, this percentage dropped back to unwounded level (Figure 3.1G) confirming the healing programme was in late proliferation phase and early remodeling phase.

Taken together, these results suggest the time-points day 2, day 5 and day 8 post-wounding represent intensive inflammation and proliferation phase, and the start of remodeling phase respectively wound healing process in mouse skin.

### **3.2.2 Myeloid cells**

To examine myeloid cells including granulocytes (mostly neutrophils), macrophages, monocytes, cDC and LCs, wounded skin were analyzed for CD11b (a marker for the majority of myeloid cells except CD11b<sup>-</sup>cDC), CD11c (expressed by cDC with high level and by LC with low level) (Romani et al., 2009), F4/80 (a marker for macrophages, monocytes, Langerhans cells as well as CD11b<sup>+</sup> cDC), and Gr-1 (a maker for neutrophils and inflamed (activated) monocytes which give rise to mature macrophages and cDC and possibly LC) (Auffray et al., 2009).

To distinguish cDC (CD11c<sup>high</sup> CD11b<sup>+/-</sup>) and LCs (CD11c<sup>low</sup> CD11b<sup>+</sup>) from the other myeloid cells (CD11c<sup>-</sup> CD11b<sup>+</sup>), I first analyzed their expression of CD11b and CD11c. A rare number of CD11c<sup>high</sup> cDCs were detected in unwounded skin, accounting for 0.1-0.2% of total skin cells (Figure 3.2A). This percentage was increased by  $1.7 \pm 0.2$  fold on day 2 post-wounding (Figure 3.2C) arising from derivation from inflamed monocytes (Figure 3.2D) and dropped back to unwounded level on day 5 and day 8 (Figure 3.2E and G), suggesting cDCs are present in skin wound healing especially at early stage of inflammation. To confirm the location of DCs, skin sections were analyzed using CD11c antibody which could detect both CD11c<sup>high</sup> cDCs and CD11c<sup>low</sup> LCs. However, I was only able to detect CD11c<sup>+</sup> cells in dermis but not in epidermis where resident LCs are constantly present, suggesting these detectable CD11c<sup>+</sup> cells were uniformly CD11c<sup>high</sup> cDCs. CD11c<sup>high</sup> DC were detected in rare dermis in unwounded skin with an rounded morphology (Figure 3.3A and B), suggesting they were immature DC with high ability to phagocytose, poor motility and low potential for antigen presentation (Delves et al., 2011). However, an increased number of these CD11c<sup>high</sup> dendritic cells were detected in dermis adjacent to the wound on day 2 post-wounding (Figure 3.3C). The morphology of the cells which were immediately adjacent to the wound became dendritic, suggesting they were mature DC with poor ability to phagocytose but with high motility that had enabled them to migrate to wound site from distal area and wound enable them to migrate to the draining lymph nodes nearby to present antigen to T cells (Delves et al., 2011). In contrast, the cells which were not immediately adjacent to the wound remained rounded suggesting these immature DC might be recently derived from inflamed monocytes recruited to the wounded dermis (Figure 3.2D). On day 5 post-wounding, less CD11c<sup>high</sup> DC were detected in dermis

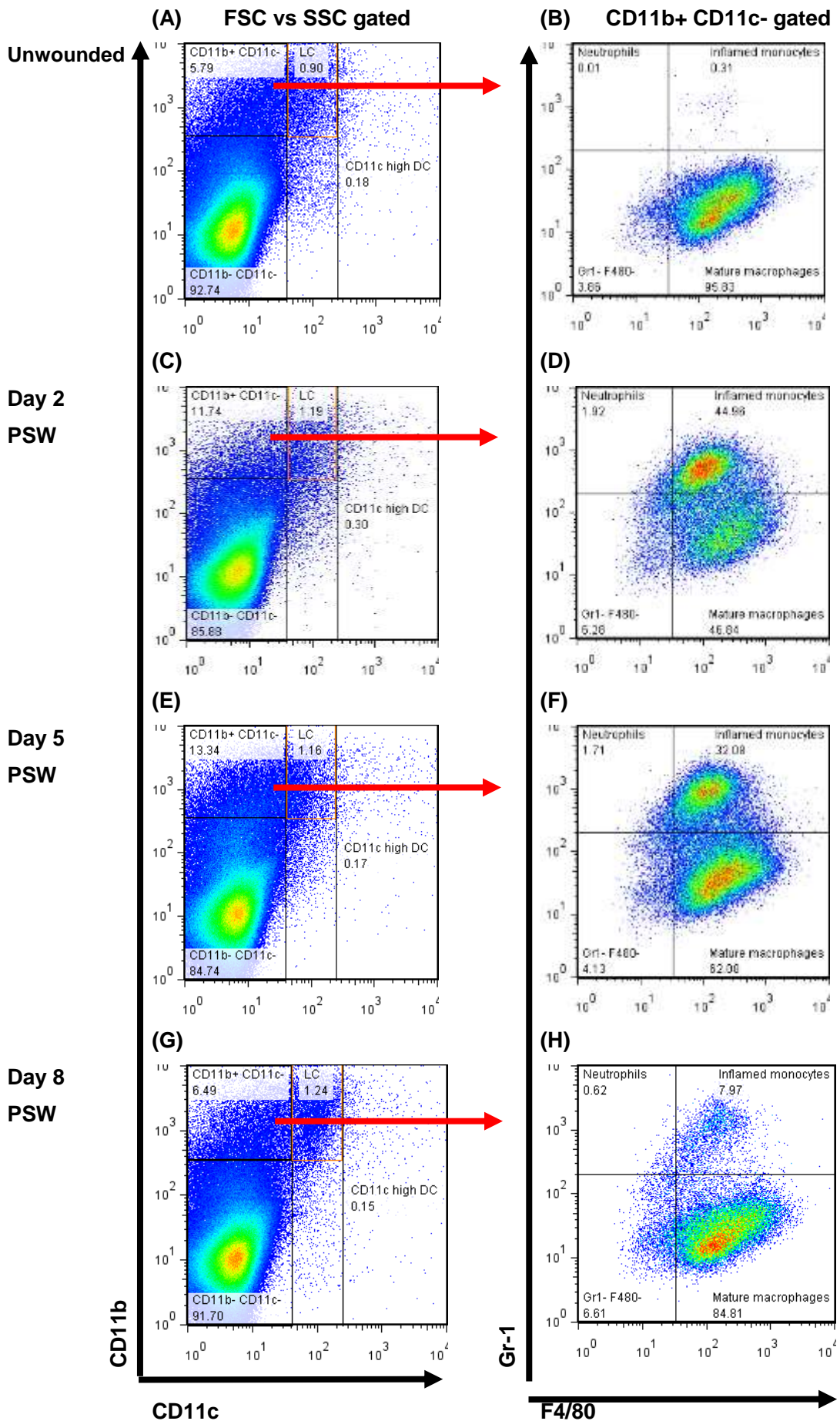
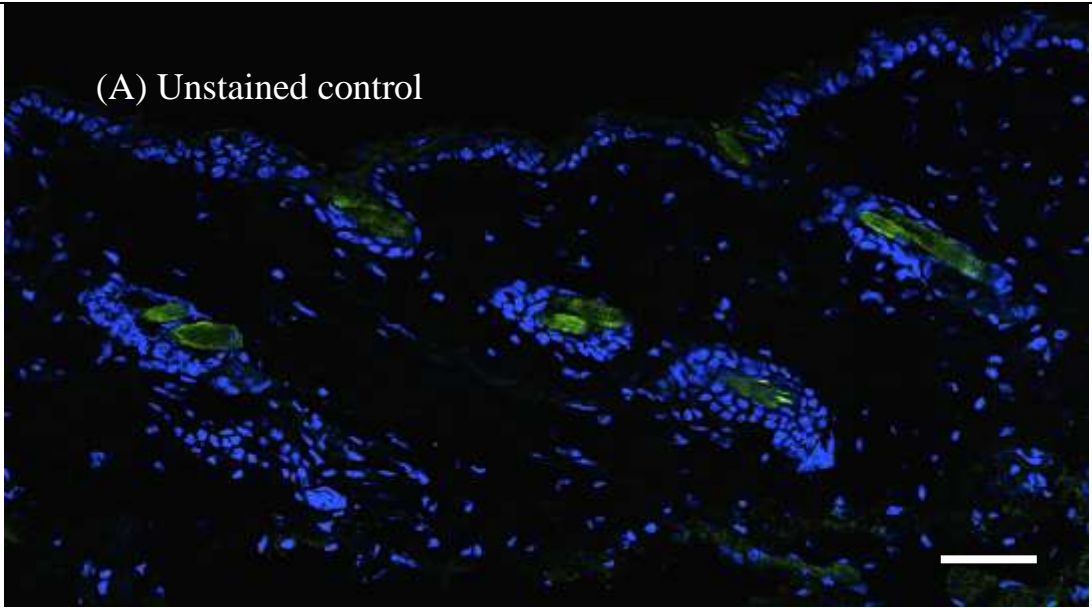


**Figure 3.2 Quantification of myeloid cells and dendritic/Langerhans cells in skin wounds.** Cells isolated from unwounded (A-B) as well as wounded mouse back skin on day 2 (C-D), 5 (E-F) and 8 (G-H) post-wounding were labelled with CD11b, CD11c, Gr1 and F4/80 antibodies and were first analyzed by flow cytometry for CD11c, CD11b to distinguish dendritic cells (DC) ( $CD11c^{high} CD11b^{+/-}$ ) and Langerhans cells (LC) ( $CD11c^{low} CD11b^{+}$ ) from the rest cells (A, C, E, G). Then  $CD11b^{+} CD11c^{-}$  myeloid cells were gated and analysed for F4/80 and Gr-1 to distinguish between neutrophils ( $Gr1^{+} F4/80^{-}$ ), mature macrophages ( $Gr1^{-} F4/80^{+}$ ) and inflamed monocytes ( $Gr1^{+} F4/80^{+}$ ). Gate frequencies are indicated in percentages. Shown one biological sample; 3 individual biological replicates were tested (not shown).

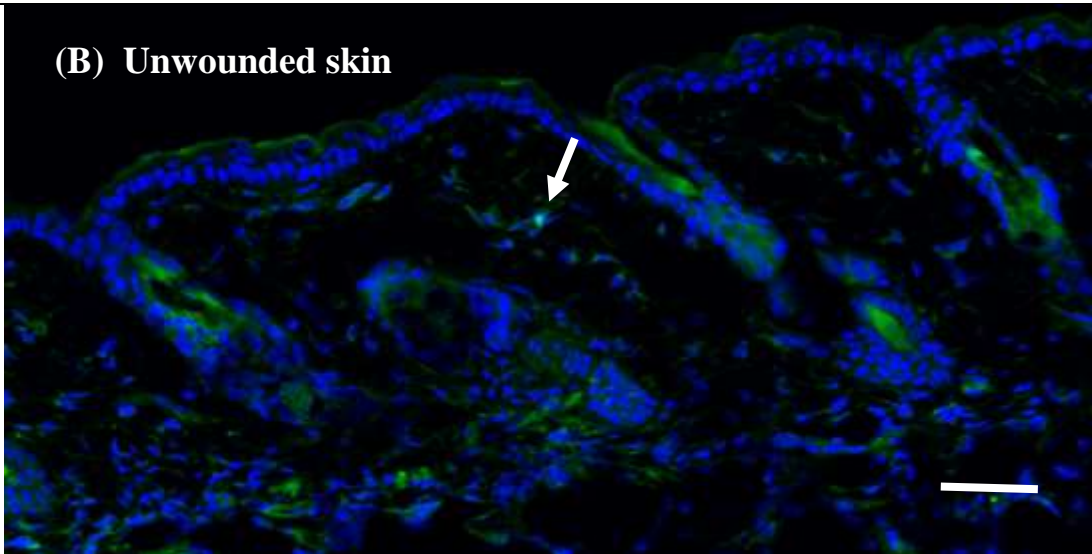


**CD11c DAPI staining**

**(A) Unstained control**



**(B) Unwounded skin**





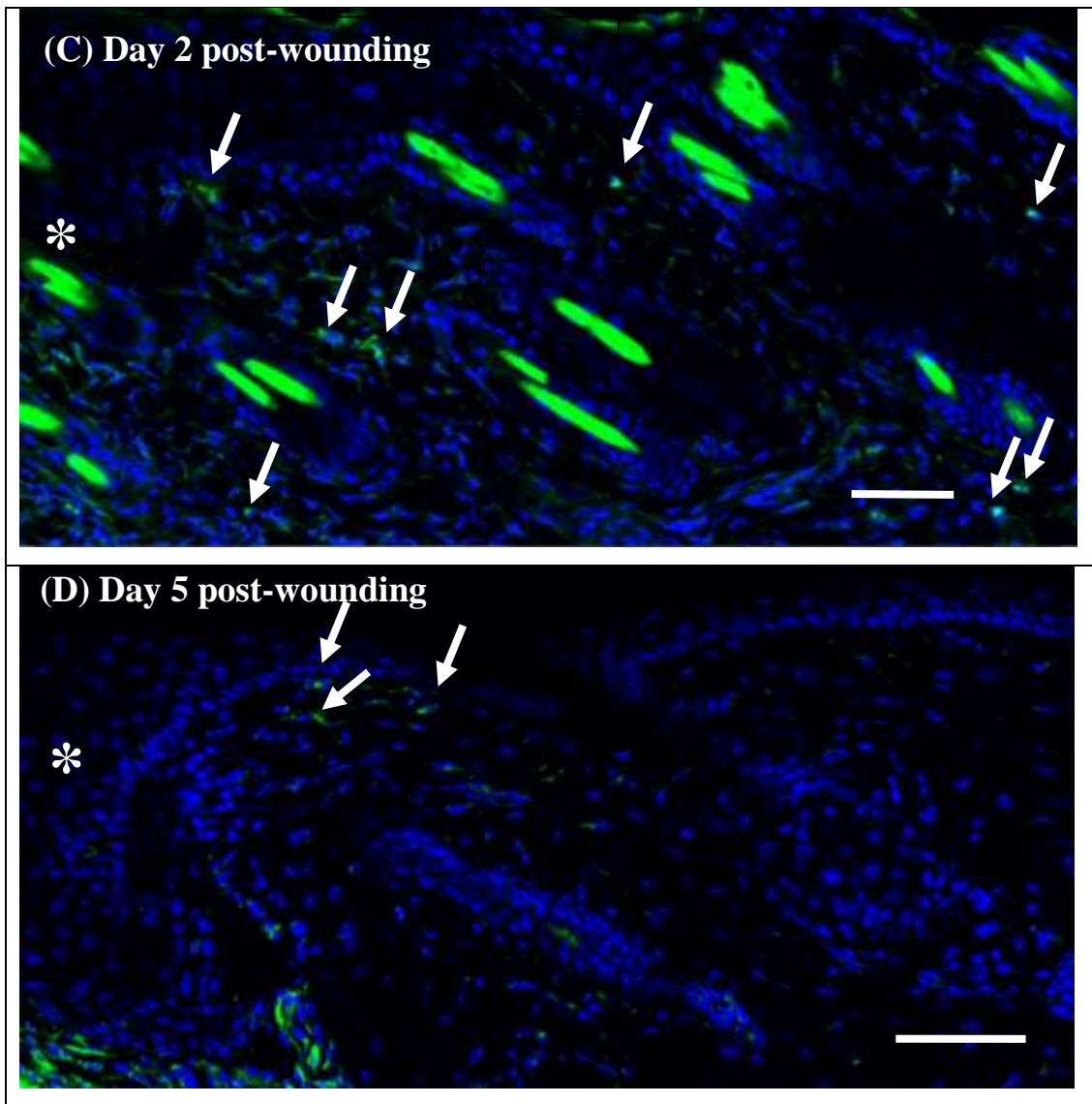


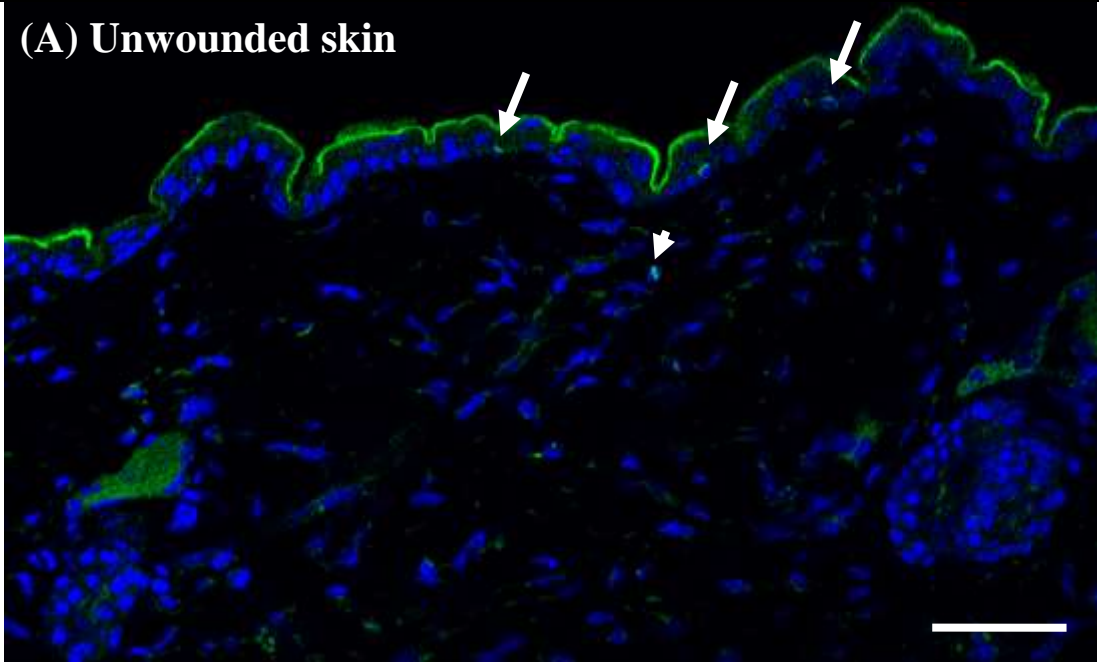
**Figure 3.3 Dendritic cells are recruited into dermis in wound edges.** Back skin tissues from unwounded (A and B) as well as wounded mice on day 2 (C) or 5 (D) post-wounding were collected. A shows unstained negative control. In B-D, sections were stained with an antibody to CD11c antigen (green) and DAPI counterstained (blue). Arrows indicates CD11c<sup>high</sup> dendritic cells. Asterisk marks wound site. Scale bars equal 100 microns.

compared to day 2 post-wounding and all of them were located immediately adjacent to the wound with dendritic morphology (Figure 3.3D), suggesting no CD11c<sup>high</sup> were being differentiated from inflamed monocytes. These results confirm that CD11c<sup>high</sup> DC are involved in skin wound healing, especially in early stage (first 2 days post-wounding) of healing programme.

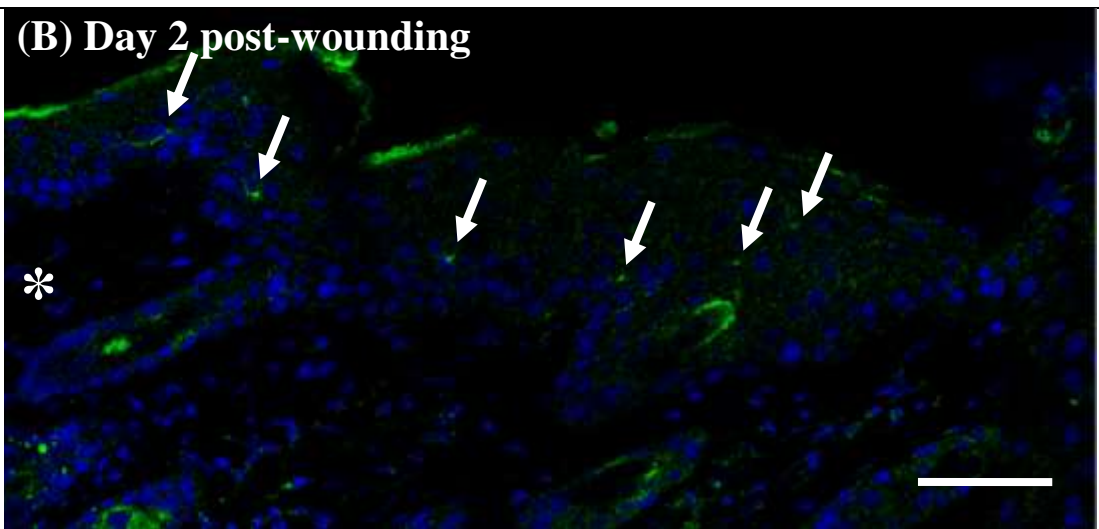
In contrast to cDCs, CD11c<sup>low</sup> CD11b<sup>+</sup> LCs were relatively abundant in unwounded skin, accounting for 0.9-1.0% of total skin cells determined by flow cytometry (Figure 3.2A). This percentage was rapidly increased by  $1.3 \pm 0.1$  fold on day 2 post-wounding (Figure 3.2C), possibly resulting from increased self-proliferation (Merad et al., 2013) and derivation from inflamed monocytes (Figure 3.2D). Subsequently, this percentage remained above unwounded levels at both day 5 (Figure 3.2E) and day 8 time-points (Figure 3.2G) probably due to their long lifespan, capability to self-proliferation and also derivation from inflamed monocytes (Merad et al., 2013; Romani et al., 2009). These results suggest that LCs constitute the predominant skin resident DCs and were accumulated upon wounding throughout the healing programme. To confirm the location of LCs, skin sections were analyzed by using CD207 (Langerin) antibody which could detect Langerhans cells as well as a recently discovered, rare subset of dermal cDC cells (Henri et al., 2009). In unwounded skin, CD207<sup>+</sup> LCs were detected in epidermis with a frequency of 4-7 cells per mm length of skin (Figure 3.4A). An increased number of CD207<sup>+</sup> LCs was detected in epidermis at wound edges with a frequency of 15-20 cells per mm length of skin on day 2 post-wounding (Figure 3.4B) and maintained afterwards on day 5 and 8 (Figure 3.4C and data not shown). These results confirm epidermal LCs constitute the predominant DC in skin and are present in skin wound

**CD207 DAPI staining**

**(A) Unwounded skin**



**(B) Day 2 post-wounding**



**(C) Day 5 post-wounding**

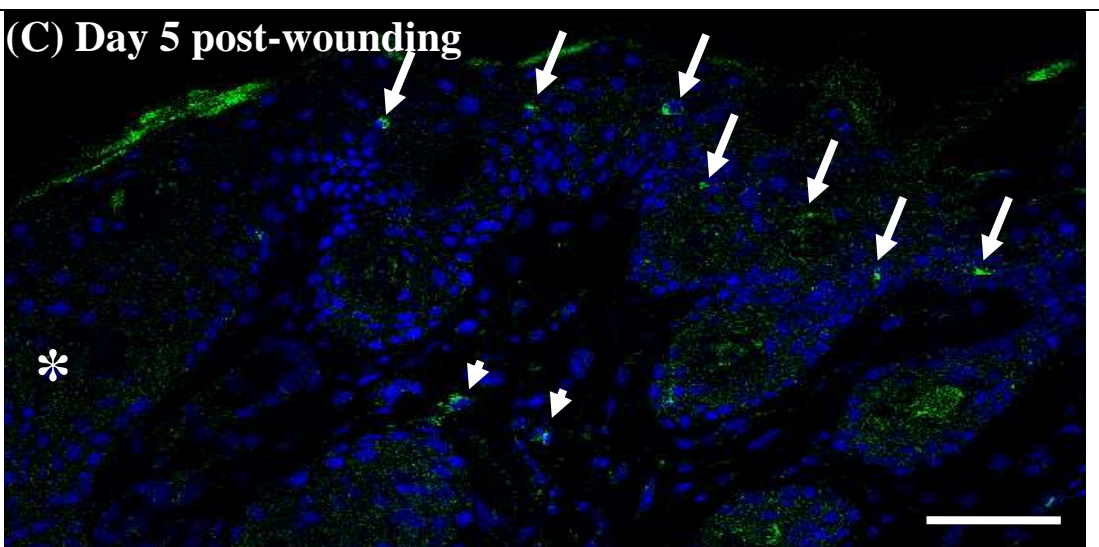


**Figure 3.4 Langerhans cells reside in epidermis and are replenished early following wound healing.** Back skin tissues from unwounded (A) as well as wounded mice on day 2 (B) or 5 (C) post-wounding were collected. Sections were stained with an antibody to CD207 antigen (green) and DAPI counterstained (blue). Long arrows indicate epidermal Langerhans cells. Arrow heads indicate either migratory Langerhans cells trafficking to lymph nodes through dermis or a rare subset of dermal dendritic cells (Langerin-expressing dermal dendritic cells). Asterisk marks wound site. Scale bars equal 100 microns.

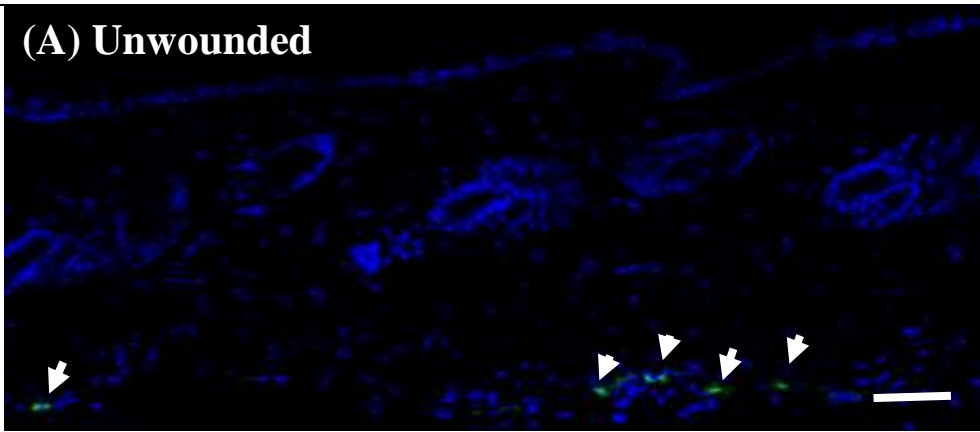
healing, probably at all stages of healing programme.

Then I analyzed CD11b<sup>+</sup> CD11c<sup>-</sup> myeloid cells, among which neutrophils (Gr-1<sup>+</sup> F4/80<sup>-</sup>), mature macrophages (Gr-1<sup>-</sup> F4/80<sup>+</sup>) and inflamed monocytes (Gr-1<sup>+</sup> F4/80<sup>+</sup>, including immature macrophages and possibly monocyte-derived Langerhans cells and dendritic cells in transition status) were distinguished by the expression of Gr-1 and F4/80. Neutrophils (CD11b<sup>+</sup> CD11c<sup>-</sup> Gr-1<sup>+</sup> F4/80<sup>-</sup>) were hardly detectable (less than 0.001% of total skin cells) in unwounded skin (Figure 3.2A and B) and were detected with a small percentage to total skin cells on day 2 ( $0.23 \pm 0.03\%$ ) and 5 ( $0.28 \pm 0.04\%$ ) post-wounding. This percentage was dramatically reduced to less than 0.05% by day 8 post-wounding. These results suggest neutrophils may be involved in early stage of skin wound healing probably within early hours. To confirm the location of neutrophils, skin sections were analyzed using Gr-1 antibody which could detect both neutrophils and inflamed monocytes which are known as precursors for mature macrophages, cDCs and possibly LCs in inflamed settings (Auffray et al., 2009). Unwounded skin was largely devoid of neutrophils (Figure 3.5A), however, a few Gr-1<sup>+</sup> cells were detected in hypodermis, which were probably circulating neutrophils in skin blood networks. On day 2 post-wounding, a large number of Gr-1<sup>+</sup> cells were detected in both dermis and hypodermis adjacent to the wound (Figure 3.5B). According to flow cytometry results, the majority of Gr-1<sup>+</sup> cells at this time-point were in deed CD11b<sup>+</sup> CD11c<sup>-</sup> Gr-1<sup>+</sup> F4/80<sup>+</sup> inflamed monocytes (Figure 3.2D) which are supposed to be located in blood vessels in hypodermis as well as in newly generated dermal granular tissues (Martin and Leibovich, 2005), while the majority of neutrophils are supposed to be outside blood vessels in dermis. To test this, skin sections were analyzed for



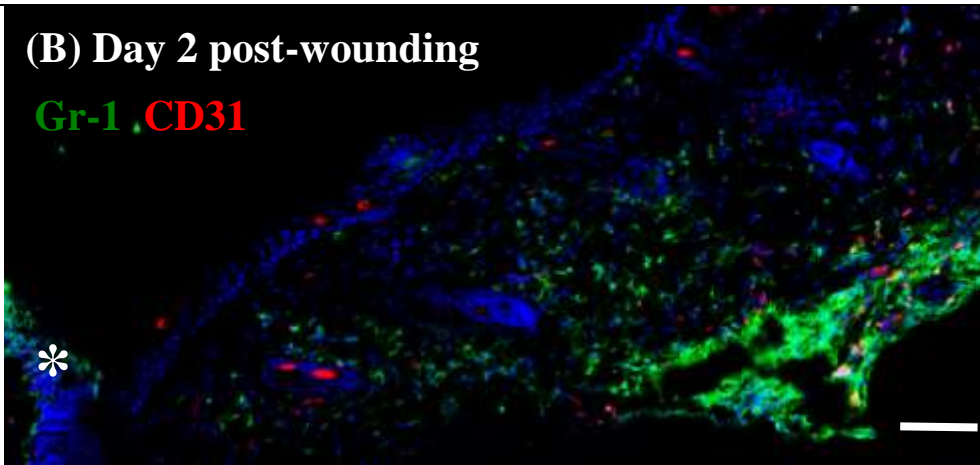
**Gr-1 DAPI staining**

**(A) Unwounded**

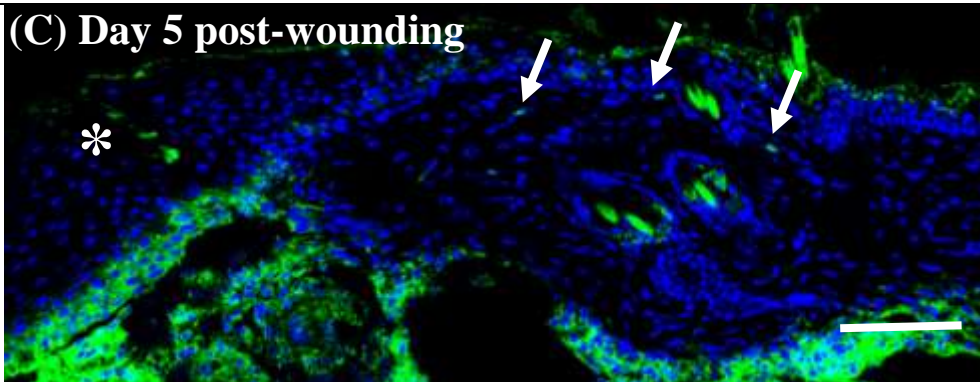


**(B) Day 2 post-wounding**

**Gr-1 CD31**



**(C) Day 5 post-wounding**



**(D) Day 8 post-wounding**

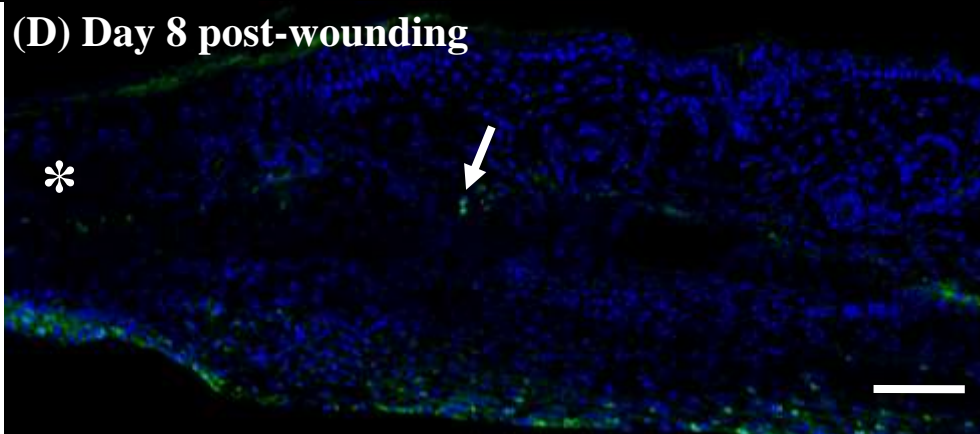


**Figure 3.5 Neutrophils are recruited into dermis in wound edges.** Back skin tissues from unwounded (A) as well as wounded mice on day 2 (B), 5 (C) or 8 (D) post-wounding were collected. Sections were stained with an antibody to Gr1 antigen (green) and DAPI counterstained (blue). Some sections were co-stained with antibodies to Gr-1 (green) and CD31 (red). Long arrows indicate neutrophils in dermis. Arrow heads indicate either neutrophils or inflamed monocytes in hypodermis blood capillaries Asterisk marks wound site scale bars equal 100 microns.

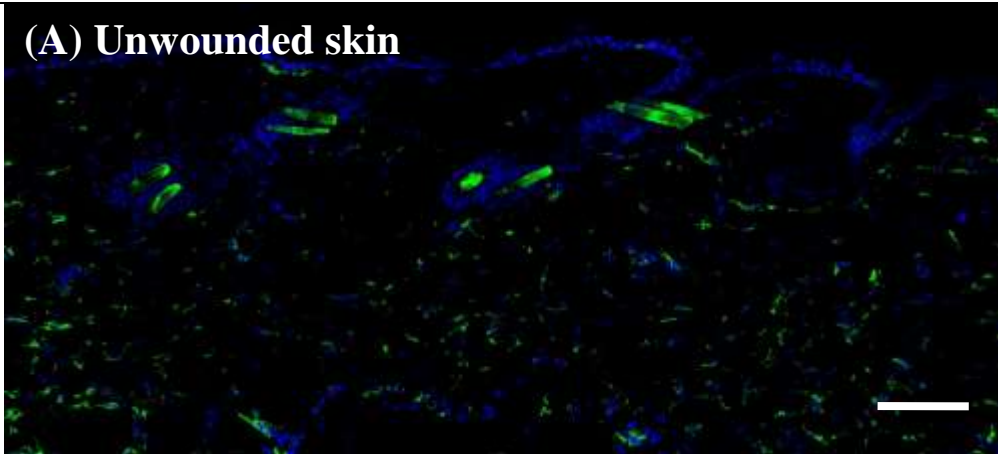
CD31 (a marker for blood vascular endothelial cells) together with Gr-1. Most of Gr-1<sup>+</sup> cells in reticular (lower part) dermis and hypodermis were surrounded by CD31<sup>+</sup> vascular endothelial cells (Figure 3.5B) confirming the dramatic increase in the number of Gr-1<sup>+</sup> cells on day 2 post-wounding were related to massive granular tissue generation in which new blood vessels were formed and massive inflamed monocytes as precursors of macrophages as well as DCs were recruited into wound site to transiently express Gr-1 (Howe et al, 2012; Hume et al., 2008). On day 5, Gr-1<sup>+</sup> cells were mostly detected hypodermis and in rare papillary dermis (upper portion of dermis), and were absent in reticular dermis (Figure 3.5C). Combined with the flow cytometry results that neutrophils remained in the wound site at a low percentage at this time-point and the percentage of inflamed monocytes were decreased compared to day 2 post-wounding (Figure 3.2F), I confirmed that those rare Gr-1<sup>+</sup> cells detected in rare papillary dermis were neutrophils, while those detected in hypodermis were primarily inflamed monocytes. In addition, the absence of Gr-1<sup>+</sup> cells in reticular dermis indicated that granular tissue might be repressed on day 5 post-wounding leading to the decrease of inflamed monocyte infiltration. These results confirmed that a small number of neutrophils were maintained in papillary dermis adjacent to the wound on day 5 post-wounding when the healing programme was in the transition from proliferation phase to remodelling phase. On day 8 post-wounding, neutrophils were hardly detectable in dermis, and the number of inflamed monocytes in hypodermis were also dramatically reduced (Figure 3.5 D), which is consistent with flow cytometry results (Figure 3.2H). All of these results suggest that neutrophils are present in skin wound healing, especially within early hours of the healing programme, and day 5 post-wounding is probably the transition point from proliferation phase to remodelling phase in mouse skin wound healing.



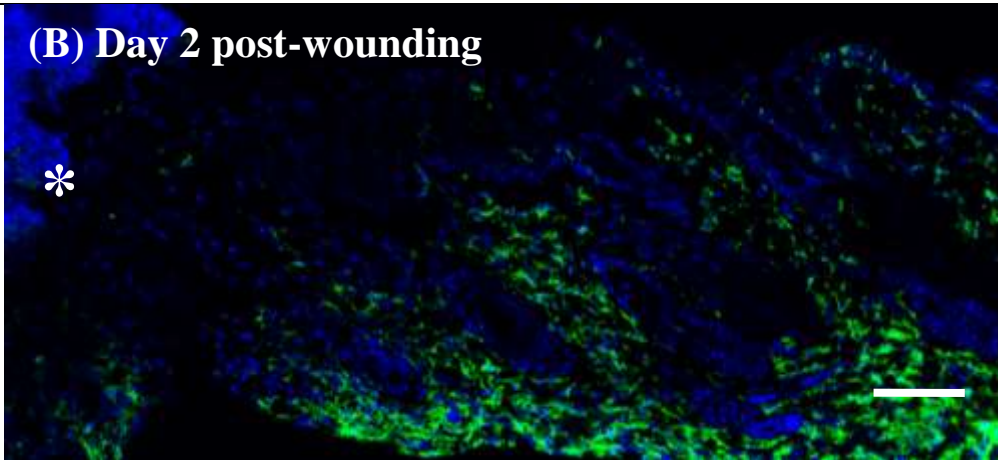
Mature macrophages ( $CD11b^+ CD11c^- Gr-1^- F4/80^+$ ) accounted for 5-6% of total skin cells in unwounded skin, which made them become the major resident immune cells in skin (Dupasquier et al, 2004). The percentage of mature macrophages to total skin cells in wounded skin was not evidently changed within the first 2 days post-wounding (Figure 3.2D). However, this percentage was rapidly increased afterwards and reached its peak with a  $1.5 \pm 0.2$  fold increase on 5 post-wounding (Figure 3.2F) resulting from derivation from massive inflamed monocytes that were recruited into wound site from approximately day 2 post-wounding (Figure 3.2D). On day 8 post-wounding, there was an sharp decrease in the recruitment of inflamed monocytes leading to an reduction in the percentage of mature macrophages to the unwounded level (Figure 3.2H). To confirm the location of macrophages, skin sections were analyzed using F4/80 antibody which could also detect LCs, some cDC (Merad et al., 2013) and inflamed monocytes the vast majority of which are recruited into skin as the precursors of mature macrophages in inflamed setting (Hume, 2008). At all time-points, the epidermal  $F4/80^+$  cells (Figure 3.6) were detected with a similar frequency to  $CD207^+$  epidermal LCs (Figure 3.4), suggesting  $F4/80^+$  cells in epidermis are uniformly LCs. Since cDC were very rare accounting for up to 0.3% of total skin cells at all time-points (Figure 3.2A, C, E and G), the dermal  $F4/80^+$  cells were considered to be primarily composed of mature macrophages and inflamed monocytes. In unwounded skin where the inflamed monocytes were not present (Figure 3.2B), skin resident macrophages were detected throughout dermis (Figure 3.6A). Following wounding, massive infiltration of  $F4/80^+$  macrophages/monocytes were detected in dermis and hypodermis adjacent to the wound on both day 2 and day 5 (Figure 3.4B and C) with different proportions (Figure 3.2F and H). On day 2 post-wounding,  $48.7 \pm 5.3\%$  of macrophage/monocytes heterogeneous population

**F4/80 DAPI staining**

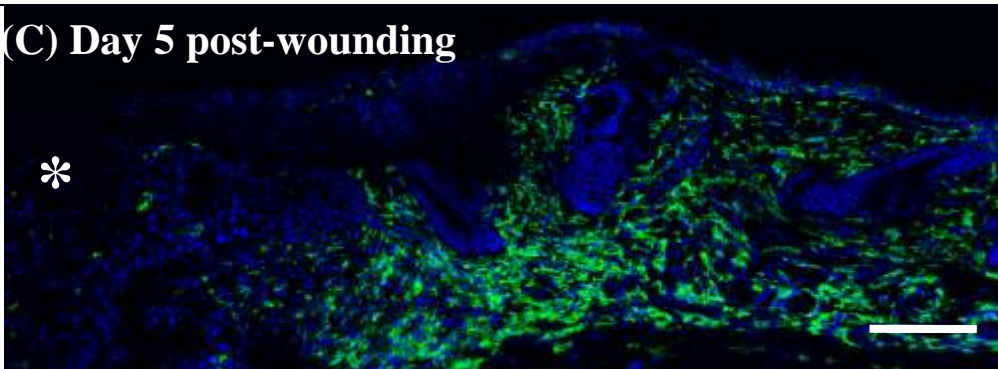
**(A) Unwounded skin**



**(B) Day 2 post-wounding**



**(C) Day 5 post-wounding**



**(D) Day 8 post-wounding**

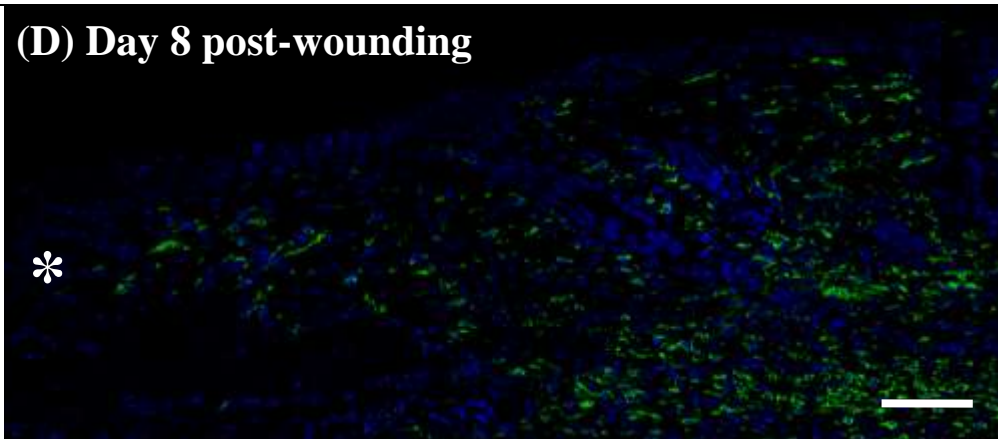


**Figure 3.6 Monocytes/Macrophages are recruited into dermis in wound edges.**

Back skin tissues from unwounded (A) as well as wounded mice on day 2 (B), 5 (C) or 8 (D) post-wounding were collected. Sections were stained with an antibody to F4/80 antigen (green) and DAPI counterstained (blue). Note F4/80<sup>+</sup> in epidermis are Langerhans cells. Asterisk marks wound site scale bars equal 100 microns.

were mature macrophages (Figure 3.2F), while this proportion was increased to  $63.7 \pm 4.2\%$  on day 5 post-wounding (Figure 3.2H) due to the conversion from inflamed monocytes to mature macrophages and reduction in the number of inflamed monocytes to mature macrophages and reduction in the number of inflamed monocytes accompanied by granular tissue degeneration (Figure 3.5C). By day 8 post-wounding, the number of dermal macrophages were dramatically reduced to unwounded level, and the number of inflamed monocytes as detected in hypodermis were also dramatically reduced to a low level (Figure 3.4D). These results suggest that dermal macrophages are the predominant skin resident immune cells, and macrophages/ monocytes constitute the predominant immune cells involved in skin wound healing. Specifically, skin resident macrophages are present in early stage (first 2 days post-wounding), while monocyte-derived macrophages are involved in later stage (after 2 days post-wounding) of healing programme.

### **3.2.3 T cells**

To examine if T cells are present in skin wound healing, wounded skin from wildtype mice were analyzed for CD45, CD3 (a pan-marker for all the T cells), TCR $\beta$  (a marker for  $\alpha\beta$  T cells), V $\gamma$ 3 (a marker for the majority of DETCs) (Jameson et al., 2004) by flow cytometry. I first gated on CD3<sup>low to high</sup> CD45<sup>+</sup> T cells, among which  $\alpha\beta$  T cells (CD45<sup>+</sup> CD3<sup>+</sup> TCR $\beta$ <sup>+</sup> V $\gamma$ 3<sup>-</sup>), DETCs (CD45<sup>+</sup> CD3<sup>+</sup> TCR $\beta$ <sup>-</sup> V $\gamma$ 3<sup>+</sup>) and dermal  $\gamma\delta$  T cells (CD45<sup>+</sup> CD3<sup>+</sup> TCR $\beta$ <sup>-</sup> V $\gamma$ 3<sup>-</sup>) were distinguishable by their expression of TCR $\beta$  and V $\gamma$ 3. In unwounded skin control,  $\alpha\beta$  T cells accounted for 1.2-1.4% of total skin cells suggesting  $\alpha\beta$  T cells are one of the major resident immune cell type in skin (Figure 3.7A and B). This percentage was continuously reduced following wounding at all time-points probably suggesting  $\alpha\beta$  T cells are not significantly involved in skin wound healing. DETCs accounted for 1.6-1.8% of total

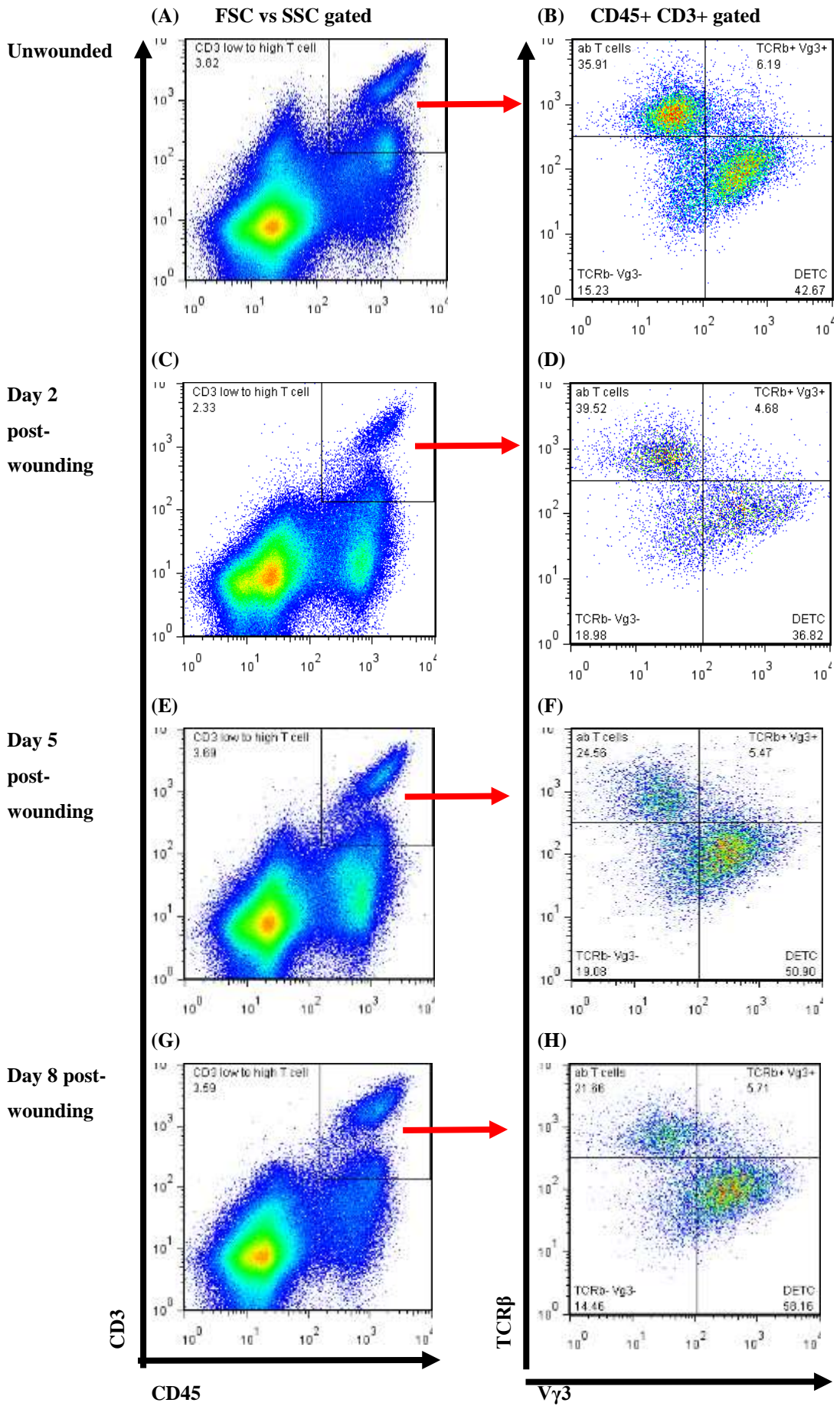


**Figure 3.7 Quantification of T cell subsets in skin wounds.** Cells isolated from unwounded (A-B) as well as wounded mouse back skin on day 2 (C-D), 5 (E-F) or 8 (G-H) post-wounding were labelled with CD3, CD45, TCR $\beta$  and V $\gamma$ 3 antibodies and were first analyzed by flow cytometry for CD3, CD45 for total T cells (CD45<sup>+</sup> CD3<sup>+</sup>) (A, C, E, G). Then CD45<sup>+</sup> CD3<sup>+</sup> T cells were gated and analyzed for TCR $\beta$  and V $\gamma$ 3 to distinguish  $\alpha\beta$  T cells (ab T cells) (TCR $\beta$ <sup>+</sup>V $\gamma$ 3<sup>-</sup>), dendritic epidermal T cells (DETCs) (TCR $\beta$ <sup>-</sup>V $\gamma$ 3<sup>+</sup>) and dermal  $\gamma\delta$  T cells (gd T cells) (TCR $\beta$ <sup>-</sup>V $\gamma$ 3<sup>-</sup>) from each other. Note  $\alpha\beta$  T cells are continuously decreased following wounding. DETCs are replenished and dermal  $\gamma\delta$  T cells are replenished after 5 days post-wounding. Gate frequencies are indicated in percentages. Shown one biological sample; 3 individual biological replicates were tested (not shown).

skin cells in unwounded skin (Figure 3.7A and B). Previous studies suggest DETCs are resident T cells specifically in rodent epidermis and the epidermal T cells are uniformly DETCs (MacLeod and Havrand, 2011; Sumuria et al., 2012). The percentage of DETCs to total skin cells was dramatically reduced by  $2.0 \pm 0.3$  fold on day 2 post-wounding (Figure 3.7C and D), partly due to the massive infiltration of other immune cells and other cell types in wound site. However, they were rapidly replenished and increased afterwards on day 5 and day 8 post-wounding (Figure 3.7E-H), probably through self-proliferation (Sumaria et al., 2011). However, the mechanism for maintenance of DETCs in injury state is yet to be determined. These results suggest that DETCs are involved in skin wound healing, especially in later stage (after 2 days post-wounding) of healing programme.

In addition, a small number of  $\gamma\delta$  T cells other than DETCs were detected in unwounded skin, accounting for 0.5-0.6% of total skin cells (Figure 3.7A and B). These  $\gamma\delta$  T have been recently determined as a mixture population of resident  $V\gamma 3^-$   $\gamma\delta$  T cells in dermis (Sumaria et al., 2011). Similar to DETCs, these  $V\gamma 3^-$   $\gamma\delta$  T cells are self-proliferative in steady state (Mumaria et al., 2011) and were not expanded until day 5 post-wounding (Figure 3.7C and D). However, the percentage of  $V\gamma 3^-$   $\gamma\delta$  T cells was reduced on day 8 compared to day 5 post-wounding (Figure 3.7E and F). These results suggest that dermal  $\gamma\delta$  T cells are involved in skin wound healing, especially in later stage (after 2 days post-wounding) of the healing programme.

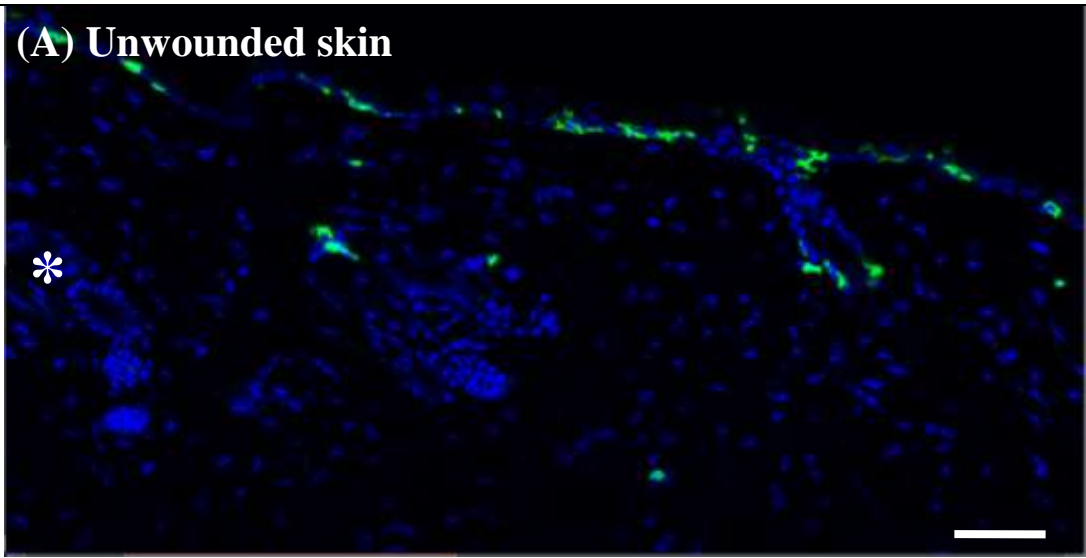
To visualize of T cells, skin section were analyzed by using CD3, which could detect all T cell subsets. DETCs cells were detected in interfollicular epidermal basal layer and hair follicle outer root sheath with dendritic morphology (Figure 3.8A), while a

few CD3<sup>+</sup> T cells were also detected in dermis, which were composed of  $\alpha\beta$  T cells and dermal  $\gamma\delta$  T cells (Figure 3.7B). On day 2 post-wounding, the number of DETCs was dramatically reduced in epidermal compartment (Figure 3.8B), which is consistent with the decreased percentage of CD45<sup>+</sup> CD3<sup>+</sup> TCR $\beta$ <sup>-</sup> V $\gamma$ 3<sup>+</sup> DETCs detected by flow cytometry (Figure 3.7C and D). However, a similar number of CD3<sup>+</sup> T cells were detected at this time-point in dermal compartment adjacent to the wound compared to the unwounded skin (Figure 3.8B), which is apparently contradicted with the substantially decreased percentages of total CD3<sup>+</sup> T cells and all T cell subsets detected by flow cytometry (Figure 3.7C and D). Although the migration of T cells from distal dermis into wound site could lead to T cell accumulation at wound edges without changing the overall T cell number in dermis, it could not explain the decrease in the number of dermal T cell subsets (Figure 3.7B and Figure 3.8B). One of the possible reasons for the loss of all T cell subsets and persistent dermal presence of T cells might be increased trafficking of resident T cells including both  $\alpha\beta$  and  $\gamma\delta$  T cells into skin draining lymph nodes in response to injury or infection (Vireling et al., 2012), some T cells detected in dermis at this time-point might be migratory DETCs that travelled through dermis. However, it yet needs to be determined since DETCs, as a specialized  $\gamma\delta$  T cells, are considered to be immobile in steady state and reside in epidermis for life-time once they get there during development of early fetus (Gray et al., 2011; MacLeod and Havran, 2011). On day 5 post-wounding, an increased number of T cells were detected adjacent to the wound especially in epidermis and reticular dermis (Figure 3.8C), suggesting DETCs and dermal  $\gamma\delta$  T cells (Figure 3.7E and F) were replenished and expanded at this time-point, probably through recruitment of blood-derived  $\gamma\delta$  T cells as well as self-proliferation (Gray et al., 2011; MacLeod and Havran, 2011). However, the

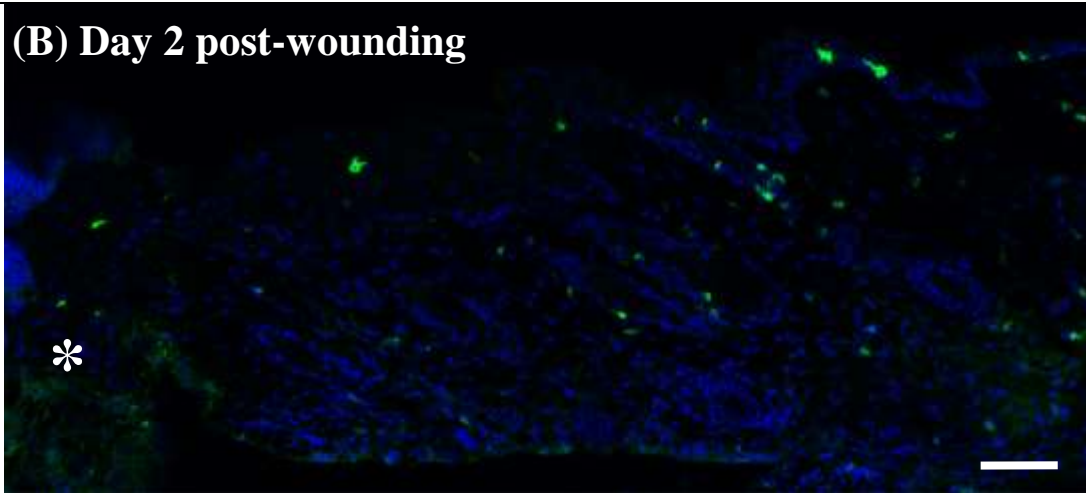


**CD3 DAPI staining**

**(A) Unwounded skin**



**(B) Day 2 post-wounding**



**(C) Day 8 post-wounding**

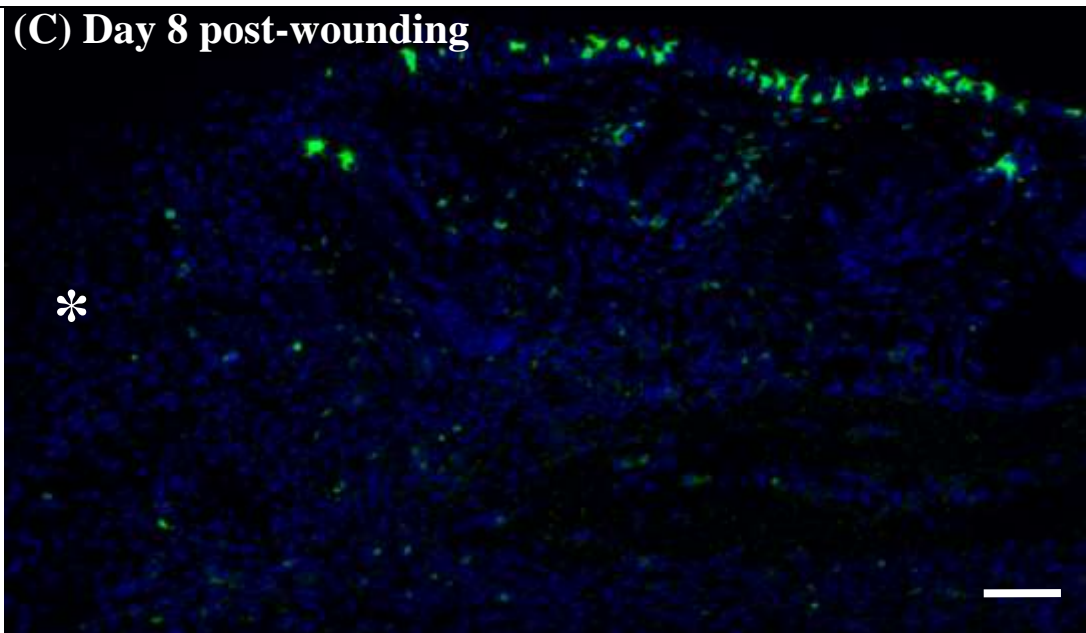


**Figure 3.8 T cells reside in epidermis and rare dermis, and are replenished late following wounding.** Back skin tissues from unwounded (A) as well as wounded mice on day 2 (B) or 8 (C) post-wounding were collected. Sections were stained with an antibody to CD3 antigen (green) and DAPI counterstained (blue). Note DETCs reside in epidermis and replenished after 5 days post-wounding. CD3<sup>+</sup> T cells in dermis include  $\alpha\beta$  T cells dermal  $\gamma\delta$  T cells and possibly DETC precursors which are trafficking from blood circulation to epidermis through dermis. Asterisk marks wound site. Scale bars equal 100 microns.

mechanism of maintenance of self-proliferative DETCs and dermal  $\gamma\delta$  T cells in inflamed settings are currently unknown (Gray et al., 2011; MacLeod and Havran, 2011) and needs to be determined. In addition, I found the morphologies of those DETCs which were most proximal to wound site became rounded in response to keratinocyte injury, which is consistent with previous results (Havran and Jameson, 2010). All of these results suggest  $\gamma\delta$  T cells including both DETCs and dermal  $\gamma\delta$  T cells are involved in skin wound healing, especially in later stage (after 2 days post-wounding) of healing programme, while  $\alpha\beta$  T cells may not be significantly involved in this healing process.

#### **3.2.4 B cells**

To examine if B lymphocytes are involved in skin wound healing, wildtype wounded mice were analyzed for CD45, CD19 (a marker for B cells) by flow cytometry. CD19<sup>+</sup> B cells were very rare in both unwounded and wounded skin at all time points with no increase during the time course, accounting for up to 0.1% of total skin cells (Figure 3.9). To verify this result, skin sections were analyzed for CD19 by using anti-CD19 antibody. B cells were detectable in neither unwounded nor wounded skin (data not shown). These results suggest B cells may not be significantly involved in skin wound healing.

#### **3.2.5 NK cells**

To examine if NK cells are involved in skin wound healing, wounded skin was analyzed for NK1.1 (a marker for NK and rare T cells known as NKT cells), CD3 (a marker for T cells) and NKp46 (also known as natural cytotoxicity triggering receptor, NCR), which is co-expressed with NK1.1 by mouse NK and NKT cells,

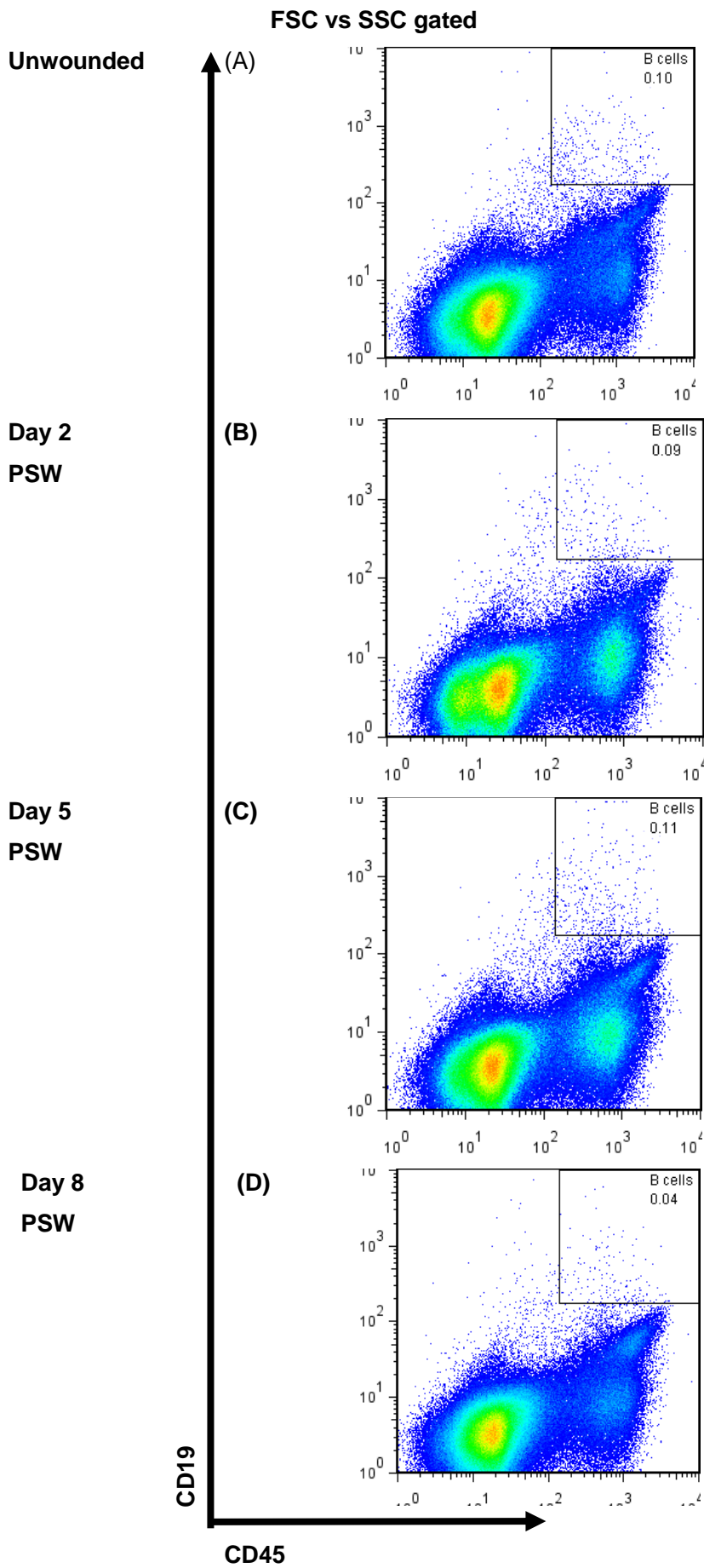


**Figure 3.9 B cells are not involved in skin wound healing.** Cells isolated from unwounded (A) as well as wounded mouse back skin on day 2 (B), 5 (C) or 8 (D) post-wounding (PSW) were labelled with CD45 and CD19 and were analyzed by flow cytometry for B cells (CD45<sup>+</sup> CD19<sup>+</sup>). Gate frequencies are indicated in percentages. Shown one biological sample; 3 individual biological replicates were tested (not shown).

and expressed by ILC22 in intestine) (Luci et al., 2009). NK cells (NK1.1<sup>+</sup> CD3<sup>+</sup>) are distinguishable from NKT cells (NK1.1<sup>+</sup> CD3<sup>-</sup>) and other immune cells by their expression of NK1.1 and lacking CD3. NKT cells were detected at a very small percentage (0.02-0.03%) to total skin cells in both unwounded and wounded skin at all time points and there was no increase during the time course up to day 8 post-wounding (Figure 3.10), suggesting NKT cells, like the other  $\alpha\beta$  T cells, may not be significantly involved in skin wound healing.

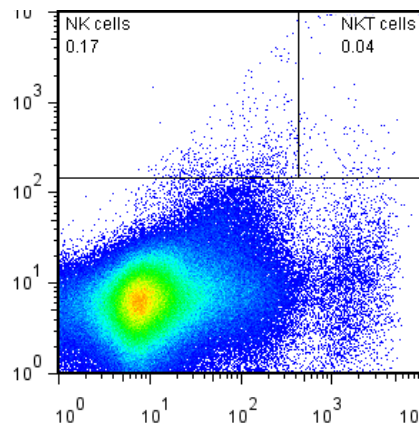
Compared to NKT cells, NK1.1<sup>+</sup> CD3<sup>-</sup> NK cells were nearly 10-fold more abundant in skin, accounting for 0.1-0.2% of total skin cells in steady state (Figure 3.10A). This percentage was considerably increased by  $2.9 \pm 0.3$  fold on day 2 post-wounding (Figure 3.10B) followed by a gradual decrease afterwards on day 5 (Figure 3.10C) and day 8 (Figure 3.10D) post-wounding. I found that all of these cell were positive for NKp46 (data not shown), which confirmed their NK cell identity. These results suggest that NK cell are recruited to the wounded skin on day 2 post-wounding and are present in skin wound healing, especially in early stage of healing programme.

To confirm the location of NK cells in skin, skin sections were analyzed by using NKp46 antibody which could detect NK cells which constitute the majority of NKp46<sup>+</sup> cells, NKT cells, and possibly ILC22 if they exist (Luci et al., 2009). In contrast to spleen (Figure 3.11A), NKp46<sup>+</sup> cells were hardly detectable in dermis in unwounded skin (Figure 3.11B). Since NK cells were increased in skin on day 2 post-wounding (Figure 3.10B), I expected a larger number of NKp46<sup>+</sup> cell detected in dermis adjacent to the wound. Surprisingly, rare NKp46<sup>+</sup> cells were detected on

FSC vs SSC gated

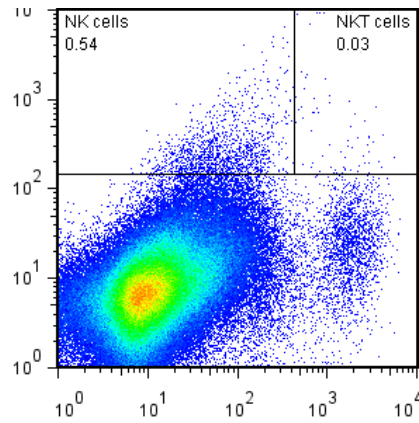
Unwounded

(A)



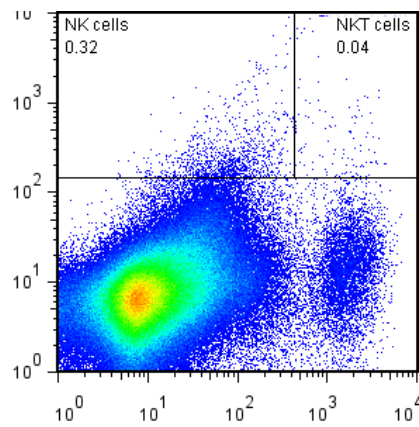
Day 2  
PSW

(B)



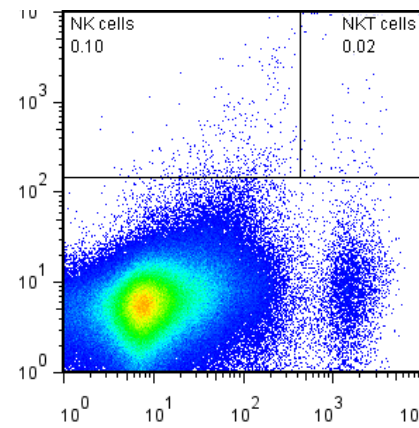
Day 5  
PSW

(C)



Day 8  
PSW

(D)



NK1.1

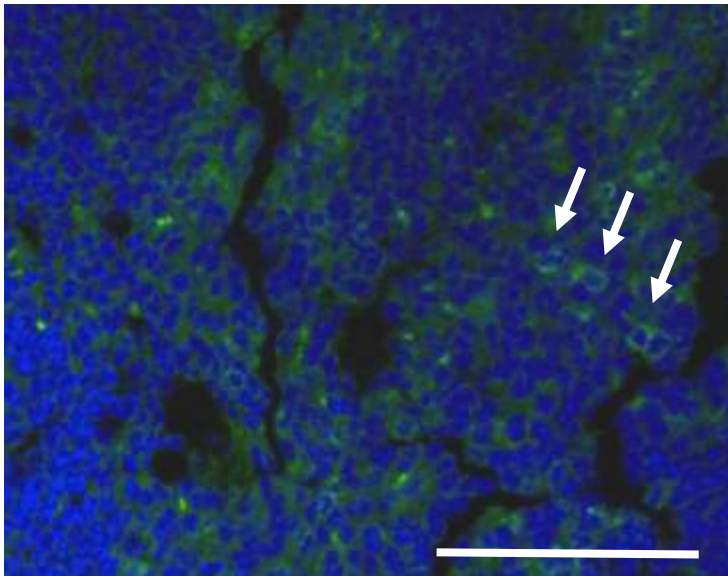
CD3

**Figure 3.10 NK cells are recruited early into wound site determined by flow cytometry.** Cells isolated from unwounded (A) as well as wounded mouse back skin on day 2 (B), 5 (C) or 8 (D) post-wounding were labelled with CD3 and NK1.1 and were analyzed by flow cytometry for NK cells (NK1.1<sup>+</sup> CD3<sup>-</sup>) and NKT cells (NK1.1<sup>+</sup> CD3<sup>+</sup>). Gate frequencies are indicated in percentages. Shown one biological sample; 3 individual biological replicates were tested (not shown).

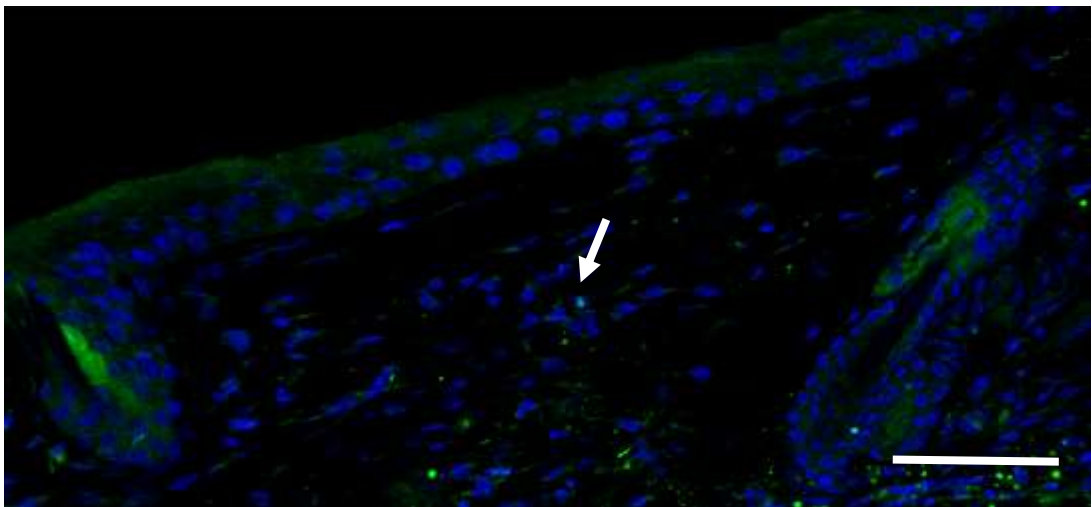


**NKp46 DAPI staining**

**(A) Spleen**



**(B) Non-wound**



**(C) Day 2 post-wounding**

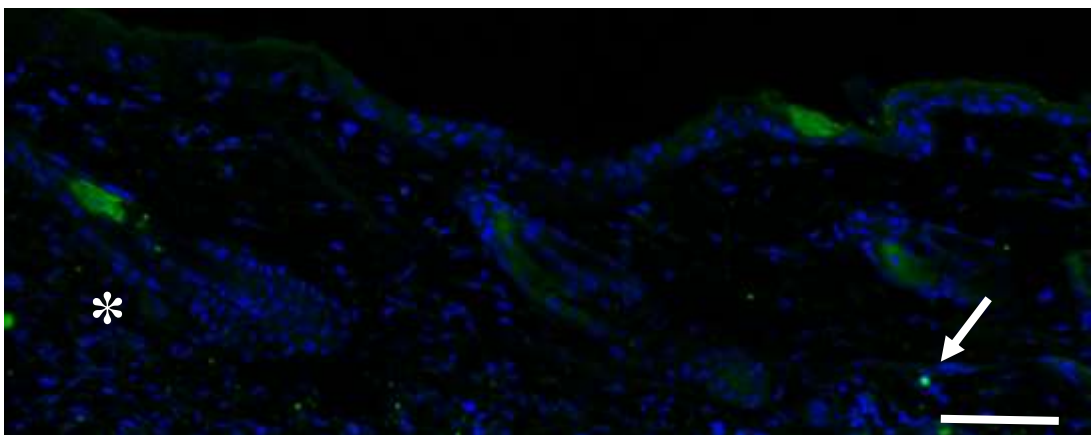


**Figure 3.11 NKp46<sup>+</sup> cells are hardly detectable in skin wound sections.** Mouse spleen (A) and back skin tissues from unwounded (B) as well as wounded mice on day 2 (C) post-wounding were collected. Sections were stained with an antibody to NKp46 antigen (green) and DAPI counterstained (blue). Arrow indicates NKp46<sup>+</sup> NK or NKT cell. Asterisk marks wound site. Scale bars equal 100 microns.

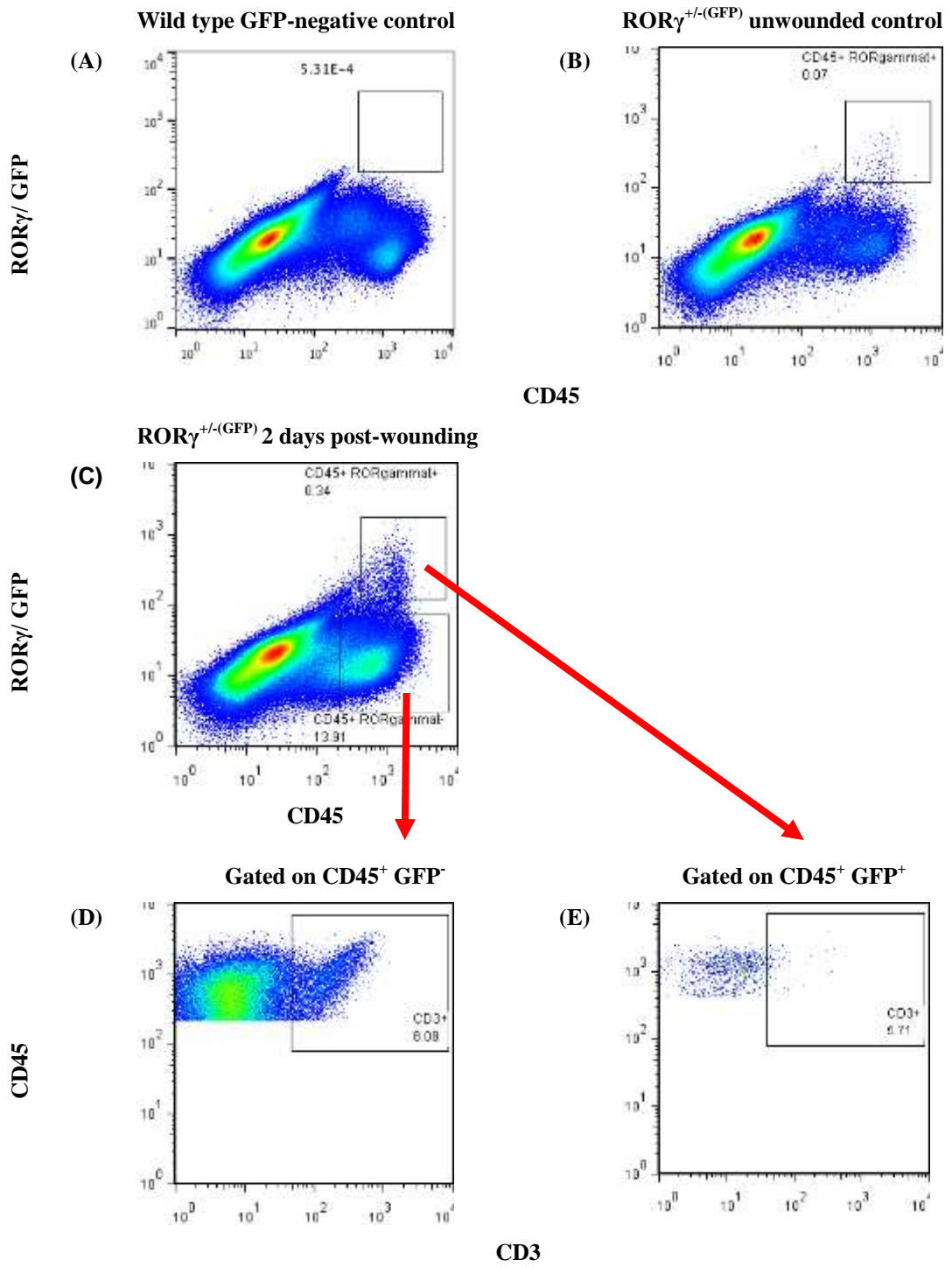
day 2 post-wounding with a frequency similar to unwounded level (Figure 3.11C). I failed to detect NK cells on day 5 post-wounding (Data not shown). These two apparently contradicted results determined by using different methods might indicate that the majority of blood-derived NK cells recruited upon wounding are likely to express a low level of NKp46, which is below the threshold of the fluorescence microscopy and only detectable by flow cytometry.

### **3.2.6 Innate lymphoid cells**

ROR $\gamma$ t<sup>+</sup> ILCs (also known as ILC3s) are an emerging group of rare innate lymphoid cells that play a central role in promoting innate immunity and epithelial tissue repair in lung and intestine (Dudakov et al., 2012) in adult human and mouse through producing IL-17 and/or IL-22 which were considered as Th17 cytokines (Spits et al., 2013). Similar to Th17 cells, they are dependent on transcriptional factor ROR $\gamma$ t for their development and function (Spits and Cupedo, 2012; Spits et al., 2013; Spits and Santo, 2011). However, they lack T cell markers such as CD3, which makes them distinguishable from ROR $\gamma$ t<sup>+</sup> T cells. In addition, the development of ILC3s is also dependent on a cytokine IL-7 through IL-7 receptor  $\alpha$  (CD127). By inducing different infections to adult mouse models, at least 3 subsets of ROR $\gamma$ t<sup>+</sup> ILCs have been identified and named according to their phenotypical markers (e.g. CD117, CD4, NKp46) and cytokine production (i.e. IL-22 or IL17 or both) (Luci et al., 2009; Sonnenberg et al., 2012; Spits and Cupedo, 2012; Spits et al., 2013; Spits and Santo, 2011). These ROR $\gamma$ t<sup>+</sup> ILCs in adults include lymphoid inducer cells (LTi cells, ROR $\gamma$ t<sup>+</sup> CD3<sup>-</sup> CD127<sup>+</sup> CD4<sup>+</sup> CD117<sup>+</sup> NKp46<sup>-</sup>) which mainly produce IL-22 but also IL-17, ILC22 (also named as NCR<sup>+</sup>ILC3s, ROR $\gamma$ t<sup>+</sup> CD3<sup>-</sup> CD127<sup>+</sup> CD4<sup>+/-</sup> CD117<sup>+</sup> NKp46<sup>+</sup>) which mainly produce IL-22, and ILC17 (also named as NCR<sup>-</sup> ILC3s,

ROR $\gamma$ t<sup>+</sup> CD3<sup>-</sup> CD127<sup>+</sup> CD4<sup>-</sup> CD117<sup>-</sup> NKp46<sup>-</sup>) which produce both IL-17 and IL-22 as well as IFN- $\gamma$ ).

To examine if ILC3s are present in skin and involved in skin wound healing and to define their phenotypes, wounded as well as unwounded ROR $\gamma$ <sup>+/-</sup> mice with ROR $\gamma$ -GFP transgene were analyzed by flow cytometry for CD45, CD3, TCR $\beta$ , TCR $\delta$ , V $\gamma$ 3, CD127, CD4, CD117 and NKp46. I first analyzed CD45<sup>+</sup> ROR $\gamma$ -GFP<sup>+</sup> cells which could include ILC3s as well as rare ROR $\gamma$ t<sup>+</sup> T cells such as Th17, Th22 and some dermal  $\gamma\delta$  T cells (Gray et al., 2011). In both unwounded skin and wounded skin, the vast majority of ROR $\gamma$ -GFP<sup>+</sup> cells are positive for CD45 (Figure 3.12A-C), suggesting ROR $\gamma$  is almost exclusively expressed by immune cells. In unwounded skin, ROR $\gamma$ -GFP<sup>+</sup> cells were very rare, accounting for 0.06  $\pm$  0.02% of total skin cells (Figure 3.12A and B). This percentage was dramatically increased to 0.28  $\pm$  0.06% on day 2 post-wounding (Figure 3.12C), suggesting ROR $\gamma$ <sup>+</sup> cells may be involved in early stage of skin wound healing. To distinguish ILC3s (CD3<sup>-</sup>) from ROR $\gamma$ t<sup>+</sup> T cells (CD3<sup>+</sup>), CD45<sup>+</sup> ROR $\gamma$ -GFP<sup>+</sup> cells were analyzed for CD3 expression. The vast majority (approximately 95%) of CD45<sup>+</sup> ROR $\gamma$ -GFP<sup>+</sup> cells were negative for CD3 (Figure 3.12D and E), suggesting the majority of ROR $\gamma$ <sup>+</sup> cells recruited into skin wound site at this time-point are not T cells. To confirm this, CD45<sup>+</sup> ROR $\gamma$ -GFP<sup>+</sup> cells were analyzed for markers for different T cell subsets, such as TCR $\beta$  and TCR $\gamma$  and V $\gamma$ 3. Similarly, the vast majority (approximately 99%) of CD45<sup>+</sup> ROR $\gamma$ -GFP<sup>+</sup> cells were negative for TCR $\beta$  and TCR $\gamma$  or V $\gamma$ 3 (data not shown). To our best knowledge, only ILC3s or certain subsets of T cells are found to express ROR $\gamma$ t (Spits et al., 2013), therefore these ROR $\gamma$ <sup>+</sup> non-T cells found in skin wounds are very likely to be ILC3s. In order to define the phenotypes and subsets of these ROR $\gamma$ <sup>+</sup>



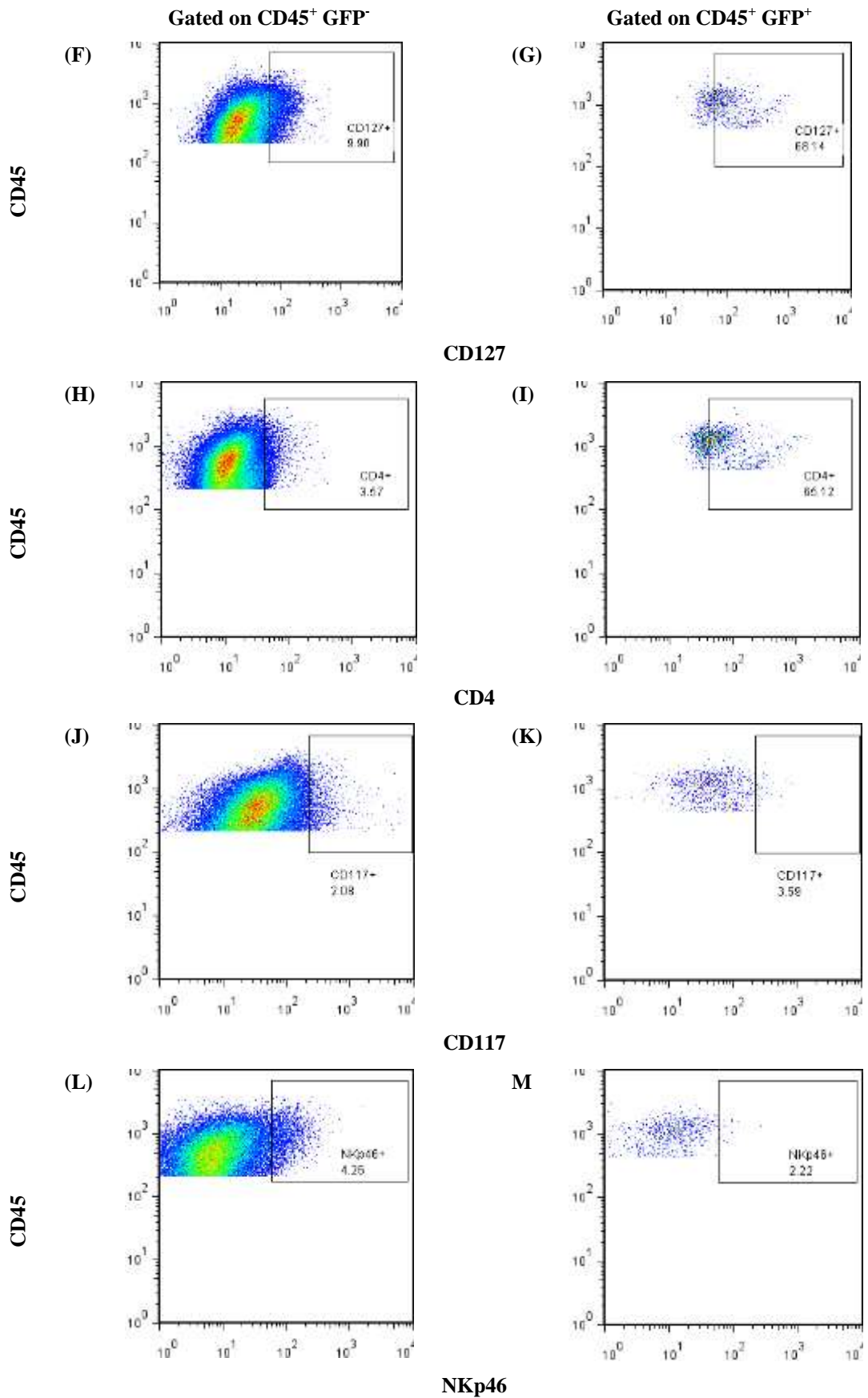




**Figure 3.12 The phenotypes of the vast majority of ROR $\gamma$ -expressing cells recruited in skin wounds are CD3<sup>-</sup> CD4<sup>dim to +</sup> CD127<sup>dim to +</sup> CD117<sup>-</sup> NKp46<sup>-</sup> ILC3s.** Cells isolated from uninjured wild type GFP-negative back skin (A), uninjured ROR $\gamma^{+/-}$ (GFP) (B) and injured ROR $\gamma^{+/-}$ (GFP) mouse back skin at day 2 (C-M) post-wounding were labelled with CD45, CD3, CD127, CD4, NKp46 and CD117 and were first analyzed for CD45<sup>+</sup> ROR $\gamma$ /GFP<sup>+</sup> cells (A-C). Then CD45<sup>+</sup> ROR $\gamma$ /GFP<sup>+</sup> cells as well as CD45<sup>+</sup> ROR $\gamma$ /GFP<sup>-</sup> cells in wounded ROR $\gamma^{+/-}$  skin on day 2 post-wounding were gated and compared for expression of CD3, CD127, CD4, NKp46 and CD117 (D-M). Gate frequencies are indicated in percentages. Shown one biological sample; 3 individual biological replicates were tested (not shown).

non-T cells, CD45<sup>+</sup> ROR $\gamma$ -GFP<sup>+</sup> cells were analyzed for expression of CD127 (IL-7 receptor, IL-7R), CD4, CD117 (C-kit receptor) and NKp46. Approximately 60-70% of CD45<sup>+</sup> ROR $\gamma$ -GFP<sup>+</sup> cells were positive for CD127 (Figure 3.12 E-F), while the rest of CD45<sup>+</sup> ROR $\gamma$ -GFP<sup>+</sup> cells expressed a very low level of CD127. Similarly, 60-70% of CD45<sup>+</sup> ROR $\gamma$ -GFP<sup>+</sup> cells were positive for CD4 (Figure 3.12 G-H), while the rest of CD45<sup>+</sup> ROR $\gamma$ -GFP<sup>+</sup> cells expressed a very low level of CD4. In contrast, the vast majority (over 95%) of CD45<sup>+</sup> ROR $\gamma$ -GFP<sup>+</sup> cells were negative for CD117 and NKp46 (Figure 3.12J-M). Similar phenotypes were detected on day 5 post-wounding (data not shown). Taken together, these results suggest the phenotypes of the vast majority of ROR $\gamma$ <sup>+</sup> cells involved in skin wound healing are CD45<sup>+</sup> CD3<sup>-</sup> CD127<sup>dim to +</sup> CD4<sup>dim to +</sup> CD117<sup>-</sup> NKp46<sup>-</sup>. Therefore, these ROR $\gamma$ <sup>+</sup> cells belong to ILC3s which by definition are innate lymphocytes (CD3<sup>-</sup>) and dependent on transcriptional factor ROR $\gamma$  (ROR $\gamma$ <sup>+</sup>) and IL-7 (CD127<sup>+</sup>) for their development (Spits and Cupedo, 2012; Spit et al., 2013; Spits and Santo, 2011). However, they may be a heterogeneous population or a distinct subset from currently known ROR $\gamma$ <sup>+</sup> ILCs, such as LTi cells (CD4<sup>+50%</sup> CD117<sup>+</sup> NKp46<sup>-</sup>), ILC22 (CD4<sup>+10%</sup> CD117<sup>+</sup> NKp46<sup>+</sup>) or ILC17 (CD4<sup>-</sup> CD117<sup>-</sup> NKp46<sup>-</sup>) because of their CD4<sup>dim to +</sup> CD117<sup>-</sup> NKp46<sup>-</sup> phenotypes.

To verify if GFP in these mice was expressed by genuine ROR $\gamma$ <sup>+</sup> cells, skin sections from wounded ROR $\gamma$ <sup>+/-</sup>(GFP) mice were analyzed by using anti-ROR $\gamma$ t and anti-GFP antibody. I confirmed that all GFP<sup>+</sup> cells were detected by anti-ROR $\gamma$ t antibody (Figure 3.13A) and thus were genuine ROR $\gamma$ <sup>+</sup> cells. Then to verify the location, identity and phenotypes of these ROR $\gamma$ <sup>+</sup> ILCs, skin sections from wounded wildtype mice were analyzed by using anti-ROR $\gamma$ t antibody together with anti-CD3, CD4, CD127, CD117 or NKp46 antibody. I confirmed that the vast majority of

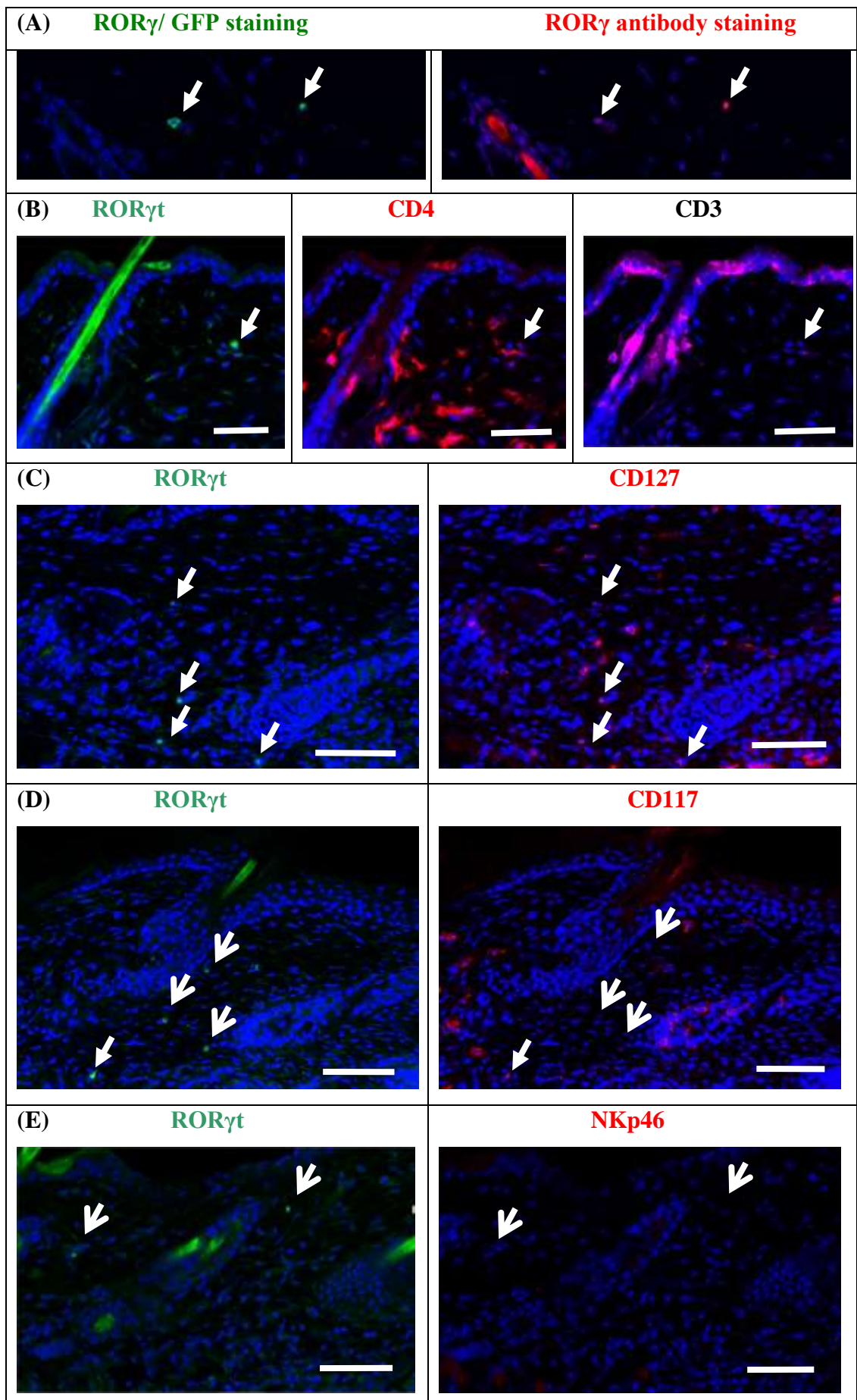




**Figure 3.13 Phenotypes of ROR $\gamma$ -expressing cells are confirmed by immunofluorescence chemistry on skin wound sections.** Back skin tissues from wounded ROR $\gamma$ / GFP mice on day 2 post-wounding (A) and wildtype mice on day 5 post-wounding (B-E) were collected. Sections were double or triple stained with antibodies to ROR $\gamma$  antigen (red in A, and green in B-E) together with CD3 (purple in B), CD4 (red in B), CD127 (red in C), CD117 (red in D) or NKp46 (red in E) and DAPI counterstained (blue). ROR $\gamma$ /GFP cells are shown in green in A. Arrows  indicate double positive ROR $\gamma$ <sup>+</sup> cells. Arrows indicate  single positive ROR $\gamma$ <sup>+</sup> cells Scale bar 100  $\mu$ m.

ROR $\gamma$ <sup>+</sup> cells were localized in dermis adjacent to the wounds and were CD3<sup>-</sup> CD4<sup>dim</sup> to + CD127<sup>dim</sup> to + CD117<sup>-</sup> NKp46<sup>-</sup> ILC3s (Figure 3.13B-E).

To examine the presence and the involvement of ILC3s at different stages of skin wound healing, dermis as well as axillary and inguinal skin draining lymph nodes from wounded wild type mice were collected on day 1, 3, 5 and 8 post-wounding and analyzed by flow cytometry using anti-CD45 and ROR $\gamma$  antibodies. At all time points, a small number of ILC3s were detected in both dermis and draining lymph nodes, accounting for less than 2% of total cells in respective tissue (Figure 3.14A). The percentage of ILC3s was rapidly increased in dermis on day 1 post-wounding and continuously increased to its peak on day 5 post-wounding. This was accompanied by a reduction in the number of ILC3s in skin draining lymph nodes to its lowest level on day 5 post-wounding, suggesting the trafficking of blood-derived ILC3s back to blood circulation via lymph might be blocked or delayed to allow more ILC3s to maintain in wounded skin. By day 8 post-wounding, the percentage of ILC3s in dermis was dramatically decreased to unwounded level. Correspondingly, this was accompanied by a considerable increase in the percentage of ILC3s in skin draining lymph nodes, suggesting ILC3s left the wound and migrated to draining lymph nodes on 8 post-wounding. To verify these results and confirm the location of ILC3s, skin sections from wounded wild type mice were analyzed by using ROR $\gamma$  antibody. While ILC3s were detected in the dermis at all time-points (Figure 3.14B-E), the maximal number of ILC3s were detected on day 5 post-wounding at wound edges (Figure 3.14D). On day 2 post-wounding, most ILC3s were found in the reticular dermis (Figure 3.14 C), however, by day 5 and day 8 post-wounding, ILC3s were detected in both the reticular and papillary dermis

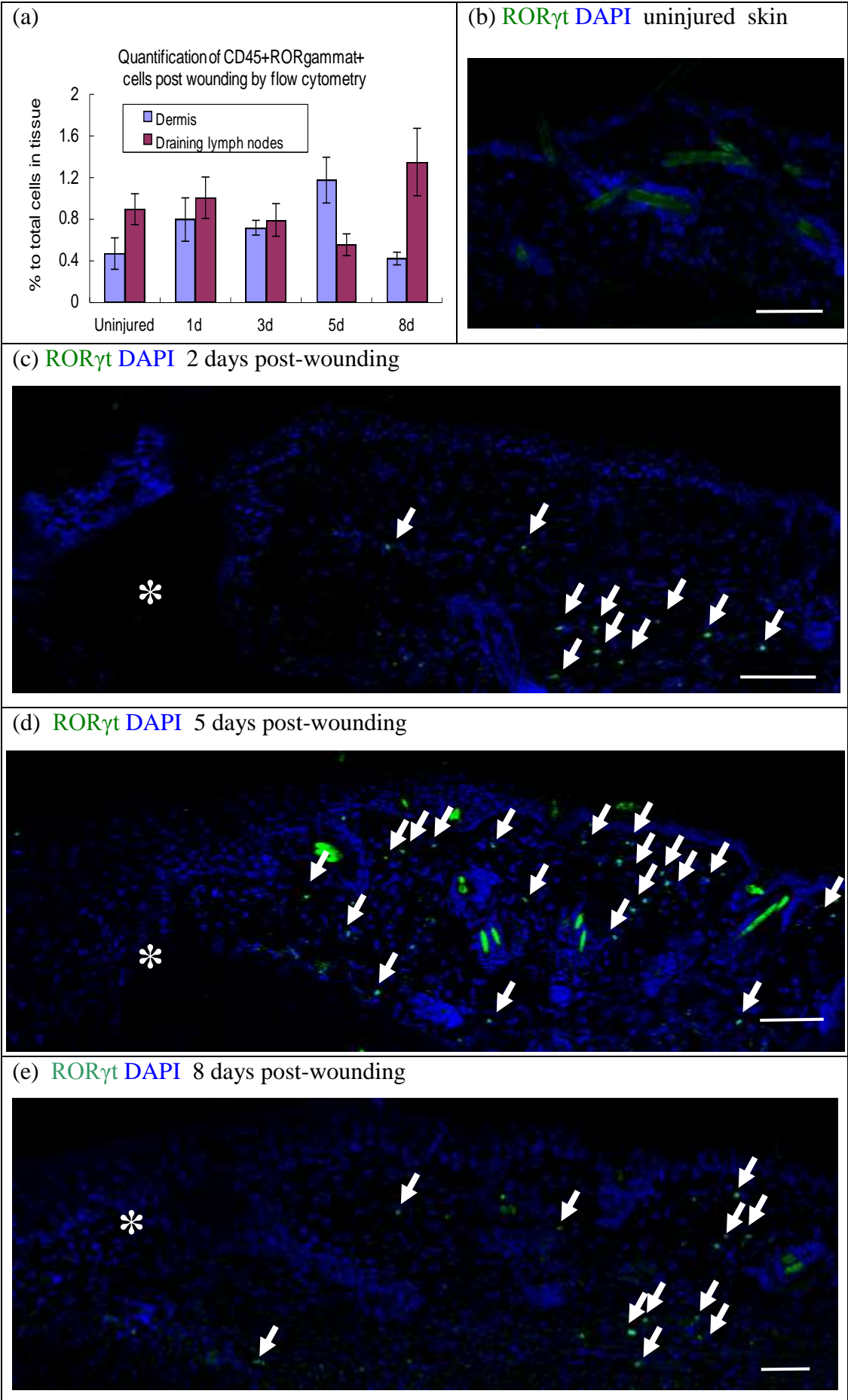
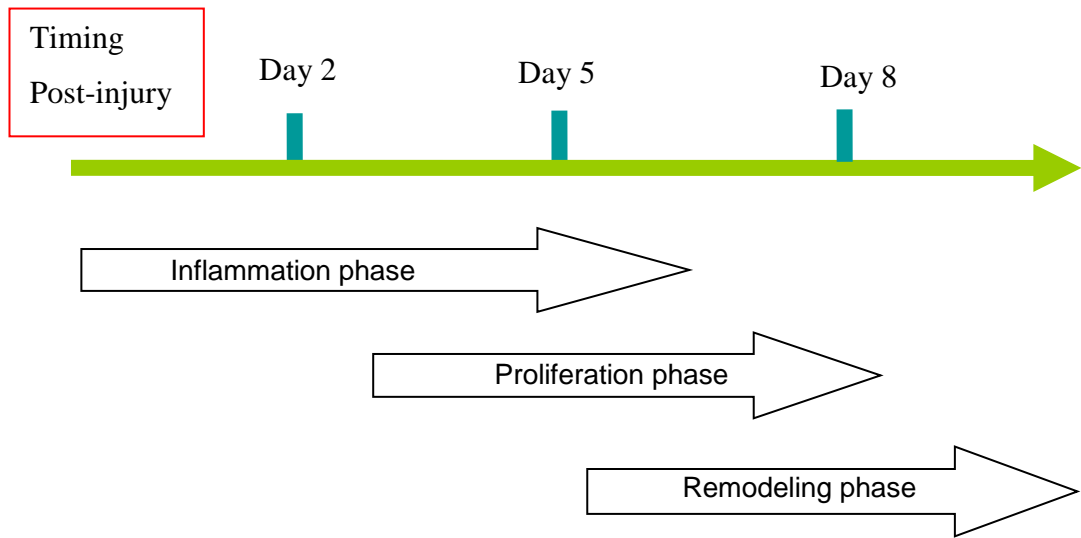


**Figure 3.14 ILC3s are recruited into dermis following wounding and are most abundant on day 5 post-wounding.** (a) The percentage of ROR $\gamma^+$  CD45 $^+$  cells in dermis and draining lymph nodes from uninjured or wounded mice at day 1, 3, 5 and 8 post-wounding were determined by flow cytometry. Graph bars represent experimental mean of biological replicates and error bars represent standard error of the mean (SEM). (b)-(e) Immunofluorescence chemistry of ROR $\gamma$  staining (green) on skin sections from uninjured (b) or wounded mice at day 2 (c), 5 (d) and 8 (e) post-wounding. Counterstained with DAPI (blue). Asterisk marks wound site. Arrow marks positive cells. Scale bar 100 micron.

(Figure 3.14 D and E) confirming active recruitment of cells from the reticular blood vascular network into the dermis. These results suggest ILC3s are involved in both early and later stages of skin wound healing.

### **3.3 Summary**

In this chapter, I examined the presence and dynamics of common immune cell types as well as an emerging group of innate lymphoid cells (i.e. ILC3s) at inflammation (day 2 post-wounding, or day 1 and 3 post-wounding), proliferation (day 5 post-wounding) and remodeling phases (day 8 post-wounding) of skin wound healing by flow cytometry and immunofluorescence chemistry using wounded mouse model. In steady state, skin was populated by resident immune cells accounting for 8-12% total skin cells, among which macrophages residing in dermis were the predominant cell type. I also detected a considerable number of dermal  $\alpha\beta$  T cells and epidermal dendritic T cells and Langerhans cells residing in unwounded skin. On day 2 post-wounding, the wound site was infiltrated by massive inflammatory cells which were either migrated from the adjacent skin or recruited from blood circulation through reticular blood capillaries. On day 5 post-wounding when the healing was in intensive proliferation phase, inflammatory infiltration at wound site was persistent but with a reduced speed of immune cell recruitment. By day 8 post-wounding when the wound was almost closed, inflammation was repressed and remodeling phase started. As for the specific cell types (Figure 3.15), most immune cells such as neutrophils, inflamed monocytes most of which gave to mature macrophages and a few of which acted as precursors for dendritic cells and possibly Langerhans cells, dendritic cells, Langerhans cells and NK cells reached their maximal number in early stage of wound healing followed by a reduction or maintenance (i.e. Langerhans



	Day 2	Day 5	Day 8
Leukocytes	↑↑↑	↑	↓↓↓
Neutrophil	↑↑	—	↓↓
Inflamed monocyte	↑↑↑	↓	↓↓
cDC	↑↑	↓↓	—
LC	↑	—	—
Macrophage	—	↑↑	↓↓
DETC	↓↓	↑↑↑	—
Dermal $\gamma\delta$ T cell	↓	↑↑	↓
$\alpha\beta$ T cell	↓	—	—
B cell	—	—	↓↓
NK cell	↑↑↑	↓↓	↓↓
ILC3	↑↑	↑↑	↓↓↓

**Figure 3.15 Summary of inflammation response in skin wound healing.** Skin wound healing initiates with inflammation phase followed by proliferation phase and remodeling phase with the indicated timing. The overall inflammation response is immediately promoted upon wounding, dramatically increased on day 2 post-wounding and persistent on day 5 post-wounding, and repressed on day 8. The cellular changes are shown in arrows. Upwards arrows indicate increase; downward arrows indicate decrease.



cells) in proliferation phase. Due to recruitment of inflamed monocytes, the numbers of mature macrophages were dramatically increased in proliferation phase. In contrast, the numbers of  $\gamma\delta$  T cells including DETCs and dermal  $\gamma\delta$  T cells were first decreased in early stage of wound healing followed by recovery in proliferation phase probably through self-proliferation as well as recruitment of blood-derived  $\gamma\delta$  T cells. However, the key cells in adaptive system,  $\alpha\beta$  T cells and B cells, appeared not to be significantly involved in skin wound healing, which is consistent with previous findings (Stout, 2010).

Most strikingly, in dermis from both unwounded and wounded mice, I detected ILC3s, a rare emerging population of innate lymphocytes which have been recently identified to play a role in local immunity and epithelial tissue repair in thymus and intestine through producing IL-22 (Dudakov et al., 2012; Spits and Cupedo, 2012; Spits et al., 2013; Spits and Santo, 2011). However, these ILC3s have unique phenotypes  $ROR\gamma^+ CD3^- CD4^{dim\ to\ +} CD127^{dim\ to\ +} CD117^- NKp46^-$ , which are distinct from currently known ILC3 subsets such as LTi cells ( $ROR\gamma^+ CD3^- CD127^+ CD4^{+50\%} CD117^+ NKp46^-$ ), ILC22 ( $ROR\gamma^+ CD3^- CD127^+ CD4^{+10\%} CD117^+ NKp46^+$ ) or ILC17 ( $ROR\gamma^+ CD3^- CD127^+ CD4^- CD117^- NKp46^-$ ).

I found these ILC3s were rapidly recruited into wound site dermis through blood vessels and reached their maximal number in proliferation phase. Interestingly, the other immune cells, such as macrophages,  $\gamma\delta$  T cells, which also had a pronounced expansion in their numbers in proliferation phase in wound healing (around day 5 post-wounding), are found to play important roles in skin repair (Bolleville et al., 2012; Macleod and Havran., 2011; Rodero and Khosrotehrani 2010; Stout 2010;

Sumaria et al., 2011). Macrophages contribute to myofibroblast-mediated wound contraction and dermal matrix deposition by producing TGF- $\beta$  (Rodero and Khosrotehrani 2010; Stout 2010). Epidermal  $\gamma\delta$  T cells (DETCs) contributes to keratinocyte proliferation and migration of macrophage by producing IGF-1, KGF and hyaluronan respectively (Bolleville et al., 2012; Macleod and Havran, 2011). Dermal  $\gamma\delta$  T cells are believed to play a similar role with DETCs in wound healing, although no evidence has been obtained (Sumaria et al., 2011). Therefore, it would be very interesting to expect a role for ILC3s in skin wound healing, and this will be tested in the next chapter.

## Chapter 4 The function of Group 3 ILCs (ILC3s) in skin wound healing

### 4.1 Introduction

Innate lymphoid cells (ILCs) are rare populations of lymphocytes that have key roles in secondary lymphoid tissue formation, homeostasis and cytokine production in response to pathogen infection or damage (Spits and Cupedo, 2012; Spits et al., 2013). One group of ILCs (Group 3 ILCs, ILC3s), also known as  $ROR\gamma^+$  ILCs, are characterized by the expression of  $ROR\gamma$  transcription factor and have key roles in adult thymus regeneration and intestinal epithelial barrier homeostasis and repair through IL22 production (Dudakov et al., 2012; Spits and Santo, 2011) which is dependent on IL23 produced by localized dendritic cell (Lee et al., 2012).

In last chapter, I presented evidence that  $ROR\gamma^+ CD3^- CD4^{dim to +} CD127^{dim to +} CD117^- NKp46^-$  ILC3s are recruited early into skin wound site with a peak in proliferation phase of the healing programme. In contrast,  $ROR\gamma^+$  T cells were hardly detectable in wounded skin especially at earlier time points, suggesting  $ROR\gamma^+$  cells recruited into wound site are primarily ILC3s. To determine whether these ILC3s play similar roles in tissue repair in skin as they do in the other epithelial tissues through producing IL-22, wounded  $ROR\gamma^{-/}$  mice lacking ILC3s as well as other  $ROR\gamma^+$  cells were analyzed and compared to control littermate in respect with wound healing rate, inflammation influx and epidermal proliferation rate. Since skin resident  $\gamma\delta$  T cells play a role in wound healing as suggested by previous studies (Bolleville et al., 2012; Macleod and Havran, 2011; Sumaria et al., 2011),  $Rag2^{-/}$  mice with deficiency in  $\gamma\delta$  T cells as well as  $\alpha\beta$  T cells and B cells were used as defective healing controls. I found that  $ROR\gamma^{-/}$  mice had poorly healed wounds compared to control littermates and  $Rag2^{-/}$  mice, which was directly caused by loss

of ILC3s. I conclude that ILC3s contribute to normal wound healing by controlling the timing of epidermal proliferation, regulating monocyte/macrophage entry into wounded dermis and supplying an important early source of IL-23-dependent IL22.

## **4.2 Results**

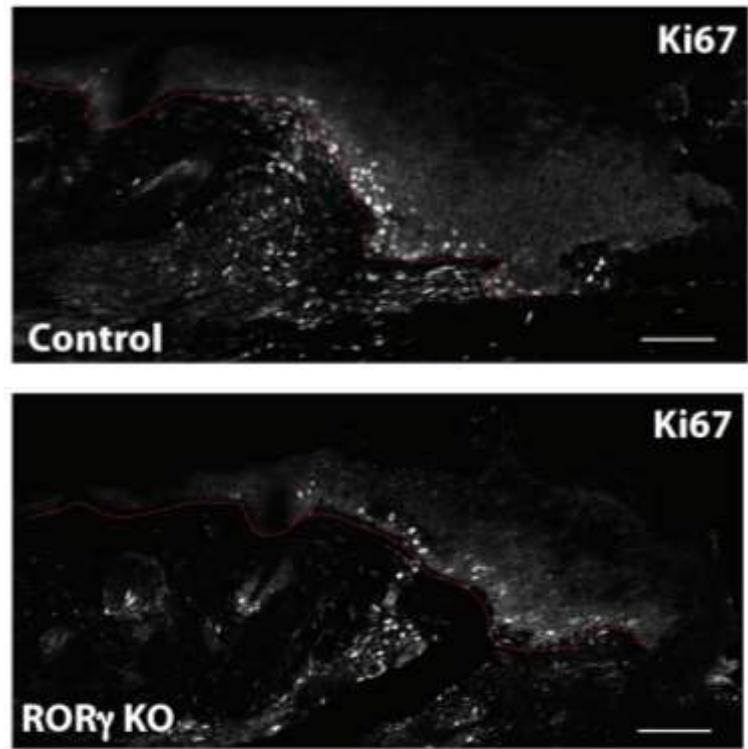
### **4.2.1 ROR $\gamma$ <sup>-/-</sup> mice have poorly healed wounds partly due to delayed epidermal proliferation**

The wound healing rate in ROR $\gamma$ <sup>-/-</sup> (Rag2<sup>+/-</sup>ROR $\gamma$ <sup>-/-</sup>, deficient in ILC3s and other ROR $\gamma$ <sup>+</sup> cells i.e. ROR $\gamma$ <sup>+</sup> T cells), Rag2<sup>-/-</sup> (Rag2<sup>-/-</sup>ROR $\gamma$ <sup>+/-</sup>, deficient in T cells and B cells) and littermate controls were analyzed. Mice were photographed daily and by day 3 post-wounding, wound size was delectably larger in ROR $\gamma$ <sup>-/-</sup> mice compared to control and Rag2<sup>-/-</sup> littermates (data not shown). By day 8 post-wounding, wounds were fully closed in control and Rag2<sup>-/-</sup> mice, while a large, crusty eschar remained in the poorly healed wounds in ROR $\gamma$ <sup>-/-</sup> mice (Figure 4.1A). Consistent with previous studies, there was some delay in wound closure in Rag2<sup>-/-</sup> mice probably due to loss of  $\gamma\delta$  T cells (Jameson et al., 2002), however ROR $\gamma$ <sup>-/-</sup> mice exhibited a severe defect demonstrating a key, previously unrecognized role for ROR $\gamma$ <sup>+</sup> cells in wound healing. As wounds in ROR $\gamma$ <sup>-/-</sup> mice remained large, I analyzed epidermal proliferation by Ki67 proliferation-marker expression; proliferation was quantified within a 0.5-millimetre distance from the wound site. On day 5 post-wounding, ROR $\gamma$ <sup>-/-</sup> mice had a marked reduction in Ki67<sup>+</sup> cells compared to controls (p=0.0006, t-test) (Figure 4.1B and C), by day 8 post-wounding, an increase in proliferative cells was detected in ROR $\gamma$ <sup>-/-</sup> mice (p=0.0143, t-test) (Figure 4.1C), suggesting the wound healing defect in ROR $\gamma$ <sup>-/-</sup> mice is partly caused by delayed epidermal proliferation.

A



B



C

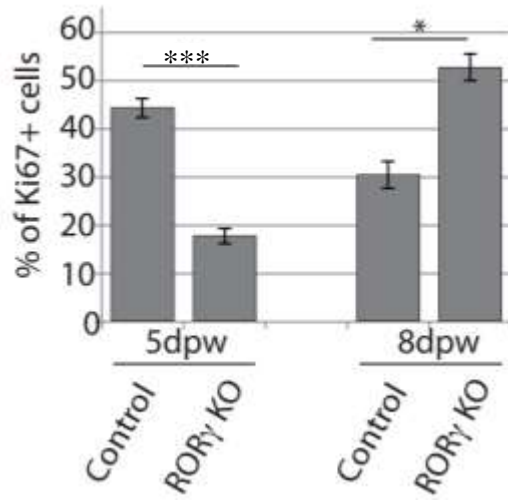


**Figure 4.1 Skin wound healing in ROR $\gamma$  KO mice are delayed partly due to reduced epidermal proliferation.** 4mm full-thickness wounds were created in 7-week-old ROR $\gamma^{+/-}$  Rag2 $^{+/-}$  (control), ROR $\gamma^{-/-}$  (ROR $\gamma$  KO) and Rag2 $^{-/-}$  (Rag2 KO) mice.(A) On day 8 post-wounding, wounds in ROR $\gamma^{-/-}$  mice remained large and crusty compared to Rag2 $^{-/-}$  and wild type controls.(B) Sections of wounded ROR $\gamma^{-/-}$  (ROR $\gamma$  KO) and control tissues collected on day 5 post-wounding were stained with antibodies to Ki67 (white). Scale bars equal 100 microns. Experiment repeated  $\geq 3$  times. (C) Graph shows percentage of Ki67 $^{+}$  basal epidermal cells within 500 microns of the wound site in control verses ROR $\gamma^{-/-}$  mice on day 5 and day 8 post-wounding. Tissues from 4 wounds (biological replicates) from both genotypes and time points were quantified. Statistics of normally distributed data compared by Student's t-test between control and ROR $\gamma$  KO samples on day 5 (p=0.0006\*\*\*) and day 8 (p=0.0143\*) post-wounding. Graph bars represent experimental mean of biological replicates and error bars represent standard error of the mean (SEM).

#### **4.2.2 CCL-3 dependent monocyte/macrophage recruitment is delayed in wounded $ROR\gamma^{-/-}$ back skin**

To examine if loss of  $ROR\gamma^+$  cells impacts the activities of the other immune cells, such as macrophages, that have key roles in skin repair, wounded  $ROR\gamma^{-/-}$  back skin sections were analyzed using anti-F4/80 antibody which could detect Langerhans cells in epidermis, macrophages including resident macrophages and blood-recruited monocytes (immature macrophages), and subsets of dermal dendritic cells which counted for less than 3% of total  $F4/80^+$  cells in skin (Figure 3.2). There was no detectable change in  $F4/80^+$  cells in epidermal compartment, however, a three-fold reduction in dermal  $F4/80^+$  cells was detected on day 2 post-wounding, compared to control ( $p=0.0315$ , t-test) and  $Rag2^{-/-}$  littermates (Figure 4.2A and data not shown). Since at this time-point, a large number of inflamed monocytes as precursors of macrophages are normally recruited into wound dermis through dermal blood networks in hypodermis and granular tissues (Figure 3.2), the reduction in the number of dermal  $F4/80^+$  cells (Figure 4.2A and B) reflects that monocyte/macrophage recruitment was impaired in  $ROR\gamma^{-/-}$  mice. These results suggest  $ROR\gamma^+$  cells but not T cells promote macrophage entry into dermis. This is consistent with a previous study which has shown DETCs do not contribute to macrophage recruitment (Macleod and Havran., 2011). By day 5 post-wounding,  $F4/80^+$  cells were plentiful within the dermis in all genotypes (Figure 4.2A right panel) suggesting that loss of ILC3s causes a delay, but not a block in macrophage infiltration. To examine the mechanism underlying the impaired macrophage recruitment, mRNA from wounded  $ROR\gamma^{-/-}$  back skin was analyzed for a chemokine CCL3 (also known as MIP1 $\alpha$ , macrophage inflammatory protein-1 $\alpha$ ) which attracts

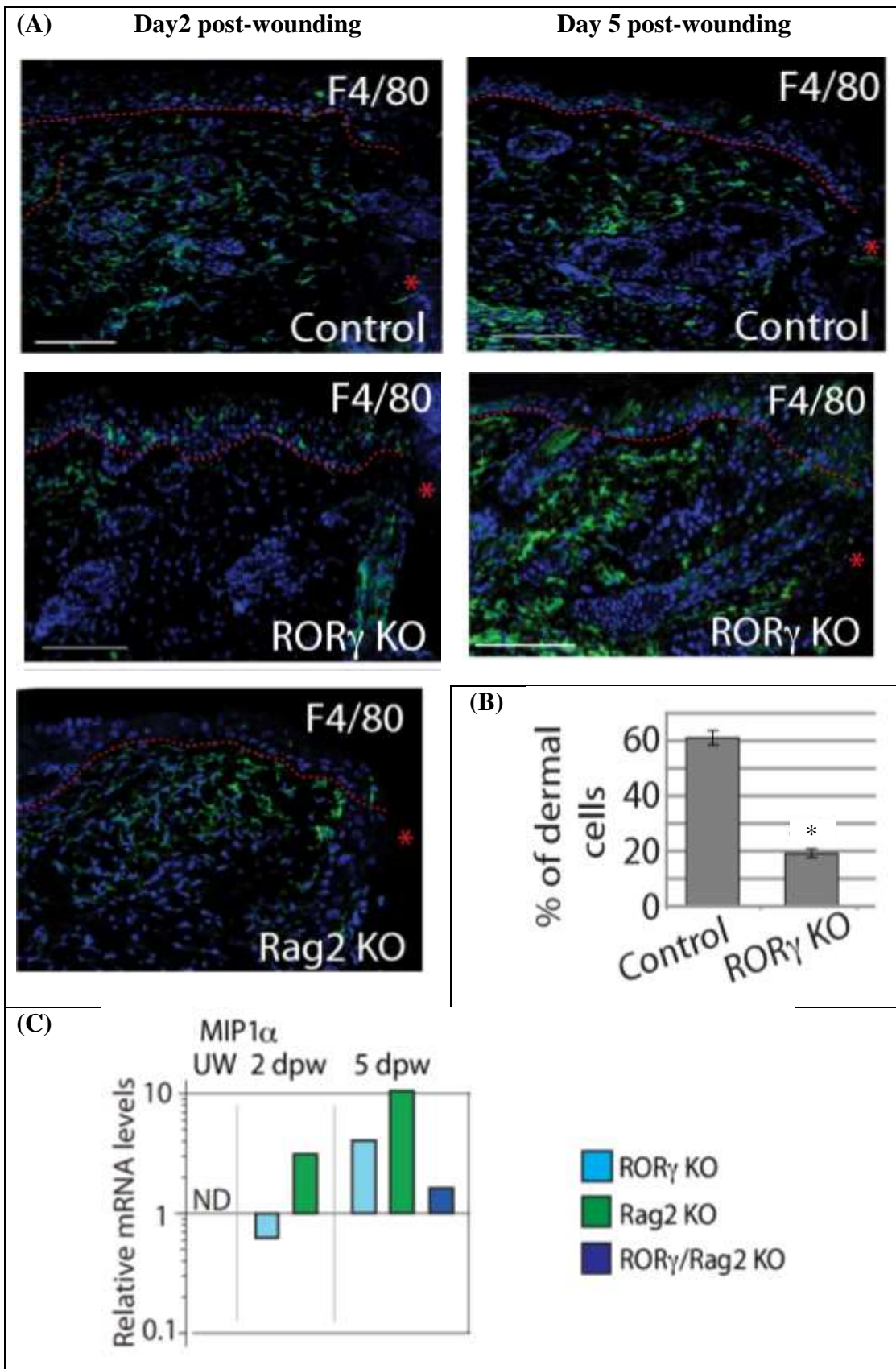




**Figure 4.2 Macrophage recruitment is delayed in wounded  $ROR\gamma^{-/-}$  back skin.**

Back skin tissues from wounded 7-week-old  $ROR\gamma^{+/+}$   $Rag2^{+/+}$  (control),  $ROR\gamma^{-/-}$   $Rag2^{+/+}$  ( $ROR\gamma$  KO) and  $ROR\gamma^{+/+}$   $Rag2^{-/-}$  ( $Rag2$  KO) were collected on day 2 or 5 post-wounding. (A) Sections were stained with an antibody to F4/80 antigen (green) and DAPI counterstained (blue). Note  $ROR\gamma$  KO wounds lack of dermal F4/80 positive cells on day 2 post-wounding, but not on day 5 post-wounding. Red, dashed line marks epidermal-dermal boundary; asterisk marks wound site scale bars equal 100 microns. (B) Graph shows percentage of F4/80<sup>+</sup> dermal cells in control verses  $ROR\gamma$  KO mice on day 2 post-wounding. Normally distributed data were compared by Student's t-test;  $p=0.0315$  (\*). Graph bars represent experimental mean of biological replicates and error bars represent standard error of the mean (3SEM). (C) Relative mRNA levels of MIP1 $\alpha$  (CCL3) quantified by quantitative PCR in unwounded back skin (UW) or wounded back skin on day 2 and 5 post-wounding from  $ROR\gamma^{-/-}$ ,  $Rag2^{-/-}$ ,  $ROR\gamma^{-/-}$   $Rag2^{-/-}$  and littermate control mice using biological replicates ( $n = 3$ ). mRNA levels were normalised to control mice on day 2 or day 5 post-wounding (designated 1). MIP1 $\alpha$  mRNA transcripts were undetectable (ND) in uninjured control skin. Note mean levels of MIP1 $\alpha$  were 1.6-fold lower in 2-day wounded  $ROR\gamma$  KO skin. Experiments were repeated  $\geq 2$  times.

the monocyte/macrophages to inflammatory sites. Compared to littermate controls,  $ROR\gamma^{-/-}$  mice had lower levels of CCL3 mRNA on day 2 post-wounding (Figure 4.2C) when the maximal number of monocytes are activated in normal wound healing (Figure 3.2), but had dramatically higher level on day 5 post-wounding (Figure 4.2C) when monocyte recruitment are unusually reduced in normal wound healing (Figure 3.2). In contrast, CCL3 mRNA level was considerably higher in wounded  $Rag2^{-/-}$  back skin than that in littermate controls on both day 2 and day 5 post-wounding (Figure 4.2C), suggesting T cells, probably skin resident  $\gamma\delta$  T cells might have a regulatory role in monocytes/macrophages recruitment. These results confirm that monocyte/macrophage recruitment is delayed in  $ROR\gamma^{-/-}$  mice in a mechanism dependent on CCL3.

#### **4.2.3 Loss of ILC3s directly causes wound healing defect in $ROR\gamma^{-/-}$ mice**

Although I have determined the vast majority of infiltrating  $ROR\gamma^{+}$  cells in wildtype skin wound are negative for CD3, TCR $\beta$  and TCR $\gamma$ , and thus are not T cells, a rare subset of  $ROR\gamma^{+}$   $\gamma\delta$  T cells are present at low levels in dermis (accounting for less than 1% of total  $ROR\gamma^{+}$  cells, Figure 3.12) (Gray et al, 2011) and might infiltrate skin wounds together with other  $\gamma\delta$  T cells at later stage of wound healing as suggested by the increase in dermal  $\gamma\delta$  T cell influx on day 5 post-wounding (Figure 3.7). In addition, since  $ROR\gamma$  is also transiently expressed by double positive CD4 $^{+}$  CD8 $^{+}$  T cells in thymus (Sun et al., 2000), T cell development and function could be disrupted or altered in  $ROR\gamma^{-/-}$  mice, although the role of  $ROR\gamma$  for T cell development is yet to be determined. Therefore, to determine if abnormal function of the remaining  $ROR\gamma^{-}$   $\gamma\delta$  T exist and impacted wound healing in  $ROR\gamma^{-/-}$  mice. I examined wound healing in  $Rag2^{-/-}ROR^{-/-}$  mice, which lack ILC3s and all T and B

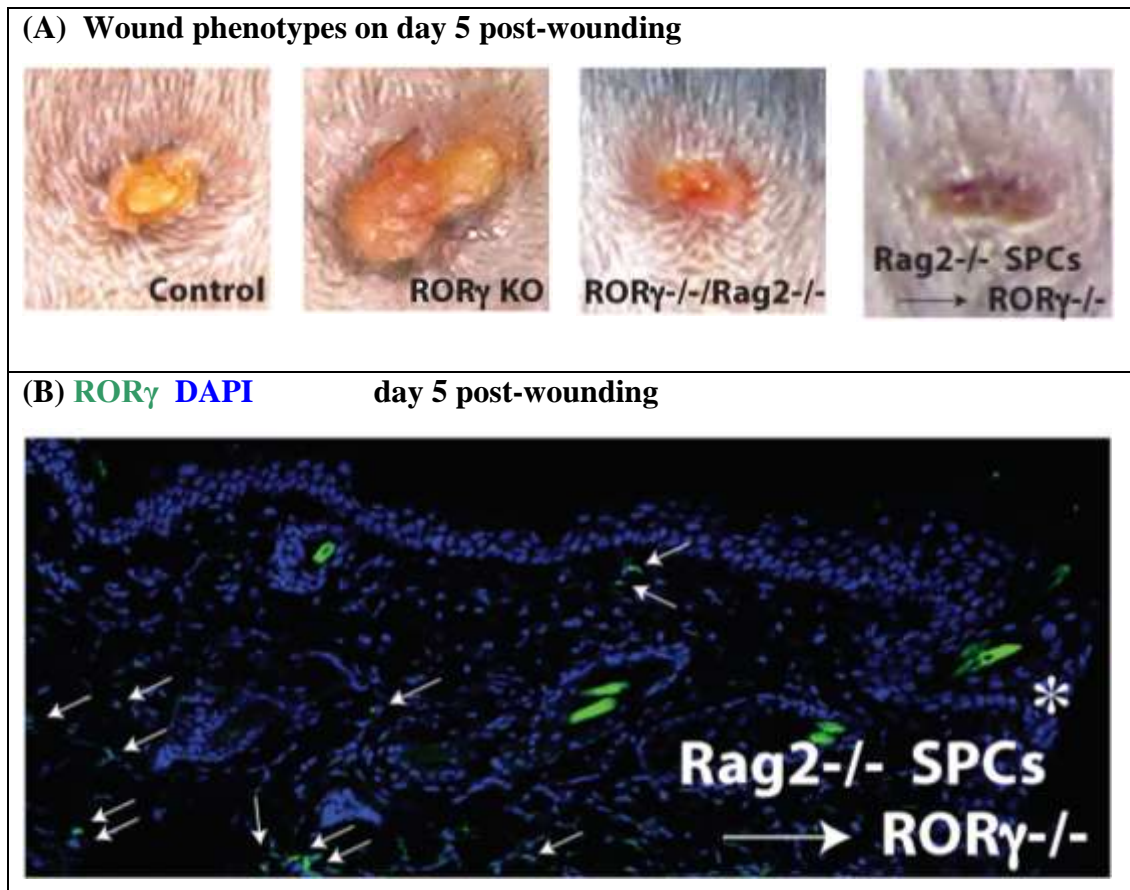


**Figure 4.3 Loss of ILC3s directly causes wound healing defects.** (A) Pictures of skin wounds taken on day 5 post-wounding show wound healing was delayed in  $ROR\gamma^{-/-}$  skin, however wound size in  $ROR\gamma^{-/-} Rag2^{-/-}$  was similar to wounded littermate controls.  $Rag2^{-/-}$  (deficient in T cells and B cells) spleen cells (SPCs) were transplanted into  $ROR\gamma^{-/-}$  mice prior to wounding (n = 3 mice). The wound size from  $ROR\gamma^{-/-}$  mice with transplanted  $Rag2^{-/-}$  spleen cells (including ILC3s, but excluding T cells) were similar to controls). (B) Tissue sections antibody stained for ROR $\gamma$  reveal ILC3s were recruited to wound sites in  $ROR\gamma^{-/-}$  skin with transplanted  $Rag2^{-/-}$  spleen cells. White arrows mark positive cells; asterisk marks wound site.

cells. Wound healing was not delayed significantly compared to control littermates (Figure 4.3), suggesting that T cells contribute to  $ROR\gamma^{-/-}$  wound pathology in some degree but that neither ILC3s nor  $ROR\gamma^{+}$  T cells are absolutely required for wound healing. To determine if the phenotype observed in the  $ROR\gamma^{-/-}$  mice was a result of loss of ILC3s rather than T cells, spleen cells from  $Rag2^{-/-}$  mice (lacking  $\alpha\beta$  and  $\gamma\delta$  T cells but containing ILC3s) were transferred into  $ROR\gamma^{-/-}$  mice 24 hours prior to wounding. Cell transplantation ameliorated wound pathology observed in control  $ROR\gamma^{-/-}$  mice and donor ILC3s could be detected adjacent to wound sites (Figure 4.3B). Therefore I conclude that the loss of ILC3s in  $ROR\gamma^{-/-}$  mice directly causes wound pathology.

#### **4.2.4 ILC3s supply early IL-22 in skin wound healing**

By definition, ILCs are innate lymphocytes that produce the cytokines which were originally thought to be produced by their corresponding counterparts T lymphocytes (Spits and Cupedo, 2002; Spits et al., 2013). Specifically, ILC3s are considered as counterparts of Th17 or Th22 cells, and produce IL17 and/or IL22 in response to IL-23 (Spits and Cupedo, 2002; Spits et al., 2013). In addition, some infiltrating  $\gamma\delta$  T cells may produce IL17 and/or IL22 (Gray et al., 2011). IL22 mediates its functions in tissues by binding to its heterodimeric receptor consisting of IL-10 receptor  $\beta$  (IL-10R $\beta$ ) and IL-22 receptor  $\alpha$  (IL-22R $\alpha$ ) (Xie et al., 2000). IL-22 signaling is typically involved in hemostasis and immunity in epithelial tissues, since IL-22R $\alpha$  is almost exclusively expressed by epithelial cells such as epidermal keratinocytes (McGee et al., 2013; Wolk et al., 2006). Furthermore, IL-22 has shown a key role in tissue repair and regeneration in thymus and intestine (Dudakov et al 2012), and promotes

keratinocyte proliferation and migration while repressing their differentiation *in vivo* (Boniface et al., 2005; Wolk et al., 2006; McGee et al., 2013). In addition McGee et al (2013) has shown that IL22 also promotes dermal repair by functioning on dermal fibroblasts. Given the results in the last chapter that ILC3s are recruited early to wound sites and promote epidermal proliferation during wound healing, I hypothesize ILC3s play this role via IL-22. To test this, IL-22 mRNA levels were examined by QPCR. In unwounded skin, IL-22 mRNA level was at the lower limit of detection by QPCR. On day 2 post-wounding, IL-22 mRNA levels in  $ROR\gamma^{-/-}$  wounds were not significantly different from unwounded controls (Figure 4.4A).  $Rag2^{-/-}$  mice also had reduced levels of IL22 consistent with a role for infiltrating  $\gamma\delta$  T cells in wound healing (Gray et al., 2011). Only control littermates displayed an evident increase in IL22 mRNA levels. Normally distributed data were compared between  $ROR\gamma^{-/-}$  and control littermates at day 2 post-wounding by Student's t-test ( $p=0.017$ ) (Figure 4.4A), suggesting a significant reduction of IL-22 mRNA levels in  $ROR\gamma^{-/-}$ . This reduction in IL-22 was not caused by lack of IL-23 as IL-23 mRNA expression was similar between  $ROR\gamma^{-/-}$  and control wounds (Figure 4.4A). These results suggest the delay in epidermal proliferation in  $ROR\gamma^{-/-}$  wounds is likely due in part to reduction in early IL22 expression.

Surprisingly, on day 5 post-wounding, increased levels of IL-22 mRNA were detected in both  $ROR\gamma^{-/-}$  and  $Rag2^{-/-}$  wounds as well as control wounds compared to unwounded control, with highest levels detected in  $ROR\gamma^{-/-}$  wounds (Figure 4.4B). Since IL-22 is known to be primarily produced by T cells (e.g. Th22) and ILC3s (Delves et al., 2011), this result suggested that some currently uncovered IL-22 producing cells might switch on IL-22 synthesis and compensate for the absence of

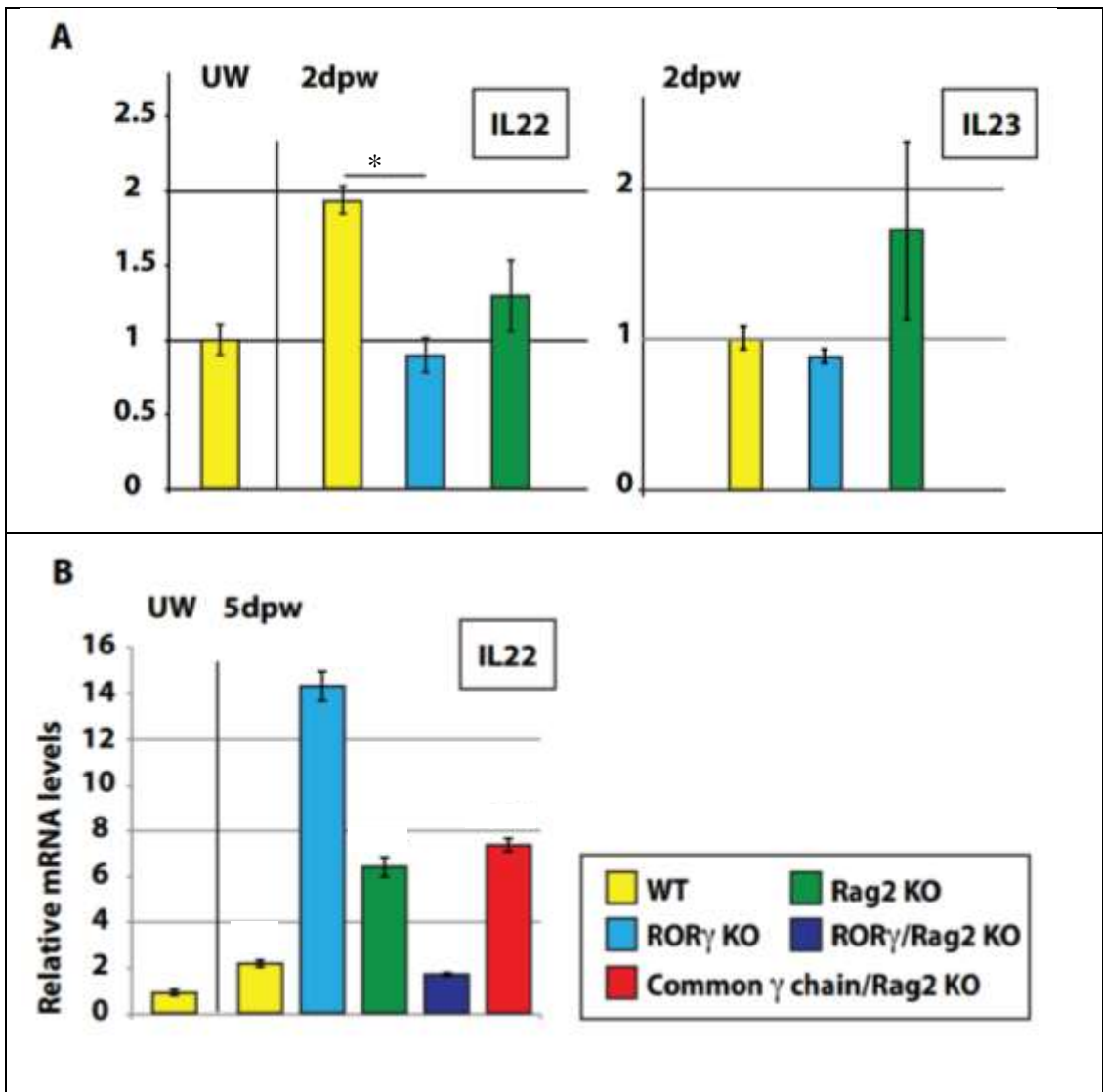


**Figure 4.4 ILC3s are an important early source of IL22.** (A) mRNA was isolated from unwounded controls or wounded  $ROR\gamma^{+/+} Rag2^{+/+}$  (WT),  $ROR\gamma^{-/-}$  (ROR $\gamma$  KO),  $Rag2^{-/-}$  (Rag2 KO),  $ROR\gamma^{-/-}/Rag2^{-/-}$ , or common  $\gamma$  chain $^{-/-} Rag2^{-/-}$  skin collected 2 days post wounding (dpw). Relative mRNA levels of IL22 and IL23 was quantified by QPCR. mRNA levels were normalised to unwounded control for IL22 (designated 1) or to wounded control mice for IL23 (designated 1). IL22 and IL23 mRNA transcripts were undetectable (ND) in uninjured control skin. Note only control mice 2 dpw ( $p=0.0170$ ) had statistically significant upregulation of IL22 compared to unwounded controls, whilst IL23 levels were not significantly different amongst genotypes. (B) By day 5 post-wounding, IL22 levels were elevated compared to unwounded controls in both wild type (WT) and leukocyte-deficient mice ( $ROR\gamma^{-/-}$ ,  $Rag2^{-/-}$ ,  $ROR\gamma^{-/-}Rag2^{-/-}$  and common  $\gamma$  chain $^{-/-} Rag2^{-/-}$ ). Error bars show standard error of the mean (SEM). For IL22, analysis = 5 or 6 biological replicates; for IL23, 3 replicates.

ILC3s or ROR $\gamma^+$  T cells at later stage of wound healing. To test this, Rag2 $^{-/-}$ ROR $\gamma^{-/-}$  wounds which lack ILC3s as well as both T cells and B cells, and  $\gamma c^{-/-}$ Rag2 $^{-/-}$  wounds which lack all lymphoid cells including NK cells were examined. Like the other immune-compromised mice examined, IL-22 mRNA levels were also elevated in day 5 wounds in Rag2 $^{-/-}$ ROR $\gamma^{-/-}$  and  $\gamma c^{-/-}$  Rag2 $^{-/-}$  mice, confirming non-lymphocyte source of IL22 exist in skin wounds and provide IL22 at later stage required for tissue repair. The ROR $\gamma^{-/-}$  wounds lacking early presence of IL-22 healed poorly despite an increased expression of IL22 at later stage, suggesting that the early IL-22 production is essential for wound healing and is dependent on ILC3s.

#### **4.2.5 IL-23 from dendritic/Langerhans cells is required for IL-22 production in skin wounds**

It is well established that IL-23, a protein formed of two subunits, P19 and p40, stimulates ILCs to produce IL-22 or IL-17 (Sonnenberg et al., 2011). Dendritic cells are considered as a source of abundant IL-23, however the IL-23 subunit p19 can be expressed by other cell types, such as colonic sub-epithelial myofibroblasts after being stimulated by TNF $\alpha$  (McGee et al, 2013). To confirm that skin dendritic cells are the source of IL-23 during wound healing, CD11c<sup>Cre</sup>Rosa26<sup>iDTR</sup> (Jung et al., 2002) were injected intraperitoneally with diphtheria toxin (DT) to deplete all dendritic cells including epidermal Langerhans cells or with PBS as a control for 4 consecutive days before wounding. Tissues were analyzed 2 or 5 days post-wounding and I confirmed that skin dendritic cells and Langerhans cells were deleted in DT-treated CD11c<sup>Cre</sup>Rosa26<sup>iDTR</sup> mice by skin section staining with CD11c and CD207 (Figure 4.5 B and C). From day 2 post-wounding, the wound sizes in DT treated animals were detectably larger than PBS-treated animals (Figure 4.5A). Both



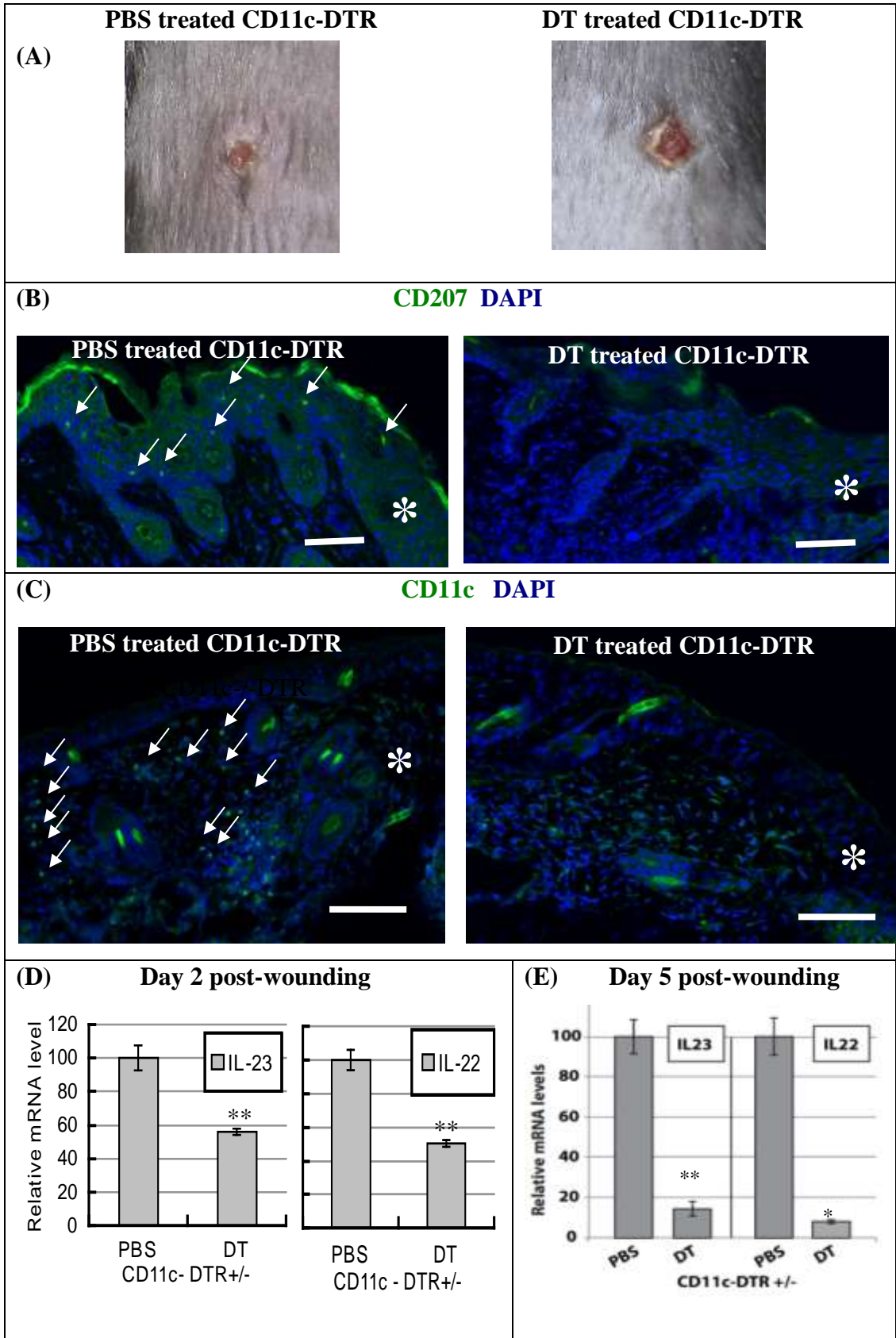


**Figure 4.5 IL22 production is dependent on IL23 supplied mainly by dendritic / Langerhans cells.** CD11<sup>cre</sup>Rosa26<sup>iDTR</sup> (CD11c-DTR) mice were injected with PBS or diphtheria toxin (DT) for 4 days prior to wounding. Back skin tissues were collected on day 2 or day 5 post-wounding. (A) Pictures were taken on day 5 post-wounding. (B-C) Tissue sections antibody stained for CD207 on day 5 post-wounding and CD11c on day 2 post-wounding confirm Langerhans cells and dendritic cells were depleted in CD11c-DTR. White arrows mark positive cells; asterisk marks wound site. Scale bars equal 100 microns. (D and E) mRNA was isolated from wounded mice and IL22 or IL23 levels quantified by QPCR. mRNA levels were normalised to PBS-injected day 2 or day 5 wounded CD11c-DTR mice (designated 100%). DT-treatment reduced IL22 and IL23 levels in wounds on both day 2 (D) and day 5 (E) post-wounding. Error bars show standard error of the mean (SEM). Statistic differences were compared by using Student's t-test in IL-23 mRNA on day 2 ( $p=0.0025^{**}$ ) and day 5 ( $p=0.0028^{**}$ ), and in IL-22 mRNA on day 2 ( $p=0.0006^{**}$ ) and day 5 ( $p=0.0054^*$ ).

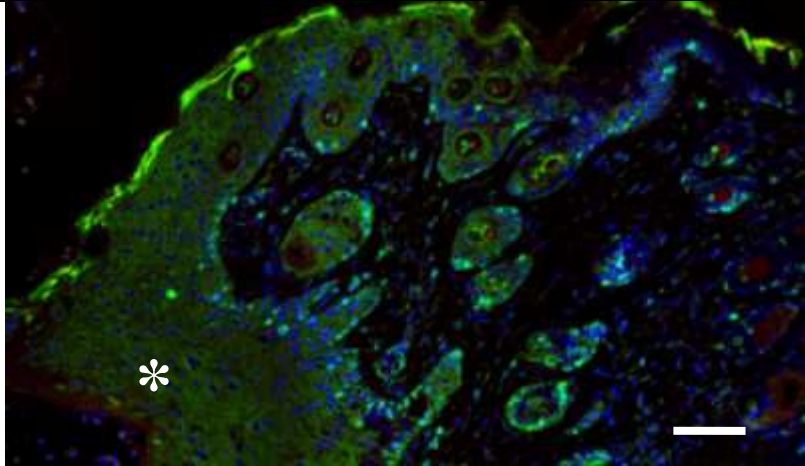
IL-23 and IL-22 mRNA levels in DT-treated animals were reduced by nearly 50% compared to PBS-treated animals ( $p=0.0025$  and  $0.0006$  for IL-23 and IL-22 respectively, t-test) (Figure 4.5D). On day 5 post-wounding, IL23 mRNA level was further substantially reduced (14% of PBS-control treated animals) ( $p=0.0028$ , t-test), correspondingly, IL-22 was also considerably reduced (8% of PBS-control treated animals) in DT-treated  $CD11c^{Cre}Rosa26^{iDTR}$  wounds ( $p=0.0054$ , t-test) (Figure 4.5E). Taken together, these results confirm that dendritic cells in skin are the main source of IL-23 which is required for IL-22 production during wound healing.

#### **4.2.6 IL23 is required for IL22-dependent epidermal proliferation but not for monocyte/macrophage recruitment**

Since differential productions of IL-22 were detected in DT-treated and PBS-treated  $CD11c^{Cre}Rosa26^{iDTR}$  due to loss of dendritic/Langerhans cell-produced IL23, epidermal proliferation rates and monocyte/macrophage recruitment were then compared between these mice in order to confirm if IL22/IL23 play a role in macrophage/monocyte recruitment as well as epidermal proliferation. Wounded skin sections were first analyzed for proliferation marker Ki67 on day 5 post wounding using an antibody specific to Ki67. As expected, a large number of  $Ki67^{+}$  cells were detected in wound edge epidermis in PBS-treated  $CD11c^{Cre}Rosa26^{iDTR}$  animals (Figure 4.6A), confirming the epidermal predominant cell type, keratinocytes, were undergoing extensive proliferation, although a small proportion of  $Ki67^{+}$  cells could be self-proliferating Langerhans cells. By contrast, the epidermal layers in DT-treated  $CD11c^{Cre}Rosa26^{iDTR}$  mice were much thinner than PBS-treated animals.

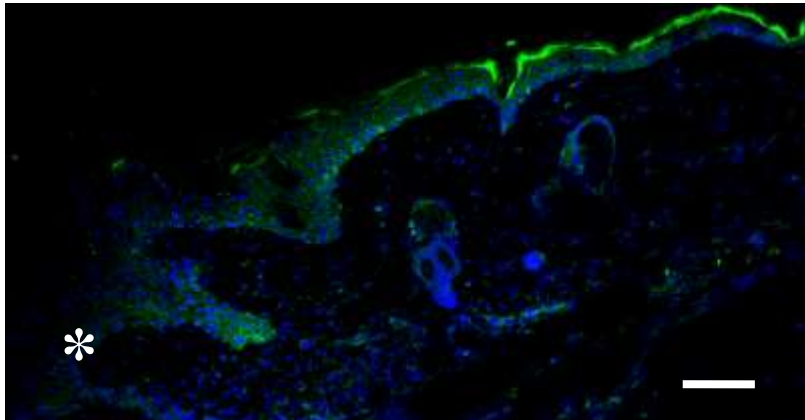
(A) **Ki67** **DAPI**

**PBS treated**  
**CD11c-DTR**



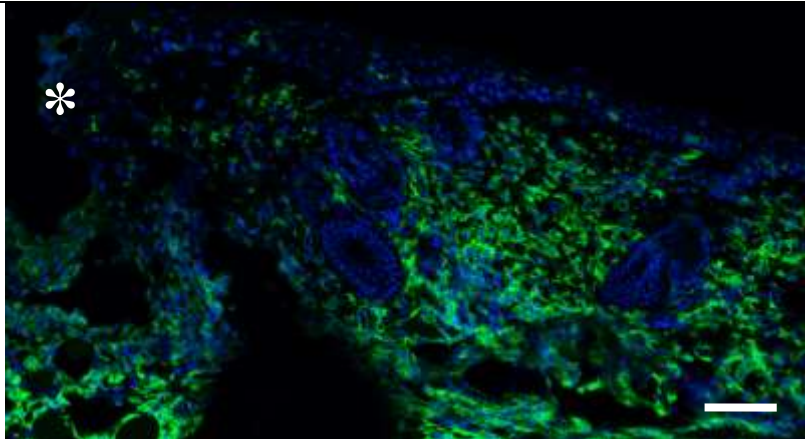
**Ki67** **DAPI**

**DT treated**  
**CD11c-DTR**



(B) **F4/80** **DAPI**

**PBS treated**  
**CD11c-DTR**



**F4/80** **DAPI**

**DT treated**  
**CD11c-DTR**

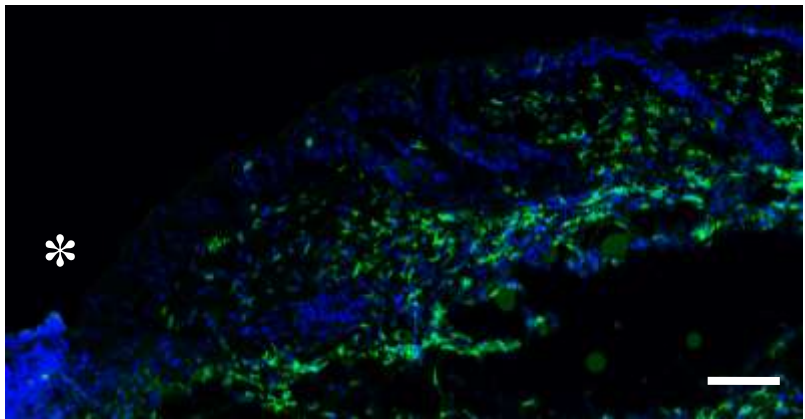


**Figure 4.6 IL23/IL22 is required for epidermal proliferation but not for macrophage/monocyte recruitment.** CD11<sup>cre</sup>Rosa26<sup>iDTR</sup> (CD11c-DTR) mice were injected with PBS or diphtheria toxin (DT) for 4 days prior to wounding. Back skin tissues were collected on day 2 or day 5 post-wounding. Tissue sections antibody stained for Ki67 (A) on day 5 post-wounding and F4/80 (B) on day 2 post-wounding reveal dramatic reduction in epidermal proliferation but apparently normal macrophage recruitment in CD11c-DTR. Asterisk marks wound site. Scale bars equal 100 microns

Correspondingly, Ki67<sup>+</sup> cells were almost undetectable. Skin sections were then analyzed for monocytes/macrophages by using an antibody to their marker F4/80 on day 2 post-wounding marker when a large number of monocytes/macrophages are normally recruited into wound site. F4/80<sup>+</sup> monocyte/macrophage were plentiful in both wound edge dermis and hypodermis in both DT and PBS treated CD11c<sup>Cre</sup>Rosa26<sup>iDTR</sup> mice (Figure 4.6B). It should be noted, the vast majority of epidermal F4/80<sup>+</sup> cells were lost in DT-treated CD11c<sup>Cre</sup>Rosa26<sup>iDTR</sup> mouse epidermis, confirming the deletion of F4/80<sup>+</sup> Langerhans cells. These results suggest epidermal proliferation but not monocyte/macrophage recruitment is dependent on IL23/IL22 signaling. Consistent with previous results (Boniface et al., 2005; Wolk et al., 2006), I have shown a co-relationship between IL22 and epidermal proliferation. In addition, I found IL22 may not be required for monocyte/macrophage recruitment, although this is to be confirmed yet by future experiments where IL-22 needs to be directly targeted.

### 4.3 Summary

In this chapter, I presented evidence that loss of ILC3s in RORγ<sup>-/-</sup> mice directly impacted the wound healing rate with delayed dependent epidermal proliferation and monocyte/macrophage recruitment due to lack of early IL-22 and CCL3 respectively. I also demonstrated loss of dendritic/Langerhans cells in DT-treated CD11c<sup>Cre</sup>Rosa26<sup>iDTR</sup> mice causes dramatic reduction of IL-23 production and its dependent IL-22 production thereby indirectly impacting wound healing. These results suggest that ILC3s play a key role in normal skin wound healing by promoting early entry of monocyte/ macrophage into wound site via CCL3, and

supplying early source of IL-22 for epidermal proliferation. Skin localized dendritic cells including both Langerhans cells and dermal dendritic cells also may play a role in wound healing by producing IL-23 that activates ILC3s and other IL22-producing non-lymphocytes to produce IL22, a key signaling in epithelial tissue repair.

## **Chapter 5 Epidermal Notch1 signaling promotes skin wound healing through recruiting ILC3s**

### **5.1 Introduction**

The Notch pathway is a key, cell-autonomous signaling pathway that directs cell fate and has pleiotropic functions in the skin (Ambler and Watt, 2010; Watt et al., 2008). Notch signaling initiates when a Notch ligand binds to one of four receptors present on mammalian cells, which causes receptor cleavage and enables the intracellular domain to undergo nuclear translocation and affect changes in gene transcription (Artavanis-Tsakonas et al., 1999). There are 4 mammalian Notch receptors, expression of all 4 receptors in the epidermis has been reported (Nickoloff et al., 2002). Genetic studies suggest Notch1 is the primary receptor needed to regulate cell differentiation required to maintain hair and skin epithelium (Ambler and Watt, 2010; Estrach et al., 2007; Kerabs et al., 2000; Kerabs et al., 2003; Pan et al., 2004; Watt et al., 2008). However, some studies suggest Notch2 also plays a non-redundant role in embryonic development and tissue maintenance (Pan et al., 2004; Saito et al., 2003). A previous study using topically-applied pan-Notch activators and inhibitors suggested that Notch might be involved in wound healing, however, the mechanistic details and site of action were unknown (Chigurupati et al., 2007). Our lab's previous work showed that forced, ectopic epidermal Notch1 activity in by applying 4OHT to K14NICDER mice resulted in extensive, epidermal proliferation and severe inflammation, two phenotypic hallmarks of skin wound healing (Ambler and Watt, 2007; Ambler and Watt, 2010; Estrach et al., 2006). Therefore, I hypothesized adult epidermal Notch signaling might play roles in skin wound healing by contributing to inflammatory cell recruitment and epidermal proliferation.



In this chapter, Notch1 and Notch2 activity was examined during skin wound healing. I found both Notch1 and Notch2 were rapidly activated in skin predominantly within epidermal compartment after injury with different timings, suggesting epidermal Notch1 and Notch2 might play different roles in skin wound healing. To investigate their individual roles, mice were pre-treated with individual Notch receptor blocking antibody, anti-NRR1 or anti-NRR2 before wounding. I found that the wound healing rate in anti-NRR1 treated were significantly impacted at early stage (2 days post-wounding) compared to control mice. However, there is no significant difference in later stage on day 5 post-wounding. I hypothesized the delay in wound healing might be caused by lack of early IL-22 following blocking Notch1. Since in the last chapter, I presented evidence that ILC3s supplies early IL-22, a key signaling in epidermal proliferation in wound healing, it is possible that Notch1 exerts its role in wound healing via ILC3s. To test this, inflammatory cellular influxes were analyzed in anti-NRR1 treated wounded mice and in 4OHT-treated uninjured K14NICDER mice where Notch1 activity can be tightly controlled in the epidermis. The K14NICDER transgene contains a truncated, Notch1 intracellular domain (NICD1) that can be temporally and spatially activated by 4-hydroxy-tamoxifen (4OHT) in the basal, keratin 14-expressing epidermis. I confirmed that ILC3 recruitment were recruited into dermis in a manner dependent on epidermal Notch1 signaling, which contributes to wound closure by producing early IL-22 as well as recruiting monocyte/macrophage early to the wound site. These results suggest epidermal Notch1 signaling promotes skin wound healing through an ILC3-mediated process.

## **5.2 Results**

### **5.2.1 Skin injury activates epidermal Notch1 and Notch2**

To determine the Notch1 and Notch2 activities in wound healing, wounded mouse back skin were collected on day 1, 3/4 and 7 days post-wounding, and analyzed by western blotting and immunofluorescence chemistry using specific antibodies to activated forms of Notch1 or Notch2. Western blotting results (Figure 5.1A) showed that wounding caused an immediate increase in Notch1 activity on day 1 post-wounding (7x) ( $p=0.0183$ , t-test) with peak activity detected on day 4 post-wounding (16x) ( $p=0.0011$ , t-test) (data collected by Soulmaz Boroumand). Notch2 activity was also immediately increased after injury with a less significant rate than Notch1. Notch2 activity reached its peak (2.5x) ( $p<0.05$ , t-test) on day 1 post-wounding and was gradually decreased afterwards, and dropped back to unwounded level by day 8 post-wounding (Data was collected by Soulmaz Boroumand). The location of Notch1 and Notch2 expression in epidermis was confirmed by immunofluorescence chemistry on skin sections (Figure 5.1B, data collected by Soulmaz Boroumand). In unwounded skin, Notch activity was detected only in rare epidermal supra-basal cells (data not shown; Ambler and Watt, 2010). However, increased Notch1 and Notch2 activity was detected in all epidermal layers (Figure 5.1 B, data collected by Soulmaz Boroumand). These results suggest skin injury results in immediate activation of Notch1 and Notch2 activity in epidermal keratinocytes. However, there is a difference in the timings and the fold-changes between Notch1 and Notch2 activity, suggesting Notch1 and Notch2 might have different roles in wound healing.

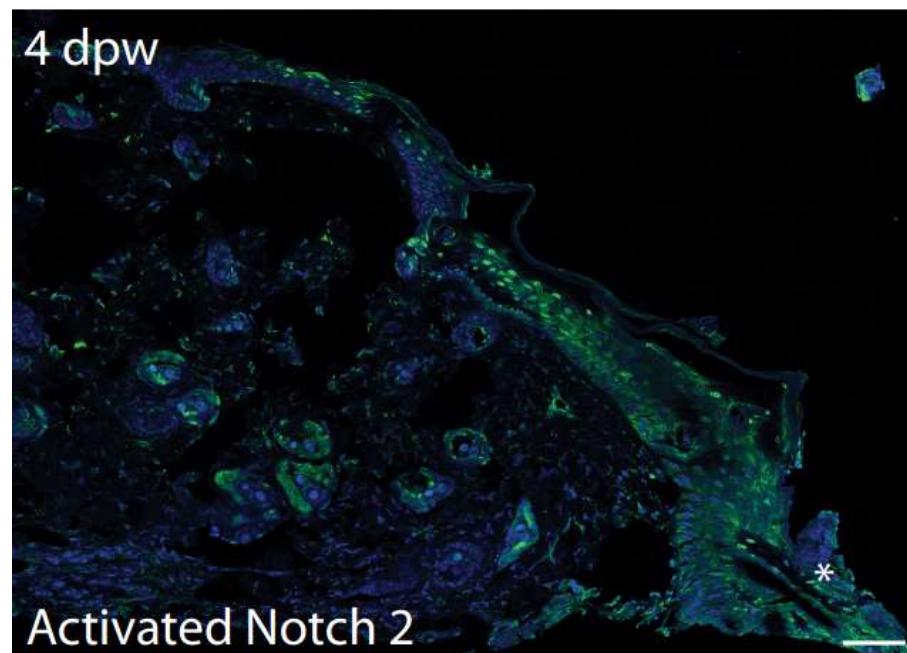
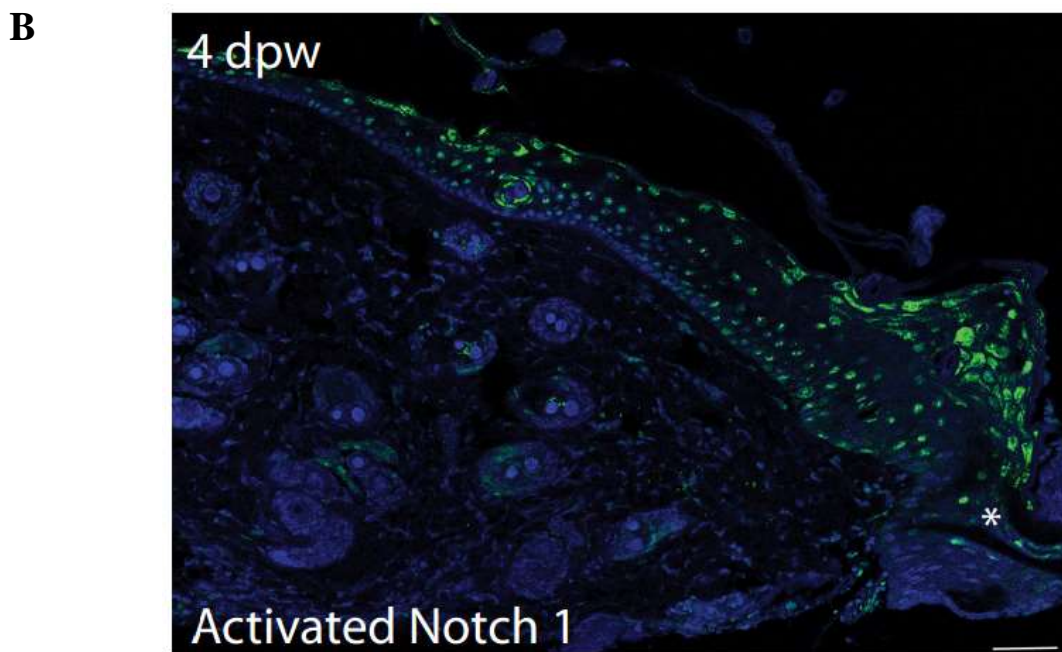
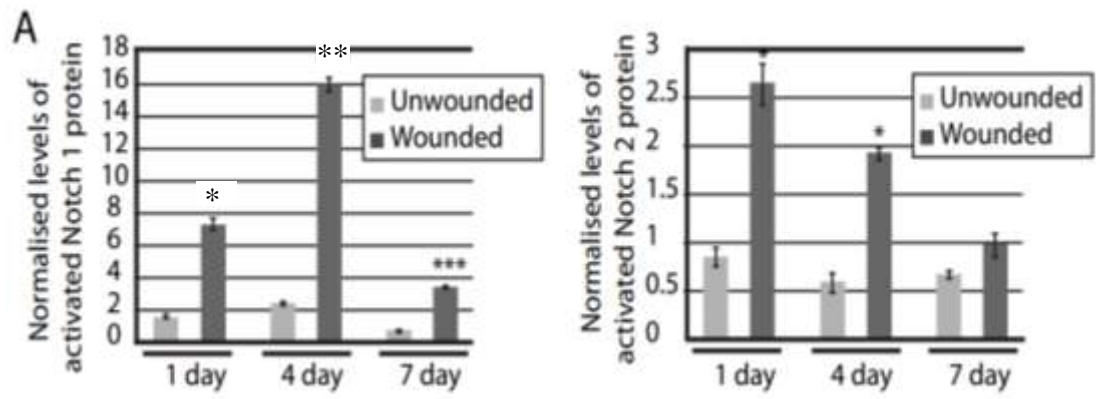


**Figure 5.1 Epidermal Notch1 and Notch2 are activated upon skin injury (Data was collected by Soulmaz Boroumand).** Back skin tissues from punch-wounded wild type mice were collected 1, 4 and 7 days post-wounding. (A) Quantified levels of cleaved, activated Notch1 and Notch2 proteins by antibody probes in a western immunoblotting assay. As loading controls, Notch1 and Notch2 levels were standardized to  $\beta$ -actin levels as a loading control and normalized to the average back skin protein levels (designated as 1) of Notch1 or Notch2 in uninjured littermate mice (n=3). Unwounded back skin was taken from a punch-wounded mouse at a distal site (minimum 2 cm) from wound site. Protein lysates from 3 different mice were analyzed for each time point post-wounding (dpw). Statistics of normally distributed data are compared by Student's t-test between wounded and unwounded samples at the stated days post-wounding. Notch1, 1 dpw p=0.0183 (\*), 4 dpw p=0.0011 (\*\*), 7 dpw p=0.0001(\*\*\*); Notch2, 1dpw p<0.05(\*). (B) Antibodies specific for activated Notch1 and Notch2 and reacted with cells adjacent to wound on day 4 post-wounding. Note activated Notch1 and Notch2 is detectable in all epidermal layers. Asterisk marks wound site. Scale bar equals to 50 microns.

### **5.2.2 Treating with anti-NRR1 and anti-NRR2 blocking antibodies specifically reduce Notch1 or Notch2 activity in wounded skin**

To investigate the role of Notch pathway in wound healing, Notch signaling was blocked prior to wounding. With the most recent pharmaceutical development of Notch-blocking antibodies, anti-NRR1 and anti-NRR2, ligand-activation of individual Notch receptor (i.e. Notch1 or Notch2) could be blocked (Wu et al., 2010). To test if anti-NRR1 and anti-NRR2 treatments were effective to block Notch signaling in our wounded mouse model, wildtype mice were injected intraperitoneally (*i.p.*) with 5mg/kg of anti-NRR1, 5mg/kg of anti-NRR2, 5mg/kg of control (anti-ragweed) or 2.5mg/kg of both anti-NRR1 and anti-NRR2 every 3 or 4 days for 7 days prior to wounding (Figure 5.2A). Since combined treatment with anti-NRR1 and anti-NRR2 are reported to cause severe adverse effects on mouse intestine and body weight loss by at least 10% due to blockage of both Notch1 and Notch2 signaling (Wu et al., 2010), the body weight of mice was scaled at the indicated days (Figure 5.2A) and compared to their body weight prior to the initial treatment. As expected, the body weight of combined anti-NRR1 and anti-NRR2 treated mice were dramatically reduced 3 days after the initial treatment and by day 7 their body weight was decreased by over 10% compared to their original body weight prior to treatment. By contrast, the mice which were treated with the other antibodies maintained their body weight (change <5%) before wounding. It is not surprising that all mice lost body weight at some degrees after wounding, since injury causes both physical and physiological stress to mice (Guo and DiPietro, 2010). These results confirmed that combined treatment with anti-NRR1 and anti-NRR2 blocking antibodies caused intestinal effects as expected in our wounded mouse model.

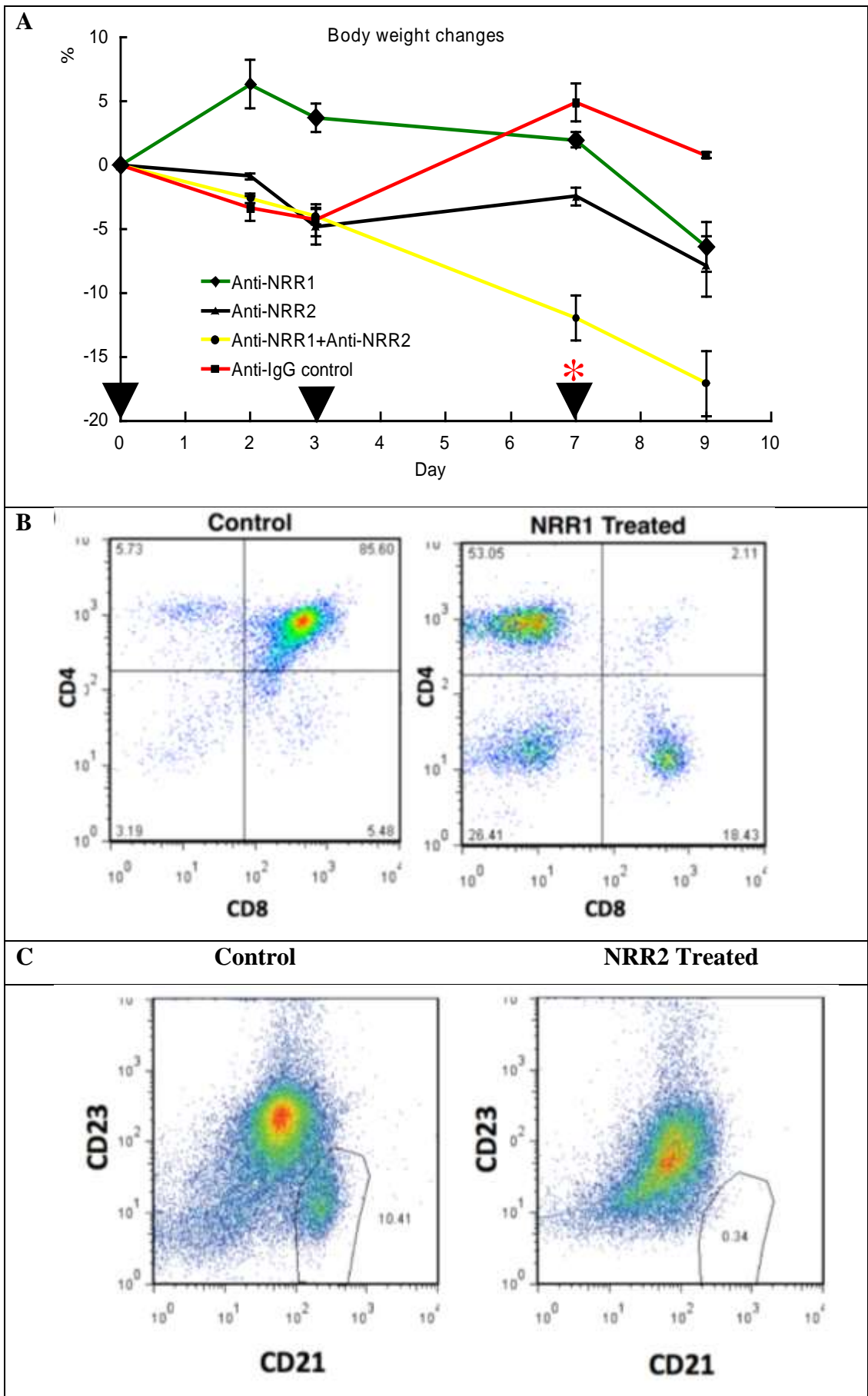


**Figure 5.2 Systemic effects of anti-NRR1 and anti-NRR2 treatment.** Punch-wounded wild type mice were injected peritoneally with 5mg/kg of anti-NRR1, 5mg/kg of anti-NRR2, 2.5mg/kg of both anti-NRR1 and anti-NRR2 antibodies or 5mg/kg anti-ragweed control for 7 days prior to wounding. (A) Body weight changes within 9 days following anti-NRR1/NRR2 treatment and wounding at day 7 (indicated by red asterisk). Arrow heads marks the timing of anti-NRR1/NRR2 treatment. Note the body weight in combined anti-NRR1 and anti-NRR2 treated mice was dramatically reduced. (B) Thymus was collected on day 2 post-wounding. Cells isolated from thymus were labelled with CD4 and CD8 antibodies and analysed by flow cytometry, only 2.1% of cells are CD4<sup>+</sup>CD8<sup>+</sup> in NRR1 treated mice. (C) Spleen was collected on day 2 post-wounding, cells isolated from spleen were labelled with CD45R (B220), CD5, CD21 and CD23, and analyzed by flow cytometry, only 0.34% of CD45R<sup>+</sup> B cells are CD21<sup>+</sup> CD23<sup>-</sup> cells. Note Notch1 activity is required for T cell maturation in thymus, while Notch2 activity is required for B cell maintenance in spleen marginal zone (Izon et al., 2001; Saito et al., 2003). (B-C) represent one biological sample, 3 individual biological replicates were tested (not shown).

To test if anti-NRR1 and anti-NRR2 are effective to specifically block Notch1 or Notch2 activity, wildtype mice were i.p. treated with 5mg/kg of anti-NRR1, 5mg/kg of anti-NRR2 or 5mg/kg of anti-ragweed control for 7 days prior to wounding, then thymus and spleen were collected on day 2 post-wounding. Previous studies have shown Notch1 activity is required for T cell maturation in thymus, while Notch2 activity is required for B cell maintenance in spleen marginal zone (Izon et al., 2001; Saito et al., 2003). Therefore, cells isolated from thymus were stained with antibodies to CD4 and CD8 to examine double positive thymocytes ( $CD4^+ CD8^+$ ) and cells isolated from spleen were stained with antibodies to CD45R (B220), CD5, CD21 and CD23 to examine the splenic marginal zone B cells ( $CD45R^+ CD21^+ CD23^-$ ) (Wu et al., 2010). As seen in Figure 5.2B, there was a sharp reduction in the percentage of double positive thymocytes ( $CD4^+CD8^+$ ) in anti-NRR1 treated mice from over 80% to below 3%, while this percentage was not significantly changed in anti-NRR2 treated mice (data not shown). As seen in Figure 5.2C, splenic marginal zone B cells were detected in anti-ragweed-treated mice, representing over 10% of total  $CD45R^+$  B cell in spleen. However, this percentage was dramatically reduced to less than 1% in anti-NRR2 treated mice. There was no significant change in the number of splenic marginal zone B cells in anti-NRR1 treated mice (data not shown). These results confirmed that treatment with anti-NRR1 or anti-NRR2 specifically and completely blocked Notch1 or Notch2 signaling in large lymphoid organs, such as spleen and thymus as expected, in our wounded mouse model.

To test if peritoneal injection with anti-NRR1 and anti-NRR2 antibodies was effective to target Notch1 or Notch2 activity in skin both of which have shown an significant increase upon wounding (Figure 5.1A), punch-wounded wildtype mice



were *i.p.* treated with 5mg/kg of anti-NRR1, 5mg/kg of anti-NRR2 or 5mg/kg anti-ragweed control for 7 days prior to wounding, then wounded skin tissues were collected and processed on day 2 post-wounding. Wounded skin sections were stained with an antibody to activated form (cleaved form) of Notch1 or Notch2 intracellular domain. As seen in Figure 5.3A-D, the detectable levels of cleaved Notch1 and Notch2 upon wounding were lowered by anti-NRR1 or anti-NRR2 treatment, however, cleaved Notch1 or Notch2 were still detectable in epidermis (indicated by arrows in Figure 5.3B and D), suggesting epidermal Notch1 and Notch2 activities, unlike the ones in thymus or spleen, was incompletely inhibited by corresponding blocking antibodies. The differential effectiveness observed between skin and central organs (i.e. Thymus and spleen) may be due to the relatively limited entry of chemicals to skin through blood circulation. To confirm if epidermal Notch1 or Notch2 was inhibited, western immunoblotting of protein lysates extracted from wounded back skin from anti-NRR1, anti-NRR2, combined anti-NRR1 and anti-NRR2, and anti-ragweed control treated mice were probed with an antibody to cleaved Notch1 or Notch2 as well as loading control  $\beta$ -actin (Figure 5.3E-F). As expected, the lowest levels of cleaved Notch1 protein were detected in anti-NRR1 as well as combined anti-NRR1 and anti-NRR2 treated mice, while the lowest levels of cleaved Notch2 protein were detected in anti-NRR2 as well as combined anti-NRR1 and anti-NRR2 treated mice. Note, compared to Notch1, less abundant levels of cleaved Notch2 protein were detected in anti-ragweed treated mice, which is consistent with our finding (Figure 5.1) that the increase in Notch2 activity upon wounding is not as evident as Notch1 activity. In summary, I confirmed that *i.p.* treatment with anti-NRR1 and anti-NRR2 blocking antibodies specifically reduced Notch1 or Notch2 activity in wounded mouse back skin (i.e. epidermis).

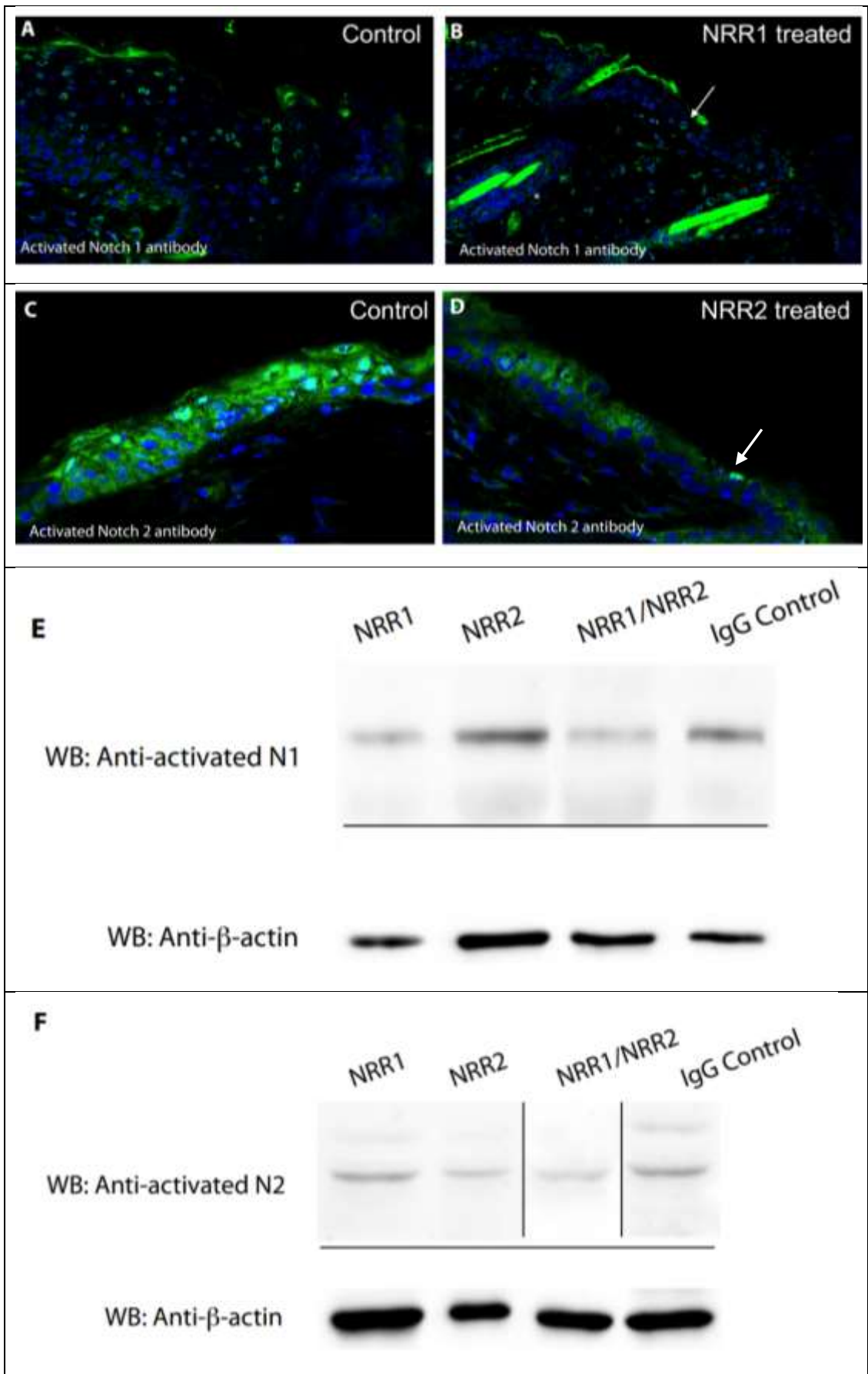


**Figure 5.3 Epidermal Notch1 and Notch2 activities are reduced by anti-NRR1 or anti-NRR2 treatment.** Punch-wounded wildtype mice were injected peritoneally with 5mg/kg of anti-NRR1, anti-NRR2, anti-ragweed control for 7 days prior to wounding. Skin tissues were collected and processed on day 2 post-wounding. (A-D) Skin sections from anti-ragweed IgG control (A, C), anti-NRR1 (B), anti-NRR2 (D) treated mice were stained with activated cleaved Notch1 (A-B) and Notch2 (C-D) respectively. Scale bars equal 50 microns. (E-F) Western immunoblotting of protein lysates were probed with antibodies to cleaved Notch1, Notch2 or  $\beta$ -actin. Shown one biological sample; 3 individual biological replicates were tested (not shown) and experiments performed twice per sample. Note, NRR1 treatment lowered detectable levels of cleaved Notch1 by in sections (B, arrows) and immunoblotting (E), however, Notch1 receptor cleavage was not completely inhibited by NRR1 blocking antibodies in wounded skin.

### **5.2.3 Inhibiting Notch1 activity causes wound healing delay partly due to lack of early IL-22**

Earlier results in this Chapter have suggested epidermal Notch1 and Notch2 activities are involved and activated in skin wound healing, and treating with anti-NRR1 or anti-NRR2 blocking antibody specifically reduces epidermal Notch1 or Notch2 activity in wounded mice. In this section, the individual roles of Notch1 and Notch2 activities in wound healing are determined by examining the wound healing rates in anti-NRR1 or anti-NRR2 treated mice with inhibited Notch1 or Notch2 activity. Wildtype mice were i.p. treated with 5mg/kg of anti-NRR1, 5mg/kg anti-NRR2 or 5mg/kg IgG control for 7 days prior to wounding, then mice were examined on day 2 or day 5 post-wounding. Wound closure rates were measured as a percentage of wound size at the time of examination to their initial size. On day 2, wounds treated with anti-NRR1 were significantly more open (77%;  $p=0.021$ , t-test) compared to control mice injected with anti-ragweed (66%) (Figure 5.4A and C). However, wounds treated with anti-NRR2 had similar sizes to anti-ragweed treated wounds (Figure 5.4 A and C). By 5 days post-wounding, wound size in anti-NRR1-treated mice did not differ from controls, however, their wounds displayed a distinct phenotype: wounds were redder, with domed margins (signs of abnormal wound granulation), compared anti-ragweed treated control wounds (Figure 5.4 B and C). Anti-NRR2 treated mice were not well and thus were not determined at this time point. Since wounds remained larger in anti-NRR1 treated mice on day 2 post-wounding, the key signaling in epidermal proliferation, IL-22 was quantified by QPCR at mRNA levels isolated from skin wounds. The IL22 mRNA levels in anti-ragweed treated wounds were used as control and designated as 1. As can be seen in Figure 5.4D, IL22 mRNA levels were significantly reduced by 50% in anti-NRR1-

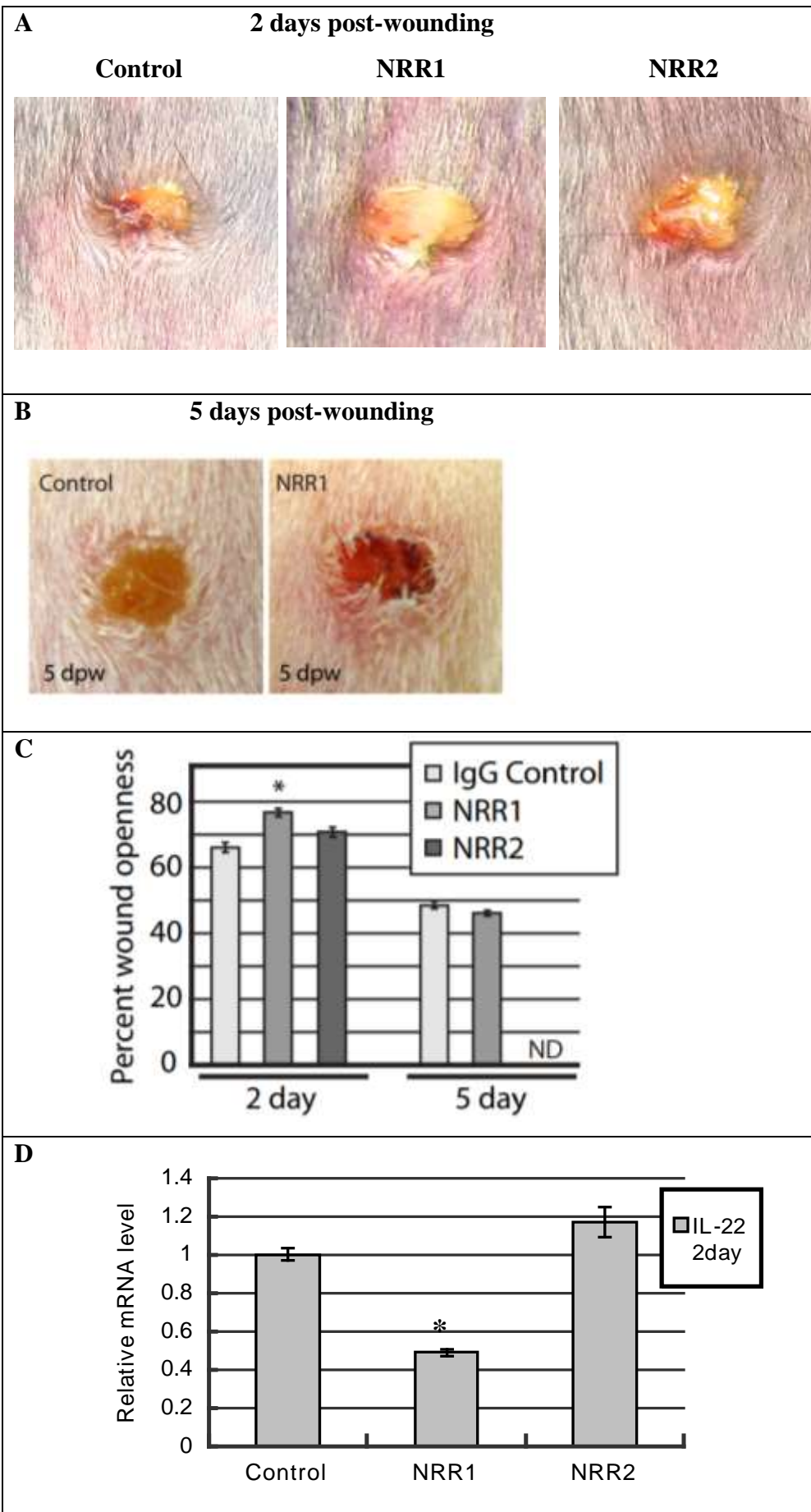


**Figure 5.4 Inhibiting Notch1 activity delays wound closure.** Punch-wounded wild type mice injected peritoneally with 5mg/kg anti-NRR1, anti-NRR2 or anti-ragweed control antibody for 7 days prior to injury. (A-B) Photos of skin wounds were taken on day 2 (A) and day 5 (B) post-wounding. Anti-NRR2 treated mice were not well and thus were not examined on day 5 post-wounding. (C) Wound openness was measured as a percent of initial wound size on day 2 and day 5 post-wounding. Note NRR1-treated wounds were significantly more open on day 2 post-wounding (\*  $p=0.0210$ ) but not on day 5. However, on day 5 wounds were redder with raised, domed margins compared to controls. (D) mRNA was isolated from wounded mice on day 2 post-wounding and IL22 levels were quantified by QPCR. mRNA levels were normalised to IgG control-injected day 2 wounded mice (designated as 1). IL22 mRNA level was significantly reduced in anti-NRR1-injected mice compared to the controls (\*  $p=0.010$ ). Graph bars represent experimental mean of biological replicates and error bars represent standard error of the mean (SEM). Statistics of normally distributed data compared by Student's t-test. All experiments were repeated  $\geq 2$  times.

injected mice ( $p=0.010$ , t-test), while IL22 mRNA levels in anti-NRR2 treated wounds did not differ from control. These results suggest that inhibiting Notch1 activity causes wound healing delay partly due to lack of early IL-22, and epidermal Notch1 activity may be required for IL22-dependent skin repair.

#### **5.2.4 IL22-producing ILC3s are recruited to dermis in a Notch1-dependent manner**

Since ILC3s are the main source of IL-22 in early wound on day 2 post-wounding (Figure 4.4), I hypothesize the reduction in IL-22 mRNA levels in anti-NRR1 treated early wounds (Figure 5.4D) are caused by lack of ILC3s. To test this, wildtype mice were *i.p* injected with anti-NRR1 and anti-ragweed control for 7 days prior to wounding, then wounded back skin tissues were collected on day 2 post-wounding. Cells isolated from anti-NRR1 or anti-ragweed treated wounded skin were labelled with antibodies to CD45 and ROR $\gamma$  and analyzed by flow cytometry, revealing that the recruitment of CD45<sup>+</sup> ROR $\gamma$ t<sup>+</sup> cells (the majority of which are ILC3s, Figure 3.12) as well as the total immune cell (CD45<sup>+</sup>) were decreased by  $2.3 \pm 0.2$  fold (Mean  $\pm$  SEM) in anti-NRR1 treated mice compared to anti-ragweed treated controls (Figure 5.5 A). Wounded skin sections from anti-NRR1 and anti-ragweed treated control mice were analyzed by using an antibody to ROR $\gamma$ , confirming ILC3 recruitment were inhibited by anti-NRR1 treatment (Figure 5.5 B). These results suggest a role of Notch1 activity, probably from epidermis, in recruiting ILC3s which produce early IL22 and in turn promote skin repair. However, blocking Notch signaling could also impact ILC3 development, since Notch signaling activity within ILC3 is required for adult ILC3 development (Possot et al., 2011). Although

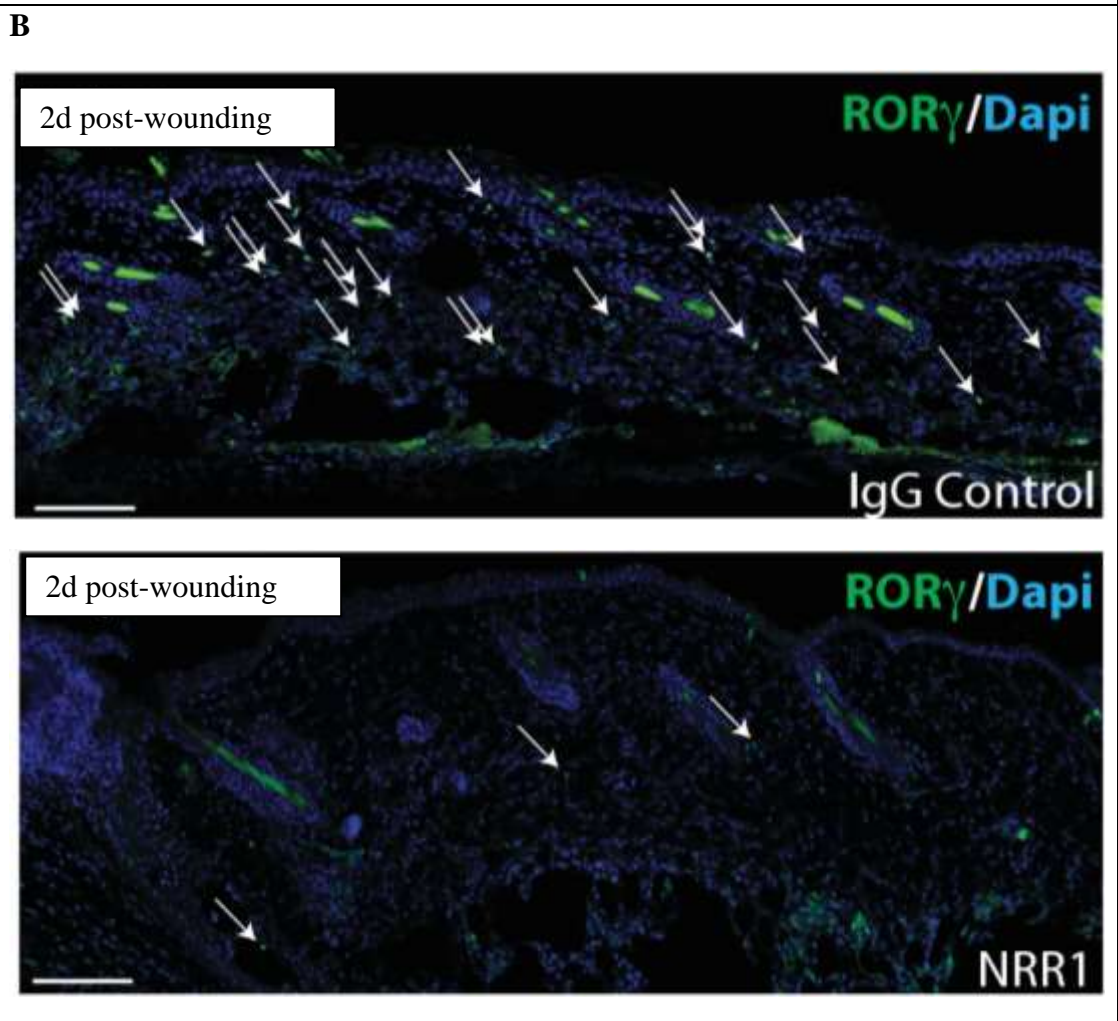
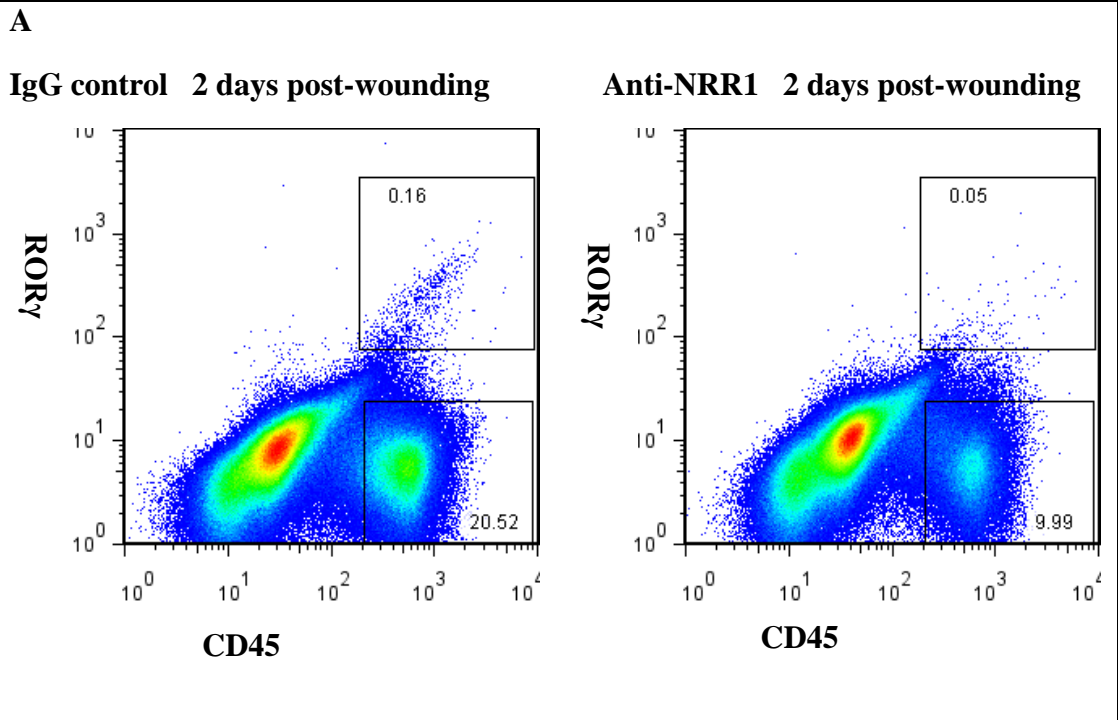
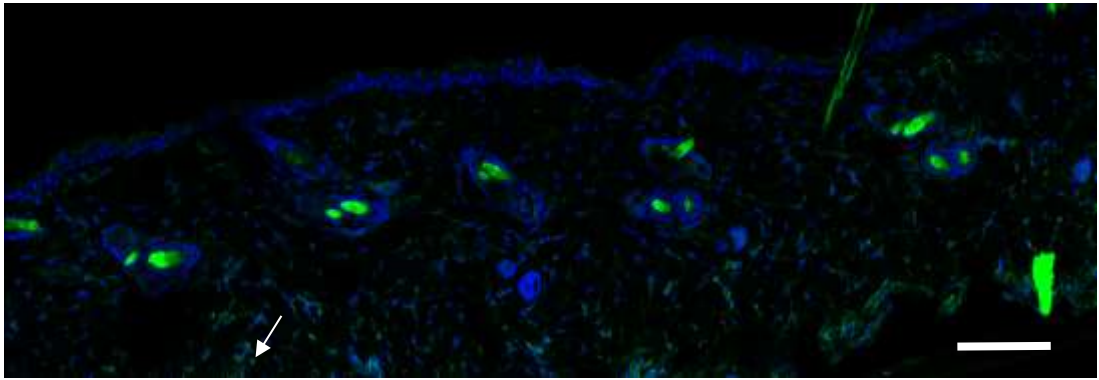




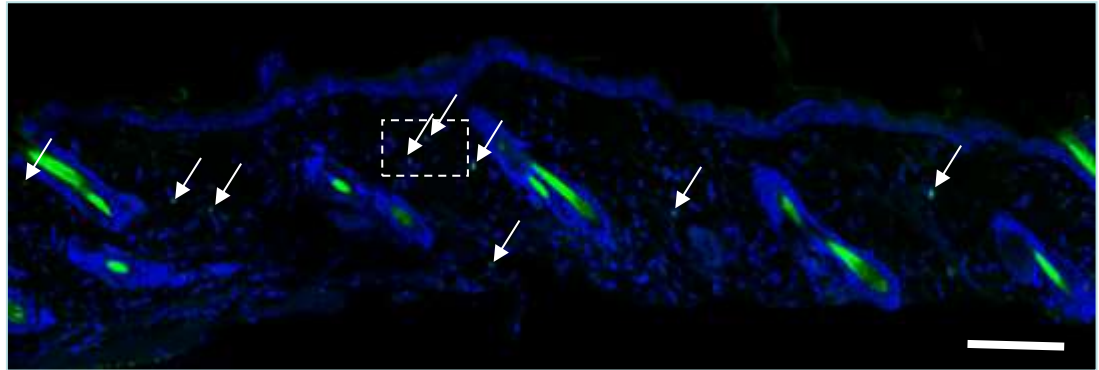
**Figure 5.5 Inhibiting Notch1 blocks ILC3 recruitment following wounding.** Punch-wounded wild type mice injected peritoneally with 5mg/kg anti-NRR1, anti-NRR2 or anti-ragweed IgG control antibody for 7 days prior to injury. Wounded back skin was collected on day 2 post-wounding. (A) Cells isolated from anti-IgG control and anti-NRR1 treated wounded skin were labelled with CD45 and ROR $\gamma$  and were analyzed by flow cytometry, confirming the ILC3s as well as total immune cell recruitment were dramatically reduced in anti-NRR1 treated mice on day 2 post-wounding. One biological sample is shown, at least 3 biological samples were analyzed (not shown). (B) Wounded skin stained with an antibody ROR $\gamma$  revealed that the infiltration of ROR $\gamma$ <sup>+</sup> cells (mostly ILC3s) was blocked in anti-NRR1 treated mice on day 2 post-wounding. Scale bars equal 100 microns. Asterisk marks wound site. Experiments were repeated  $\geq 3$  times.

blocking Notch1 alone is unlikely to influence ILC3 development (Possot et al., 2011), to confirm if ILC3 recruitment into skin is dependent on epidermal Notch1 signaling, uninjured back skin from K14NICDER mice carrying a ectopic functional fragment of Notch1 intracellular domain as well as littermate controls were topically treated with 4OHT for 3 days to activate ectopic Notch1 signaling specifically in epidermis. 4OHT treated uninjured skin sections were analyzed for ILC3 recruitment in skin by using an antibody to ROR $\gamma$ t. ROR $\gamma$ t<sup>+</sup> cells were dramatically accumulated in 4OHT-treated K14NICDER dermis compared to 4OHT-treated littermate controls (Figure 5.6 A and B), confirming the active recruitment of ILC3s by epidermal Notch1 signaling. To confirm the phenotypes of these ROR $\gamma$ t<sup>+</sup> cells in uninjured skin, back skin sections from 3-day-4OHT- treated K14NICDER were co-stained with antibodies to ROR $\gamma$ t together with one or two of the following antibodies to CD3, CD4 or CD127 (Figure 5.6 C and D). I confirmed that the ROR $\gamma$ t<sup>+</sup> cells recruited in uninjured skin by Notch1 signaling were CD3<sup>-</sup> CD4<sup>dim to +</sup> CD127<sup>+</sup> ROR $\gamma$ t<sup>+</sup> ILC3s, which is consistent with the phenotypes of ILC3s recruited in skin wounds. These epidermal Notch1-recruited ILC3s may also produce IL-22 in uninjured skin in 4OHT-treated K14NICDER mice, which could lead to epidermal hyper-proliferation as detected previously (Ambler and Watt, 2010; Estrach et al., 2006). In summary, I confirmed that ILC3s are recruited to dermis in an epidermal Notch1-dependent manner, which is an important early source of IL-22, a key signaling to skin repair.

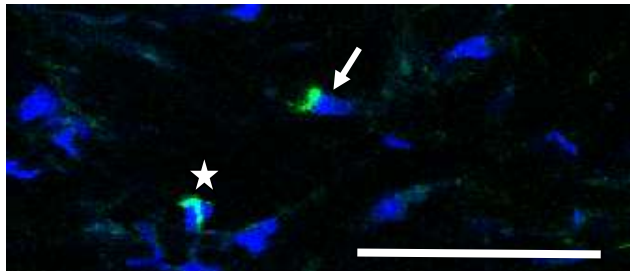
(A) **RORrt** / **DAPI** 4OHT treated WT



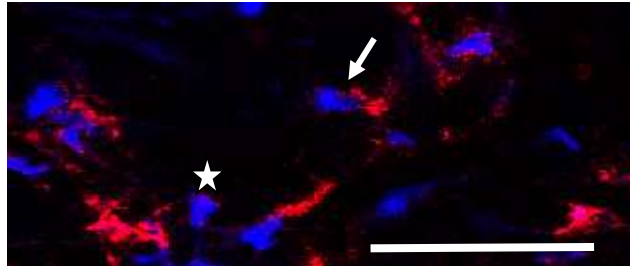
(B) **RORrt** / **DAPI** 4OHT treated K14NICDER



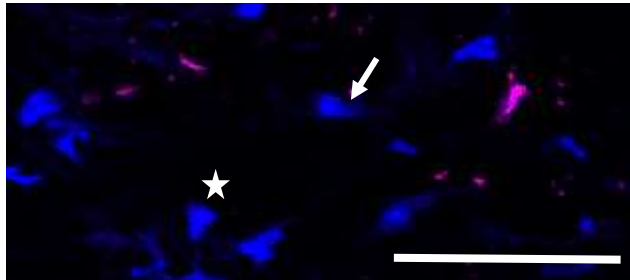
(C1) **RORrt** / **DAPI** 4OHT treated K14NICDER



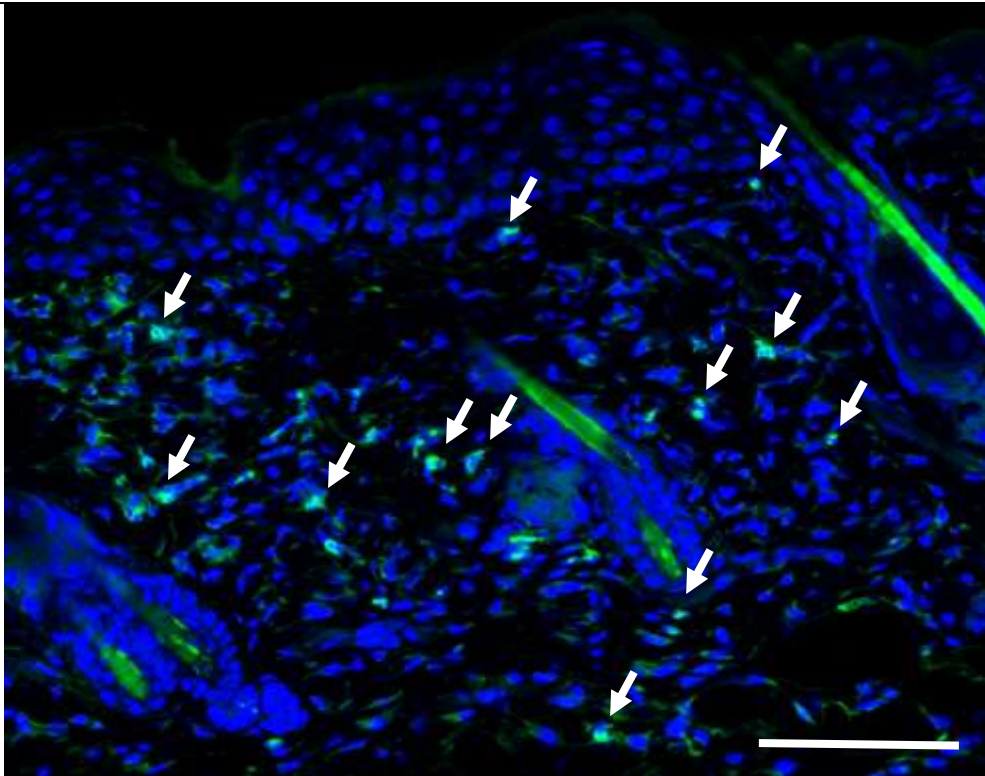
(C2) **CD4** / **DAPI** 4OHT treated K14NICDER



(C3) **CD3** / **DAPI** 4OHT treated K14NICDER



(D1) RORrt / DAPI 4OHT treated K14NICDER



(D2) CD127 / DAPI 4OHT treated K14NICDER

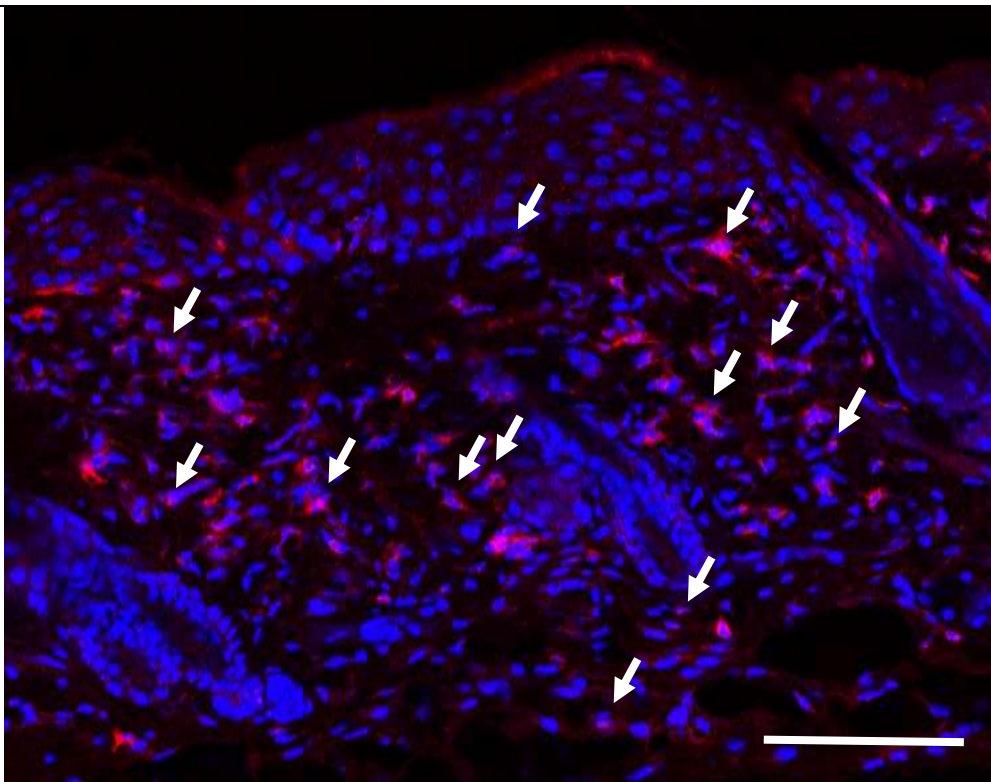


**Figure 5.6 Ectopic activation of Notch1 signaling promotes ILC3 recruitment into uninjured skin dermis.** K14NICDER mice and wildtype littermates were topically treated with 4OHT for 3 days. (A-B) Skin sections from 4OHT treated wildtype and K14NICDER were stained with an antibody to ROR $\gamma$ t (green, indicated by arrows) and counterstained with DAPI (blue). (C1-C3) show higher magnification view of the indicated area in (B) from 4OHT treated K14NICDER and was co-stained with ROR $\gamma$ t (green), CD4 (red) and CD3 (purple). Arrows indicate CD3<sup>-</sup>CD4<sup>+</sup> ROR $\gamma$ t<sup>+</sup> cells; star marks CD3<sup>-</sup>CD4<sup>low</sup> ROR $\gamma$ t<sup>+</sup> cells. Counterstained with DAPI (blue). (D1-2) Skin section from 3-day-4OHT-treated K14NICDER mice were co-stained with ROR $\gamma$ t (green) and CD127 (red) and counterstained with DAPI (blue). Arrows mark CD127<sup>+</sup> ROR $\gamma$ t<sup>+</sup> cells. Scale bar equals to 100 microns.

### **5.2.5 Recruitment of monocytes/macrophages, but not of neutrophils or dendritic/Langerhans cells, is dependent on epidermal Notch1 signaling**

I have presented evidence in last Chapter that ILC3s promote early monocyte/macrophage recruitment into wound site dermis via CCL3 (Figure 4.2), which partly contribute to ILC3-mediated skin repair. M2 macrophages have been considered as the master regulator in wound healing through switching on cytokine production of TGF- $\beta$  that is in favor of tissue repair by inducing angiogenesis for granulation tissue formation and activating myofibroblast differentiation for dermal extracellular matrix deposition and wound contraction (Rodero and Khosrotehrani 2010). Therefore I hypothesize monocyte/macrophage recruitment might be impaired in anti-NRR1 treated wounds due to loss of ILC3s. To test this, wildtype mice were *i.p.* treated with anti-NRR1 and anti-ragweed control for 7 days prior to wounding, and wounded back skin tissues were collected on day 2 post-wounding. Cells isolated from wounded back skin from anti-NRR1 and anti-ragweed control treated mice were labelled with antibodies to CD11b, CD11c, F4/80 and Gr-1 and were analyzed by flow cytometry. To distinguish monocytes/macrophages (CD11c<sup>-</sup> CD11b<sup>+</sup>) from dermal dendritic cells (CD11c<sup>high</sup> CD11b<sup>+/-</sup>) and Langerhans cells (CD11c<sup>low</sup> CD11b<sup>+</sup>), I first analyzed their expression of CD11b and CD11c, revealing the cell number of Langerhans cells and dermal dendritic cells were not significantly changed in anti-NRR1 treated mice compared to control (Figure 5.7) (p=0.29, t-test), while the percentage of CD11c<sup>-</sup>CD11b<sup>+</sup> myeloid cells including monocytes/macrophages were dramatically reduced by nearly 50% in anti-NRR1 treated mice on day 2 post-wounding compared to wounded control (p=0.0068, t-test). Since dermal dendritic cells are normally recruited and reach their maximal number at this time-point (Figure 3.2), these results suggested that Notch1 signaling or its recruited

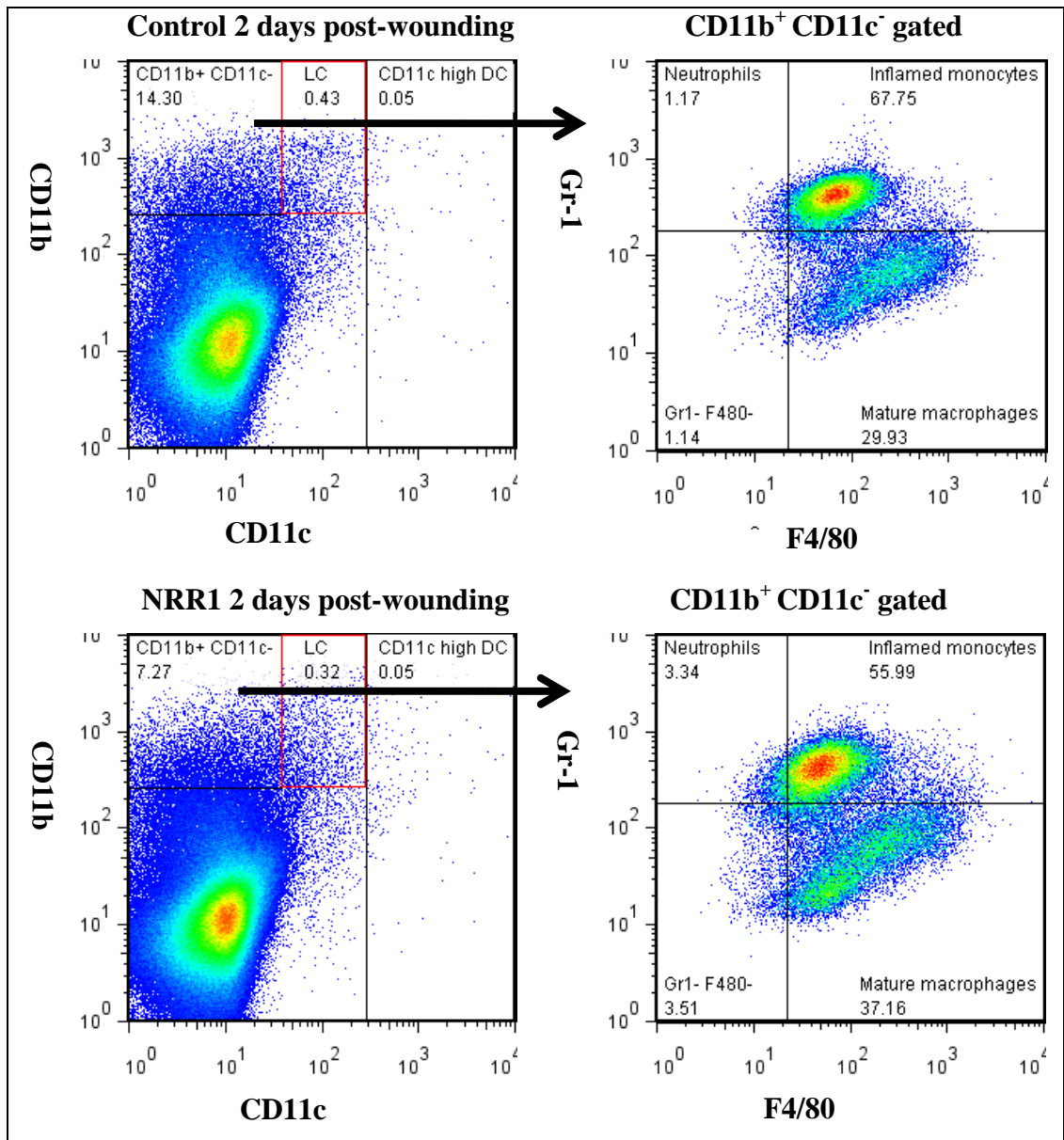


**Figure 5.7 Inhibiting Notch1 activity reduces monocyte/ macrophage recruitment.** Punch-wounded wild type mice injected peritoneally with 5mg/kg anti-NRR1 or anti-ragweed control antibody for 7 days prior to injury. Wounded back skin was collected on day 2 post-wounding. Cells isolated from wounded skin were labelled with CD11b, CD11c, F4/80 and Gr-1 were analyzed by flow cytometry, revealing monocyte/macrophage recruitment was dramatically reduced in anti-NRR1 treated mice on day 2 post-wounding. One biological sample is shown, at least 3 biological samples were analyzed (not shown). Experiments were repeated  $\geq$  3 times.

ILC3s do not have a significant role in recruiting or replenishing dendritic/Langerhans cells during normal wound healing. Then I analyzed CD11b<sup>+</sup>CD11c<sup>-</sup> myeloid cells, among which neutrophils (Gr-1<sup>+</sup>F4/80<sup>-</sup>), mature macrophages (Gr-1<sup>-</sup>F4/80<sup>+</sup>) and inflamed monocytes (Gr1<sup>+</sup>F4/80<sup>+</sup>) were distinguished from each other by Gr-1 and F4/80 expression. In anti-NRR1 treated wounds, the percentage of inflamed monocytes (p=0.0002, t-test) and mature macrophages (p=0.0011, t-test) to the total skin cells were both significantly reduced compared to anti-ragweed treated wounds, while the percentage of neutrophils to the total skin cells were not even increased, suggesting Notch1 activity is required for recruitment of monocytes/macrophages but not for neutrophils, probably through ILC3-mediated process (i.e. ILC3-dependent CCL3).

However, recent studies have suggested Notch1 activity inside macrophages is required for macrophage recruitment, since Notch1<sup>+/-</sup> mice had fewer macrophages at wound site (Outtz, et al., 2010; Outtz et al., 2011). To confirm if monocyte/macrophage recruitment is dependent on epidermal Notch1 signaling through a ILC3-mediated process, uninjured back skin from K14NICDER mice as well as littermate controls were topically treated with 4OHT for 3 days to activate ectopic Notch1 signaling specifically in epidermis and skin sections were stained with an antibody to monocyte/macrophage marker F4/80 (Figure 5.8 A), revealing that monocytes/ monocytes were dramatically recruited to dermis in Notch1 activated back skin, co-related to recruitment of ILC3s. In addition, the number of epidermal F4/80<sup>+</sup> cells was not significantly increased confirming epidermal Notch1 signaling has no effect on Langerhans cell self-proliferation or expansion. Since some dermal dendritic cells also express F4/80, to confirm the vast majority of accumulated



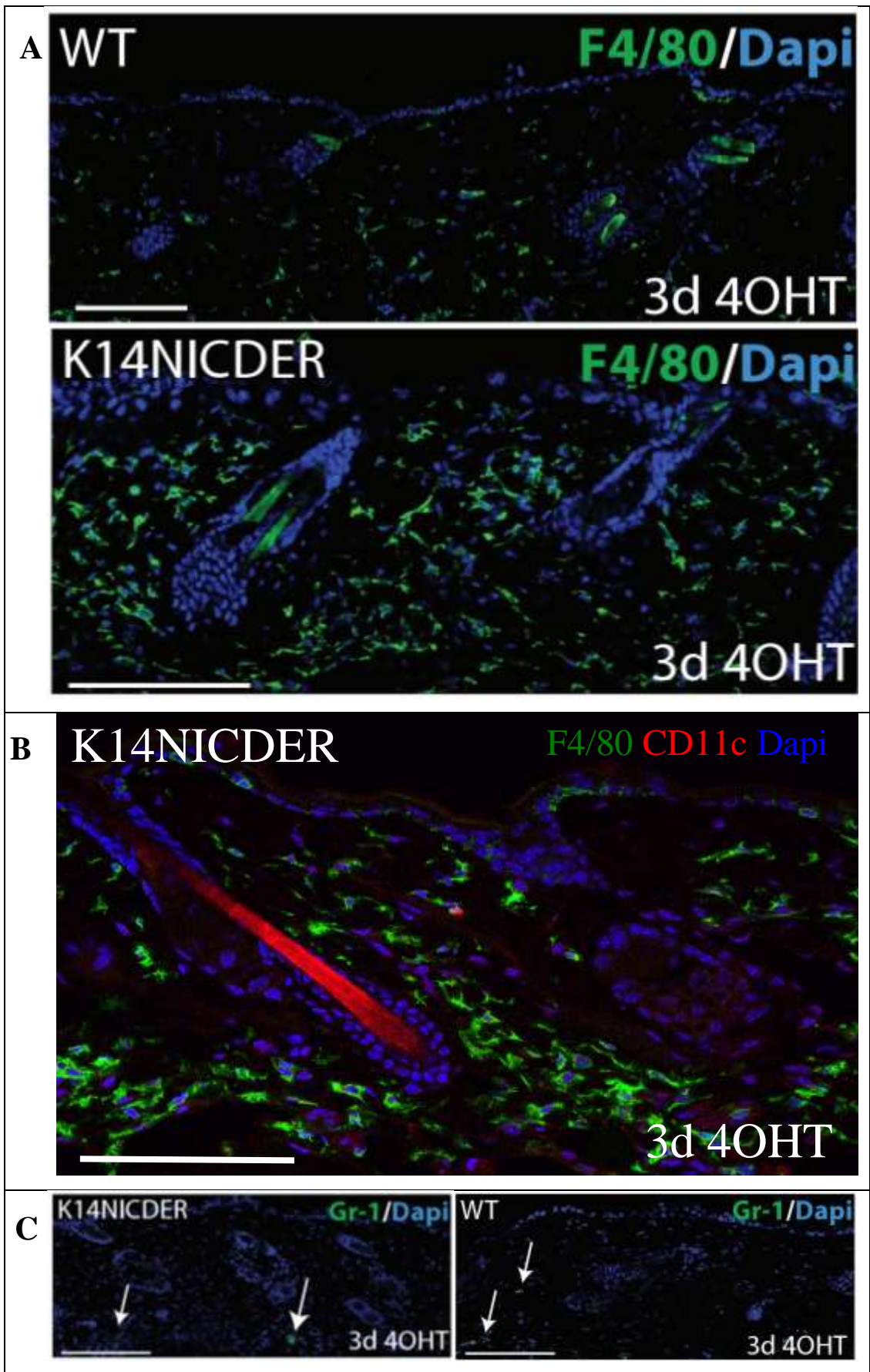


**Figure 5.8 Ectopic activation of epidermal Notch1 activity results in monocyte/macrophage recruitment in uninjured skin dermis, but has no evident effects on neutrophils or dendritic/Langerhans cells.** K14NICDER mice and wildtype littermates were topically treated with 4OHT for 3 days. (A) Skin sections from 4OHT treated wildtype and K14NICDER were stained with an antibody to F4/80 (green) and counterstained with DAPI (blue). (B) Skin sections from 4OHT treated K14NICDER were stained with antibodies to F4/80 (green), CD11c (red) and counterstained with DAPI (blue). (C) Skin sections from 4OHT treated wildtype and K14NICDER were stained with an antibody to Gr-1 (green) and counterstained with DAPI (blue). Arrows mark positive cells. Scale bar equals to 100 microns.

F4/80<sup>+</sup> cells were indeed monocytes/ macrophages, 3 day-4OHT-treated K14NICDER back skin sections were co-stained with F4/80 and CD11c. As expected, CD11c<sup>high</sup> dermal dendritic cells, unlike monocytes/ macrophages, were not accumulated in Notch1 activated uninjured skin (Figure 5.8B). Similarly, Gr-1<sup>+</sup> neutrophils were not accumulated in uninjured skin with ectopic epidermal Notch1 signaling (Figure 5.8C). Taken together, these results suggest that the recruitment of monocytes/macrophages but not of neutrophils or dendritic/Langerhans cells into skin is dependent on epidermal Notch1 signaling, probably through ILC3-mediated process.

#### **5.2.6 Notch1 signaling has no significant effect on NK cell recruitment**

Since a small number of NK cells are normally recruited into skin wounds early on day 2 post-wounding (Figure 3.10), to determine if Notch1 signaling has a role in NK cell recruitment upon wounding, wildtype mice were *i.p.* treated with anti-NRR1 and anti-ragweed control for 7 days prior to wounding, then wounded back skin tissues were collected on day 2 post-wounding. Cells isolated from wounded back skin from anti-NRR1 and anti-ragweed control treated mice were labelled with antibodies to CD3, NK1.1 and were analyzed by flow cytometry (Figure 5.9), revealing Notch1 activity has no significant effect on NK (CD3<sup>-</sup> NK1.1<sup>+</sup>) ( $p=0.057$ , t-test) or NKT (CD3<sup>+</sup> NK1.1<sup>+</sup>) cell recruitment.

#### **5.2.7 Epidermal Notch1 signaling may have a role in regulating maintenance of dendritic epidermal T cells**

Dendritic epidermal T cells (DETCs), a specialized  $\gamma\delta$  T cells residing in rodent epidermis and uniquely expressing invariant TCR V $\gamma$ 3 (MacLeod and Havran, 2011),

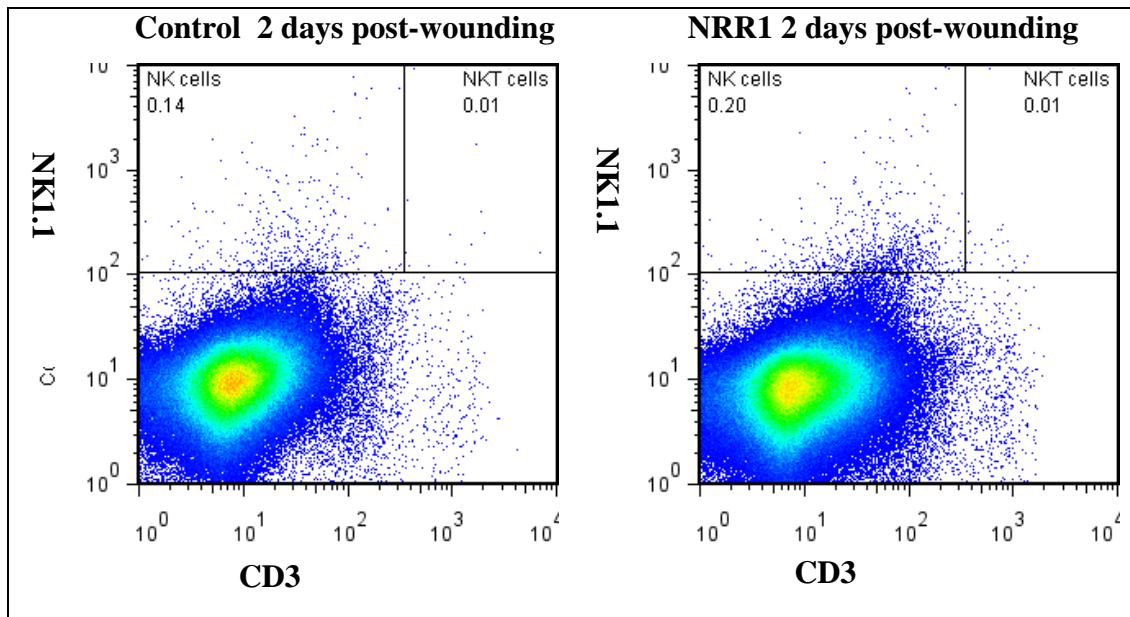


**Figure 5.9 Inhibiting Notch1 activity has no significant effects on NK cell recruitment.** Punch-wounded wild type mice injected peritoneally with 5mg/kg anti-NRR1 or anti-ragweed control antibody for 7 days prior to injury. Wounded back skin was collected on day 2 post-wounding. Cells isolated from wounded skin were labelled with NK1.1 and CD3 and were analyzed by flow cytometry, revealing NK/NKT cell recruitment was not significantly changed in anti-NRR1 treated mice on day 2 post-wounding. Shown one biological sample, at least 3 biological samples were analyzed (not shown). Experiments were repeated  $\geq 3$  times.

have been reported to be critically important for skin wound healing by producing IGF-1 and KGF for epidermal keratinocyte proliferation and by promoting macrophage migration via hyaluronan (Jameson et al., 2002; MacLeod and Havran, 2011). However, DETCs were down-regulated in early wounds on day 2 post-wounding (Figure 3.7 and Figure 3.8) and were replenished via a currently undetermined mechanism (Jameson and Havran, 2007; MacLeod and Havran, 2011) in later wounds on day 5 post-wounding (Figure 3.7 and Figure 3.8), suggesting they may only play their roles in wound healing at later stage and thus are not of our main interest. Furthermore, the interpretation of epidermal Notch1 effects on T cell recruitment or replenishment in anti-NRR1 treated mice is complicated since the role of Notch1 signaling has been well established in T cell development in thymus (Izon et al., 2001; Robey et al., 1996). Nevertheless, unexpectedly, a dramatically increased clonal expansion of  $V\gamma 3^+ CD3^+$  T cells was detected following epidermal Notch1 signaling activation in 4OHT treated K14NICDER skin. Cells isolated from 7-day 4OHT-treated K14NICDER and wildtype littermate control ear skin were stained with antibodies to CD45, CD3, TCR $\beta$  and  $V\gamma 3$  and were analyzed for DETCs ( $CD45^+CD3^+TCR\beta^-V\gamma 3^+$ ) and other T cell subsets, such as  $\alpha\beta$  T cells ( $CD45^+CD3^+TCR\beta^+V\gamma 3^-$ ) and dermal  $\gamma\delta$  T cells ( $CD45^+CD3^+TCR\beta^-V\gamma 3^-$ ). I detected a 3 to 4 -fold increase in DETCs population while  $\alpha\beta$  T cells and dermal  $\gamma\delta$  T cells did not differ from 4OHT treated wildtype controls (Figure 5.10 A). Back skin sections from 3-day 4OHT treated K14NICDER and wildtype control mice were stained with an antibody to CD3, revealing T cells were dramatically accumulated in 4OHT treated K14NICDER dermis (Figure 5.10 B). I concluded that these T cells accumulated in 3-day 4OHT treated K14NICDER dermis might be the precursors of DETCs, which would eventually migrate to epidermis to replenish

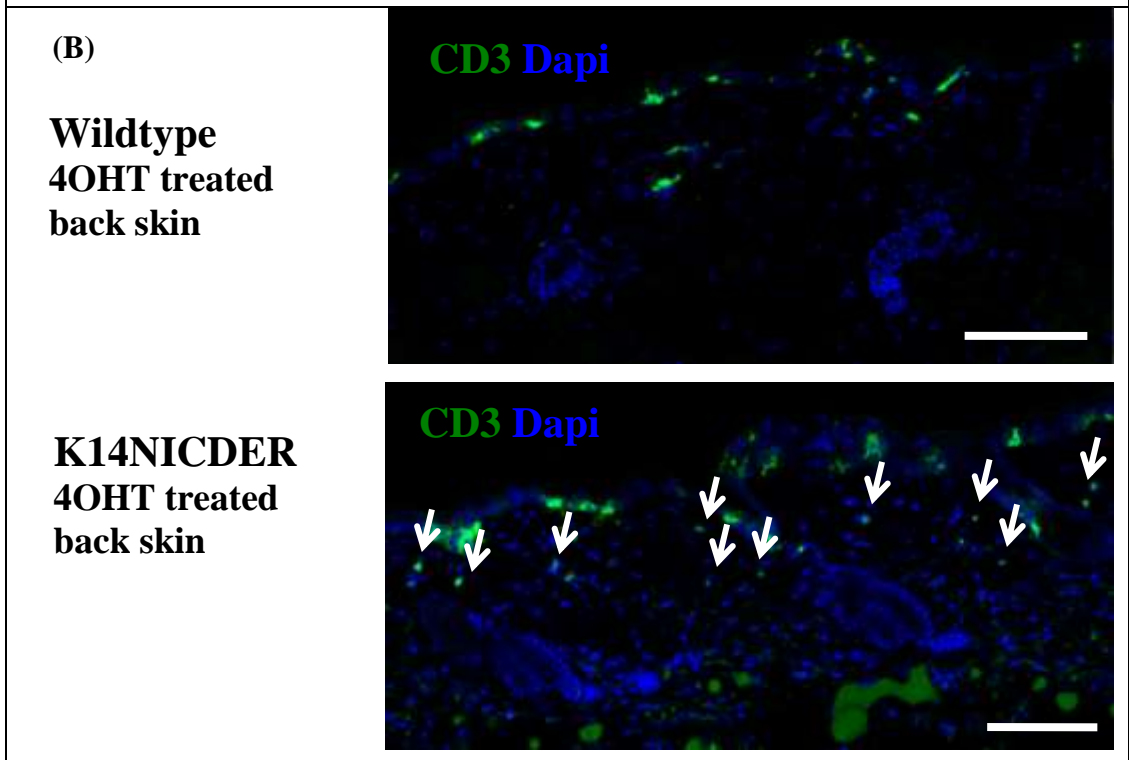
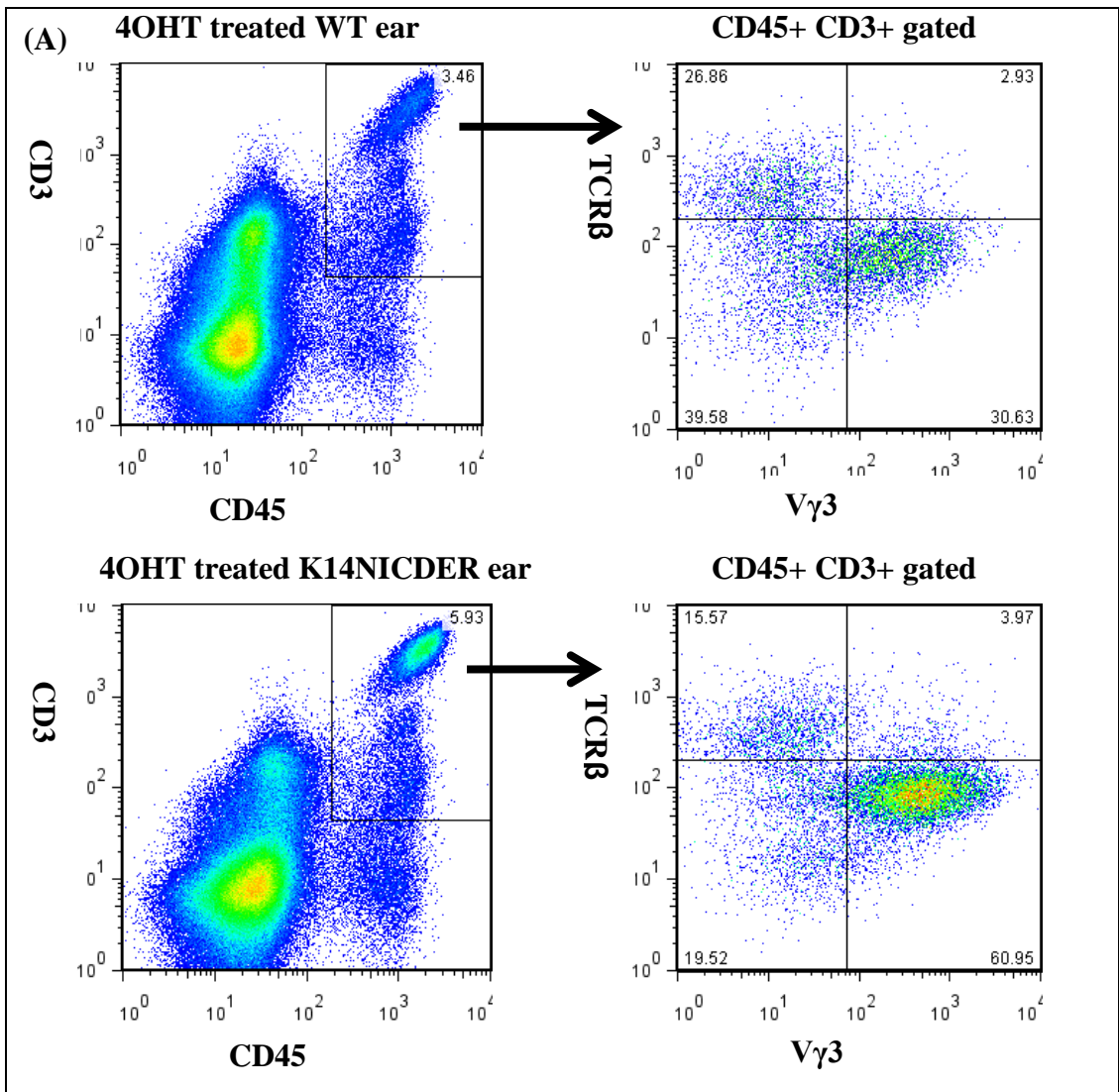


**Figure 5.10 Ectopic activation of Notch1 activity causes the expansion of epidermal dendritic T cell.** (A) Ears of K14NICDER mice and wildtype littermates were topically treated with 4OHT for 7 days. Cells isolated from 4OHT treated ears were labelled with CD45, CD3, TCR $\beta$  and V $\gamma$ 3 and were analyzed by flow cytometry, suggesting the number of epidermal dendritic cells (DETCs) were significantly increased in 4OHT treated K14NICDER ears. (B) Back skin of K14NICDER mice and wildtype littermates were topically treated with 4OHT for 3 days. Back skin sections were stained with antibodies to CD3 (green), and counterstained with DAPI (blue). Arrows mark CD3<sup>+</sup> cells in dermis, the majority of which were probably the precursors of DETCs or migratory DETCs to lymph nodes. Scale bar equals to 100 microns.

DETCs and cause clonal expansion of DETCs as detected in 7-day 4OHT treated K14NICDER skin. However, since there might be some differences in the distribution of immune cells between ear skin and back skin, further experiments are needed to confirm the role of Notch signaling in DETC maintenance. These results uncover a possible mechanism of DETC maintenance regulated by epidermal Notch1 signaling through recruiting precursors of DETCs from circulating  $\gamma\delta$  T cells.

### **5.3 Summary**

In this chapter, I presented evidence that Notch1 and Notch2 activities are immediately and robustly activated upon skin injury predominantly in epidermal keratinocytes. Interestingly, activated Notch1 levels are correlated with the number of immune cell accumulation at the wounded skin. By seven days post-wounding, during the remodeling phase when the epidermis has almost closed (Figure 3.1B) (Shaw et al., 2009) and there is very low risk of pathogen infection, Notch activity and immune cell number returns unwounded to skin levels (Figure 3.1 G and Figure 5.1A). By using chemical tools including blocking antibodies specific to Notch1 or Notch2 receptor, I have shown that inhibition of Notch1 inhibits wound closure, ILC3 recruitment, and correspondingly IL22 production and monocyte/macrophage recruitment, while inhibition of Notch2 did not differ from the controls, suggesting Notch1 signaling has an indispensable role in promoting skin wound healing especially at early stage by recruiting ILC3s that produce IL-22 for epidermal proliferation and facilitate the recruitment of monocytes/macrophages to the wound site. I further confirmed that these Notch1-regulated immune responses in skin wound healing is specifically dependent on epidermal Notch1 signaling by using genetic tools including a transgenic mouse (K14NICDER) where Notch can be



controllably activated specifically in the epidermis by 4OHT drug application. In conclusion, epidermal Notch1 signaling promotes skin wound healing through ILC3-mediated process. However, since all 4 Notch receptors have been detected in skin, and Notch2 activity is increased upon wounding, it may be possible that the other Notch receptors play redundant roles or contribute to other aspects in skin wound healing.

## **Chapter 6 Mechanism of how epidermal Notch1 regulate ILC3s**

### **6.1 Introduction**

In last chapter, I have presented evidence that epidermal Notch1 signaling promotes skin wound healing through recruiting ILC3s, the key roles of which in wound healing have been determined in Chapter 4. In this chapter, I will investigate the mechanism of how Notch1 regulates ILC3s in terms of recruitment and activation. The cell-autonomous role for Notch signaling in determining the fate of cells expressing a Notch receptor within both adaptive and innate immune systems has been well established (Radtke et al., 2013). However, how epidermal keratinocytes Notch receptor activity regulates immune cell may be different from some of the currently established mechanisms, and may be rely on cytokines and chemokines soluble factors (Ambler and Watt, 2010). Using 4OHT-treated K14NICDER mouse model where Notch1 signaling can be controllably and specifically activated in epidermis, 4 key cytokine or chemokine candidates, including TNF $\alpha$ , CCL20, CXCL13 and IL23, have been identified by micro-array (NIH GEO:GSE 782, Ambler and Watt, 2008; NIH GEO: GSE29777, Reynders et al., 2011) as Notch-regulated factors that can function on ILC3s through their cell surface receptor, such as TNF receptor superfamily (TNFRSF), CCR6, CXCR5 and IL12 receptor beta1 subunit (IL12RB1) / IL23 receptor (IL23R) respectively. Among these factors, IL23 have been determined to be largely expressed by dendritic/Langerhans cells (Figure 4.5) and required for IL22 production by ILC3s for epidermal proliferation (Figure 4.5 and Figure 4.6). To test the roles of the rest factors in recruiting ILC3s, each factor was blocked either by genetic or chemical tool in mice prior to wounding, then the number of ILC3s recruited in the wound site as well as the wound healing rate were examined. I found CXCL13<sup>-/-</sup> mice had normal ILC3 recruitment and normal

healing rate, suggesting CXCL13 is not required for ILC3 recruitment in skin. Strikingly, I found both the number of ILC3s infiltrating in wound site and the wound closure rate were co-related with the level of TNF $\alpha$  by applying chemical drug recombinant TNF $\alpha$  or TNF $\alpha$  antagonist (Adalimumab) to the wound, suggesting TNF $\alpha$  is a key cytokine required for ILC3 recruitment. However, since TNF $\alpha$ , as a cytokine, usually acts transiently and in a relatively short range, other soluble factors are required to transmit this signaling. By stimulating dermal fibroblasts with TNF $\alpha$ , I demonstrated that CCL20 and IL22 can be expressed by dermal fibroblasts. I conclude that epidermal Notch1 regulates ILC3 recruitment in a mechanism dependent on TNF $\alpha$ / CCL20. However, due to the availability of CCL20 genetic or chemical tools, we were not able to directly demonstrate the role of CCL20 regulates ILC3 recruitment.

## **6.2 Results**

### **6.2.1 Epidermal Notch1 up-regulates cytokine and chemokine production, including TNF $\alpha$ , CCL20, CXCL13 and IL-23.**

Previously, our lab has shown that Notch activity, via jagged1, stimulates epidermal production of pro-inflammatory TNF $\alpha$  (Ambler and Watt, 2010). To investigate the mechanism by which Notch1 leads to ILC recruitment, dermal and epidermal gene expression profiles of 10-day 4OHT treated, uninjured K14NICDER transgenic mouse back skin (NIH GEO:GSE 782, Ambler and Watt, 2008) were examined. Ingenuity Pathway Analysis software was used to identify secreted factors up-regulated in 4OHT-treated K14NICDER skin (6x or greater) that could facilitate immune cell infiltration into the dermis and the subsequent activation. Analysis identified seven key candidates (Figure 6.1) (4 epidermal: IL-23(10.3x),

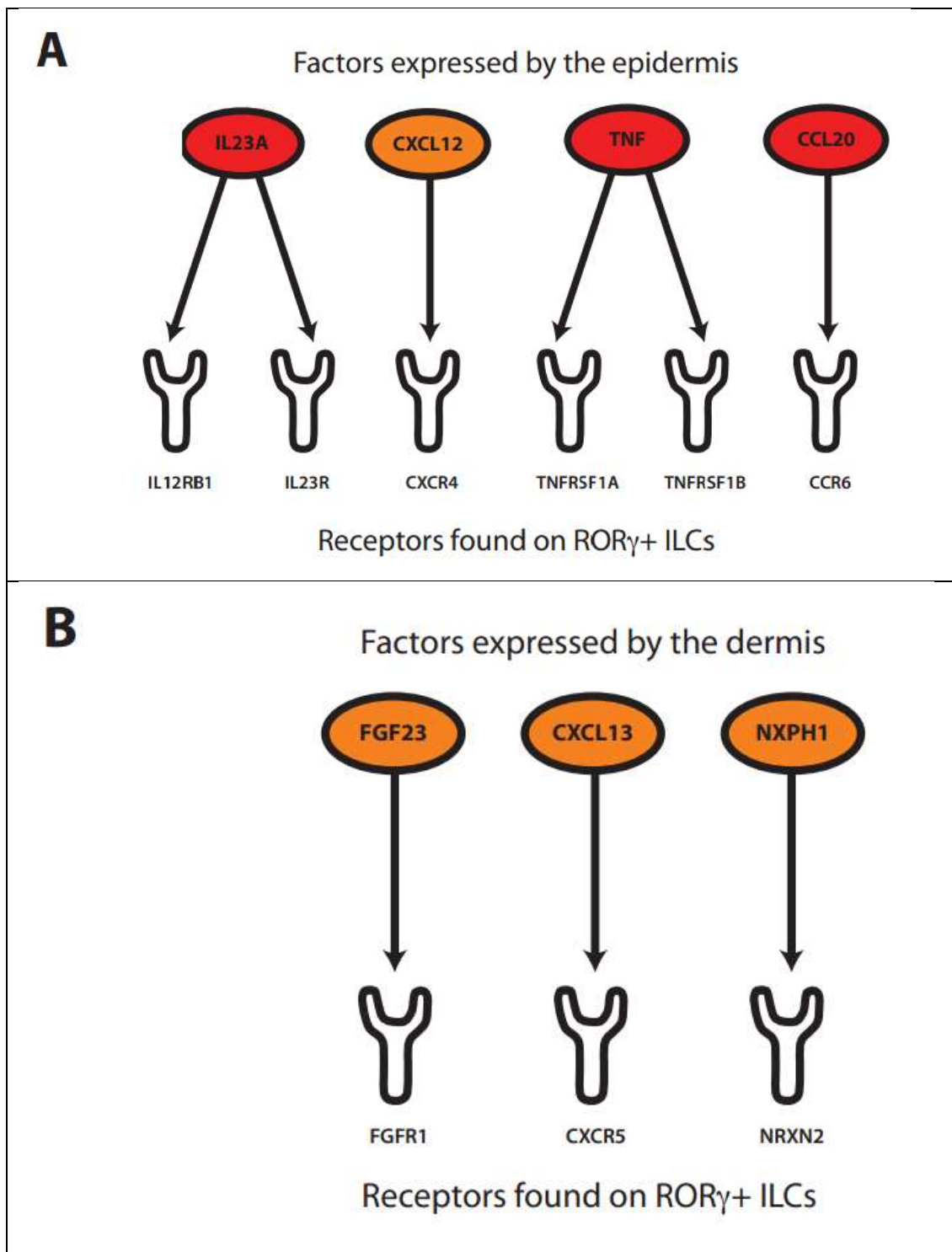


**Figure 6.1 Ingenuity Pathway Analysis of secreted factors that can interact with receptors expressed on ILC3s (ROR $\gamma$ <sup>+</sup> ILCs).** (A) Factors expressed by epidermis. (B) Factors expressed by dermis. (NIH GEO: GSE 782, Ambler and Watt, 2008; NIH GEO: GSE29777, Reynders et al., 2011)

TNF- $\alpha$  (17.1x), CXCL12 (8.0x), CCL20 (14.1x) and 3 dermal: CXCL13 (6.5x), FGF23 (5.4x), neurexophilin-1 (6.0x) that could regulate innate immune cell recruitment and activation (NIH GEO: GSE29777, Reynders et al., 2011). Of these Notch-regulated factors TNF $\alpha$ , CCL20, CXCL13 and IL23 were of particular interest as these factors regulate ILC3s through cell surface receptor TNF receptor superfamily (TNFRSF), CCR6, CXCR5 and IL12 receptor beta1 subunit (IL12RB1) / IL23 receptor (IL23R) respectively (Marchesi et al., 2009).

### **6.2.2 CXCL13 is not required for ILC3 recruitment**

It has been reported that CXCL13 expression in the gut promotes accumulation of ILC3s and formation of isolated lymphoid follicles (Marchesi et al., 2009). To test if CXCL13 expression in skin also promotes ILC3 recruitment, CXCL13<sup>-/-</sup> mice and wildtype littermate controls were wounded and the number of ILC3s recruited into wound site and wound healing rate were examined. Surprisingly, CXCL13<sup>-/-</sup> mice did not show evident wound healing defects and no difference in ILC3 recruitment was detected in wounded skin sections between CXCL13<sup>-/-</sup> mice and littermate controls by using an antibody to ROR $\gamma$  (Figure 6.2 and data not shown), suggesting CXCL13 is not required for ILC3 recruitment in wound healing. However, it may play a redundant role in recruiting ILC3s.

### **6.2.3 Notch regulated factor TNF $\alpha$ mediates ILC3 recruitment**

To confirm that TNF $\alpha$  mediates ILC3 recruitment, wildtype mice were punch-wounded and then treated with recombinant TNF $\alpha$ , TNF $\alpha$  antagonist (Adalimumab)

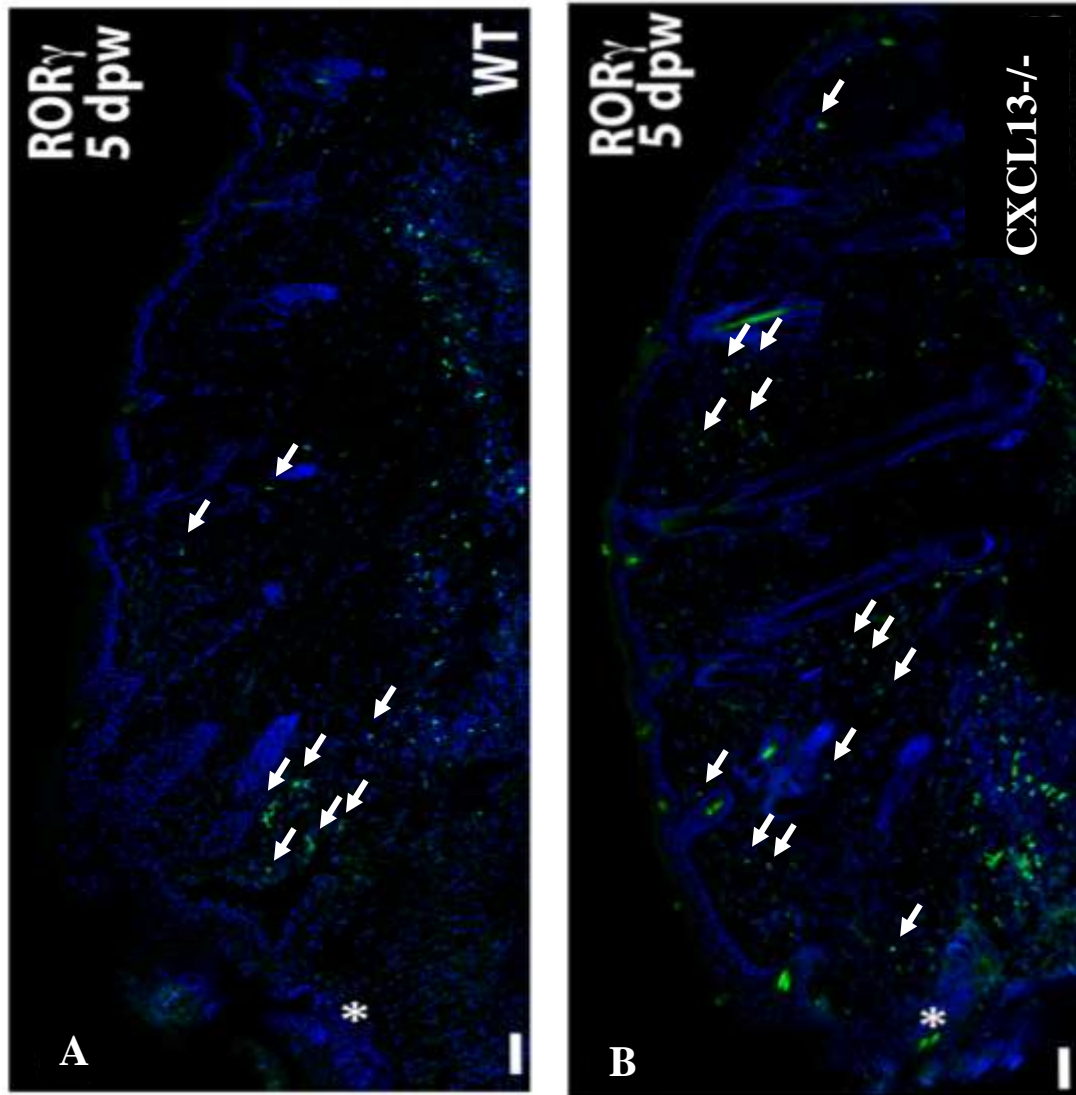


**Figure 6.2 CXCL13 is not required for ILC recruitment into skin wounds.** (a, b) Sections of wounded back skin 5 days post injury from CXCL13<sup>-/-</sup> (B) and wild type (WT) control mice (A). Antibody labelling of RORγ (green) and DAPI counterstained (blue). No difference in ILC recruitment in CXCL13<sup>-/-</sup> wounds; asterisk marks site of wound; scale bars equal 100 microns; arrows mark positive cells in dermis; experiments were repeated  $\geq 2$  times.

(Calabrese 2003) or PBS daily. By day 5 post-wounding, a substantial difference was observed between the three groups of mice (Figure 6.3): TNF $\alpha$  accelerated wound closure and ILC3 recruitment (1.8x), while the antagonist inhibited wound closure and ILC recruitment (0.4x). Moreover, injection of adalimumab for 7 days prior to 4OHT-activation of Notch in unwounded K14NICDER transgenic mice blocked Notch-mediated ILC recruitment into the skin (Figure 6.4) confirming that a Notch/TNF $\alpha$  mechanism recruits of ILC3s in to the skin dermis.

#### **6.2.4 TNF $\alpha$ regulates ILC3 recruitment by inducing CCL20 expression in dermal fibroblasts**

I have determined that Notch-regulated factor TNF $\alpha$  has a key role in recruiting ILC3s, however, as a cytokine, TNF $\alpha$  action is transient and usually short range and thus is not present in blood circulation (Delves et al., 2011). Therefore, TNF $\alpha$  may have to play its role in recruiting ILC3s through other soluble molecules (e.g. chemokines) which usually act in a longer range (Delves et al., 2011). Since TNF $\alpha$  can direct CCL20 expression in the skin (Tohyama et al., 2001), a key recruitment factor for ILC3s in lymphoid tissues, I hypothesize TNF $\alpha$  regulates ILC3 recruitment by inducing CCL20 expression in skin. CCL20 mRNA levels were measured 4, 8, 16, 24 and 40 hours after injury by QPCR and CCL20 levels were elevated immediately following wounding and returned to background levels by 24 hours post injury (Figure 6.5A) and were sustained at low levels 48-72 hours (Figure 6.5B) post-wounding in a TNF $\alpha$ -dependent process (Figure 6.5C, data collected by Rebecca Lamb). Primary dermal cells were treated with TNF $\alpha$  for 6 hours *in vitro* leading to increased CCL20 expression (13x) (Figure 6.5C, data collected by

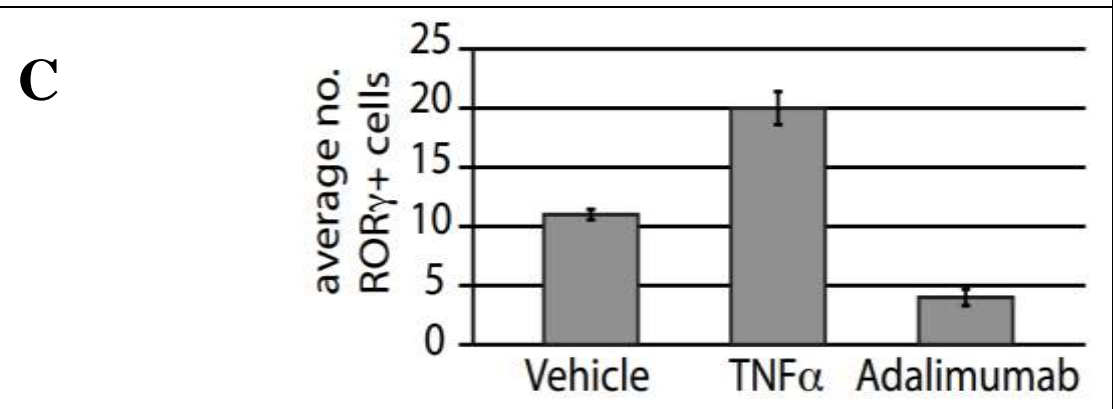
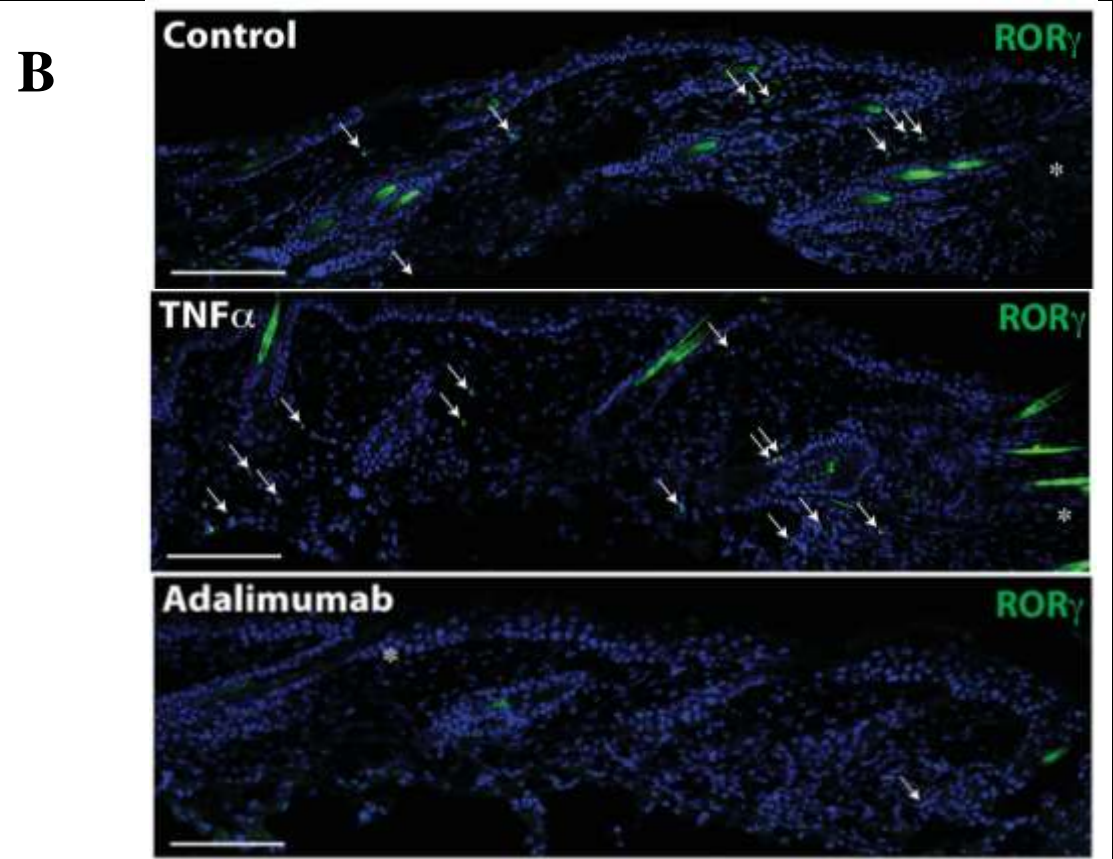




**Figure 6.3 Notch-regulated factor TNF $\alpha$  regulates ILC3 recruitment and activation.** (A) Punch wounds treated with PBS (vehicle), TNF $\alpha$  or TNF $\alpha$  antagonist (Adalimumab) were photographed on day 2 and day 5 post-wounding. Note red, inflamed tissues were evident adjacent to TNF $\alpha$ -treated day 2 wounds. Experiment repeated twice (total animal numbers; n = 4 control; n = 7 TNF $\alpha$  antagonist; n = 8 TNF). (B) ROR $\gamma$ t (green) antibody stained back skin sections from punch-wounded mice treated with PBS (control), TNF $\alpha$  or TNF $\alpha$  antagonist (Adalimumab) collected 2 days post-wounding. DAPI counterstained. Positive cells are marked by white arrows. Asterisk marks wound site; scale bars equal 100 microns. (C) Quantification of dermal ROR $\gamma$ <sup>+</sup> cells in wounded back skin from mice treated with vehicle, TNF $\alpha$  or TNF $\alpha$  antagonist on day 2 post-wounding (n = 3 control; n = 5 TNF $\alpha$  antagonist; n = 5 TNF $\alpha$ ). Sample number equals biological replicates; quantified area < 1600 micrometres distal to wound site). Error bars represent standard error of the mean (SEM).

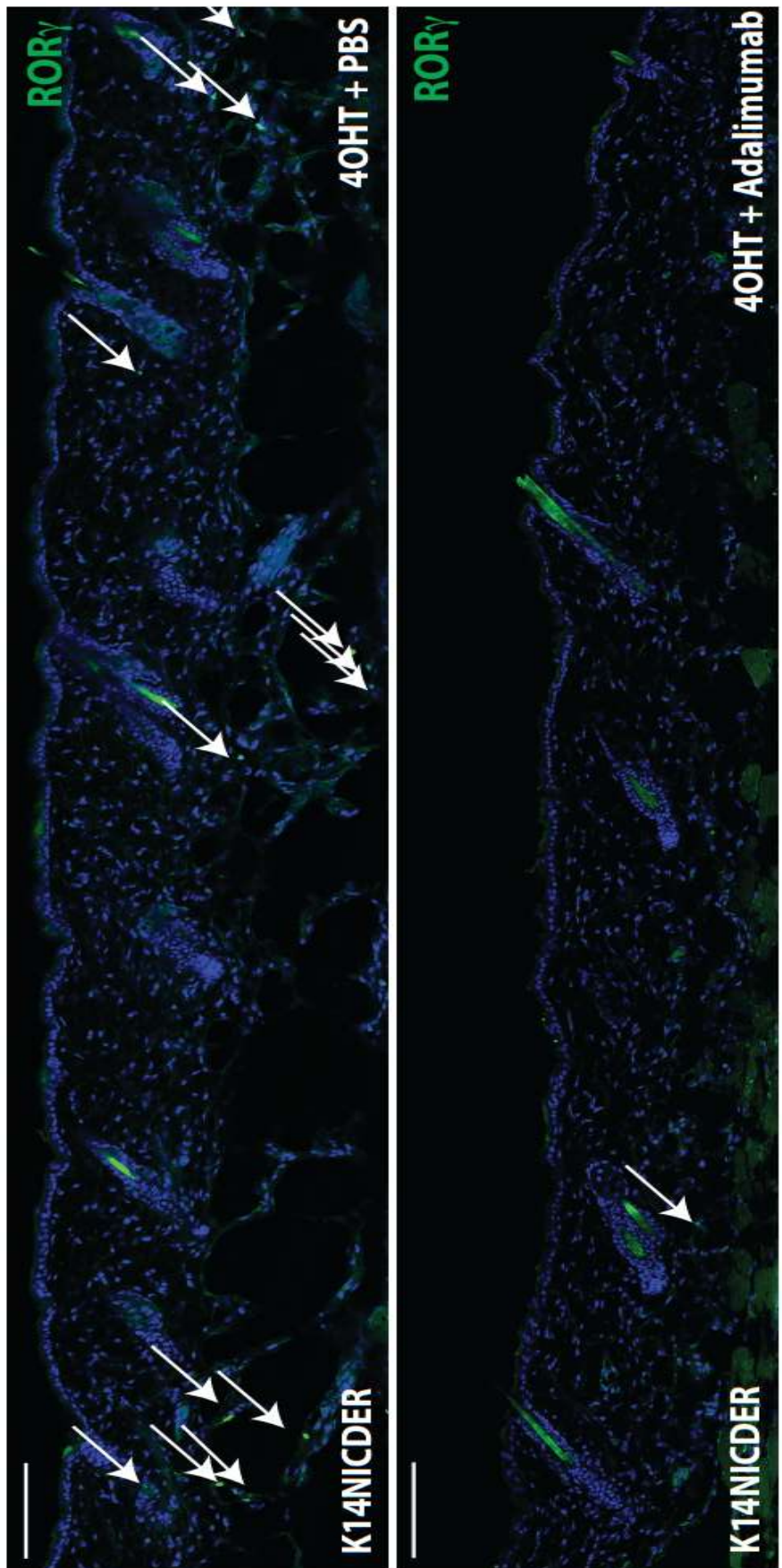
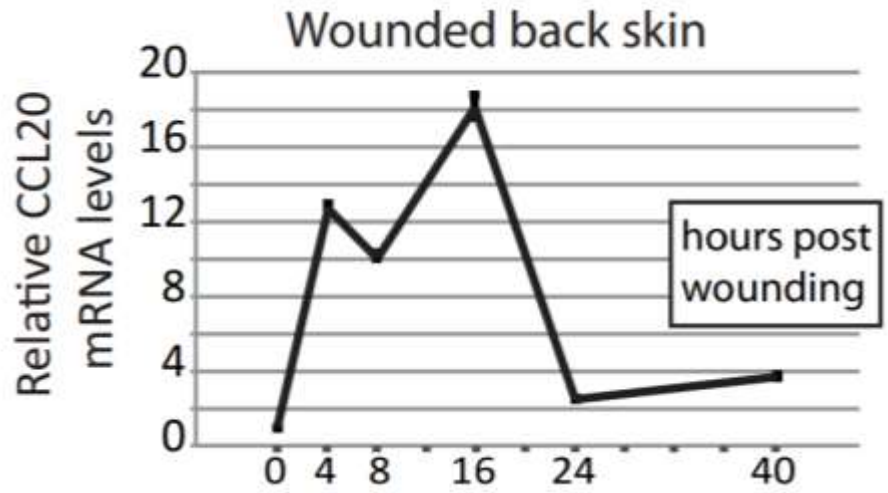
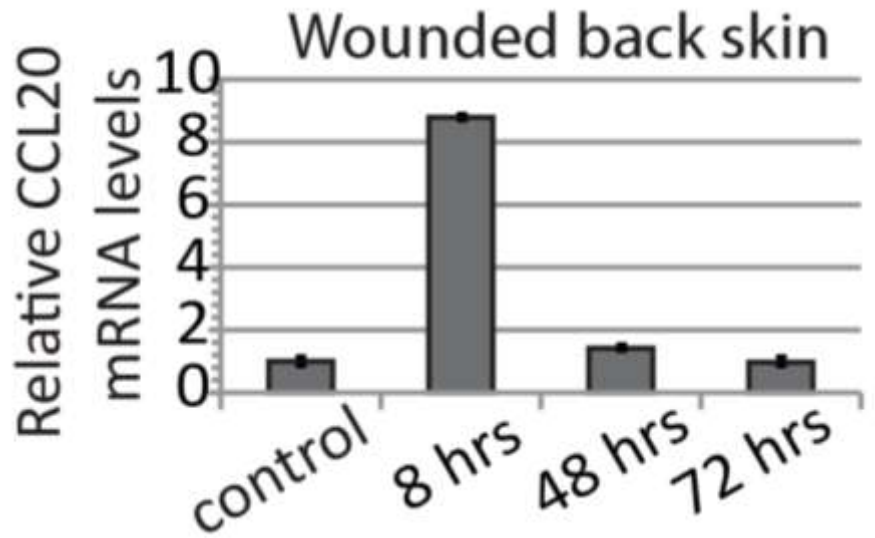


**Figure 6.4 TNF $\alpha$  antagonist (Adalimumab) blocks Notch1-induced ILC3 recruitment.** Uninjured K14NICDER transgenic mice treated with PBS or Adalimumab for 7 days followed by 2 days of 4OHT -treatment to activate the transgene. Skin sections were stained with an antibody to ROR $\gamma$  (green) and counterstained with DAPI. Positive cells are marked by white arrows. Asterisk marks wound site; scale bars equal 100 microns.

**A**



**B**



**C**

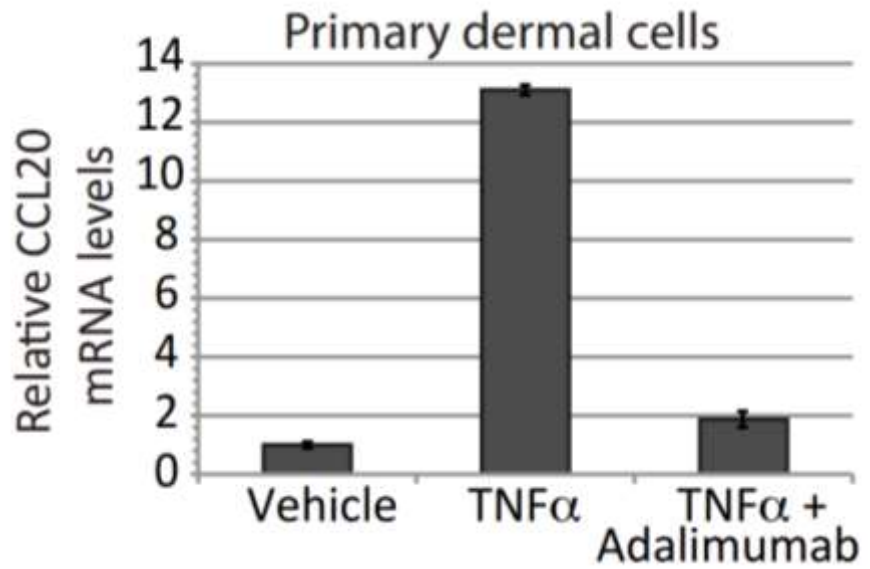


**Figure 6.5 CCL20 are immediately produced in skin wounds and can be expressed by dermal fibroblasts after stimulation by TNF $\alpha$ .** (A) mRNA levels of CCL20 quantified by quantitative RT-PCR in unwounded and wounded back skin 4, 8, 16, 24 and 40 hours post-wounding. mRNA levels were normalised to unwounded skin. (B) mRNA levels of CCL20 quantified by quantitative RT-PCR in wounded back skin 8, 24 or 72 hours post-wounding. mRNA levels were normalised to unwounded skin (designated as 1). (C) mRNA levels of CCL20 quantified by QPCR in primary dermal cells treated *in vitro* with TNF $\alpha$  or TNF $\alpha$  Adalimumab for 6 hours. mRNA levels were normalised to vehicle-only treated cells. Experiment repeated twice. Graph bars represent experimental mean of technical replicates (n = 3) and error bars represent standard error of the mean (SEM).

Rebecca Lamb). Taken together these results show that activating the TNF $\alpha$  pathway either chemically or via Notch activation resulted in a correspondingly increased CCL20 expression in dermal fibroblasts linking TNF $\alpha$  to ILC3 recruitment.

### **6.2.5 Epidermal Notch1 signaling might stimulate Langerhans cells to secrete IL23 that is required for ILC3s as well as dermal fibroblasts to produce IL22**

Previous studies suggested IL23 is required for ILCs to secrete IL22 in intestine (Sonnenberg et al., 2011). I have also determined that Langerhans/ dendritic cells are the main source of IL23 that is required for IL-22 production by ILC3s as well as other IL22-producing cells including non-lymphocytes in skin (Figure 4.4), although the candidate cell types which produce IL22 at skin wounds at later stage in the absence of ILC3 or T have not been determined. Since we have determined dermal fibroblasts can express CCL20 upon stimulated by TNF $\alpha$ , I hypothesize fibroblasts might be able to produce IL-22 as well in certain conditions. To test this, we used recombinant TNF $\alpha$  to stimulate primary dermal cells (Figure 6.6) and confirmed dermal fibroblasts have the capability to produce IL22.

Since Langerhans cells are at least 4-fold more abundant than dermal dendritic cells at all stages of wound healing (Figure 3.2 and Figure 5.7), and epidermal Notch1 induced IL23 expression are most significantly detected in epidermis (NIH GEO:GSE 782, Ambler and Watt, 2010), it is logical to deduce that epidermal Notch1 might activate Langerhans cells to secrete IL-23. However, we cannot exclude that some other cell types may also express IL23 following Notch activation,

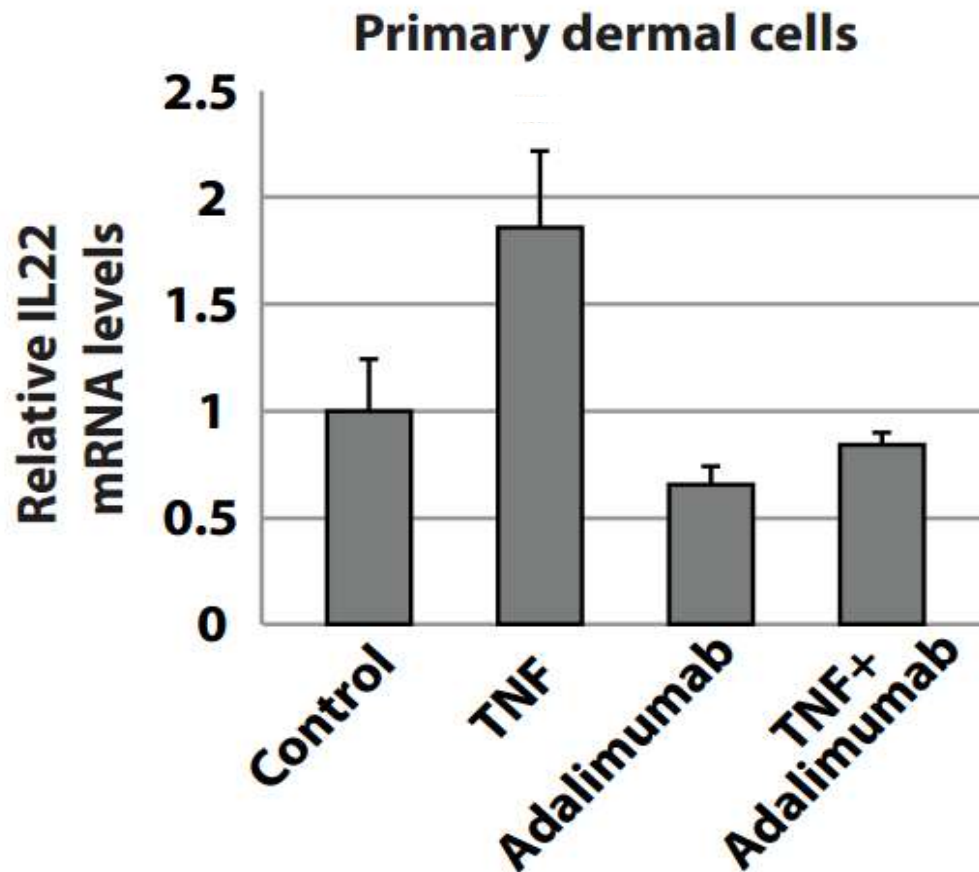


**Figure 6.6** IL-22 can be produced by dermal fibroblasts after stimulation by **TNF- $\alpha$** . mRNA levels of IL22 in primary dermal cells treated with vehicle control, **TNF- $\alpha$** , **TNF- $\alpha$**  antagonist (adalimumab) or both **TNF $\alpha$** , adalimumab. **TNF- $\alpha$**  treatment induces IL22 expression in dermal fibroblasts. Experiment repeated twice. mRNA levels were normalised to vehicle-only treated cells. Graph bars represent experimental mean of technical replicates (n = 3) and error bars represent standard error of the mean (SEM).

and epidermal Notch1 signaling does not appear to have a significant role in Langerhans cell number expansion as suggested by no change in epidermal F4/80<sup>+</sup> cell number in 4OHT-treated K14NICDER back skin (Figure 5.8). Taken together, these results suggest epidermal Notch1 signaling might stimulate Langerhans cells to secrete IL23 that is required for ILC3s as well as dermal fibroblasts to produce IL22

### **6.3 Summary**

In this chapter, using genetic and chemical tools including CXCL13<sup>-/-</sup> mice and recombinant TNF $\alpha$  or TNF $\alpha$  antagonist (Adalimumab), I analyzed the effects of blocking the key Notch-regulated soluble factors that are known to function on ILC3s through their respective cell surface receptor, suggesting epidermal Notch1 signaling recruits ILC3s in a mechanism dependent on TNF $\alpha$ / CCL20, and activates ILC3s and dermal fibroblasts to produce IL22 by inducing epidermal expression of IL23 probably by Langerhans cells.

However, due to the availability of genetic and chemical tools on targeting CCL20, we do not have direct evidence suggesting CCL20 recruits ILC3s through CCR6. I demonstrated that Notch1 stimulation of TNF $\alpha$  directly regulates CCL20 in wounded skin. However, although CCL20 expression is very rapidly expressed and it is transcriptionally down-regulated within 24-hours of wounding suggesting other factors in addition to TNF $\alpha$  tightly control CCL20 expression. CXCL13 is expressed in the wound site (data not shown) and might contribute to ILC3 recruitment and retention, however analysis of CXCL13 deficient mice show no evident defects in



wound healing or dermal ILC recruitment indicating that CXCL13 is either redundant or not key in this process.

## Chapter 7 Discussion

The normal wound healing is a highly coordinated process consisting of three sequential and overlapping phases: inflammation, proliferation and remodeling (Table 7.1) (Guo and DiPietro, 2010). The postponed, incomplete, or uncoordinated healing process usually causes pathologic inflammation, leading to delayed acute wounds or chronic wounds like ulcers. Non-healing wounds are associated with diabetes and other diseases, affecting about 3 to 6 million people in the United States, especially the elderly people (Mathieu et al., 2006). Treating and caring of these non-healing wounds cost more than 3 billion dollars per year according to estimation (Mathieu et al., 2006). Better understanding of how wound healing is regulated will help us to find a more efficient and economic solution for the delayed or non-healing wounds.

In this thesis, I first analyzed normal immune responses in wound healing by using a surgical wounding mouse model. Consistent with previous results, I found that monocytes/ macrophages are the predominant immune cells residing in unwounded skin and infiltrating in wounded skin, and are recruited early into wound site at approximately day 2 post-wounding (Figure 3.2; Figure 3.6), while  $\gamma\delta$  T cells including dendritic epidermal T cells are dramatically replenished at later stage approximately from day 5 post-wounding (Figure 3.7; Figure 3.8), confirming these cells are heavily involved in normal skin wound healing and important for this process (Delavary et al 2011; Dupasquier et al 2004; Havran and Jameson 2010; Jameson et al, 2002; Jameson and Havran 2007; Rodero and Khosrotehrani 2010; Stout 2010). However, I am the first to Group 3 demonstrate innate lymphoid cells

### Normal skin wound healing process

Phase	Major cellular events
Inflammation	<ol style="list-style-type: none"><li>1. Neutrophil recruitment and infiltration</li><li>2. Innate lymphoid cell recruitment and infiltration</li><li>3. Monocyte recruitment, infiltration and differentiation into macrophage</li><li>4. Epidermal dendritic T cell replenishment</li></ol>
Proliferation	<ol style="list-style-type: none"><li>1. Keratinocyte division (re-epithelialization, epidermal proliferation)</li><li>2. Fibroblast differentiation into myofibroblast (dermal collagen synthesis, wound contraction)</li><li>3. Vascular endothelial cell division (granulation tissue formation)</li></ol>
Remodeling	<ol style="list-style-type: none"><li>1. Vascular endothelial cell apoptosis (granulation tissue repression)</li><li>2. Dermal collagen type switch</li></ol>

**Table 7.1 Major cellular events of normal skin wound healing process.**

(ILC3s) which were only identified in lymphoid tissues and some other epithelial tissues such as intestine, are recruited into skin wound site early on day 2 post-wounding and continue to infiltrate the wounded skin on day 5 post-wounding, and participate in normal skin wound healing. I have determined that the phenotypes of these ILCs are  $CD45^+ROR\gamma^+CD3^-CD127^{dim\ to\ +}CD4^{dim\ to\ +}CD117^-NKp46^-$ , which belong to Group 3 ILCs (ILC3), but are different from current subsets identified in other sites. Although  $ROR\gamma^+$  is also reportedly expressed by some dermal  $\gamma\delta$  T cells (Gray et al., 2011), I confirmed that the vast majority (> 90%) of  $ROR\gamma^+$  cells at wound site are non-T cells ( $CD3^-$ ) and thus are ILCs.

I then analyzed the function of these ILC3s in skin wound healing. I have shown loss of ILC3 causes severely delayed wound healing partly due to lack of early IL22-dependent epidermal proliferation and early CCL3-dependent monocyte/macrophage recruitment during wound healing, while transfer of ILC3 to the recipients inhibits the wound pathology. Furthermore, I have demonstrated IL23 signaling from localized dendritic/Langerhans cells is required for the production of IL22 in ILC3. Thus I suggest that ILC3 play key roles in skin repair through promoting epidermal proliferation via supplying early IL22 which is dependent on IL23 secreted by dendritic/ Langerhans cells and recruitment of monocytes/ macrophages via supplying early CCL3, which is consistent with previous studies on the role of ILC3s in tissue repair in thymus and intestine through IL-22 (Dudakov et al., 2012; Sonnenberg et al., 2012). Given the new evidence that IL22 receptor $\alpha$  is also expressed by dermal fibroblasts (McGee et al., 2013), IL-22 may have roles in both epidermal and dermal compartment and thus may be a key signaling to skin repair. However, I am the first to uncover a role of ILC3 in regulating monocyte/

macrophage recruitment via CCL3. The recruitment of monocytes/ macrophages are reportedly unrelated to the resident macrophages (MacDonald et al., 2010) and are thought to be partly regulated by neutrophils via an array of cytokines including CCL3 (Amulic et al., 2012). However, in our models neutrophil infiltration is not affected by absence of ILC3, confirming ILC3 has a specific role in regulating early macrophage/ monocyte recruitment into wound site via CCL3. Increasing evidence has shown that macrophages in wounds have complex phenotype in different stages of healing: in the initial inflammation phase (1 day post-wounding) (Daley et al., 2010), the majority of macrophages are classically activated by interferon- $\gamma$  (IFN- $\gamma$ ) (M1 macrophages) to perform extensive phagocytosis to clear wound of any debris including the short-life neutrophils and secrete pro-inflammatory cytokines such as TNF- $\alpha$ , IL-1 $\beta$ , IL-6 (Rodero and Khosrotehrani, 2010), while as the healing progresses M1 macrophages are converted to M2 macrophages which are activated by distinct cytokines (alternatively activated), thought to be IL4 and IL13, and play a key role in inflammation resolution and tissue repair (e.g. granulation tissue generation, dermal extracellular matrix deposition and wound contraction) via producing TGF- $\beta$  (Delavary et al., 2011; Martin and Leibovich, 2005; Rodero and Khosrotehrani, 2010). However, the timing of macrophage phenotype conversion and the cytokines involved in this conversion are currently less clear (Daley et al., 2010). I propose that the skin resident macrophages may display M1 phenotype to undertake phagocytosis, while ILC3-recruited macrophages may exert M2 phenotype to provide an early signaling for tissue repair. However, further experiment to analyze the macrophage activation cytokines is required to confirm this.

More strikingly, I have demonstrated that epidermal Notch1 signaling promotes wound healing through an ILC3-mediated process. Previous studies suggested that Notch is implicated in wound healing by using topically-applied Notch activator and inhibitor, however, the mechanistic detail or the site of action was unknown (Ambler and Watt, 2010; Chigurupai et al., 2007; Estrach et al., 2006). Using surgical wounding mouse models, I have shown that both Notch1 and Notch2 activities are robustly activated in wound edge skin predominately in epidermal keratinocytes after injury. Using chemical and genetic tools including blocking antibodies specific for Notch1 or Notch2 (Wu et al., 2010) and a transgenic mouse (K14NICDER) where Notch1 can be controllably activated in the epidermis by 4OHT drug application, I have shown that Notch1 signaling from non-immune cells (i.e. epidermal keratinocytes) rather than from immune cells has an essential temporal role in the wound healing process via regulating wound immune responses specifically recruiting ILC3 and monocytes/ macrophages, and inhibition of Notch1 inhibits wound closure (Figure 5.4). Since I have demonstrated ILC3 recruits monocytes/ macrophages via CCL3 in Chapter 4, I propose epidermal Notch1 signaling indirectly promotes macrophage/ monocyte recruitment through ILC3-dependent CCL3. This is partly supported by recent studies where Notch1<sup>+/-</sup> mice had fewer macrophages in wound site (Outtz, et al., 2010; Outtz et al., 2011), although the authors concluded these defects in macrophage recruitment and inflammatory response are caused by lack of Notch1 activity within macrophages, without giving further evidence to show the sites of Notch activity in normal wound healing. However, in our wounding model, Notch1 activity is hardly detectable in dermal compartment where massive immune cells are normally infiltrating suggesting loss of Notch1 signaling from epidermal compartment was likely to cause decreased

macrophage response in Notch1<sup>+/-</sup> mice. I have uncovered a novel connection between Notch signaling in epithelium and initiation of the immune response, which would become an important paradigm in understanding epithelial tissue repair and homeostasis. The capacity of ectopically activated epidermal Notch1 signaling to recruit ILC3 in unwounded skin, suggesting ILC3 recruitment is dependent on neither pathogen stimulation nor pattern recognition receptor. However, all 4 Notch receptors are expressed in skin epithelial, therefore it will be interesting to determine if other Notch receptors have a contributing role in other aspects in wound healing.

Finally, I demonstrated the mechanism of how epidermal Notch1 recruits ILC3s and regulates their function during skin repair. I have shown that epidermal Notch1 signaling stimulates epidermal production of TNF $\alpha$  which controls ILC3 recruitment to the wound site partly through inducing CCL20 synthesis in dermal fibroblasts, and induces IL23 production (Figure 5.1; NIH GEO: GSE 782, Ambler and Watt, 2008) probably by Langerhans cells which together with dermal dendritic cells have been demonstrated as the main source of IL23 in skin wounds (Figure 4.5) in order to activate ILC3 to function through IL22 production. Interestingly, I have shown dermal fibroblasts also have the capacity to secrete IL22 following stimulation by TNF $\alpha$  (Figure 6.6) and may compensate for the absence of ILC3 to supply IL-22 in later stage of wound healing (Figure 4.4). Given the evidence showing fibroblasts are the key candidate phagocytes in the absence of macrophage during wound healing (Martin et al., 2003) and responsive to IL22 signaling (McGee et al., 2013), I suggest dermal fibroblasts are a versatile candidate playing roles in a wide range of events during wound healing.

In conclusion, I uncovered that the classic developmental signal Notch directs innate immune response after skin damage. The skin wounding activates Notch pathway robustly in epidermal keratinocytes (Figure 7.1). This injury induced Notch1 activity up-regulates epidermal cytokine  $\text{TNF}\alpha$ , which induces CCL20 in fibroblasts, and recruits innate lymphoid cells (i.e. ILC3) to the wound site. ILC3 at the wound site are activated by Notch-stimulated production of IL23 from Langerhans cells to produce early IL22 and CCL3 which subsequently promotes epidermal proliferation and monocyte/ macrophage recruitment, two key events in normal skin wound healing programme. Thus we propose that epidermal Notch1 signaling acts as a damage “sensor” transmitting a “stress/injury signal” instigating skin repair through an ILC mediated process. This signaling may be conserved among different epithelial tissues in the body playing a key role in tissue homeostasis and repair.

However, the cytokines and chemokines were only determined and compared at mRNA levels in this thesis. There might be some proportion of cytokines or chemokines that are preformed and secreted by cells after activation, for example, the preformed  $\text{TNF}\alpha$  can be released by skin mast cells via degranulation (Gibbs et al., 2001), and this might not be reflected in mRNA levels. Further studies using intracellular staining by flow cytometry or protein assay (e.g. enzyme-linked immunosorbent assay, ELISA) are required to determine both newly generated and preformed cytokines and chemokines. In addition, I did not find a direct link between  $\text{TNF}\alpha$  and CCL20 in skin wound healing context. Further studies using recombinant  $\text{TNF}\alpha$  or  $\text{TNF}\alpha$  antagonist at early hours in wounded mice are required to confirm CCL20 is regulated by  $\text{TNF}\alpha$ . In this thesis, CD3, CD4, CD117, CD127, NKp46 were ROR $\gamma$  were used to characterize the phenotypes of ILC3s,



however, more ILC3 markers such as CCR6 (receptor for CCL20), CD25 and CD90 may need to be tested to confirm the phenotypes and subsets of ILC3s in skin wounds preferably using flow cytometry. Since  $CD11c^{Cre}Rosa^{DTR}$  mice deficient in Langerhans and dendritic cells had poorly wound healing, specific depletion of skin Langerhans cell by using DT treated  $Langerin^{Cre}Rosa^{iDTR}$  mice would be our next interest to examine their wound healing rate and cytokine production (e.g. IL-23, IL-22), and compare them to DT treated  $CD11c^{Cre}Rosa^{iDTR}$  as well as wildtype wounds. This future study would confirm whether Langerhans cells or skin conventional dendritic cells had a more critical role in producing IL-23 that activates ILC3 functioning on wound healing.

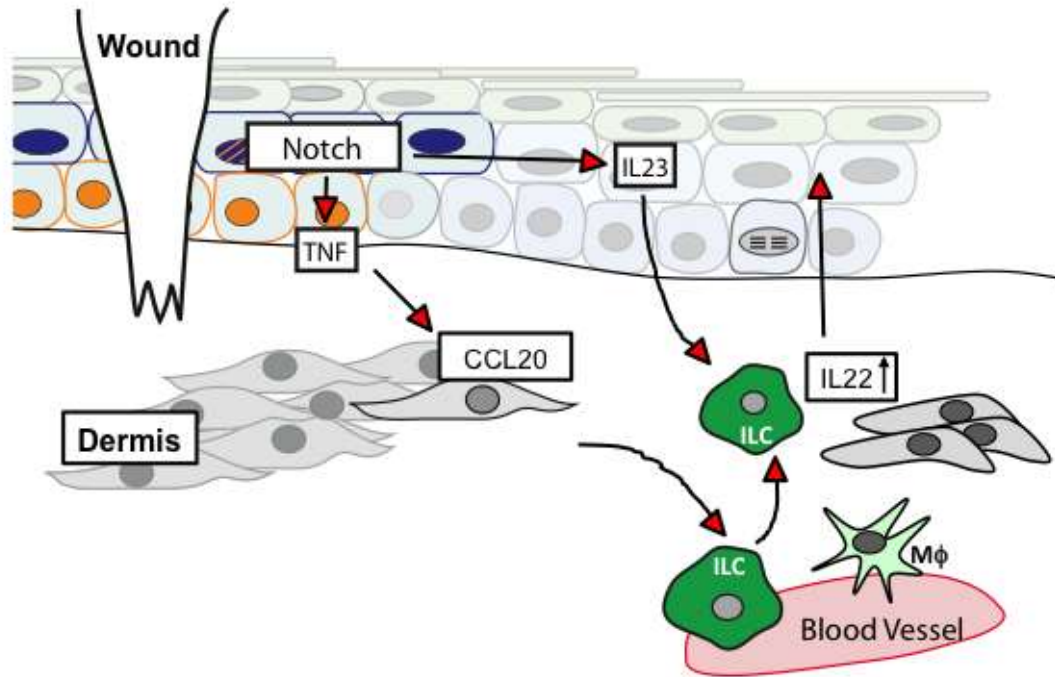


**Figure 7.1 Notch1 orchestrates wound healing through control of Innate Lymphoid Cells (i.e. ILC3s).** Skin wounding activates Notch pathway (orange cells) in the basal and suprabasal epidermis. Injury induced Notch1 activity upregulates TNF $\alpha$  (TNF), which induces CCL20 in fibroblast cells (grey cells), and recruits ILC3s (green cells) to the wound site. ILCs at the wound site are activated by Notch-stimulated production of IL23 to produce IL22 and CCL3 (MIP1 $\alpha$ ) which subsequently influence epidermal proliferation and macrophage (M $\phi$ ) recruitment, two key events in the skin wound-healing programme.

## **Bibliography**

Afshar M and Gallo RL. (2013) Innate immune defense system of the skin. *Veterinary Dermatology*, 24(1):32-8

Alonso L and Fuchs E. (2006) The hair cycle. *Journal of Cell Science*, 119: 391-3

Ambler CA and Watt FM. (2007) Expression of Notch pathway genes in mammalian epidermis and modulation by beta-catenin. *Developmental Dynamics*, 236: 1595-160116

Ambler CA and Watt FM. (2010) Adult epidermal Notch activity induces dermal accumulation of T cells and neural crest derivatives through upregulation of Jagged 1. *Development*, 137: 3569-3579

Amulic B, Cazalet C, Hayes GL, Metzler KD and Zychlinsky A. (2012) Neutrophil function: from mechanism to diseases. *Annual Reviews of Immunology*, 30: 459-89

Ansel KM, Ngo VN, Hyman PL, Luther SA, Förster R, Sedgwick JD, Browning JL, Lipp M and Cyster JG. (2000) A chemokine-driven positive feedback loop organizes lymphoid follicles. *Nature*, 406: 309-14

Ansell DM, Kloepper JE, Thomason HA, Paus R, Hardman MJ. (2011) Exploring the "hair growth-wound healing connection": anagen phase promotes wound re-epithelialization. *Journal of Investigative Dermatology*, 131(2): 518-28.

Artavanis-Tsakonas S, Rand MD and Lake RJ. (1999) Notch signaling: cell fate control and signal integration in development. *Science*, 284: 770-776.

Baroni A, Buommino E, De Gregorio V, Ruocco E, Ruocco V and Wolf R. (2012) Structure and function of the epidermis related to barrier properties. *Clinics in Dermatology*, 30(3):257-62.

Benhra N, Vignaux F, Dussert A, Schweisguth F and Le Borgne R (2010). Neuralized promotes basal to apical transcytosis of delta in epithelial cells. *Molecular Biology of the Cell*, 21: 2078–2086.

Bielez B, Sirin Y, Si H, Niranjana T, Gruenwald A, Ahn S, Kato H, Pullman J, Gessler M, Haase VH and Susztak K. (2010) Epithelial Notch signaling regulates interstitial fibrosis development in the kidneys of mice and humans. *Journal of Clinical Investigation*, 120; 4040-4054

Blanpain C and Fuchs E. (2006) Epidermal stem cells of the skin. *Annual Review of Cell and Developmental Biology*, 22: 339-73.

Blanpain C, Lowry WE, Pasolli HA and Fuchs E. (2006) Canonical notch signaling functions as a commitment switch in the epidermal lineage. *Genes and Development*, 20(21):3022-35

Blum JS, Wearsch PA and Cresswell P. (2013) Pathways of antigen processing. *Annual Review of Immunology*, 31:443-73

Bonneville M. (2012) Semaphorins: new cues for skin healing by  $\gamma\delta$  T cells. *Immunity*, 37(2):194-6

Borregaard N, Theilgaard-Monch K, Cowland JB, Stahle M and Sorensen OE. (2005) Neutrophils and keratinocytes in innate immunity--cooperative actions to provide antimicrobial defense at the right time and place. *Journal of Leukocyte Biology*, 77: 439-443

Bray SJ. (2006) Notch signalling: a simple pathway becomes complex. *Nature Reviews Molecular Cell Biology*, 7(9): 678-89.

Buch T, Heppner FL, Tertilt C, Heinen TJ, Kremer M, Wunderlich FT, Jung S, Waisman A. (2005) A Cre-inducible diphtheria toxin receptor mediates cell lineage ablation after toxin administration. *Nature Methods*, 2(6): 419-26.

Bugeon L, Gardner LM, Rose A, Gentle M and Dallman MJ. (2008) Cutting edge: Notch signaling induces a distinct cytokine profile in dendritic cells that supports T cell-mediated regulation and IL-2-dependent IL-17 production. *Journal of Immunology*, 181: 8189-8193

Calabrese LH. (2003) Molecular differences in anticytokine therapies. *Clinical and Experimental Rheumatology*, 21: 241-248

Cameron AL, Kirby B, Fei W and Griffiths CE. (2002) Natural killer and natural killer-T cells in psoriasis. *Archives of Dermatological Research*, 294(8):363-9.

Chastagner P, Israël A and Brou C. (2008) AIP4/Itch regulates Notch receptor degradation in the absence of ligand. *PLoS One*, 3(7): e2735.

Chen H, Chen H, Ko G, Zatti A, Di Giacomo G, Liu L, Raiteri E, Perucco E, Collesi C, Min W, Zeiss C, De Camilli P and Cremona O. (2009) Embryonic arrest at midgestation and disruption of Notch signaling produced by the absence of both epsin 1 and epsin 2 in mice. *Proceedings of the Natural Academy of Sciences of the United States of America*, 106:13838–13843.

Chiba S. (2006) Notch signaling in stem cell systems. *Stem Cell*, 24(11):2437-47

Chigurupati S, Arumugam TV, Son TG, Lathia JD, Jameel S, Mughal MR, Tang SC, Jo DG, Camandola S, Giunta M, Rakova I, McDonnell N, Miele L, Mattson MP and Poosala S. (2007) Involvement of notch signaling in wound healing. *PloS One*, 2: e1167

Chillakuri CR, Sheppard D, Lea SM and Handford PA. (2012) Notch receptor-ligand binding and activation: insights from molecular studies. *Seminars in Cell and Developmental Biology*, 23(4):421-8

Daley JM, Brancato SK, Thomay AA, Reichner JS and Albina LE. (2010) The phenotype of murine wound macrophages. *Journal of Leukocyte Biology*, 87(1): 59-67.

Delves PJ, Martin SJ, Burton DR and Roitt IM. (2011) *Roitt's Essential Immunology*, 12<sup>th</sup> Edition. West Sussex: Wiley-Blackwell.

Demehri S, Morimoto M, Holtzman MJ and Kopan R. (2009) Skin-derived TSLP triggers progression from epidermal-barrier defects to asthma. *PLoS Biology*, 7: e1000067

Dexter JS. (1914) The analysis of a case of continuous variation in *Drosophila* by a study of its linkage relations. *American Naturalist*, 48: 712–58.

Dovi, JV, He LK and DiPietro LA. (2003) Accelerated wound closure in neutrophil-depleted mice. *Journal of Leukocyte Biology*, 73: 448–455

Dudakov JA, Hanash AM, Jenq RR, Young LF, Ghosh A, Singer NV, West ML, Smith OM, Holland AM, Tsai JJ, Boyd RL and van den Brink MR. (2012) Interleukin-22 drives endogenous thymic regeneration in mice. *Science*, 336: 91-95

Dupasquier M, Stoitzner P, van Oudenaren A, Romani N and Leenen PJ. (2004) Macrophages and dendritic cells constitute a major subpopulation of cells in the mouse. *Journal of Investigative Dermatology*, 123(5):876-9.

Egozi EI, Ferreira AM, Burns AL, Gamelli RL and DiPietro LA. (2003) Mast cells modulate the inflammatory but not the proliferative response in healing wounds. *Wound Repair Regeneration*, 11: 46–54

Ellisen LW, Bird J, West DC, Soreng AL, Reynolds TC, Smith SD and Sklar J. (1991) TAN-1, the human homolog of the *Drosophila* notch gene, is broken by chromosomal Translocations in T lymphoblastic neoplasms. *Cell*, 66(4): 649–61.

Emery G, Hutterer A, Berdnik D, Mayer B, Wirtz-Peitz F, Gaitan MG and Knoblich JA. (2005) Asymmetric Rab 11 endosomes regulate delta recycling and specify cell fate in the *Drosophila* nervous system. *Cell*, 122: 763–773.

Estrach S, Ambler CA, Lo Celso C, Hozumi K, and Watt FM. (2006) Jagged 1 is a beta-catenin target gene required for ectopic hair follicle formation in adult epidermis. *Development*, 133: 4427-4438

Favier B, Fliniaux I, Thélu J, Viallet JP, Demarchez M, Jahoda CA and Dhouailly D. (2000) Localisation of members of the notch system and the differentiation of vibrissa hair follicles: receptors, ligands, and fringe modulators. *Developmental Dynamics*, 218(3):426-37

Ferguson MW and O'Kane S. (2004) Scar-free healing: from embryonic mechanisms to adult therapeutic intervention. *Philosophical transactions of the Royal Society of London. Series B, Biological sciences*, 359: 839-850

Foldi J, Chung AY, Xu H, Zhu J, Outtz HH, Kitajewski J, Li Y, Hu X and Ivashkiv LB. (2010) Autoamplification of Notch signaling in macrophages by TLR-induced and RBP-J-dependent induction of Jagged1. *Journal of Immunology*, 185(9):5023-31



Fortini ME. (2009) Notch signaling: the core pathway and its posttranslational regulation. *Developmental Cell*, 16(5):633-47

Fuchs E. (2007) Scratching the surface of skin development. *Nature*, 455: 834-42

Gawronska-Kozak B, Bogacki M, Rim, JS, Monroe WT, and Manuel JA. (2006) Scarless skin repair in immunodeficient mice. *Wound Repair and Regeneration*, 14: 265-276.

Gibbs BF, Wierecky J, Welker P, Henz BM, Wolff HH, Grabbe J (2001) Human skin mast cells rapidly release preformed and newly generated TNF-alpha and IL-8 following stimulation with anti-IgE and other secretagogues. *Experimental Dermatology*, 10(5):312-20

Girardi M, Lewis J, Glusac E, Filler RB, Geng L, Hayday AC and Tigelaar RE. (2002) Resident skin-specific gammadelta T cells provide local, nonredundant regulation of cutaneous inflammation. *Journal of Experimental Medicine*, 195: 855-867

Gordon WR, Arnett KL and Blacklow SC. (2008) The molecular logic of Notch signaling--a structural and biochemical perspective. *Journal of Cell Science*, 121:3109-3119.

Goren I, Allmann N, Yogev N, Schurmann C, Linke A, Holdener M, Waisman A, Pfeilschifter J and Frank S. (2009) A transgenic mouse model of inducible

macrophage depletion: effects of diphtheria toxin-driven lysozyme M-specific cell line-age ablation on wound inflammatory, angiogenic, and contractive processes. *American Journal of Pathology*, 175: 132-147.

Gray EE, Suzuki K and Cyster JG. (2011) Cutting edge: Identification of a motile IL-17-producing gammadelta T cell population in the dermis. *Journal of Immunology*, 186(11):6091-5

Gröne A. (2002) Keratinocytes and cytokines. *Veterinary Immunology and Immunopathology*, 88(1-2):1-12.

Guo S and Dipietro LA. (2010) Factors affecting wound healing. *Journal of Dental Research*, 89(3):219-29

Guruharsha KG, Kankel MW and Artavanis-Tsakonas S. (2012) The Notch signalling system: recent insights into the complexity of a conserved pathway. *Nature Reviews Genetics*, 13(9): 654-66

Hao Z and Rajewsky K. (2001) Homeostasis of peripheral B cells in the absence of B cell influx from the bone marrow. *Journal of Experimental Medicine*, 194(8): 1151-64.

Havran WL and Jameson JM. (2010) Epidermal T cells and wound healing. *Journal of Immunology*, 184: 5423-5428.

Henri S, Poulin LF, Tamoutounour S, Ardouin L, Guilliams M, de Bovis B, Devilard E, Viret C, Azukizawa H, Kissenpfennig A and Malissen B. (2010) CD207<sup>+</sup> CD103<sup>+</sup> dermal dendritic cells cross-present keratinocyte-derived antigens irrespective of the presence of Langerhans cells. *Journal of Experimental Medicine*, 207(1): 189-206

Iso T, Kedes L and Hamamori Y. (2003) HES and HERP families: multiple effectors of the Notch signaling pathway, *Journal of Cellular Physiology*, 194(3):237-55.

Ito M, Liu Y, Yang Z, Nguyen J, Liang F, Morris RJ and Cotsarelis G. (2005) Stem cells in the hair follicle bulge contribute to wound repair but not to homeostasis of the epidermis. *Nature Medicine*, 11(12): 1351-4

Ito M, Yang Z, Andl T, Cui C, Kim N, Millar SE and Cotsarelis G. (2007) Wnt-dependent de novo hair follicle regeneration in adult mouse skin after wounding. *Nature*, 447(7142): 316-20.

Ito M and Cotsarelis G (2008) Is the hair follicle necessary for normal wound healing? *Journal of Investigative Dermatology*, 128(5): 1059-1061

Izon DJ, Punt JA, Xu L, Karnell FG, Allman D, Myung PS, Boerth NJ, Pui JC, Koretzky GA and Pear WS. (2001) Notch1 regulates maturation of CD4<sup>+</sup> and CD8<sup>+</sup> thymocytes by modulating TCR signal strength. *Immunity*, 14: 253-264

Jafar-Nejad H, Andrews HK, Acar M, Bayat V, Wirtz-Peitz F, Mehta SQ, Knoblich JA and Bellen HJ. (2005) Sec15, a component of the exocyst, promotes notch signaling during the asymmetric division of *Drosophila* sensory organ precursors. *Developmental Cell*, 9: 351–363.

Jahoda CA., Horne KA and Oliver RF. (1984) Induction of hair growth by implantation of cultured dermal papilla cells. *Nature*, 311: 560-562

Jameson J, Ugarte K, Chen N, Yachi P, Fuchs E, Boismenu R and Havran WL. (2002) A role for skin gammadelta T cells in wound repair. *Science*, 296: 747-749

Johnston A, Fritz Y, Dawes SM, Diaconu D, Al-Attar PM, Guzman AM, Chen CS, Fu W, Gudjonsson JE, McCormick TS and Ward NL. (2013) Keratinocyte overexpression of IL-17C promotes psoriasiform skin inflammation. *Journal of Immunology*, 190: 2252-2262

Jung S, Unutmaz D, Wong P, Sano G, De los Santos K, Sparwasser T, Wu S, Vuthoori S, Ko K, Zavala F, Pamer EG, Littman DR and Lang RA. (2002) In vivo depletion of CD11c+ dendritic cells abrogates priming of CD8+ T cells by exogenous cell-associated antigens. *Immunity*, 17: 211-220.

Kageyama R, Ohtsuka T and Kobayashi T (2007) The Hes gene family: Repressors and oscillators that orchestrate embryogenesis. *Development*, 134 (7): 1243–1251

Kim S, Han S and Kim MY. (2010) Heterogeneity of IL-22-producing Lymphoid Tis IL-22-producing Lymphoid Tissue Inducer-like Cells in Human and Mouse. *Immune Network*, 10(4):115-9.

Krebs LT, Xue Y, Norton CR, Shutter JR, Maguire M, Sundberg JP, Gallahan D, Closson V, Kitajewski J, Callahan R, Smith GH, Stark KL and Gridley T. (2000) Notch signaling is essential for vascular morphogenesis in mice. *Genes & Development*, 14: 1343-1352.

Krebs LT, Xue Y, Norton CR, Sundberg JP, Beatus P, Lendahl U, Joutel A and Gridley T. (2003) Characterization of Notch3-deficient mice: normal embryonic development and absence of genetic interactions with a Notch1 mutation. *Genesis*, 37: 139-143.

Kushwah R and Hu J. (2011) Complexity of dendritic cell subsets and their function in the host immune system. *Immunology*, 133(4):409-19

Lai EC, Deblandre GA, Kintner C and Rubin GM. (2001) Drosophila neutralized is a ubiquitin ligase that promotes the internalization and degradation of delta. *Developmental Cell*, 1:783–794.

Laitman LE and Dahan S. (2012) Taking inflammatory bowel disease up a Notch. *Immunologic Research*, 54: 69-74

Lanz TA, Karmilowicz MJ, Wood KM, Pozdnyakov N, Du P, Piotrowski MA, Brown TM, Nolan CE, Richter KE, Finley JE, Fei Q, Ebbinghaus CF, Chen YL, Spracklin DK, Tate B, Geoghegan KF, Lau LF, Auperin DD and Schachter JB. (2006) Concentration-dependent modulation of amyloid-beta in vivo and in vitro using the gamma-secretase inhibitor, LY-450139. *The Journal of Pharmacology and Experimental Therapeutics*, 319: 924–33.

Lee J, Basak JM, Demehri S and Kopan R. (2007) Bi-compartmental communication contributes to the opposite proliferative behavior of Notch1-deficient hair follicle and epidermal keratinocytes. *Development*, 134: 2795-2806

Lee JS, Cella M, McDonald KG, Garlanda C, Kennedy GD, Nukaya M, Mantovani A, Kopan R, Bradfield CA, Newberry RD and Colonna M. (2012) AHR drives the development of gut ILC22 cells and postnatal lymphoid tissues via pathways dependent on and independent of Notch. *Nature Immunology*, 13, 144-151

Leibovich SJ and Ross R. (1975) The role of the macrophage in wound repair: A study with hydrocortisone and antimacrophage serum. *American Journal of Pathology*, 78: 71–100

Lewis J. (1998) Notch signaling and the control of cell fate choices in vertebrates. *Cell and Developmental Biology*, 9: 583 – 589

Lin MH, Leimeister C, Gessler M and Kopan R. (2000) Activation of the Notch pathway in the hair cortex leads to aberrant differentiation of the adjacent hair-shaft layers. *Development*, 127(11):2421-32

Liu J, Sun Y, Oster GF and Drubin DG. (2010) Mechanochemical crosstalk during endocytic vesicle formation. *Current Opinion in Cell Biology*, 22:36–43.

Louvi A and Artavanis-Tsakonas S. (2012) Notch and disease: a growing field. *Seminars in Cell and Developmental Biology*, 23(4):473-80

Lowell S, Jones P, Le Roux I, Dunne J and Watt FM. (2000) Stimulation of human epidermal differentiation by delta-Notch signaling at the boundaries of stem-cell clusters. *Current Biology*, 10: 491-500

Lucas T, Waisman A, Rannan R, Roes J, Krieg T, Muller W, Roers A and Eming SA. (2009) Differential Roles of Macrophages in Diverse Phases of Skin Repair. *Journal of Immunology*, 184(7):3964-77

Luci C, Reynders A, Ivanov II, Cognet C, Chiche L, Chasson L, Hardwigsen J, Anguiano E, Banchereau J, Chaussabel D, Dalod M, Littman DR, Vivier E and Tomasello E. (2009) Influence of the transcription factor ROR $\gamma$  on the development of NKp46<sup>+</sup> cell populations in gut and skin. *Nature Immunology*, 10(1): 75-82

Luther SA, Lopez T, Bai W, Hanahan D, Cyster JG. (2000) BLC expression in pancreatic islets causes B cell recruitment and lymphotoxin-dependent lymphoid neogenesis. *Immunity*, 12(5): 471-81.

MacDonald KP, Palmer JS, Cronau S, Seppanen E, Olver S, Raffelt NC, Kuns R, Pettit AR, Clouston A, Wainwright B, Branstetter D, Smith J, Paxton RJ, Cerretti DP, Bonham L, Hill GR and Hume DA. (2010) An antibody against the colony-stimulating factor 1 receptor depletes the resident subset of monocytes and tissue- and tumor-associated macrophages but does not inhibit inflammation. *Blood*, 116(19): 3955-63

Macleod AS and Havran WL. (2011) Functions of skin-resident  $\gamma\delta$  T cells. *Cellular and Molecular life Sciences*, 68(14): 2399-408

Mahdavian Delavary B, van der Veer WM, van Egmond M, Niessen FB and Beelen RH. (2011) Macrophages in skin injury and repair. *Immunobiology*, 216, 753-762.

Marchesi F, Martin AP, Thirunarayanan N, Devany E, Mayer L, Grisotto MG, Furtado GC and Lira SA. (2009) CXCL13 expression in the gut promotes accumulation of IL-22-producing lymphoid tissue-inducer cells, and formation of isolated lymphoid follicles. *Mucosal Immunology*, 2: 486-494

Martin B, Hirota K, Cua DJ, Stockinger B and Veldhoen M. (2009) Interleukin-17-producing gammadelta T cells selectively expand in response to pathogen products and environmental signals. *Immunity*, 31: 321-330



Martin P, D'Souza D, Martin J, Grose R, Cooper L, Maki R and McKercher SR. (2003) Wound healing in the PU.1 null mouse--tissue repair is not dependent on inflammatory cells. *Current Biology*, 13: 1122-1128

Martin P and Leibovich SJ. (2005) Inflammatory cells during wound repair: the good, the bad and the ugly. *Trends Cell Biology*, 15: 599-607

Mathieu D, Linke J-C, Wattel F (2006). Non-healing wounds. In Mathieu DE, *Handbook on hyperbaric medicine*, Netherlands: Springer, 401-427

Mestas J. and Hughes CCW (2004) Of Mice and Not Men: Differences between Mouse and Human Immunology. *The Journal of Immunology*, 172: 2731-2738.

McGee HM, Schmidt BA, Booth CJ, Yancopoulos GD, Valenzuela DM, Murphy AJ, Stevens S, Flavell RA and Horsley V. (2013) IL22 Promotes Fibroblast-Mediated Wound Repair in the Skin. *Journal of Investigative Dermatology*, 133(5): 1321-9

Merad M, Sathe P, Helft J, Miller J and Mortha A. (2013) The dendritic cell lineage: ontogeny and function of dendritic cells and their subsets in the steady state and the inflamed settings. *Annual Review of Immunology*, 31:563-604

Mirza R, DiPietro LA and Koh TJ. (2009) Selective and specific macrophage ablation is detrimental to wound healing in mice. *American Journal of Pathology*, 175: 2454-2462.

Moriyama M, Durham AD, Moriyama H, Hasegawa K, Nishikawa S, Radtke F and Osawa M. (2008) Multiple roles of Notch signaling in the regulation of epidermal development. *Developmental Cell*, 14(4):594-604

Mueller SN, Gebhardt T, Carbone FR, Heath WR. (2013) Memory T cell subsets, migration patterns, and tissue residence. *Annual Review of Immunology*, 31:137-61

Musse AA, Meloty-Kapella L and Weinmaster G. (2012) Notch ligand endocytosis: mechanistic basis of signaling activity. *Seminars in Cell and Developmental Biology*, 23(4):429-36

Nestle FO and Nickoloff BJ. (2007) Deepening our understanding of immune sentinels in the skin. *The Journal of Clinical Investigation*, 117(9):2382-5

Nickoloff BJ, Qin JZ, Chaturvedi V, Denning MF, Bonish B and Miele L. (2002) Jagged-1 mediated activation of notch signaling induces complete maturation of human keratinocytes through NF-kappaB and PPARgamma. *Cell Death and Differentiation*, 9: 842-855

Nichols JT, Miyamoto A, Olsen SL, D'Souza B, Yao C and Weinmaster G. (2007) DSL ligand endocytosis physically dissociates Notch1 heterodimers before activating proteolysis can occur. *Journal of Cell Biology*, 176(4):445-58

Nicolas M, Wolfer A, Raj K, Kummer JA, Mill P, van Noort M, Hui CC, Clevers H, Dotto GP and Radtke F. (2003) Notch1 functions as a tumor suppressor in mouse skin. *Nature Genetic*, 33(3): 416-21.

Niyonsaba F, Ushio H, Nakano N, Ng W, Sayama K, Hashimoto K, Nagaoka I, Okumura K and Ogawa H. (2007) Antimicrobial peptides human beta-defensins stimulate epidermal keratinocyte migration, proliferation and production of pro-inflammatory cytokines and chemokines. *Journal of Investigative Dermatology*, 127(3):594-604

Obata Y, Takahashi D, Ebisawa M, Kakiguchi K, Yonemura S, Jinnohara T, Kanaya T, Fujimura Y, Ohmae M, Hase K and Ohno H. (2012) Epithelial cell-intrinsic Notch signaling plays an essential role in the maintenance of gut immune homeostasis. *Journal of Immunology*, 188: 2427-2436

Oh HS and Smart RC. (1996) An estrogen receptor pathway regulates the telogen-anagen hair follicle transition and influences epidermal proliferation. *Proceedings of the National Academy of Science of the United States of America*, 93(22):12525-30.

Okamoto R, Tsuchiya K, Nemoto Y, Akiyama J, Nakamura T, Kanai T and Watanabe M. (2009) Requirement of Notch activation during regeneration of the intestinal epithelia. *American Journal of Physiology*, 296: G23-35

Okuyama R, Tagami H and Aiba S. (2008) Notch signaling: its role in epidermal homeostasis and in the pathogenesis of skin diseases. *Journal of Dermatological Science*. 49(3):187-94.

Outtz HH, Tattersall IW, Kofler NM, Steinbach N and Kitajewski J. (2011) Notch1 controls macrophage recruitment and Notch signaling is activated at sites of endothelial cell anastomosis during retinal angiogenesis in mice. *Blood*, 118: 3436-3439

Outtz HH, Wu JK, Wang X and Kitajewski J. (2010) Notch1 deficiency results in decreased inflammation during wound healing and regulates vascular endothelial growth factor receptor-1 and inflammatory cytokine expression in macrophages. *Journal of Immunology*, 185: 4363-4373

Pan Y, Lin MH, Tian X, Cheng HT, Gridley T, Shen J and Kopan R. (2004) Gamma-secretase functions through Notch signaling to maintain skin appendages but is not required for their patterning or initial morphogenesis. *Developmental Cell*, 7:731-743

Parks AL, Klueg KM, Stout JR and Muskavitch MA. (2000) Ligand endocytosis drives receptor dissociation and activation in the Notch pathway. *Development*, 127:1373–1385.

Penton AL, Leonard LD and Spinner NB. (2012) Notch signaling in human development and disease. *Seminars in Cell and Developmental Biology*, 23(4):450-7

Plikus MV, Gay DL, Treffeisen E, Wang A, Supapannachart RJ and Cotsarelis G. (2012) Epithelial stem cells and implications for wound repair. *Seminars in Cell and Developmental Biology*, 23(9):946-53

Possot C, Schmutz S, Chea S, Boucontet L, Louise A, Cumano A and Golub R. (2011) Notch signaling is necessary for adult, but not fetal, development of ROR $\gamma$ t(+) innate lymphoid cells. *Nature Immunology*, 12(10):949-58

Powell BC, Passmore EA, Nesci A and Dunn SM. (1998) The Notch signalling pathway in hair growth. *Mechanisms of Development*, 78(1-2):189-92

Radtke F, Macdonald HR and Tacchini-Cottier F. (2013) Regulation of innate and adaptive immunity by Notch. *Nature Reviews Immunology*, 13: 427-437

Rajan A, Tien AC, Haueter CM, Schulze KL and Bellen HJ. (2009) The Arp2/3 complex and WASp are required for apical trafficking of Delta into microvilli during cell fate specification of sensory organ precursors. *Nature Cell Biology*, 11: 815–824.

Rangarajan A. (2001) Notch signaling is a direct determinant of keratinocyte growth arrest and entry into differentiation. *The EMBO Journal*, 20(13):3427-36.

Reynders A, Yessaad N, Manh TV, Dalod M, Fenis A, Aubry C, Nikitas G, Escalière B, Renauld JC, Dussurget O, Cossart P, Lecuit M, Vivier E and

Tomasello E (2011) Identity, regulation and in vivo function of gut NKp46<sup>+</sup>RORγt<sup>+</sup> and NKp46<sup>+</sup>RORγt<sup>-</sup> lymphoid cells. *The EMBO Journal*, 30: 2934-2947

Robey E, Chang D, Itano A, Cado D, Alexander H, Lans D, Weinmaster G and Salmon P (1996) An activated form of Notch influences the choice between CD4 and CD8 T cell lineages. *Cell*, 87, 483-492

Rodero MP and Khosrotehrani K. (2010) Skin wound healing modulation by macrophages. *Journal of Clinical Experimental Pathology*, 3(7): 643–653

Romani N, Clausen BE and Stoitzner P. (2010) Langerhans cells and more: Langerin-expressing dendritic cell subsets in the skin. *Immunological Reviews*, 234(1):120-41

Romera-Hernandez M, Aparicio-Domingo P and Cupedo T. (2013) Damage control: RORγt<sup>+</sup> innate lymphoid cells in tissue regeneration. *Current Opinion in Immunology*, 25(2):156-60

Ross DA and Kadesch T. (2004) Consequences of Notch-mediated induction of Jagged1. *Experimental Cell Research*, 296(2):173-82.

Saito T, Chiba S, Ichikawa M, Kunisato A, Asai T, Shimizu K, Yamaguchi T, Yamamoto G, Seo S, Kumano K, Nakagami-Yamaguchi E, Hamada Y, Aizawa S

and Hirai H. (2003) Notch2 is preferentially expressed in mature B cells and indispensable for marginal zone B lineage development. *Immunity*, 18: 675-685

Segre JA. (2006) Epidermal barrier formation and recovery in skin disorders. *The Journal of Clinical Investigation*, 116(5): 1150–1158

Shaw TJ and Martin P. (2009) Wound repair at a glance. *Journal of Cell Science*, 122: 3209-3213

Shimomura Y and Christiano AM. (2010) Biology and genetics of hair. *Annual Review of Genomics and Human Genetics*, 11:109-32

Simpson, D.M. and Ross, R. (1972) The neutrophilic leukocyte in wound repair. A study with antineutrophil serum. *Journal of Clinical Investigation*, 51: 2009–2023

Small D, Kovalenko D, Kacer D, Liaw L, Landriscina M, Di Serio C, Prudovsky I and Maciag T. (2001) Soluble Jagged 1 represses the function of its transmembrane form to induce the formation of the Src-dependent chord-like phenotype. *The Journal of Biological Chemistry*, 276: 32022–32030

Sonnenberg GF, Monticelli LA, Elloso MM, Fouser LA and Artis D. (2011) CD4(+) lymphoid tissue-inducer cells promote innate immunity in the gut. *Immunity*: 34, 122-134

Spencer ML, Theodosiou M and Noonan DJ (2004). NPDC-1, a novel regulator of neuronal proliferation, is degraded by the ubiquitin/proteasome system through a PEST degradation motif. *The Journal of Biological Chemistry*, 279 (35): 37069–78.

Spits H and Cupedo T. (2012) Innate lymphoid cells: emerging insights in development, lineage relationships, and function. *Annual Review of Immunology*, 30:647-75

Spits H and Di Santo JP. (2011) The expanding family of innate lymphoid cells: regulators and effectors of immunity and tissue remodeling, *Nature Immunology*, 12(1): 21-7

Spits H, Artis D, Colonna M, Diefenbach A, Di Santo JP, Eberl G, Koyasu S, Locksley RM, McKenzie AN, Mebius RE, Powrie F and Vivier E. (2013) Innate lymphoid cells--a proposal for uniform nomenclature. *Nature Reviews. Immunology*, 13(2):145-9

Stone KD, Prussin C and Metcalfe DD. (2010) IgE, Mast Cells, Basophils, and Eosinophils. *The Journal of Allergy and Clinical Immunology*, 125(2 Suppl 2): S73–S80.

Stout RD. (2010) Macrophage functional phenotypes: no alternatives in dermal wound healing. *Journal of Leukocyte Biology*, 87: 19-21



Sumaria N, et al. (2011) Cutaneous immunosurveillance by self-renewing dermal gammadelta T cells. *The Journal of Experimental Medicine*, 208(3):505-18

Sun Z, Unutmaz D, Zou YR, Sunshine MJ, Pierani A, Brenner-Morton S, Mebius RE and Littman DR. (2000) Requirement for ROR $\gamma$  in thymocyte survival and lymphoid organ development. *Science*, 288; 2369-2373

Thélu J, Rossio P and Favier B. (2002) Notch signalling is linked to epidermal cell differentiation level in basal cell carcinoma, psoriasis and wound healing. *BMC Dermatology*, 2:7

Tohyama M, Shirakara Y, Yamasaki K., Sayama K. and Hashimoto K.. (2001) Differentiated keratinocytes are responsible for TNF-alpha regulated production of macrophage inflammatory protein 3alpha/CCL20, a potent chemokine for Langerhans cells. *Journal of Dermatological Science*, 27, 130-139

Tolia A and De Strooper B. (2009) Structure and function of  $\gamma$ -secretase. *Seminars in Cell and Developmental Biology*, 20: 211–8.

Uyttendaele H, Panteleyev AA, de Berker D, Tobin DT and Christiano AM. (2004) Activation of Notch1 in the hair follicle leads to cell-fate switch and Mohawk alopecia. *Differentiation*, 72(8):396-409

Wang W and Struhl G. (2005) Distinct roles for Mind bomb, Neuralized and Epsin in mediating DSL endocytosis and signaling in Drosophila. *Development*, 132:2883–2894.

Watt FM, Estrach S and Ambler CA. (2008) Epidermal Notch signalling: differentiation, cancer and adhesion. *Current Opinion in Cell Biology*, 20(2):171-9

Weinmaster G and Fischer JA. (2011) Notch ligand ubiquitylation: what is it good for? *Developmental Cell*, 21(1):134-44.

Windler SL and Bilder D. (2010) Endocytic Internalization Routes Required for Delta/Notch Signaling. *Current Biology*, 20:538–543

Wolk K, Kunz S, Witte E, Friedrich M, Asadullah K and Sabat R. (2004) IL-22 increases the innate immunity of tissues. *Immunity*, 21: 241-254

Wolk K, Haugen HS, Xu W, Witte E, Waggie K, Anderson M, Vom Baur E, Witte K, Warszawska K, Philipp S, Johnson-Leger C, Volk HD, Sterry W and Sabat R. (2009) IL-22 and IL-20 are key mediators of the epidermal alterations in psoriasis while IL-17 and IFN-gamma are not. *Journal of Molecular Medicine*, 87: 523-536

Wolk K, Warszawska K, Hoeflich C, Witte E, Schneider-Burrus S, Witte K, Kunz S, Buss A, Roewert HJ, Krause M, Lukowsky A, Volk HD, Sterry W and Sabat R. (2011) Deficiency of IL-22 contributes to a chronic inflammatory disease: pathogenetic mechanisms in acne inversa. *Journal of Immunology*, 186: 1228-1239

Wynn TA and Barron L. (2010) Macrophages: master regulators of inflammation. *Seminars in Liver Disease*, 30(3):245-57

Wu Y, Cain-Hom C, Choy L, Hagenbeek TJ, de Leon GP, Chen Y, Finkle D, Venook R, Wu X, Ridgway J, Schahin-Reed D, Dow GJ, Shelton A, Stawicki S, Watts RJ, Zhang J, Choy R, Howard P, Kadyk L, Yan M, Zha J, Callahan CA, Hymowitz SG and Siebel CW. (2010) Therapeutic antibody targeting of individual Notch receptors. *Nature*, 464: 1052-1057

Yamaguchi E, Chiba S, Kumano K, Kunisato A, Takahashi T, Takahashi T and Hirai H (2002) Expression of Notch ligands, Jagged1, 2 and Delta1 in antigen presenting cells in mice. *Immunology Letters*. 81(1):59-64.

Zhu J, Yamane H and Paul WE. (2010) Differentiation of effector CD4 T cell populations. *Annual Review of Immunology*, 28:445-89